T H E U N I V E R S I T Y O F M I C H I G A N

COLLEGE OF ENGINEERING
Department of Mechanical Engineering
Heat Transfer Laboratory

Final Report

CONVECTIVE AND RADIATIVE HEAT TRANSFER TO SUPERHEATED STEAM IN UNIFORMLY AND NONUNIFORMLY HEATED TUBES

Poul S. Larsen
Herbert A. Lord

ORA Project 08742

supported by:

WESTINGHOUSE ELECTRIC CORPORATION
ATOMIC POWER DIVISION
PITTSBURGH, PENNSYLVANIA

administered through:

OFFICE OF RESEARCH ADMINISTRATION ANN ARBOR

February 1969

ACKNOWLEDGMENT

Several graduate students of the Department of Mechanical Engineering contributed to this study, Mr. J. S. Gellerstedt in the design of loop and test sections and preliminary shake-down, Mr. S. A. Korpela and Mr. D. Gőzűm in the taking of data.

Measurement of emissivity of surface samples was made at the Infrared Physics Laboratory of the Institute of Science and Technology of The University of Michigan.

TABLE OF CONTENTS

TABLE OF CONTENTS (Concluded)

LIST OF TABLES

LIST OF FIGURES

LIST OF FIGURES (Concluded)

NOMENCLATURE

Roman

A	Laminarization parameter, Eq. (3-27)
AW	Nondimensional wall area, Eq. (2-2)
B	Radiosity
C_p	Constant pressure specific heat
C_w	Pressure correction factor, Eq. (3-22)
D	Inside diameter
G	Mass velocity
h	Enthalpy, heat transfer coefficient
H	Incident radiation
k	Thermal conductivity
Nu	Nusselt number, $h D/k$
p	Pressure
Pr	Prandtl number, $\mu C_p/k$
$\mathcal{P}$	Planck number, $\alpha k/4\sigma T^3$
q	Heat flux
Re	Reynolds number, GD/μ
Re_{wb}	Modified wall-bulk Reynolds number, $(GD/\mu_w)(\rho_w/\rho_b)$
T	Temperature
V	Velocity
x	Axial coordinate measured from inlet to heated length
z	Nondimensional axial coordinate, x/D

Greek

α	Absorptivity
δ	Boundary layer thickness
ϵ	Emissivity
η	Nondimensional radial coordinate, $2r/D$
Θ	Temperature ratio, T/T_w
θ	Temperature difference, $T_w - T_b$
κ	Absorption coefficient
Λ	Velocity profile parameter, Eq. (3-26)
μ	Dynamic viscosity
ν	Kinematic viscosity
ρ	Density
σ	Constant, 0.171×10^{-8} Btu/°R^{4}ft^{2}hr
τ	Optical thickness, κD
ϕ	Function, Eq. (3-6)

Subscript

b	Bulk
e	Equivalent hydraulic
f	Film
g	Gas, bulk
U	Uniform flux value
NU	Nonuniform flux value
w	Wall

Superscript

C	Convection
L	Laminar
R	Radiative
T	Total

ABSTRACT

Total heat transfer by convection and radiation to superheated steam was measured at 12 local stations along 36-in. long by 0.5 in. I.D. uniformly and nonuniformly heated tubes. Parameter ranges were: pressure (25, 50, 75 psia), inlet temperature (300, 700, 1100°F), bulk inlet Reynolds number (1900-35,000), lowest local bulk Reynolds number (420), wall temperatures (400-1800°F), and wall-to-bulk temperature ratio (1.1-2.11).

Uniform flux test sections of type 310 stainless steel and zircaloy-2 and a nonuniform flux test section of type 310 stainless steel having a modified cosine flux distribution with a maximum to mean heat flux ratio of 1.66 were employed.

At constant heat flux fully turbulent convective heat transfer data for a transparent gas (nitrogen) agree with the McEligot correlation. Total convective and radiative heat transfer data to steam 26 or more diameters downstream of the entrance agree with the Dittus-Boelter correlation, $Nu_b^T = 0.023\ Re_b^{0.8}\ Pr_b^{0.4}$, to within $\pm 5\%$ for $Re_b > 6000$ and to within +10% and -20% for $1000 < Re_b < 6000$ for all pressures investigated. Retransition from turbulent to laminar flow was observed for Reynolds numbers as high as 5300, and onset of laminarization was correlated empirically.

Analysis shows that axial radiant transfer can be neglected. One-dimensional radiative transfer for turbulent and laminar flow is well predicted based on the thin gas limit of the absorption coefficient for steam at the higher pressures and smaller optical depths.

At nonuniform heat flux fully turbulent convective heat transfer can be approximately predicted from superposition with uniform flux correlation, despite property variation.

1. INTRODUCTION

1.1. BACKGROUND

The increased interest in heat transfer to gases in forced convection at elevated temperatures in recent years stems from engineering problems of effective and safe design of components such as rocket engines and gas cooled nuclear reactors.

The present investigation is directed at heat transfer to saturated and superheated steam at conditions typical of those arising during a later phase of a loss of coolant accident of a water cooled nuclear reactor. Following a hypothesized primary system pipe rupture, expulsion of coolant and bottom flooding of the reactor core its decay heat is to be removed by evaporating water flowing up through the core while gaining superheat. The system pressure during this phase is approximately that of the vapor containment, ranging typically from 1 to 5 atm. Safe design requires accurate prediction of cladding surface temperature which is determined by the heat transfer characteristics of superheated steam in forced convection in nonuniformly heated channels.

Heat transfer to forced gas flow at relatively high heat flux and elevated temperatures includes the following possible areas of complexity,

Thermal entrance effect
Variable thermophysical properties
Variable heat flux
Radiative heat transfer
Laminarization
Dissociation and ionization.

The present study includes and explores all but the last mentioned effects. The equilibrium composition of molecular hydrogen formed by dissociation of water vapor at 2000°F is less than 1/10 of 1% and ionization is not important except at considerably higher temperatures. Among the remaining effects few can be entirely isolated for experimental study. However, by suitable choice of parameter ranges and fluids certain effects may be sufficiently suppressed that those remaining dominate. This approach is taken in design and interpretation of the present study.

1.2. LITERATURE SURVEY

In regard to the several areas of complexity mentioned in the section above consideration is given first to studies involving heat transfer to transparent gases, or gases at low temperature level, for which radiative heat transfer may be ignored.

For fully developed turbulent flow at Reynolds numbers above about 10,000 heat transfer to gases without property variation is well correlated by a Dittus-Boelter type correlation of the form

$$Nu = \text{const.}\ Re^{n}\ Pr^{m} \qquad (1\text{-}1)$$

Eddy diffusivity analyses based on the momentum and heat transfer analogy such as the Karman-Boelter-Martinelli theory (see e.g., Refs. 1 or 2) yield results in agreement with Eq. (1-1) for which the empirically determined constant is taken to be 0.021 for constant flux heat transfer to a gas. The Prandtl number exponent is 0.4 and the Reynolds number exponent is 0.8. Because of the linearity of the constant property problem heat transfer in the thermal entrance length of a fully developed velocity profile may be treated analytically,[3] although not without labor.

The effect of variable properties substantially alters the problem since the flow becomes two dimensional and, in principle, a state of fully developed heat transfer is no longer a reality. Because of the increased analytical complexity empirical correlations including variable property and thermal entrance effects continue to have practical interest. Variable properties are accounted for either through the use of thermophysical properties evaluated at wall, wall-bulk or film temperature, or by multiplying Eq. (1-1) by a wall-to-bulk viscosity or temperature ratio raised to some exponent. At moderate wall-to-bulk temperature ratios (less than about 2.5) an exponent of -0.5 is recommended,[4] while at higher ratios the exponent may decrease to -0.7.[5] Reference 6, in fact, suggests that the exponent depend on the magnitude of the wall-to-bulk temperature ratio, wherefore use of a constant value may be expected to be a reasonable approximation only for a narrow range of temperature ratios.

The entrance effect is accounted for empirically through an additional factor in Eq. (1-1) of the form[4] $(1 + (x/D)^{-0.7})$ for temperature ratios up to 2.5 and of the form[5] $(1 + (T_w/T_b)^{0.7}\ (x/D)^{-0.7})$ for higher temperature ratios up to 7.5. Such simple functional relations are reasonable approximations only several diameters downstream of the beginning of the heated length.

Recent detailed summaries of investigations of heat transfer to transparent gases with variable properties appear in Refs. 4 and 5. A distinction should be made between overall average,[7] incremental average,[8] and local[4,5] heat transfer results. While earlier studies considered average heat transfer only, more recent studies, as well as the present investigation, have considered local heat transfer. The parameter ranges of the study of McEligot *et al.*,[4] most closely coincide with those for fully turbulent flow of the present study, and it may be expected that best agreement is obtained with the correlation developed by these investigators.

Constant property turbulent heat transfer with variable axial heat flux distribution may be treated analytically by applying the superposition integral to the constant heat flux solution. The validity of this procedure has been verified by experiment.[9] Although not directly applicable to the variable property case some success in using this procedure in data reduction has been reported.[6]

Although equally important, heat transfer to gases at low Reynolds numbers and in the transition regime has received less study. Average heat transfer below 8-10,000 Reynolds number is usually presented in terms of the Coburn j-factor vs. bulk Reynolds number.[10] A similar graphical representation was employed for local data obtained more recently.[11] It is characteristic that heat transfer data in the transition regime cover a broad band when displayed in a manner yielding a unique relation for fully turbulent or fully laminar data. Additional parameters are required to fully describe this complex developing heat transfer process. A recent study[12] of heat transfer to constant property gases at Reynolds numbers less than 15,000 presents an empirical correlation which includes the Reynolds number in the axially dependent development term.

Experiments of laminar convective heat transfer to gases indicate[2] that variable properties has a small effect on developed heat transfer. However, heat transfer in the thermal development length is influenced by variable property effects, essentially as in regard to the length coordinate. Data is well correlated by the constant property Graetz solution if the axial coordinate $(2x/D)/Re \cdot Pr$ is replaced by its integrated value from the inlet, as suggested by analysis.[11]

While there are several analytical studies of simultaneous convective and radiative heat transfer to duct flow of absorbing and emitting gases (see e.g., Refs. 13, 14, and 15) there is virtually no experimental study for geometry and parameter ranges of the present investigation. Although heat transfer to superheated and saturated steam is a commonplace process it appears that no recent study has been made in which the convective and radiative heat transfer were separately considered.

1.3. PRESENT STUDY

It is the purpose of the present investigation to study experimentally and analytically heat transfer to superheated steam, particularly at lower Reynolds numbers, and to examine the role of thermal radiation. The specific objectives are summarized below.

Experiment:

(i) Measurement of total local heat transfer to forced flow of water vapor at low to intermediate Reynolds numbers (from 1000 to 30,000),

in the pressure range of 25 to 75 psia and at wall temperatures to 1800°F.

(ii) Sample measurements of convective heat transfer to a transparent gas (nitrogen).

(iii) Determination of the effect of nonuniform axial heat flux distribution on convective and radiative heat transfer.

(iv) Determination of the effect of wall emissivity.

Analysis:

(v) Separation of convective and radiative contributions to total heat transfer.

(vi) Comparison of convective heat transfer to existing correlations developed for transparent gases.

(vii) Separate prediction of radiative and convective heat transfer for uniform and nonuniform heat flux distribution.

(viii) Correlation for prediction of retransition to laminar flow.

The present report summarizes the experimental study, data reduction and correlation, and the analysis according to the above objectives. A second report, Ref. 15, describes detailed analyses of convection-radiation interaction of both laminar and turbulent duct flow, including the thermal entrance effects.

2. EXPERIMENT

2.1. GENERAL

Local heat transfer data was obtained in three 36-in. long by 0.5 in. I.D. test sections, successively placed in an open loop test facility designed and constructed for the present study. The open loop was supplied with either dry bottled nitrogen or shop steam at the upstream end and vented to the atmosphere at the downstream end.

Test sections were heated electrically by passing an AC current through the tube wall. Outside wall temperatures were measured with attached sheathed thermocouples. The heated test sections and power lugs were guard heated and insulated to minimize ambient heat transfer. Inlet and exit fluid temperatures were measured by radiation shielded thermocouples placed in mixing chambers. Flow was measured with a square edge orifice flow meter.

Surface samples were cut from test sections for measurement of normal spectral emissivity of inside wall.

2.2. LOOP

2.2.1. General Description

The open loop designed and built for this study is shown in Figures 1 and 2 and the flow diagram is shown in Figure 3 (see Table I for list of components). To allow thermal expansion downwards the loop is suspended from above through insulated pipe hangers from a basic Unistrut structure which forms a frame for a 1/2-in. plywood enclosure surrounding the loop for personnel protection. The front side of the enclosure serves as instrument panel (Figure 2) for all instruments except flow meter manometers which are mounted on a separate panel.

Either shop steam or bottled gas may be supplied to the open loop, which in the direction of flow consists of the following main components (see Figure 3 and Table I): upstream automatic pressure control valve (9), orifice flow meter (11), precooler (14), preheater (16), flow development section (19), test section (21), exit cooler (23), pneumatically operated flow control valves (24) and (25), exhaust vent to the ambient.

Since single phase superheated steam conditions are maintained at the flow meter both a precooler and a preheater are included in the design so that the steam state at the inlet to the test section may be adjusted to the desired value, ranging from a near saturated state to a superheated state up to 1100°F. To ensure a fully developed velocity profile at the inlet to the heated test

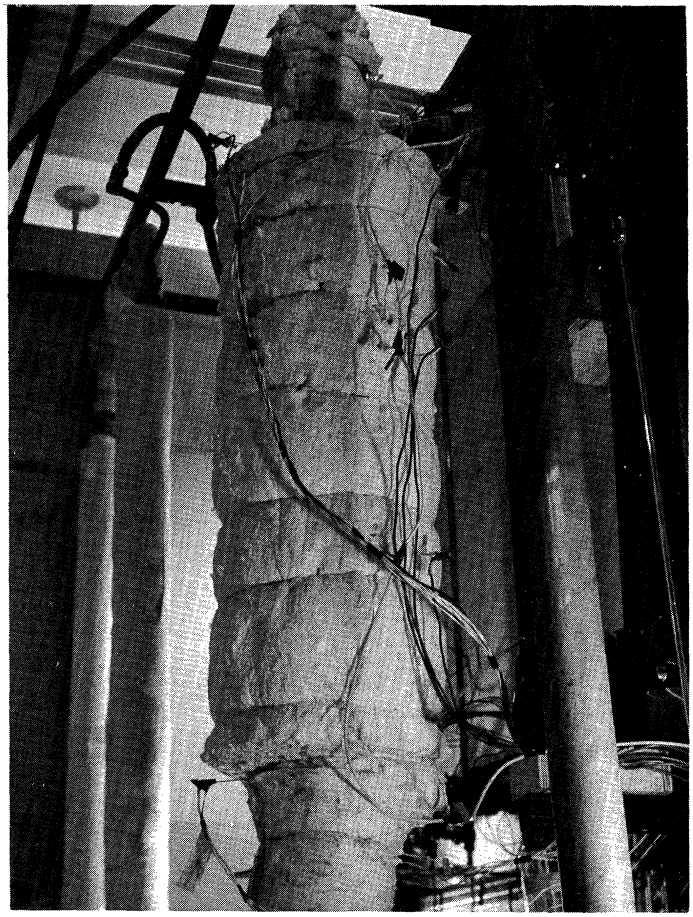

Figure 1. Insulated test section in loop.

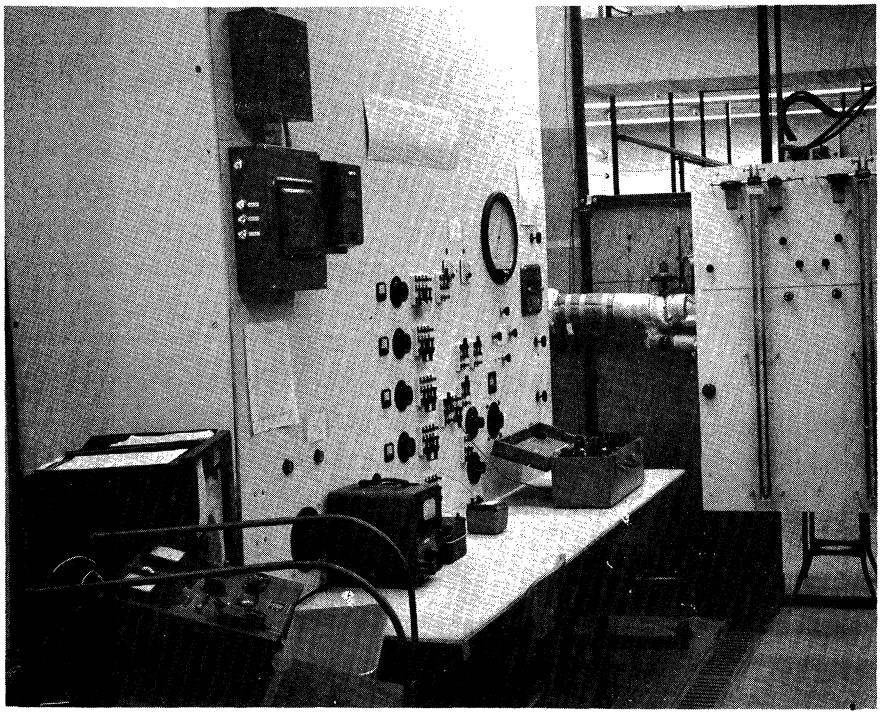

Figure 2. Loop operating panel and flow meter manometers.

TABLE I

LOOP COMPONENTS

Item	Description
1	Filter separator
2	Condensate drain line
3	Steam superheater
4	Steam pressure regulator
5	Nitrogen pressure regulator
6	Six bottles dry nitrogen. Manifold with station valves
7	By-pass to drain
8	By-pass for pressure control valve
9	Pressure control valve, 1/4"-Trim G
10	Pneumatic controller
11	Orifice flow meter
12	Water cooler for horizontal orifice pressure tap lines
13	Two parallel flow rate manometers
14	Precooler
15	Electrical insulation gland
16	Preheater
17	Electrical insulation gland
18	Mixing chamber for inlet fluid thermocouple
19	Flow development section
20	Test section pressure tap (at inlet)
21	Test section
22	Mixing chamber for exit fluid thermocouple
23	Exit cooler
24	Flow control valve, 1/4"-Trim I
25	Flow control valve, 1/2"-Trim A
26	Exhaust manifold and vent to ambient
27	Air filter regulator
28	Pressure gauge

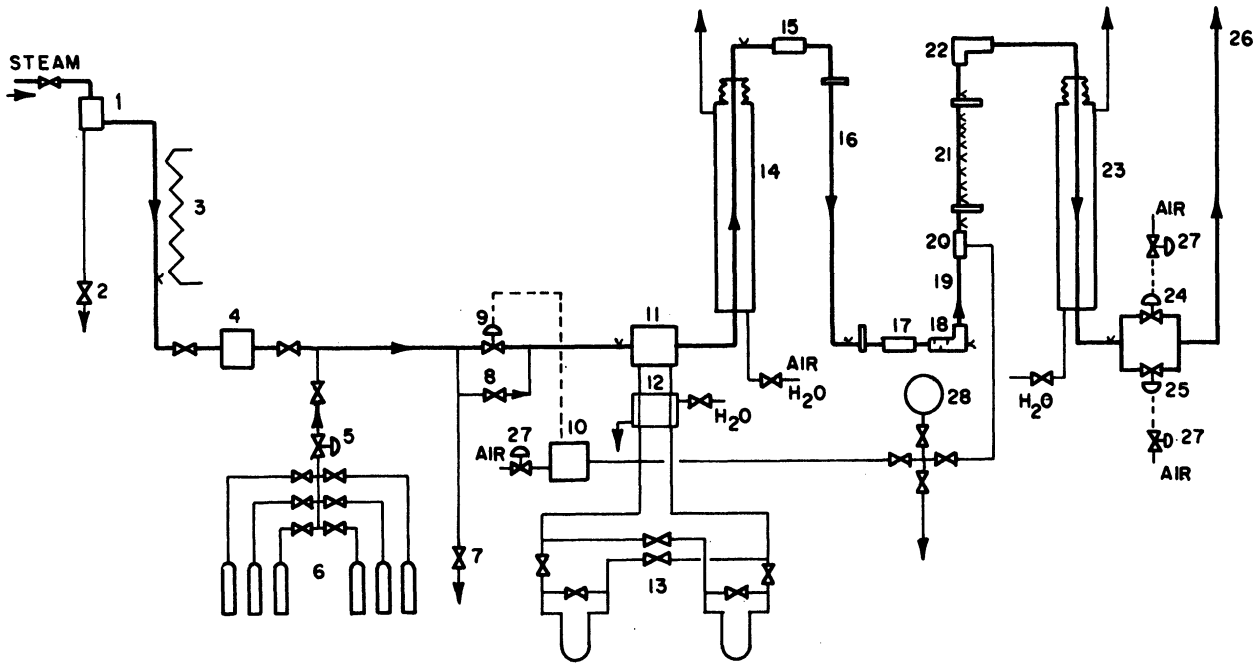

Figure 3. Open loop flow diagram (see Table I for component list).

section length the test section is preceded by a 30-in. long flow development section. The use of a Swagelok union (20) joining smoothly the test section tubing to that of the development section, both of same inside diameter, provides effectively a 68 L/D unheated flow development section. To not disturb the velocity profile fluid temperature is measured upstream of the flow development section at the mixing chamber (18). The purpose of the exit cooler is to protect flow control valves (24) and (25) against temperature levels in excess of their design limit of about 700°F and furthermore to reduce the specific volume of the fluid at the flow control valves thereby reducing the required control range.

The general design conditions for the loop are as follows:

Fluid:	Saturated/superheated steam, bottled gas
Pressure:	25-75 psia
Flow Rate:	5-50 lbm/hr
TS Inlet Temperature:	Saturation to 1100°F (steam)
	Ambient to 1100°F (gas)

In the following sections the individual loop components are described in detail.

2.2.2. Loop Component Description

2.2.2.1. Steam supply. The shop steam is provided by two oil fired boilers supplying respectively 6 x 10^6 and 10 x 10^6 Btu/hr saturated steam at 130 psig, nominal. The feed water is treated with sodium sulfide to scavenge dissolved oxygen, hence the oxygen content of the steam is estimated to be less than about 8 ppm based on the air solubility in water at 70°F of 33 ml air per liter water. Steam is supplied to the loop area in insulated black iron piping and arrives with a considerable moisture content. The inlet portion of the loop up to the flow control valve is constructed from 3/4 in. and 1/2 in. black iron pipe, schedule 40 in standard fiberglass insulation and comprises: filter separator (1) (Adams TR-AC Poro-Carbon filter, 1/2 in. line) drained through a long uninsulated line (2) of 1/4 in. copper tubing, serving effectively as air-cooled condenser and cooler for the separated moisture-steam mixture. Steam superheater (3), which consists of a 10-ft length of 3/4 in. black iron pipe, wrapped with 3 pc. 786 watt 1 in. by 96 in. heating tape (Briskeat, BIH-81, 115v) and insulated outside, a capped 1/4 in. black pipe is placed inside the 5-ft long vertical run of this superheater to enhance heat transfer and ensure that wall temperatures do not exceed about 900°F, particularly at low flow rates. The three heating tapes are connected in parallel and supplied with power from a manually operated autotransformer (Variac, W102G) adjusted to maintain about 400°F steam temperature at the orifice flow meter. At low test section flow rates this may be achieved only by by-passing a portion of the steam supply through the superheater to the drain (7) to avoid overheating of the superheater. Pressure reducing and regulating valve (4) (Macarco, No. 4674M, 1/2 in., iron body, bronze trim) is preset to reduce and control the periodically changing steam supply pressure, ranging from about 120 to 135 psig, to about 80 psig for added loop stability. In addition the steam supply line is equipped with standard brass body shut-off gate valves.

2.2.2.2. Nitrogen gas supply. Extra dry nitrogen (less than 0.01% moisture) from up to six 214 scft bottles, joined through a manifold with station valves (6) (Matheson, six station double row with No. 580 fittings and bushing valves) is supplied through pressure regulator (5) and shut-off valve to the loop pressure control valve. In usual operation all bottles are open to provide a large supply reservoir.

2.2.2.3. Loop piping. The loop piping from pressure control valve (7) to exit mixing chamber (22) is constructed from standard 5/8 in. O.D., gauge 16 (1/2 in. I.D.) stainless steel tubing joined with type 316 stainless steel Swagelok fittings or welding. The section through precooler (14) up to first electrical insulating gland (15) is type 304 while the remaining section is type 310. These sections are insulated with respectively standard glass fibre insulation and special high temperature insulation (Babcock and Wilcox Kaowool Ceramic fiber, 3/4 in. thick blanket: 6 lb/cu ft, 1 $in.^2$ strip, 8 lb/cu ft). The loop piping from exit mixing chamber to exhaust manifold is uninsulated and

is constructed from type 304 stainless steel 1 in. O.D., gauge 16 tubing, joined with Swagelok fittings or welded.

2.2.2.4. Control valves. Test section pressure and flow rate is set and controlled by the inlet pressure control valve (9), 1/4 in. Trim G, fail closed, and either one or both of the flow control valves (24), 1/4 in. Trim I, or (25), 1/2 in. Trim A, both fail open, having the following common specifications: Research Control Type 78S, diaphragm control valve, SS-316 globe style body with linear inner valve.

The pressure control valve (9) is automatically controlled by the pneumatic controller (10) (Sivalls and Bryson, Type 72-14-1, SS-316 Bourdon tube, proportional band) according to the pressure sensed at the inlet to the flow meter. The two flow control valves (24) and (25) are remotely set by use of manually operated air filter regulators (27) (Sivall and Bryson, Type 73-26-1) functioning as pneumatic loaders for the valves. A by-pass (8) for the pressure control valve is used at high flow rates and high pressure to maintain control.

2.2.2.5. Precooler and exit cooler. These single pass concentric tube heat exchangers are each constructed from type 304 stainless steel. A 65-in. long, 2-1/2 in. O.D., gauge 16 tubing forms the shell side, while a 75-in. long, 5/8 in. O.D., gauge 16 tubing forms the tube side. The upper end of the shell is joined through a plate to a type 304 stainless steel bellows which in turn joins to the upper end plate. Upper and lower end plates are welded to the inner tube. All other joints are silver soldered. Coolant (air or water) is supplied in 1/4 in. tubing through the lower end plate and vented through 1 in. tube from the side of the shell near its upper end. The shell side is equipped with a sight tube for manual control of water level in the cooler. In most cases, it was found to be unnecessary to operate the precooler. For near saturated test section inlet conditions it was operated on air. The exit cooler was operated on water, adjusting manually the water level (usually 4-6 in.) so as to maintain a temperature less than 750°F as measured on a wall thermocouple attached to the loop piping upstream of the tee branching for the flow control valves. Excessive cooling at the exit gave rise to condensation, two-phase flow, and loop instability.

2.2.2.6. Preheater. The preheater (16) consists of a 10.25-ft length of type 310 stainless steel loop piping (5/8 in. O.D., gauge 16 tubing) heated electrically by passing a DC current through its wall between two 1/4 in. thick by 1-3/4 in. x 8 in. power lugs welded to the tube. The power source is a 50 kw DC (2000 amp and 25v) germanium rectifier.

2.2.2.7. Test section power supply. The test section is heated electrically by passing an AC current through its wall between two lugs. A 115v/12v AC transformer (Westinghouse S10n05S07D, 7.5 kVA) controlled manually by an autotransformer (3 gang VARIAC W20 G3 with 50P-1 and 50P-2 chokes) serves as power supply.

2.2.2.8. Electrical insulation of loop sections. The loop upstream of preheater and downstream of test section, hence test section exit power lug, is electrically grounded. The preheater is isolated from loop and ground by two electrical insulating glands (15) and (17) (constructed by slight modification of Conax electrical conducting scaling gland, EG-500-A, without conductor, 0.500 in., Lava seal).

2.2.2.9. Mixing chamber for fluid thermocouples. To ensure accurate measurement of mixed mean fluid temperatures up- and downstream of test section two mixing chambers with radiation shields (18) and (22) were constructed from type 304 stainless steel tubing and Swagelok components. The 1/8 in. sheathed and grounded chromel-alumel thermocouple, sealed through a Conax gland with Lava seal, is positioned concentrically in a 1 in. O.D. tube downstream of four perforated plate baffles and surrounded by a long spiral wound 0.015 in. thick plate, effectively providing three concentric radiation shields, since conduction in the shield is small compared to fluid convection.

2.2.2.10. Flow meter. A small size square edge orifice flow meter (11) was constructed from a standard 5/8 in. Swagelok bulk head union and placed in the loop downstream of a 1-in. long straight section. The orifice plate (0.625 in. O.D., 0.212 in. I.D. by 0.100 in. thick) was silver soldered in place to prevent leakage. Pressure tap holes of 1/16 in. were placed one diameter upstream and one-half diameter downstream of the orifice plate. Two uninsulated 12-in. long, 1/4 in. tubing pressure taps, welded to the bulk head union, extend to one side in the horizontal plane. The 1/4 in. copper tubing pressure lines leading to the manometers continue in the same horizontal plane through a 10-in. long water cooled jacket (12) before changing elevation. When operating on steam this arrangement ensures that the liquid meniscus in both pressure lines is at the same elevation. Flow meter pressure drop is read on either or both of two 50-in. parallel connected U-tube manometers (Merriam, model 10AA-WM25) equipped with traps and bleed lines. The flow meter in place in up- and downstream loop piping sections was calibrated on tap water measuring flow rates by stopwatch and weighing tank.

2.2.3. Loop Instrumentation

2.2.3.1. Pressure. Test section inlet pressure and pressure at the upstream flow meter pressure tap is measured with a bourdon tube precision gauge (28) (Heise, H42041, 0-100 psig, 12 in.) corrected for hydrostatic pressure difference between pressure tap and gauge positions when operating on steam. Absolute pressure is obtained by adding atmospheric pressure read on a precision barometer corrected for elevation and thermal expansion. The uncertainty on absolute pressure is estimated to be less than ± 0.5 psi.

2.2.3.2. Flow. The test section flow rate is calculated from

$$\dot{m} = CA_2 Y\sqrt{2\rho_1(\rho_m - \rho_{1m})\Delta h} \qquad (2\text{-}1)$$

where

$\dot{m}$	mass flow rate
$C = C_d/\sqrt{1 - \beta^4}$	orifice discharge coefficient
$\beta = D_2/D_1$	diameter ratio
D_1	tube I.D., 0.500 in.
D_2	orifice I.D., 0.2125 in.
$A_2 = \pi D_2^2/4$	orifice flow area
ρ_1	fluid density upstream of orifice
ρ_m	manometer fluid density
ρ_{1m}	density of fluid superposed manometer fluid
Δh	manometer deflection
Y	compressibility factor

The compressibility factor, Y, is a function of pressure ratio across the orifice, P_2/P_1, the isentropic exponent, k, and the geometry

$$Y = \sqrt{\frac{\frac{k}{k-1}(p_2/p_1)^{2/k}\left[1 - (p_2/p_1)^{(k-1)/k}\right]}{1 - p_2/p_1}}\sqrt{\frac{1 - \beta^4}{1 - \beta^4(p_2/p_1)^{2/k}}} \qquad (2\text{-}2)$$

Orifice calibration using water yielding a discharge coefficient of

$$C_D = \begin{cases} 0.6604 \pm 0.4\%; & 5000 < Re < 20{,}000 \\ 0.6604 + 0.0888 \log\left(\frac{5000}{Re}\right); & 1000 < Re \leq 5000 \end{cases} \qquad (2\text{-}3)$$

The discharge coefficient is evaluated on the basis of the upstream Reynolds number, $Re_1 = 4\dot{m}/(\pi\mu_1 D_1)$. The fluid density upstream of the orifice plate, ρ_1, is evaluated from the equation of state of the fluid based on measured absolute pressure and temperature at that point. The orifice pressure drop is read from either of two 50-in. U-tube manometers, using mercury, s.g. oil 2 or s.g. oil 1.25. For the case of steam water at room temperature was superposed on the manometer fluid.

2.2.3.3. Fluid temperatures. Mixed mean fluid temperatures are measured at mixing chambers (18) and (22) with radiation shielded, ungrounded, 1/8 in. sheathed chromel-alumel thermocouples (Conax, Type INC 12K-U-T4-MPG125AL-12 in.). Radiation correction is negligible but correction according to calibration is made. Each of the thermocouple leads is soft soldered to shielded copper extension leads, the junctions being kept at the ice point. Copper extension leads are connected to knife switches for selection of strip chart recorder or manual read-out on precision portable potentiometer (Leeds and Northrup Model 8662) or digital voltmeter (Hewlet-Packard, 3444A). Thermocouple readings are corrected according to calibration but no conduction or radiation correction is made.

2.2.3.4. Test section power. Test section power is made directly with a special order precision watt meter indicating true RMS power (Sensitive Research Instruments, University Model, full scale ranges, 18.75, 37.5, 75 watts; 7.5- and 15-v input; 2.5- and 5-amp input; 0.75% accuracy at full scale) used with one or four primary windings on a 100:1 current transformer (Weston, 641 Type 5, 0.2% accuracy). A total of four different range combinations is used for maximum accuracy as follows:

Test Section Power (kw)	Scale	Coupling	Primary Windings
0.094 - 0.380	low	series	4
0.375 - 1.250	low	series	1
0.750 - 2.500	middle	parallel	1
2.000 - 7.500	high	parallel	1

2.2.3.5. Auxiliary instrumentation. For safety and purpose of steady state loop operation temperatures are measured at: superheater exit (not to exceed 900°F), flow meter inlet (to exceed about 100°F superheat), precooler

exit and flow control valve inlet (not to exceed 700°F). Thermocouples measuring the outisde wall temperature at respectively the preheater exit and the test section hot spot are each connected to a meter relay (Assembly Products, Model 351-C, adjustable upper limit set point 0-2500°F for C-A thermocouple). When the maximum temperature set-points are exceeded or when pressure control valve is closed power to preheater and test section is automatically cut off. Loop temperatures as well as selected test section temperatures are recorded on a 24-point strip chart recorder. This record serves to help attain steady loop operation.

2.3. TEST SECTIONS

The test sections employed in the experiment have the same geometry, comprising a 44-in. long by 0.5-in. I.D. tube joined to the loop by Swagelok unions. The heated length between (12 in. x 1-1/2 in. x 3/8 in., type 304 stainless steel) power lugs, heliarc welded to the tube wall, is 36 in. (see Figure 4). Wall thermocouple attachment and guard heater arrangement is the same for all test sections. The test sections differ in wall material (SS-310 and Zr-2) and in heat flux distribution according to the outside diameter variation.

2.3.1. Uniform Flux Test Sections

One test section was fabricated from type 310 stainless steel tubing (5/8 in. O.D., 16-gauge, seamless, annealed temper), another from Zr-2 tubing. To heliarc weld SS-304 power lugs to the Zr-2 tubing a silicon-bronze filler rod was used. Because of the smaller outside diameter of the Zr-2 tubing 2-1/2 in. long by 0.625 in. O.D., SS-310 sleeves were press-fit and seal welded at each end of the test section to facilitate the use of standard 5/8 in. Swagelok unions as for the SS-310 test sections. Type 310 stainless steel was chosen because its creep and oxidation properties at temperatures up to 2000°F are superior to those of 18-8 steels.

Actual dimensions of the tubing as received are:

	I.D. (in.)	O.D. (in.)
SS-310	0.498	0.627
Zr-2	0.499	0.572

The axial position of 14 wall thermocouple stations for the uniform flux test sections, measured from the inlet to the heated test section, are listed below:

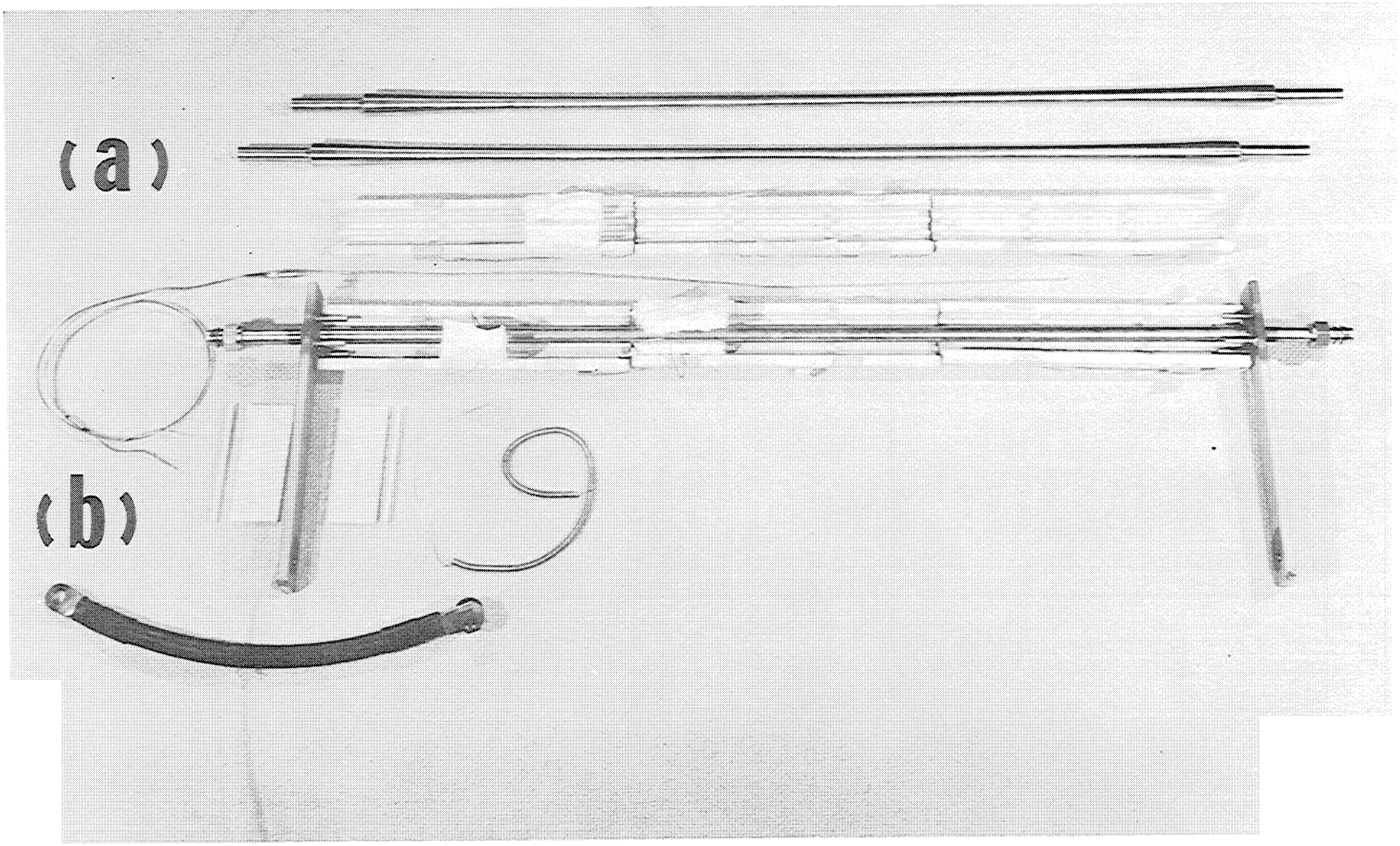

Figure 4. (a) Nonuniform flux test sections without power lugs. (b) Uniform flux test sections with power lugs, guard heaters before assembly.

TC Station	x ± 0.1 (in.)	z = (x/D)
1	-2.12	-4.26
2	0.50	1.00
3	1.75	3.51
4	3.75	7.51
5	6.0	12.02
6	9.0	18.03
7	13.0	26.05
8	18.0	36.10
9	23.0	46.10
10	27.0	54.20
11	30.0	60.20
12	33.0	66.20
13	35.50	71.20
14	38.0	76.40

2.3.2. Nonuniform Flux Test Section

Two identical test sections (Figure 4) were fabricated from type 310 stainless steel (1-1/4 in. O.D. by 4 ft long, round stock, annealed temper) by gun drilling and subsequent lathe machining of the outside diameter to a number of prescribed tapered sections, leaving a wall area variation which for constant electrical current and resistivity approximates the modified cosine heat flux distribution given by

$$q''(x)/q''_{max} = \frac{A_{w,min}}{A_w(x)} = 0.46 \cos\left(2.76 \frac{2x - L}{L}\right) + 0.54 \qquad (2\text{-}4)$$

$$q''_{max}/q_{mean} = 1.66$$

$$q''_{max}/q_{min} = 8.70$$

One test section was employed in the study, the other being a reserve. Table II summarizes the dimensions and axial thermocouple positions for the test section, where AW denotes the wall area divided by the tube I.D.,

$$AW = \frac{\pi}{4 \times 12} [(O.D./I.D.)^2 - 1] \quad . \qquad (2\text{-}5)$$

TABLE II

NONUNIFORM FLUX SS-310 TEST SECTION DIMENSIONS
AND THERMOCOUPLE STATIONS

D = 0.501 ± 0.0005 in.

Thermocouple Station	Axial Position from Inlet x(in.)	$z = x/D_i$	Measured OD* D_o(in.)	AW(x) (ft.in.)	$\frac{q(x)}{q_{max}}$
1	-2.25	-4.24	0.634	0.039	--
	0	0	(1.000)	--	--
2	1	1.99	0.912	0.1514	0.152
	2	--	(0.8182)	0.09108	(0.211)
3	3	5.99	0.7748	0.05626	0.253
	5	--	(0.6832)		(0.410)
4	6	11.98	0.6701	0.05164	0.447
5	9	17.96	0.6218	0.03537	0.652
6	12	23.95	0.5970	0.02748	0.839
7	15	29.94	0.5866	0.02426	0.951
8	18	35.93	0.5826	0.02306	1.000
9	21	41.92	0.5866	0.02426	0.951
10	24	47.90	0.5970	0.02748	0.839
11	27	53.89	0.6218	0.03537	0.652
12	30	59.88	0.6701	0.05164	0.447
13	33	65.87	0.7748	0.05626	0.253
	36	71.856	(1.000)	0.09108	--
14	37.9	75.80	0.634	0.039	--

*Assuming symmetry, mean value is used.

Equation (2-4) together with $q(x)/q_{max}$ of Table II, based on measured area variation, is compared in Section 4.3.3, Figure 17, to the heat flux distribution under experimental conditions of nonuniform temperature.

2.3.3. Wall Thermocouples

Outside wall temperature is measured with 1/16 in. O.D. sheathed and ungrounded thermocouples (Thermoelectric, CES-10-116-K, SS-310 sheath, chromel-alumel) wrapped 180° around the tube and held in position by two 0.1-in. wide by 0.0035-in. thick Nichrome straps, spot welded to the outside tube wall (Figure 5). The thermocouple attachment zone is covered with a layer of ceramic cement (Aremco Products, Ceramacoat 512) for addition strength (Figure 6).

A sample of 5 thermocouples were calibrated at melting points of zinc, aluminum, and copper. Based on comparison with standard tables a deviation

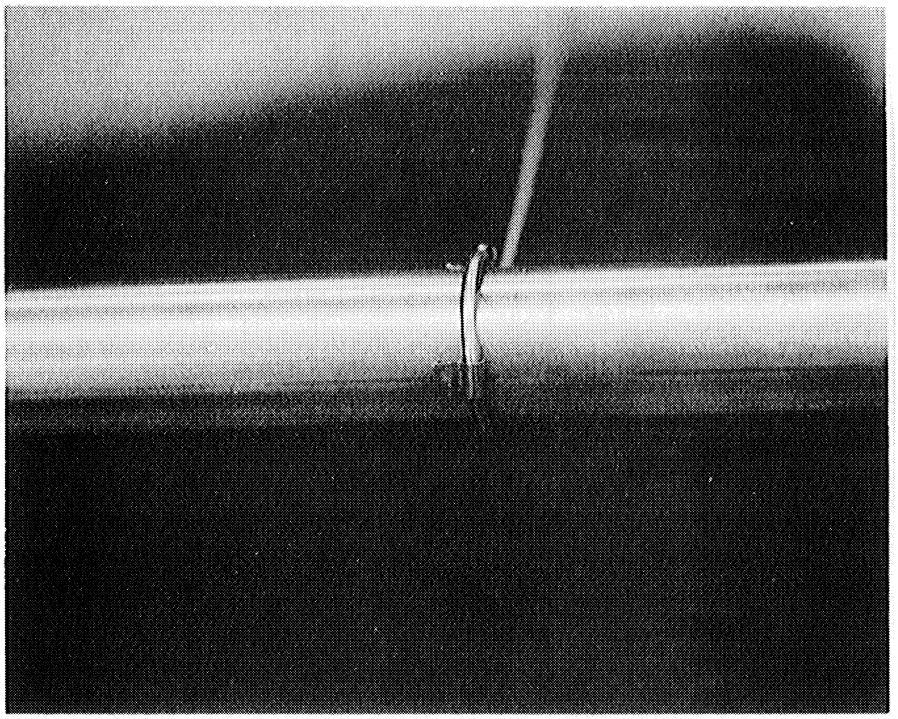

Figure 5. Sheathed thermocouple (1/16 in. O.D.) attachment with spot welded straps.

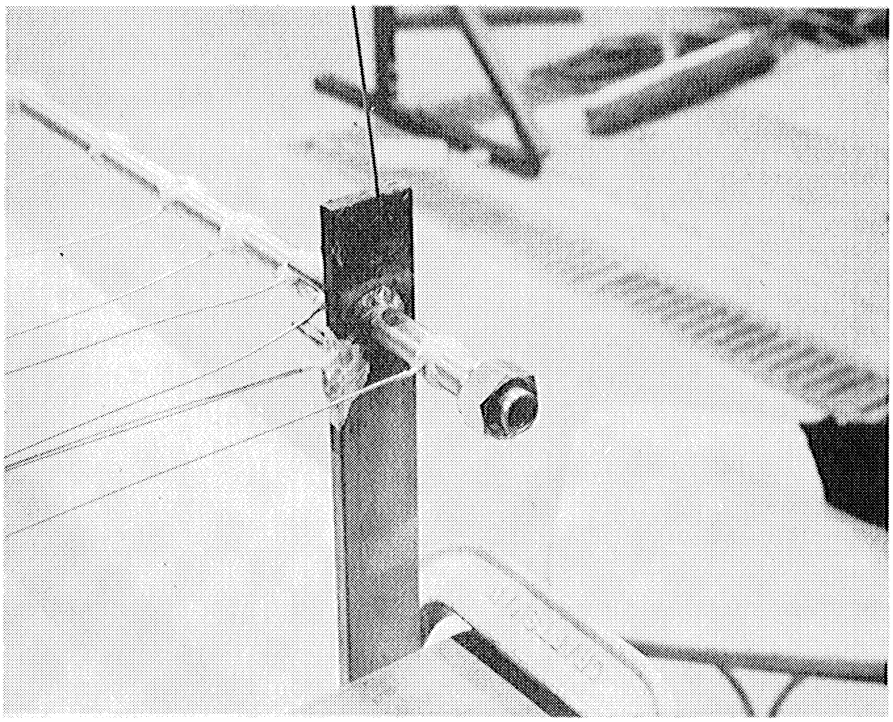

Figure 6. Uniform flux test section. Thermocouples covered with ceramic cement.

curve was constructed. Corrections are made in the data reduction program as described in Appendix A.

Thermocouple extension leads of chromel-alumel are soft soldered to copper extension leads, these junctions being kept at the ice point. All leads are shielded electrically and only pure copper switches are employed.

2.3.4. Guard Heaters

To minimize ambient heat transfer from the heated test section the 36-in. tube length is wrapped with about 1/2-in. thick layer of high temperature insulation (Kaowool) and enclosed by three guard heater sections each comprising two half-cylindrical shells (Linberg, Hevi-Duty, Model 50132, type 1712-KSP, 115v AC, 670 watt, 12-in. long by 2-5/8 in. O.D., and 1-3/4 in. I.D.) (see Figure 4). This assembly is surrounded by six layers of high temperature insulation (Kaowool), yielding a total outside diameter of about 12 in. (see Figure 1). The power to each of the three guard heaters is separately controlled by a transformer (Variac, type W5, 0.94 kVA), manually adjusted to zero the temperature difference between the wall thermocouple at the guard heater midpoint and another thermocouple located between insulation and guard heater inner wall at the same axial position. This arrangement attempts to establish three isothermal zones along the test section. However, the test section wall temperature varies axially and some heat transfer to and from the test section will occur. This correction, being small, is incorporated in the data reduction program (Appendix A).

To reduce conductive heat transfer along the power lugs these are also guard heated. The lug is covered with a 1/8-in. thick insulation sleeve (Lava) which in turn is wound with resistance wire covered with ceramic cement and insulation. The power to inlet and exit lug guard heater is individually controlled by a transformer (Variac, type W5, 0.94 kVA), manually adjusted to zero the temperature difference between two thermocouples imbedded in the center of the lug, respectively 1-1/2 in. and 2 in. from the tube centerline.

2.4. EXPERIMENTAL PROGRAM

The experimental study involved a dummy test section for shake down and three fully instrumented test sections providing data, as summarized in Table III. The first uniformly heated SS-310 test section was equipped with only one set of guard heaters and only partially instrumented. It served as a dummy test section for loop shake-down, design check and for providing SS-310 surface samples exposed to either steam or both steam and then nitrogen at elevated temperatures for surface emissivity measurements (see Appendix D).

After approximately 50 hr of operation on steam at wall temperatures ranging from 300°F to 1500°F this test section was removed and a 4-in. sample

TABLE III

EXPERIMENTAL SERIES

TS	Material	Flux	Fluid	Purpose	No. of Runs
1	SS-310	Uniform	N_2, steam	Shake-down/samples	--
2	SS-310	Uniform	N_2, steam	Basic data	93
3	Zr-2	Uniform	Steam	Check data/samples	22
4	SS-310	Nonuniform	Steam	Check data	9

was cut near the downstream heated end. A copper lug was brazed to the test section which was subsequently operated on nitrogen for 7 hr at temperatures ranging to 1100°F. The downstream end of the heated length was cut to provide a surface sample having been exposed to both steam and nitrogen at elevated temperatures. A third sample cut from the uniform SS-310 tubing as received serves as reference. The second uniformly heated SS-310 test section was fully instrumented and provided basic data for both steam and nitrogen for direct comparison of the effect of wall to gas radiative transfer. The purpose of the third test section, uniformly heated Zr-2, was to provide steam data for a different surface material. The fourth test section, having a chopped cosine heat flux distribution, was designed to illustrate the proper interpretation and application of uniform heat flux data to predict heat transfer under conditions of variable axial heat flux distribution.

At the beginning of each test series several heat balance runs were made to check instrumentation and evaluate ambient heat transfer. Wall thermocouple readings were frequently checked against saturation temperatures in the pressure range of 25-75 psia by maintaining saturated loop conditions. Low temperature in-place calibration of this kind indicated deviations less than 1°F.

One test section failure occurred during the last run (123) planned for the Zr-2 test section.

The failed test section after removal of instrumentation is shown in Figure 7. Fracture occurred about 2-1/2 in. from the exit of the heated section, originally 36-in. long but elongated about 3/4 in. during failure. The dimensions of the tube and locations of samples D, E, and F cut for inside surface emissivity measurements are shown in Figure 8. The sample cut from the tubing as received is denoted G. Figure 8 also shows the outside wall temperature distribution typical of a run from the second series of tests where maximum wall temperature was limited to 1400°F.

The outside surface had a black appearance over the upstream half of the heated length. From the mid-point a light-brown layer of oxide of increasing thickness extended downstream. The failure area showed considerably increased diameter due to flaring which cracked the oxide layer in this region. The in-

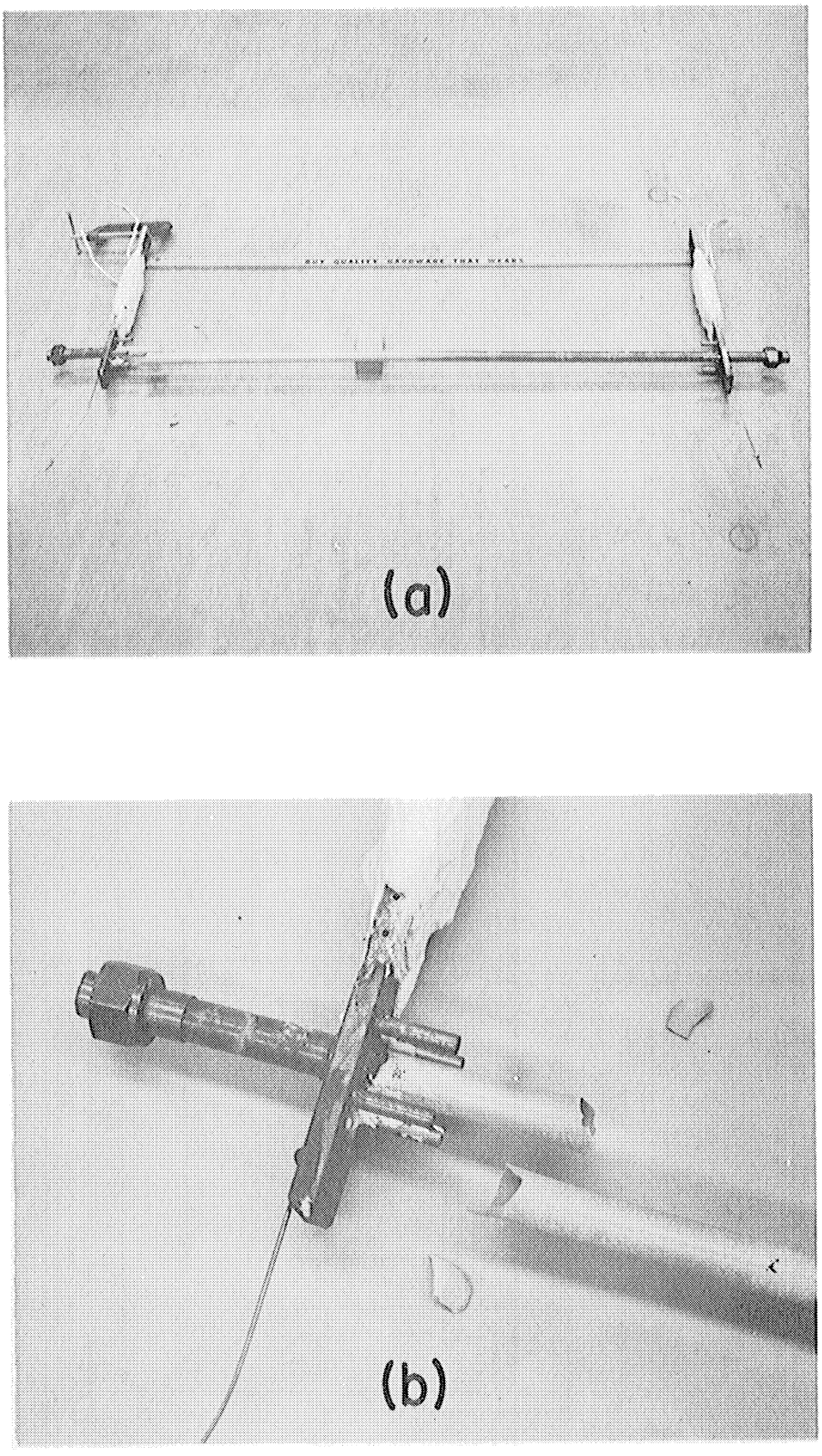

Figure 7. Failed Zr-2 test section. (a) Inlet shown to the right. (b) Close-up of exit section.

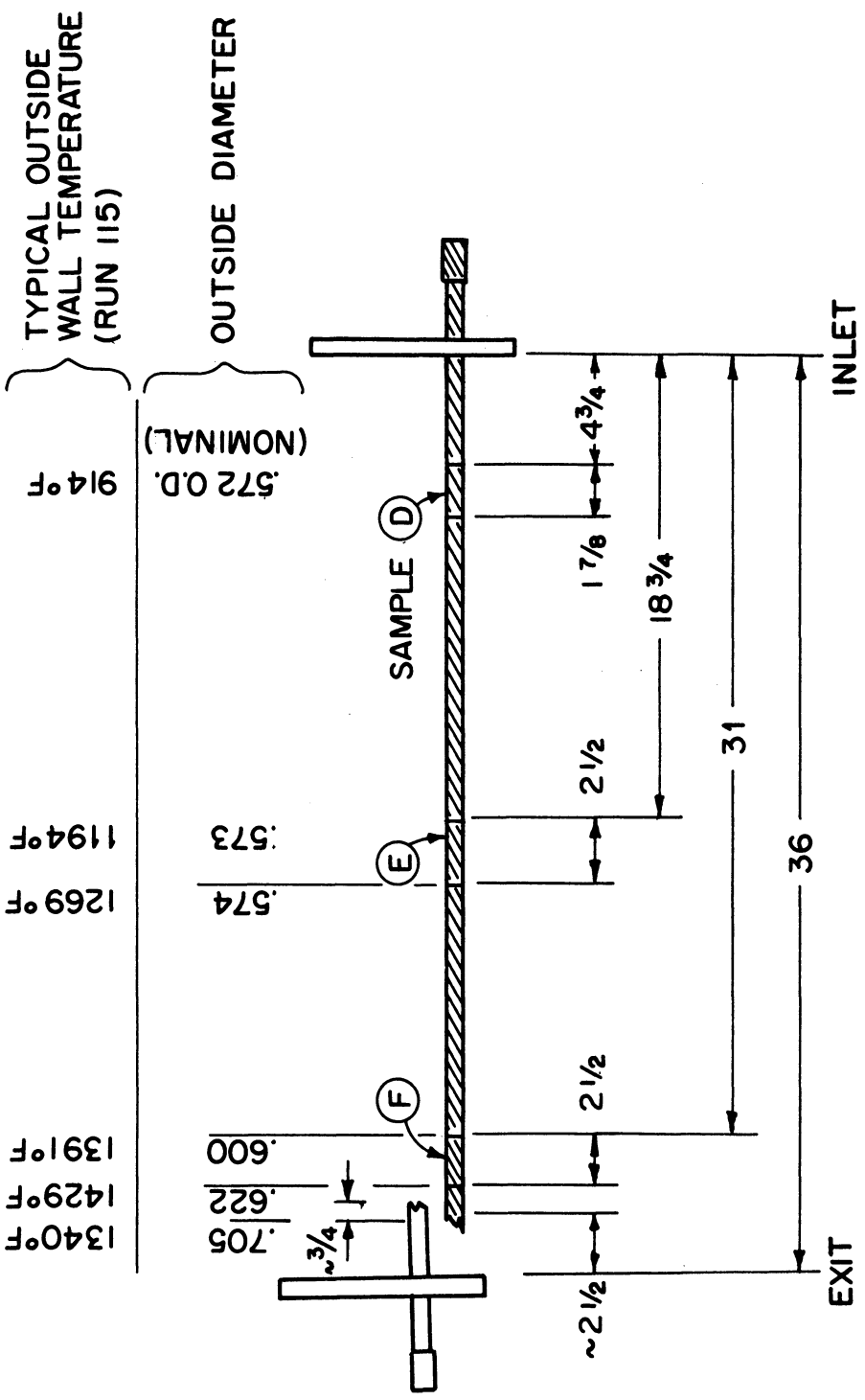

Figure 8. Failed Zr-2 test section dimensions and sample locations.

side surface had a uniform shiney, apparently thin layer of light-brown oxide. Failure is believed to have been caused by excessive oxidation of outside surface exposed to air, particularly during second sequence of runs performed at temperatures to 1400°F. The reduction of metal wall thickness, thermal cycling, and axial load of test section, guard heaters, insulation, and in part, the horizontal run of the preheater ultimately caused failure. The internal pressure (50 psia) caused some flaring at ultimate failure.

The experiments with the Zr-2 test section were such that the average operating time per run was approximately 4 hr. The conditions were as follows:

Run	Avg. Temp.	Max. Temp.	Time (hr)
101-104	400-700°F	400-800°F	20
105-114	~ 700°F	900°F	40
115-122	~ 1100°F	1400°F	30

3. ANALYSIS

3.1. INTRODUCTION

For the present study the experimental data obtained for the total heat transfer by convection and radiation from a point of the tube wall to the gas is analyzed in terms of a superposition model whenever the flow is turbulent. The basic assumption is that convective and radiative heat transfer each may be determined separately given the bulk properties of the gas and wall temperature and emissivity. The validity of this approach rests on the assumption that the radiative transfer merely changes the level of the gas temperature but does not alter its distribution. This assumption is reasonable for fully developed turbulent flow of a gas of moderate optical thickness but is expected to become increasing less valid as the Reynolds number decreases and the optical thickness increases. Specifically, for laminar flow of a gas of intermediate to large optical thickness absorption of radiant energy from the wall will tend to raise the gas temperature in particular adjacent to the wall, hence alter the temperature distribution to reduce the convective heat transfer as compared to that of a transparent gas. Thermal radiation from wall to gas thus tends to insulate the wall from a convection view point and laminar convective heat transfer to an absorbing and emitting gas will be less than that to a transparent gas. The total heat transfer, however, will always exceed that of the transparent gas case.

The case of radiation-convection interaction for laminar flow will be treated in detail in a separate report.[15] In the following discussion of turbulent flow superposition is assumed to be valid,

$$Nu^{T} = Nu^{c} + Nu^{R} \quad . \tag{3-1}$$

The separate evaluation of each term in Eq. (3-1) is next examined for conditions where laminarization does not take place.

3.2. CONVECTIVE HEAT TRANSFER UNIFORM FLUX

Based on the comparison in section 4.2 of five existing correlations to the fully turbulent data obtained with nitrogen (which can be considered to be a transparent gas) the McEligot correlation[4]

$$Nu_b = 0.021\ Re_b^{0.8} Pr_b^{0.4} (T_w/T_b)^{-0.5} [1+(x/D)^{-0.7}] \tag{3-2}$$

$$x/D > 5;\ Re_b > 6000,\ T_w/T_b < 2.5$$

is found to be best suited for the parameter range of the present study. The correlation assumes that a fully developed turbulent velocity profile exists at the inlet to the uniformly heated section. Given axial position, local gas bulk properties, wall and gas bulk temperature the heat transfer coefficient for convection may be evaluated explicitly from Eq. (3-2).

3.3. CONVECTIVE HEAT TRANSFER NONUNIFORM FLUX

Forced convection heat transfer data for duct flow are generally obtained for either constant wall temperature or constant wall heat flux, the latter being the more common. Although less important for turbulent than for laminar flows experimental data should be qualified in regard to the actual boundary condition. If neither of these classical boundary conditions were actually maintained it would be desirable to appropriately correct data to a common base, in the present study to that of constant heat flux.

For fully developed constant property flow a condition of fully developed heat transfer (constant heat transfer coefficient) results downstream of the entrance region for only three boundary conditions, constant wall temperature, constant heat flux and exponentially varying heat flux along the duct. For any other boundary condition and in all cases of variable properties no condition of fully developed heat transfer exists. The appropriate analytical solution to this class of problems based on developing two-dimensional flow with property dependent eddy diffusivity expression is very complex but has revealed that quasi-developed analysis is inadequate. Nevertheless, data for constant heat flux variable property transparent gases correlate well with a Dittus-Boelter type relation such as Eq. (3-2). This correlation suggests that results are well approximated downstream by a temperature ratio corrected quasi-developed flow. The relatively simple correction factor for the entrance effect represents a reasonable approximation only, as evident from comparison with the exact series solution for the constant property case.[3]

As well-known, the solution to a problem having an arbitrarily prescribed varying boundary condition may readily be obtained from the same problem subject to a constant boundary condition by the use of the Duhamel superposition integral, provided the problem is linear. For example, in case of the constant property fully developed laminar or turbulent duct flow the resulting local heat transfer for an arbitrary heat flux

$$q = \begin{cases} 0 & x < 0 \\ q(x) & x \geq 0 \end{cases} \qquad (3\text{-}3$$

has the solution

$$h(x) = q(x)/\theta(x) \qquad (3\text{-}4)$$

$$\theta(x) = T_w - T_b = q(0)\phi(x) + \int_o^x \frac{dq(x')}{dx'}\,\phi(x-x')dx' \tag{3-5}$$

where

$$\phi(x) = 1/h_u(x) \tag{3-6}$$

represents the solution for the wall-to-bulk temperature difference for the same problem for the case of a unit constant heat flux

$$q_u = \begin{cases} 0 & x < 0 \\ 1 & x \geq 0 \end{cases} \tag{3-7}$$

This procedure does not formally apply to cases where variable property effects are significant because of the nonlinear nature of such problems. However, experience from variable property convection[6] suggests that reasonably satisfactory results may nevertheless be obtained by superposition. The validity of the procedure will be examined in the present study. Both the uniform flux data and the chopped cosine flux data will be reduced to the common base of uniform flux results following the scheme outlined below.

Since the constant flux solution $\phi(x)$ is presently not known a priori, but rather $\theta(x)$ and $q(x)$ have been determined experimentally it is necessary to solve the integral equation, Eq. (3-5), for $\phi(x)$. This is accomplished by successive approximation through the following iterative procedure. The first trial function, $\phi_o(x)$, for $\phi(x)$ may, for example, be obtained by assuming the heat flux is constant, hence ignoring the integral of Eq. (3-5). Using this solution in the convolution integral of Eq. (3-5) an improved solution $\phi_1(x)$ may be evaluated, and so on. The iteration may be summarized as follows

$$\begin{aligned} \phi_o(x) &= \theta(x)/q(x) \\ \phi_1(x) &= [\theta(x) - \int_o^x \frac{dq(x')}{dx'}\,\phi_o(x-x')dx']/q(0) \\ &\vdots \\ \phi_m(x) &= [\theta(x) - \int_o^x \frac{dq(x')}{dx'}\,\phi_{m-1}(x-x')dx']/q(0) \end{aligned} \tag{3-8}$$

In finite difference form Eq. (3-8) is written at the r-th of $N = L/\Delta x$ points along the heated length as follows

$$\phi_m(x_r) = [\theta(x_r) - \sum_{i=1}^{r} [q(x_i) - q(x_{i-1})]\phi(x_{r-i+1})]/q(0) \tag{3-9}$$

This form requires that $q(0)$ be known, while the singularity associated with

$\phi(0)$ and $\theta(0)$ is avoided.

The criterion for termination of the iteration according to Eq. (3-8) has arbitrarily been chosen as an acceptable small RMS deviation between successive results

$$\left[\frac{\sum_{r=1}^{N}\left|\frac{\phi_m(x_r)-\phi_{m-1}(x_r)}{\phi_m(x_r)}\right|^2}{N-1}\right]^{1/2} < \varepsilon$$

Then, the reciprocal of $\phi_m(r)$ is interpreted as being the equivalent constant heat flux value of the heat transfer coefficient. Accordingly, the equivalent uniform flux convective Nusselt number, Nu_u^c, is evaluated as

$$Nu_u^c(x) = Nu^c(x)\,\frac{\phi_o(x)}{\phi_m(x)} \tag{3-10}$$

If this procedure is applicable Nu_u^c from Eq. (3-10) is expected to correlate according to Eq. (3-2). Conversely local heat transfer coefficients for a given nonuniform heat flux distribution are to be evaluated from Eqs. (3-4, 3-5, 3-6) where $h_u(x)$ of Eq. (3-6) is evaluated from the appropriate uniform flux correlation including the thermal development effect. For constant property from infinite series solutions for $h_u(x)$ of constant heat flux turbulent flow are available[3,2] for selected values of Re and Pr. The development correction, $1+(x/D)^{-0.7}$, of Eq. (3-2) is of course only a crude approximation to the exact solution in some region, such as $x/D > 5$. Nevertheless, the effect of nonuniform flux may be approximated in terms of a convolution with this factor, yielding the nonuniform flux convective Nusselt number

$$Nu_{Nu}^c = Nu_u^c\,\frac{q(x)}{\dfrac{q(0)}{1+(x/D)^{-0.7}} + \displaystyle\int_o^x \frac{\partial q(x')}{\partial x'}\,\frac{dx'}{1+\left(\frac{x-x'}{D}\right)^{-0.7}}} \tag{3-11}$$

In using this form the effect of variable properties is not counted in the convolution but is considered to be local as contained in Nu_u^c of Eq. (3-2).

3.4. RADIATIVE HEAT TRANSFER

Evaluation of radiative heat transfer is not complicated by a nonuniform axial heat flux distribution as long as convection-radiation interaction is ignored. Depending on the optical thickness of the gas two different methods of analysis are appropriate in predicting the radiative heat transfer from wall to the gas.

For an optically thick gas, $\tau_g = \kappa_g D \gg 1$, the radiation streaming from the wall is absorbed by the gas over a distance small compared to the diameter of the tube. Axial transfer can therefore be ignored and the wall to gas radiant transfer is evaluated from a one-dimensional analysis.

For an optically thin gas, $\tau_g = \kappa_g D \ll 1$, the radiation streaming from the wall travels a distance large compared to the diameter of the tube before being absorbed. In this case axial transfer between wall elements, between gas and wall as well as to the ends of the tube cannot be ignored in principle. However, because the magnitude of the radiant flux from wall to gas in this case is small compared to the convective flux an elaborate thin gas analysis is hardly warranted. The first-order effect to be considered is a correction to the wall heat flux due to radiant exchange between wall elements and tube ends. Sample calculations for several experimental data sets indicate that for turbulent flow the wall heat flux correction is less than about 1%. The resulting correction to the heat transfer coefficient would be of the same order of magnitude.

Based on these considerations all steam data of the present study are treated by the one-dimensional analyses described below.

3.4.1. Method Based on Gas Absorption Coefficient

At each axial position along the tube the radiative heat transfer from wall to gas is calculated based on the assumption that the tube is of infinite length of constant inside wall temperature, T_w, and that the gas is at a uniform temperature, T_g. Denoting the radiosity of the wall by B, the grey gas emissivity at T_g by $\epsilon_g(T_g)$ and the grey gas absorptivity for wall radiation by $\alpha_g(T_w)$ the radiant heat flux becomes

$$q^R = \alpha_g(T_w)B - \epsilon_g(T_g)\sigma T_g^4 \qquad (3\text{-}12)$$

The radiosity of the wall is

$$B = \epsilon_w \sigma T_w^4 + (1-\epsilon_w)H \qquad (3\text{-}13)$$

where ϵ_w is the wall emissivity at T_w and the incident radiation, H, is composed of gas emission and transmitted wall radiation

$$H = \epsilon_g(T_g)\sigma T_g^4 + [1-\alpha_g(T_w)]B \ . \qquad (3\text{-}14)$$

Note that the gas transmissivity, $1-\alpha_g(T_w)$, for the wall radiosity is evaluated at the wall temperature, a good approximation for wall emission dominated heat transfer from wall to gas. Assuming local equilibrium, gas absorptivity and emissivity are equated, $\alpha_g(T) = \epsilon_g(T)$.

Given wall and gas bulk temperatures the radiosity is then evaluated explicitly from Eq. (3-13) and (3-14) as

$$B = \frac{\sigma[\epsilon_w T_w^4 + (1-\epsilon_w)\epsilon_g(T_g)T_g^4]}{1-(1-\epsilon_w)[1-\epsilon_g(T_w)]} , \qquad (3\text{-}15)$$

and the radiant heat flux is evaluated from Eq. (3-12), which in terms of emissivities becomes

$$q^R = \epsilon_g(T_w)B - \epsilon_g(T_g)\sigma T_g^4 . \qquad (3\text{-}16)$$

The wall emissivity depends on the surface and its temperature and is generally well approximated by an expression of the form,

$$\epsilon_w(T_w) = \epsilon_A + \epsilon_B \ln T_w , \qquad (3\text{-}17)$$

where ϵ_A and ϵ_B are experimental constants for the particular surface and temperature range in question (see Appendix D).

The present method deviates from that of Hottel[1] in that it evaluates gas emissivity from the absorption coefficient κ_g by the expression

$$\epsilon_g(T) = 1-\exp[-\tau_g(T)] \qquad (3\text{-}18)$$

which is a good approximation for small to moderate optical thickness, $\tau_g = \kappa_g D$, of the circular tube geometry. Here, κ_g, is calculated from the impirical expression for steam

$$\kappa_g = p[5.6(1000/T)^2 - 0.3(1000/T)^4] , \qquad (3\text{-}19)$$

where the units are κ_g(feet^{-1}), p(atm) and T(°R). Equation (3-19) was obtained from the thin gas analysis of existing spectral data for water vapor presented by Abu-Romia and Tieu[16]. While the thin gas analysis indicates that the mass absorption coefficient, κ_g/p, is independent of the pressure, a similar thick gas analysis suggests an inverse pressure effect which increases with increasing optical thickness. This secondary effect has not yet been well established and is not included in the present analysis.

3.4.2. Method Based on Gas Emissivity Chart

Following the method of Hottel[1] for the case of wall emission dominated radiant transfer from wall to gas use is made of a single gas emissivity and

absorptivity, α_{gw}, based on the effective beam length of the tube geometry. Equations (3-15) and (3-16) then may be combined to yield

$$q^R = \frac{\sigma(T_w^4 - T_g^4)}{1/\epsilon_w + 1/\alpha_{gw} - 1} \quad . \tag{3-20}$$

For water vapor α_{gw} is evaluated from

$$\alpha_{gw} = \epsilon_g\{T_w, (pL) \times (T_w/T_g)\} \times C_w \times (T_w/T_g)^{-0.45} \tag{3-21}$$

where L = D, and the pressure correction of Hottel, C_w, is extrapolated for current use as

$$C_w = \begin{cases} 0.4 \times (p+3) & p \leq 2 \text{ atm} \\ 2.0 & p > 2 \text{ atm} \end{cases} \quad . \tag{3-22}$$

The following approximation obtained from the Hottel chart[1] for H_2O is used for the gas emissivity in the ranges $500 < T < 3000°R$ and $0.05 < PL < 0.40$ ft-atm,

$$\epsilon_g = \exp[K3 - K2 \times (T-1400)] \quad , \tag{3-23}$$

where

$$10^5 \times K2 = \begin{cases} 56 - 44\sqrt{PL - 0.05}; & T < 1400°R \\ 76.8 - 55\sqrt{PL - 0.033}; & T \geq 1400°R \end{cases} \tag{3-24}$$

$$K3 = -3.34 + 2.75\sqrt{PL - 0.033} \quad , \tag{3-25}$$

where T is in (°R) and PL is in (ft-atm).

The reliability of this procedure for evaluating the radiant flux depends on the availability of gas emissivity data for the appropriate conditions of pressure, temperature, and path-length. Unfortunately, the gas emissivity data reported by Hottel, and here approximated by Eq. (3-23), are valid for zero partial pressure of water vapor and a total pressure of 1 atm, and are not recommended for different total pressures. Furthermore, the data was obtained for path-lengths large compared to those of the present study.

3.5. LAMINARIZATION

Transition from laminar to turbulent flow is well-known. Local theory for constant property flow indicates that for duct flow a single parameter, the Reynolds number, and for boundary flow in addition the velocity profile shape describe the onset of transition. The laminar velocity profile of simple boundary flows is related to the pressure gradient, or acceleration, of the free stream. A single parameter profile as employed in the Karman-Pohlhausen integral procedure is characterized by the quantity[17]

$$\Lambda = \frac{\delta^2}{\nu} \frac{dU}{dx} \tag{3-26}$$

Where δ denotes the boundary layer thickness. For a given Reynolds number increasing positive values of Λ enhances stability. Decreasing Reynolds numbers for a given value of Λ has the same effect. Experimental studies[2] indicate that reverse transition from turbulent to laminar flow, here denoted laminarization, appears at conditions close to those of usual transition.

For duct flow of gases with heat transfer from wall to gas laminarization is promoted by three effects: decreasing bulk Reynolds number, preferential increase in fluid viscosity near wall, and acceleration of the flow. It is postulated that the following single parameter characterizes laminarization

$$A = \frac{\Lambda}{(Re_b)^2} = \frac{1}{Re_b} \frac{D_e \rho_b}{G} \frac{dV_b}{dx} \tag{3-27}$$

Where Λ, evaluated in terms of $\delta = D$ and $\nu = \nu_b$, accounts for the two latter effects mentioned above. The axial bulk velocity gradient is evaluated as follows. The lumped form of the continuity equation yields

$$\begin{aligned} \frac{d}{dx}(\rho_b V_b) &= 0 \\ \frac{dV_b}{dx} &= -\frac{V_b}{\rho_b} \frac{d\rho_b}{dx} \end{aligned} \tag{3-28}$$

From the equation of state in the form $\rho = \rho(h,p)$ the density gradient is written

$$\frac{d\rho_b}{dx} = \left(\frac{\partial \rho}{\partial h}\right)_p \frac{dh_b}{dx} + \left(\frac{\partial \rho}{\partial p}\right)_h \frac{dP_b}{dx} .$$

Ignoring the small axial pressure gradient of the flow Eq. (3-28) becomes

$$\frac{dV_b}{dx} = - \frac{V_b}{\rho_b} \left(\frac{\partial \rho}{\partial h}\right)_p \frac{dh_p}{dx} , \tag{3-29}$$

where the axial bulk enthalpy gradient is determined from the lumped energy equation for the constant area duct flow

$$\frac{d}{dx} (\rho_b V_b h_b) = \frac{4q''_w}{D_e}$$

$$\frac{dh_b}{dx} = \frac{4q''_w}{G D_e} \tag{3-30}$$

From Eqs. (3-27), (3-29), and (3-30) the laminarization parameter becomes

$$A = - \frac{1}{\rho_b} \left(\frac{\partial \rho}{\partial h}\right)_p \frac{4q''_w}{G Re_b} \tag{3-31}$$

For a perfect gas Eq. (3-31) reduces to

$$A_{gas} = \frac{4q''_w}{C_p T_b G Re_b} \tag{3-32}$$

It is noted that A_{gas} of Eq. (3-32) is proportional to the ratio of the heat flux parameter, $q''_w/C_p T_b G$, of variable property analyses[4,11] and the bulk Reynolds number. The latter accounts on an average for the level of bulk turbulence expected, while the former determines both the acceleration of the bulk flow, modifying the velocity profile, and the extent of property variation. The low Reynolds number data is examined for laminarization in terms of the parameter A in section 4.4.

3.6. RADIATION-CONVECTION INTERACTION FOR LAMINAR FLOW

The results of the detailed analysis of Ref. 15 for the case of developing and fully developed laminar flow is summarized below.

Employing the constant property assumption, the energy equation for fully developed laminar flow may be expressed in the form

$$\frac{q''R_o}{kT_w}(2\eta-\eta^3) = \frac{\partial\theta}{\partial\eta} - \frac{\tau_o}{8\mathcal{P}_w}\left[\frac{\epsilon_w+(1-\epsilon_w)\tau_o\int_o^1\theta^4(\eta')G(\tau_o,\eta')d\eta'}{1-(1-\epsilon_w)[1+H(1,\tau_o)]}H(\eta,\tau_o)\right.$$

$$\left. + \eta\tau_o\int_o^{1/\eta}\theta^4(\eta')G(-\tau_o,\frac{\eta'}{\eta})d(\frac{\eta'}{\eta})\right] , \qquad (3\text{-}33)$$

where $\theta = T/T_w$, $\eta = 2r/D$, $\tau_o = \kappa D$, $\mathcal{P}_w = \kappa k/4\sigma T_w^3$, and G and H are functions describing the decay of radiant energy emitted by the gas and emitted and reflected from the walls, respectively. A solution to Eq. (3-33) is assumed of the form

$$\theta(\eta) = a_o + a_2\eta^2 + a_4\eta^4 + \ldots a_{2n}\eta^{2n} .$$

Such a profile may be forced to satisfy the condition $\theta(1) = 1$ and n additional conditions. The simplest proceedure is to satisfy Eq. (3-33) at n points $\eta = \eta_i$, i = 1,n. This results in a set of n + 1 simultaneous linear equations for the unknown coefficients which are solved numerically, and which in turn permits evaluation of the Nusselt number, $Nu(\tau_o,\mathcal{P}_w,\epsilon_w)$. Examination of a solution obtained in a related manner for small τ_o for the entrance length reveals that the primary effect of radiation is simply to add a constant to the Nusselt number, independent of axial position. Extrapolation of this finding to larger values of τ_o results in the expression

$$Nu^T(\frac{2x/D}{RePr},\tau_o,\mathcal{P}_w,\epsilon_w) = Nu^c(\frac{2x/D}{RePr}) + Nu^T_\infty(\tau_o,\mathcal{P}_w,\epsilon_w) - Nu^c_\infty , \qquad (3\text{-}34)$$

where the subscript ∞ refers to fully developed flow. Results of numerical calculations of Nu^T_∞ ignoring the temperature dependency of κ in the gas are presented in Figure 9. κ is a strong function of temperature for steam, approximately proportional to T^{-2} (Eq. (3-19)). Including this approximation in calculating the energy emitted by the gas it can be shown (see Ref. 15 for details) that τ and $\mathcal{P}$ should be evaluated at the wall temperature. Nu^c is taken from Ref. 11 in which it is proposed to account for the effect of variable properties in terms of a modified nondimensional axial coordinate

$$x^+ = \int_o^{2x/D}\frac{d(2x'/D)}{Re_b Pr_b} , \qquad (3\text{-}35)$$

rather than $(2x/D)/(Re\cdot Pr)$ employed in constant property analysis. This procedure acknowledges a variable property effect on laminar convection only in the entrance length coordinate.

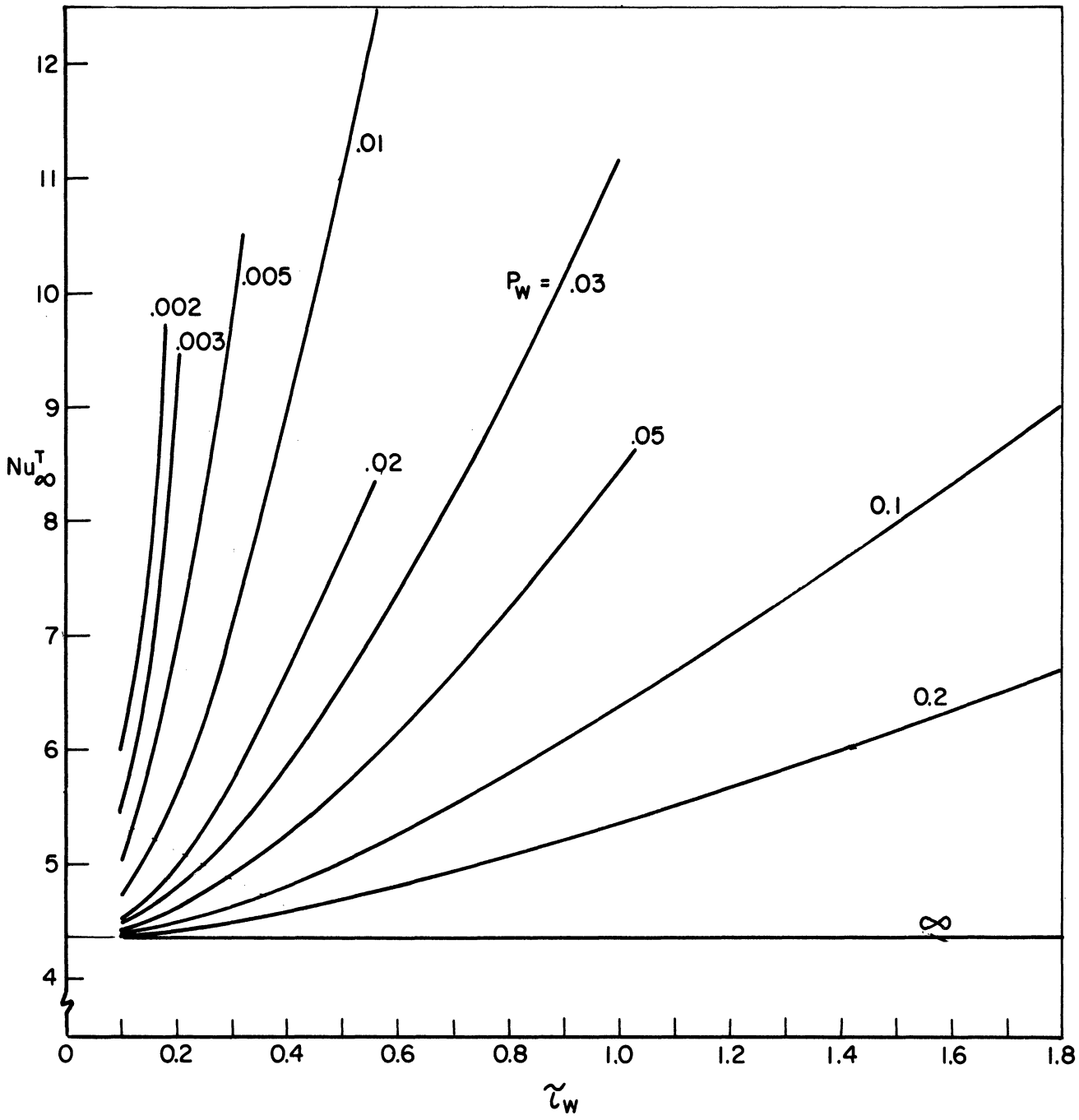

Figure 9. Total bulk Nusselt number by fully developed laminar flow. (Based on gas absorption coefficient evaluated at the wall temperature.

3.7. DATA REDUCTION

The data reduction analysis and procedure, being rather elaborate, are discussed separately in Appendix A.

Based on the raw data input of each run and the general test section data and calibration data listed at the end of the computer program local heat flux, q_w, inside wall temperature, T_w, and gas bulk temperature, $T_b = T_g$, as well as appropriate thermophysical properties are evaluated at each of 12 axial wall thermocouple stations along the heated section. The program furthermore evaluates the various analyses of the previous sections. A complete sample printout for a single run is reproduced in Appendix A. The thermophysical properties employed in the data reduction are also described in this appendix. The reduced data is tabulated in Appendix B.

4. EXPERIMENTAL RESULTS (DISCUSSION)

This section summarizes the results of the experimental study including comparison with existing correlations and with the analysis of Section 3. Each experimental run yielded 12 data points for local heat transfer along the heated test section. Among these two first and two last points, positioned a few diameters downstream of inlet and upstream of exit, respectively, are ignored because conduction and radiation losses could not be accurately accounted for. Laminarization appeared in uniform heat flux runs for bulk Reynolds numbers less than approximately 6000. All of this data is treated in a separate section following the presentation and discussion of fully turbulent data. The fully laminar data is discussed in the last section.

4.1. HEAT BALANCE DATA. EXPERIMENTAL ERROR AND UNCERTAINTY

Establishment of an accurate heat balance is particularly important for the present study because inlet and exit fluid temperatures are measured respectively 36 in. upstream and 10 in. downstream of the heated test section to not obstruct the fully developed velocity profile and to use mixing chambers to attain mixed mean bulk temperatures and eliminate radiation correction.

Several heat balance runs for each test section were made to measure the enthalpy change associated with ambient heat transfer from the well insulated inlet and exit sections. Careful balance of test section guard heaters reduced extraneous heat transfer from the heated test section to less than 2% of the normal test section power and could be ignored in the heat balance checks, although included in the data reduction of power runs. The measured ambient heat transfer was compared to that calculated for the given flow conditions, geometry, insulation material, and ambient conditions. Using the manufacturer's values for thermal conductivity of the insulation the predicted ambient heat transfer was found to be consistently low by about 30%. Due to variations in actual density of the packed insulation this is not an unreasonable deviation.

The main sources of error and uncertainty in the final uniform flux heat transfer data are associated with gas inlet temperature and test section power, both related to the heat balance calculations made for each data run as described in Appendix A. Analysis of the data shows that the accuracy of results from a low power run, such as run 55, is

mass flow rate:	±2%
heat flux:	±2.8%
$T_w - T_g$:	±2.3%
$\bar{Nu}_b$:	±3.6%
$\bar{Re}_b$:	±2.2%

For some runs the power reading amounted to somewhat less than 1/4 of full scale on the instrument having a calibrated accuracy of 0.75% of full scale. The uncertainty on the resulting Nusselt number would not exceed 4.3%, however. For the bulk of the data, having considerably higher power levels than run 55 considered above, the uncertainties are less than quoted.

For the nonuniform flux data the accuracy is further dependent on the uncertainty associated with the nonuniform wall thickness variation along the test section. Measurements of the inside and outside diameters suggest an additional uncertainly of 2-3% in wall area, hence calculated heat flux, raising the uncertainty on the Nusselt number in the high heat flux center portion of the test section to approximately 4.8%.

4.2. NITROGEN DATA. UNIFORM FLUX SS-310 TEST SECTION

The test conditions for the nitrogen runs 50-56, 90-93 are listed in Table VI of Appendix C. Among these, run 90 was unsuccessful, runs 53-55 were questionable, and run 91 was poor in regard to loop steadiness and heat balance. Examination of the data for selfconsistency, however, does not suggest that any runs except 90 and 91 be rejected, leaving a total of 9 runs for evaluation. These are divided into two groups

Fully Turbulent: Runs 53, 54, 56
Laminarization: Runs 50, 51, 52, 55, 92, 93

All of the data for these runs, $7.5 \leq z \leq 60.2$, is plotted in Figures 10a-e for comparison with the following correlations

Dittus-Boelter (Figure 10a)

$$Nu_b = 0.023\ Re_b^{0.8}\ Pr_b^{0.4} \tag{4-1}$$

Humble et al.,[7] (1952) (Figure 10b)

$$Nu_w = 0.023\ Re_{wb}^{0.8}\ Pr_w^{0.4} \tag{4-2}$$

McEligot et al.,[4] (1965). (X/D > 5) (Figure 10c)

$$Nu_b = 0.021\ Re_b^{0.8}\ Pr_b^{0.4}\ (Tw/Tb)^{-0.5}[1 + z^{-0.7}] \tag{4.3}$$

Perkins, Worsoe-Smith[5] (1965) (Figure 10d)

$$Nu_b = 0.024\ Re_b^{0.8}\ Pr_b^{0.4}(Tw/Tb)^{-0.7}[1 + (Tw/Tb)^{0.7}\ z^{-0.7}] \tag{4-4}$$

Reynolds, Jr.[12] (1968) (Figure 10e) (modified with $(Tw/Tb)^{-0.5}$)

$$Nu_b = 0.021\, Re_b^{0.8}\, Pr_b^{0.4} (Tw/Tb)^{-0.5} [1 + 0.8(1 + 70000\, Re_b^{-3/2}) z^{-1}] \quad (4\text{-}5)$$

The modified wall-bulk Reynolds number of Eq. (4-2) is defined by

$$Re_{wb} = (GD/\mu_w)(\rho_w/\rho_b).$$

Ignoring the entrance effect Figure 10a shows clearly the effect of variable properties on the fully turbulent data in reducing the bulk Nusselt number. Humble et al.,[7] correlated their data for fully developed turbulent flow for $1.1 \leq T_w/T_b \leq 2.5$ for $Re_{wb} > 10^4$ by Eq. (4-2). For $Re_{wb} < 10^4$ the data fell on a curve reproduced in Figure 10b. The present fully developed turbulent data fall above this line. It should be noted, however, that Humble et al., considered average, not local, heat transfer.

Although the following three correlations, Eqs. (4-3), (4-4), and (4-5), were developed on the basis of results obtained with the same experimental facility, Eq. (4-3) was based on temperature ratios of 1.1 - 2.5 using air, He and N_2, Eq. (4-4) on $(T_w/T_b) = 1.24 - 7.5$ using N_2, while Eq. (4-5) (without the temperature correction which tentatively is proposed here) was based on low Reynolds number data for N_2 and He for $(T_w/T_b) = 1 - 1.4$. From Figures 10c, d, e it appears that Eq. (4-3) yields the best general agreement for all of the fully turbulent data. None of the correlations can appropriately handle the data showing laminarization, however.

On the basis of this comparison Eq. (4-3) is selected to best represent fully turbulent heat transfer to a transparent gas for the present parameter ranges, in particular for $z > 5$ and $Re_b > 6000$.

The low Reynolds number data indicating retransition to laminar flow will be discussed in section 4.4.

4.3. STEAM DATA

Total convective and radiative heat transfer to steam was measured in three test sections referred to as: (i) uniform flux SS-310, (ii) uniform flux Zr-2, and (iii) nonuniform flux SS-310. The first test section provides the bulk of the data for a complete parameter study. The second one investigates the effect of surface emissivity, while the third one explores the effect of nonuniform heat flux distribution. The flow geometry is the same for all test sections. The reduced data is tabulated in Appendix B.

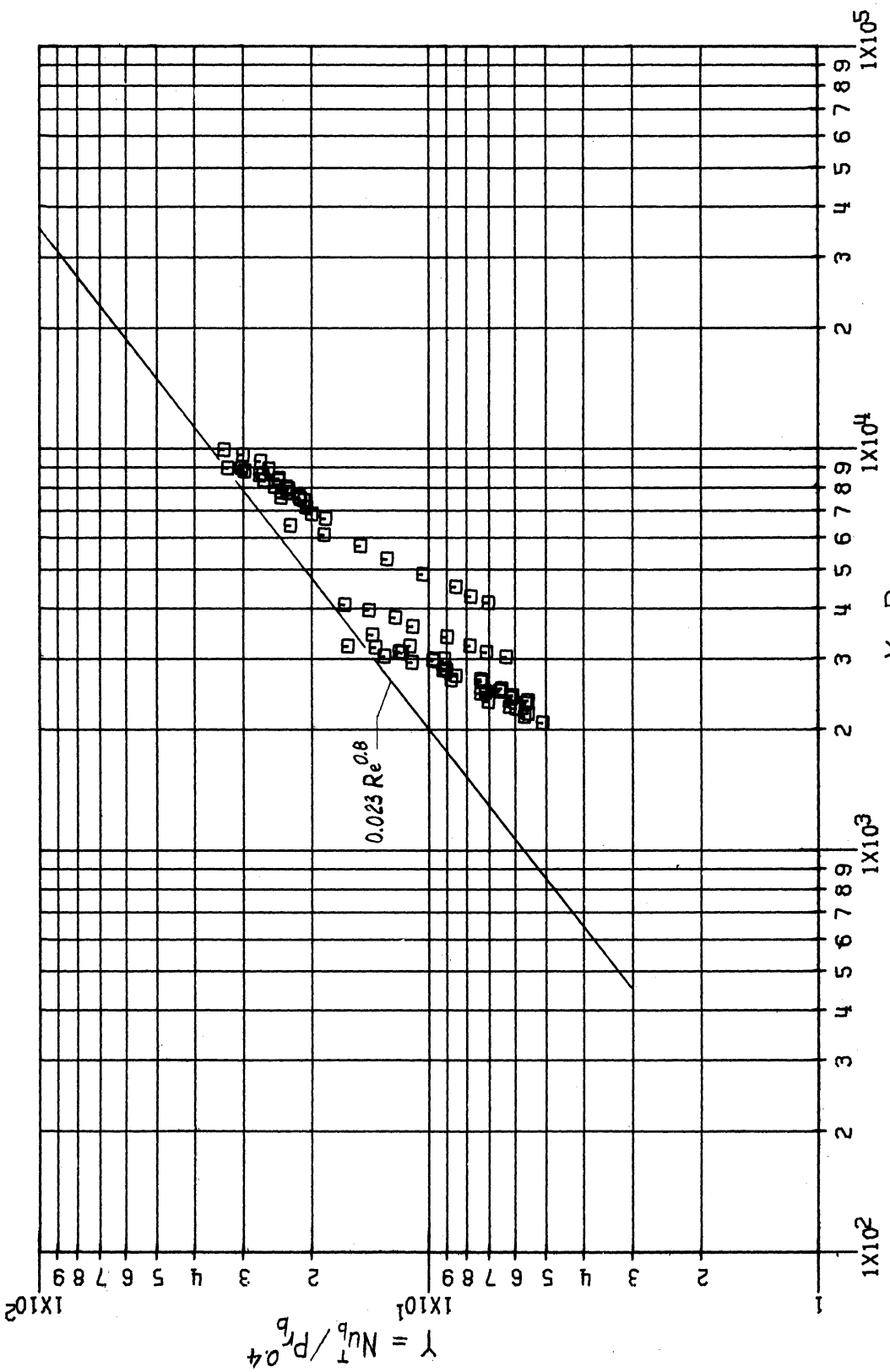

Figure 10. Nitrogen data. Uniform flux SS-310 test section.

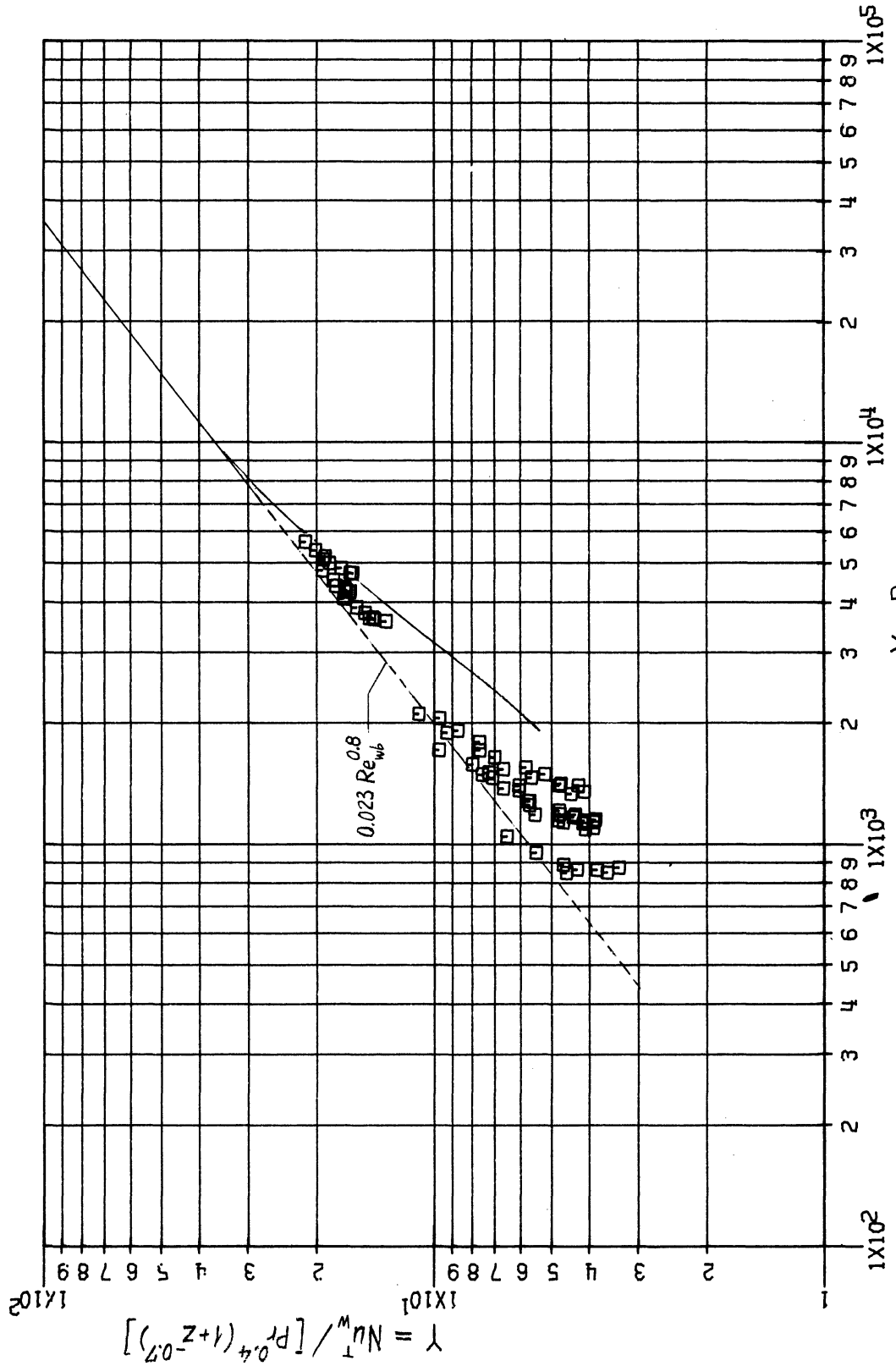

Figure 10. (continued)

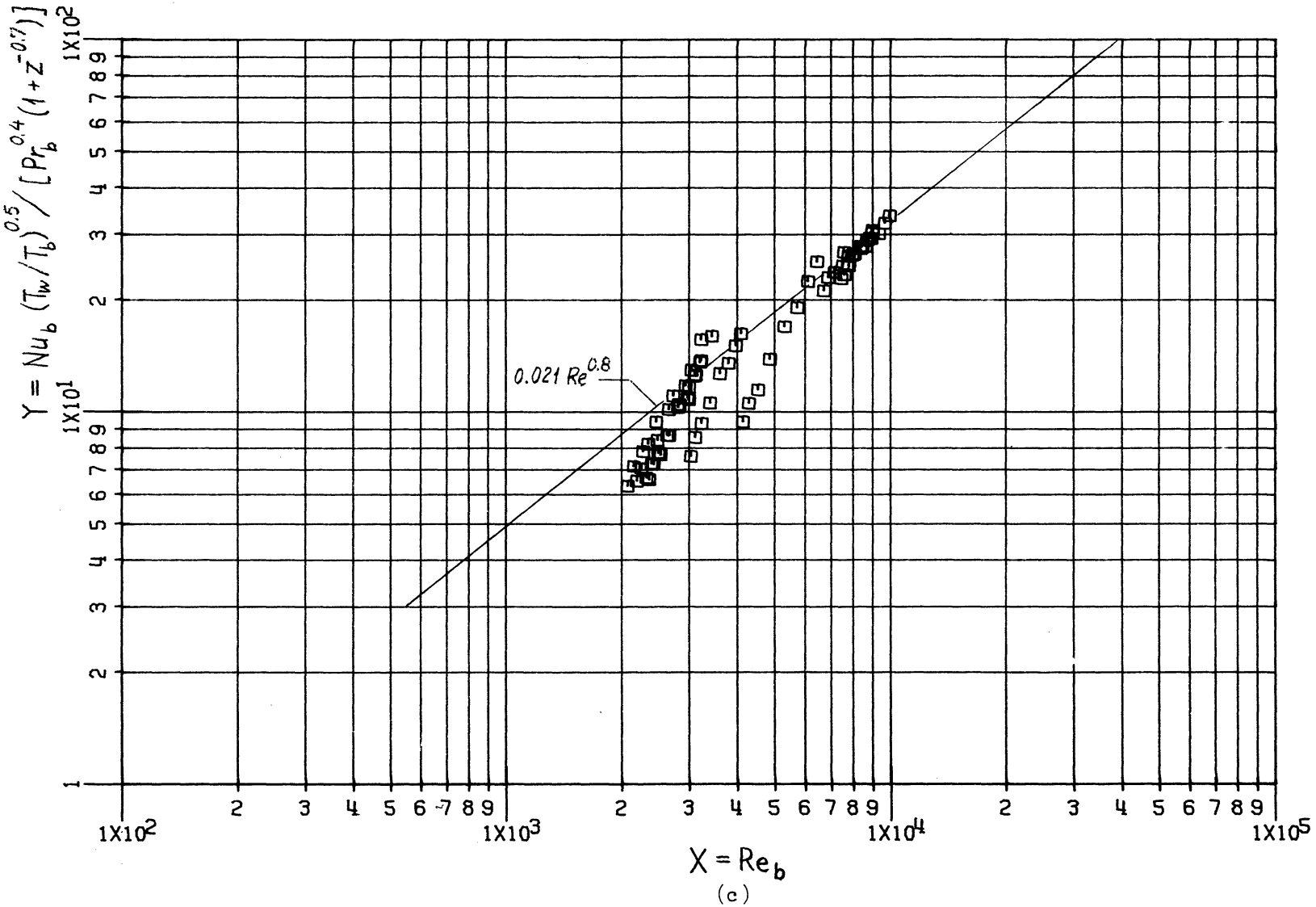

(c)

Figure 10. (continued)

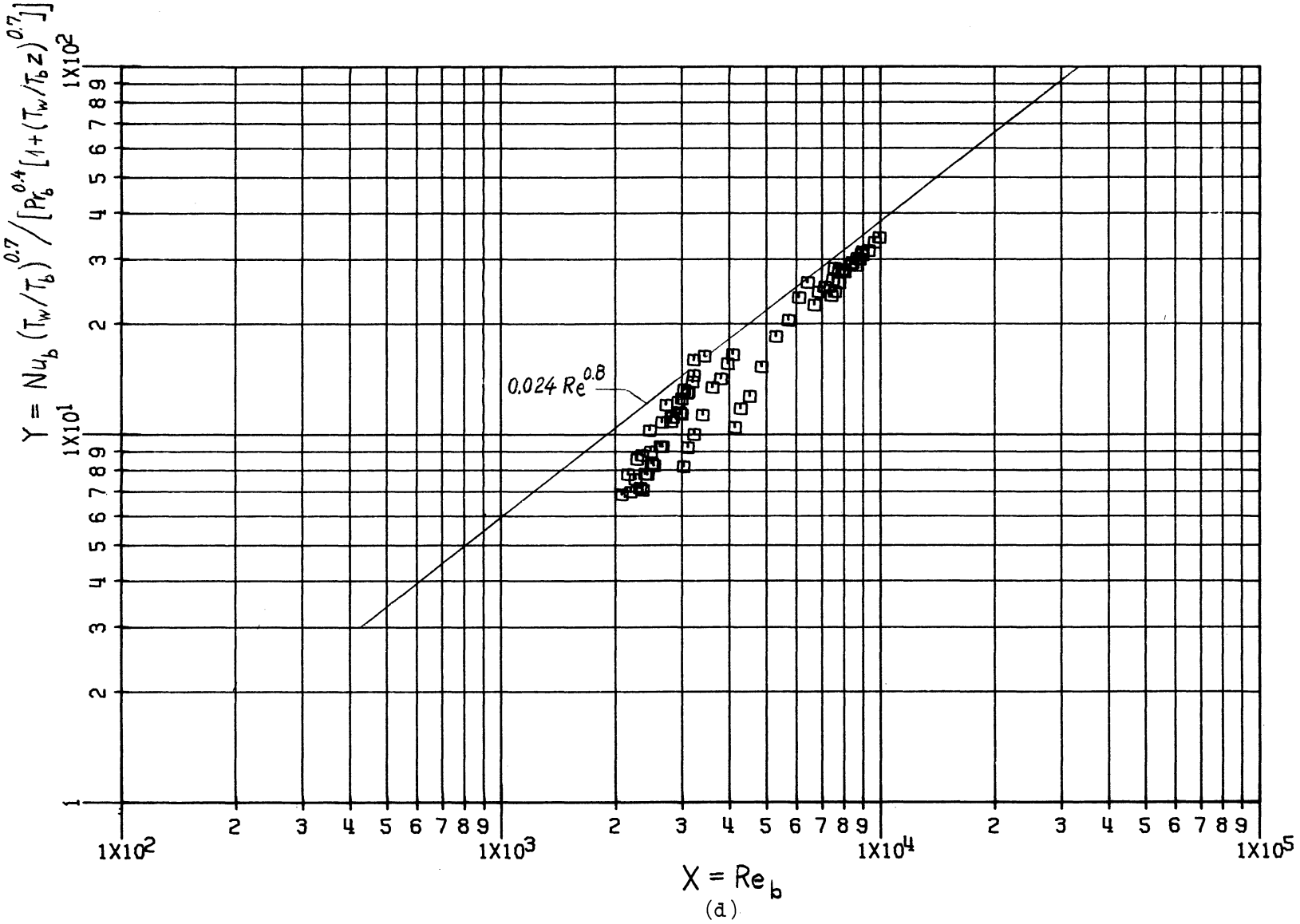

(d)

Figure 10. (continued)

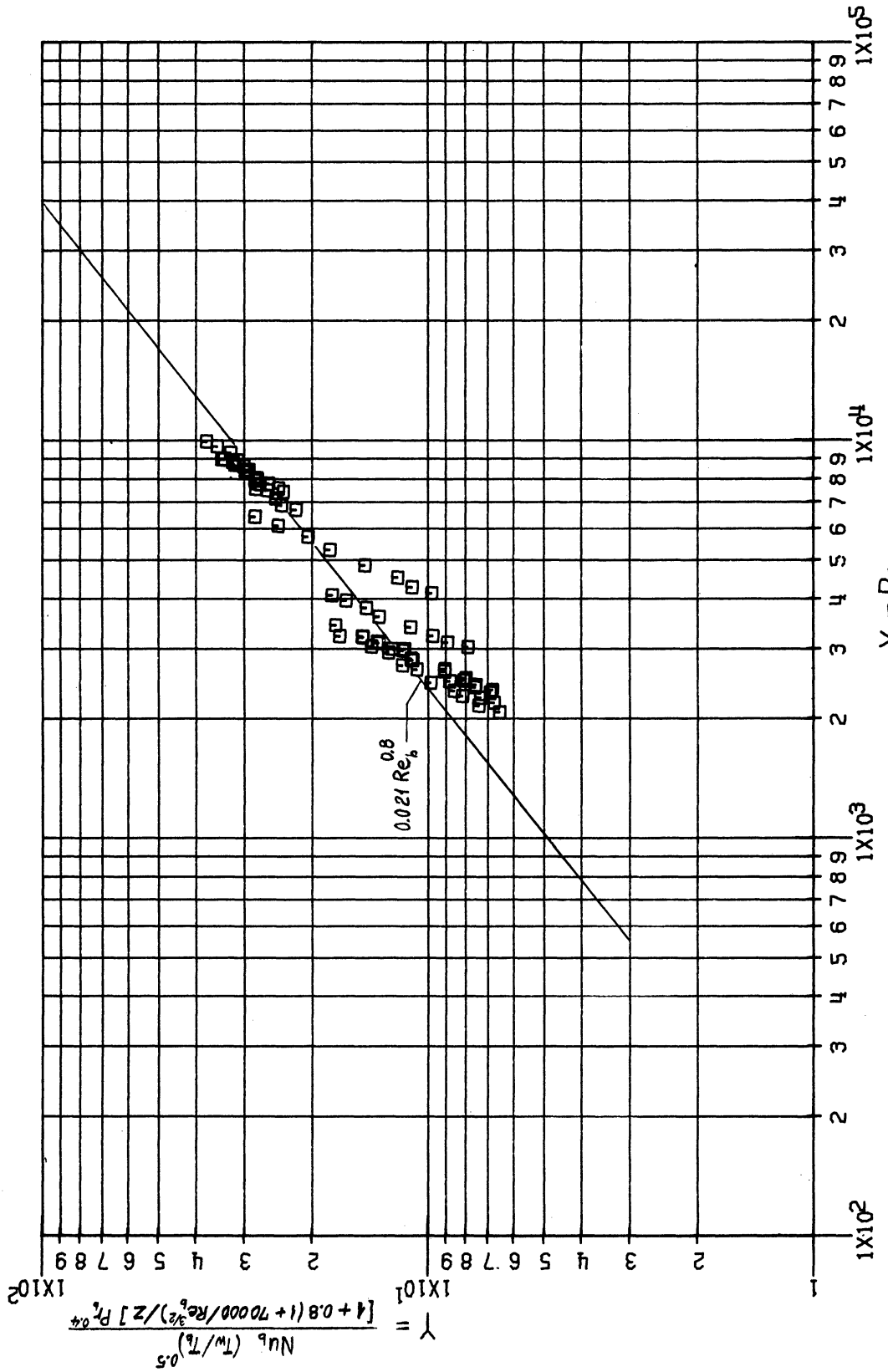

Figure 10. (concluded)

4.3.1. Uniform Flux SS-310 Test Section

The test conditions and qualification of the runs are listed in Table VII of Appendix C. Of a total of 71 runs, 46 were labeled questionable before data reduction. However, after further examination of reduced data only 6 runs could be rejected as being in error or inconsistent with the remaining data. These were runs 26, 27, 30, 37, 44, 79, 80. Ignoring the two first axial stations (Z = 1 and Z = 3.51) and the last two stations (Z = 66.2 and Z = 71.2), this leaves a total of 8 x 65 = 520 useful local data points.

The parameter ranges of the data are listed in Table IV.

TABLE IV

PARAMETER RANGES
(Uniform Flux SS-310 Test Section Steam Data)

p	25, 50, 75 psia
T_{in}	Sat., 300, 700, 1100°F
G	1700 - 40,000 lbm/hr ft^2
Re_{in}	1900 - 35,000
q_w	2400 - 31,000
z	7.5 - 60.2
T_w	400 - 1800°F
T_g	300 - 1500°F
T_w/T_g	1.1 - 2.11
Re_b	420 - 33,000
Re_w	383 - 21,000
Pr_b	0.7 - 1.1
Pr_w	0.87 - 0.98
$\mathcal{P}_b$	0.0043 - 0.0803
τ_b	0.107 - 1.79

The reduced data is presented graphically in terms of the following relations for each of three pressures (25, 50, and 75 psia)

Y	X	Figures
$\bar{Nu}_b^T/Pr_b^{0.4}$	Re_b	11a, b, c
$Nu_b^c(T_w/T_b)^{0.5}/[Pr_b^{0.4}(1 + Z^{-0.7})]$	Re_b	12a, b, c
Nu_b^T(measured)	Nu_b^T(predicted, Eq. (4-3), (3-16))	13a, b, c
$\bar{Nu}_b^T$(measured)	$\bar{Nu}_b^T$(predicted, Eq. (4-3), (3-20))	14a, b, c

Figures 11a, b, c show that total convective and radiative local heat transfer for $26 \leq Z \leq 60.2$ correlates with the Dittus-Boelter Eq. (4-1) to within ±5% for all pressures for $Re_b > 5\text{-}6000$ and to within +10% -20% for $Re_b < 5\text{-}6000$, including retransition data. It appears that the radiative transfer approximately makes up for the expected reduction in convective heat transfer due to variable properties in the fully turbulent range and in addition makes up for part of the reduction in convective heat transfer due to laminarization at low Reynolds numbers. Comparison between Figures 11a, b, c indicates no pressure effect in the correlation at high Reynolds numbers but a definite shift upwards of the data with increasing pressure at low Reynolds numbers.

In Figures 12a, b, c the local convective heat transfer for $7.5 \leq Z < 60.2$ is compared to the McEligot correlation, Eq. (4-3). The convective Nusselt number, $\bar{Nu}_b^c$, is obtained from the total measured Nusselt number by subtracting the radiative transfer evaluated according to Eq. (3-16). At 25 psia, excluding the data showing retransition, the results from runs having a high inlet temperature of about 700 and 1100°F agree with the correlation to within ±5%, while data from runs of low inlet temperature of about 300°F fall high by as much as 20%. A similar trend is shown by the laminarization data. At 50 psia the high Reynolds number data show a similar trend although the low inlet temperature data fall high by only 15%. At 75 psia most data at high Reynolds numbers fall within ±10% of the correlation.

Since the grey gas absorption coefficient, κ, increases with increasing pressure and decreasing temperature the correlation trend of the present data is in agreement with that expected. The radiative transfer is predicted on the basis of the thin gas approximation, Eq. (3-19), for the absorption coefficient which ignores the path length dependent inverse pressure effect suggested in the discussion following Eq. (3-19). The radiation transfer is therefore underestimated for the data of lower pressure and higher optical thickness.

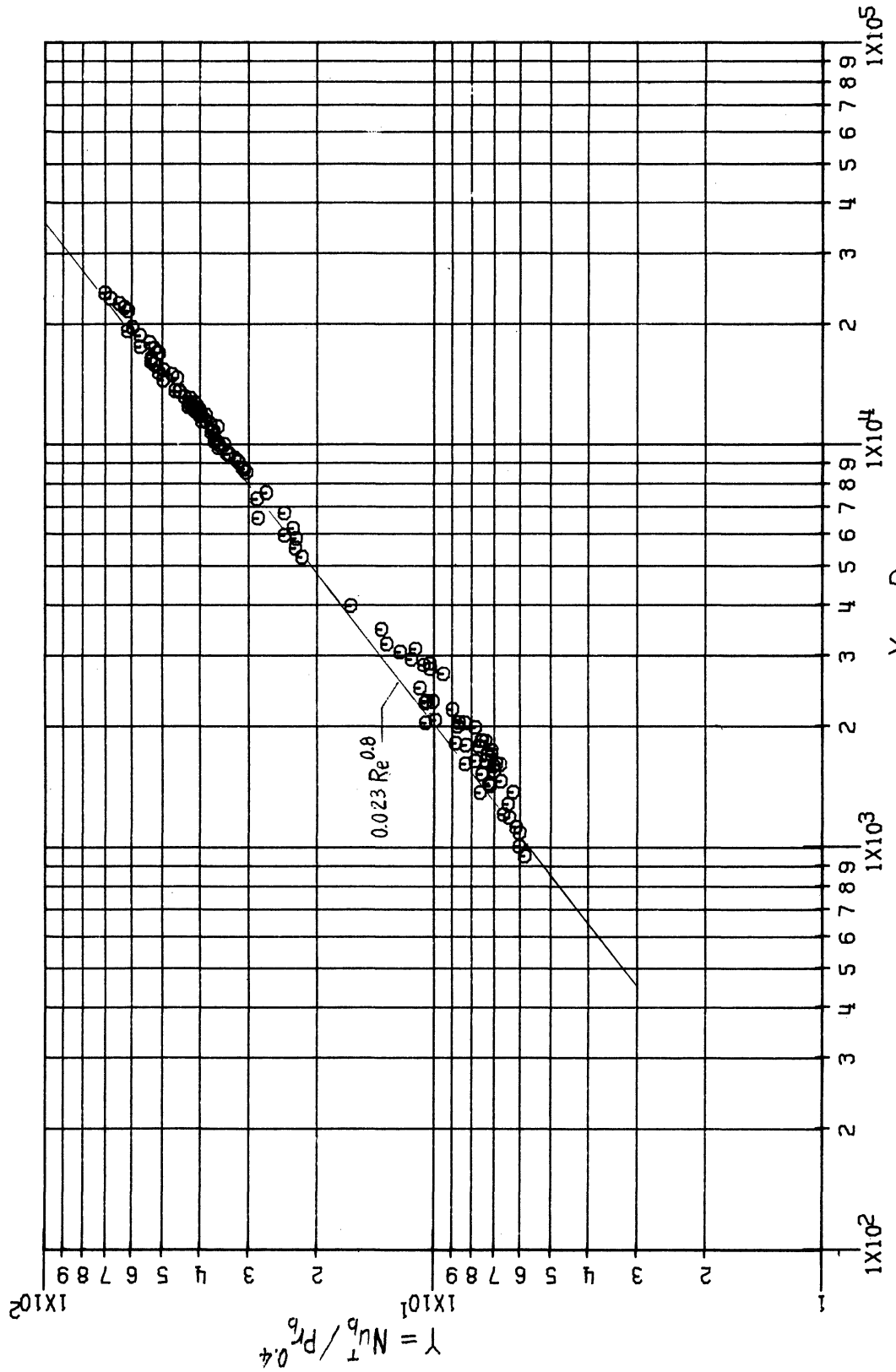

(a) 25 psia

Figure 11. Steam data. Uniform flux SS-310 test section.

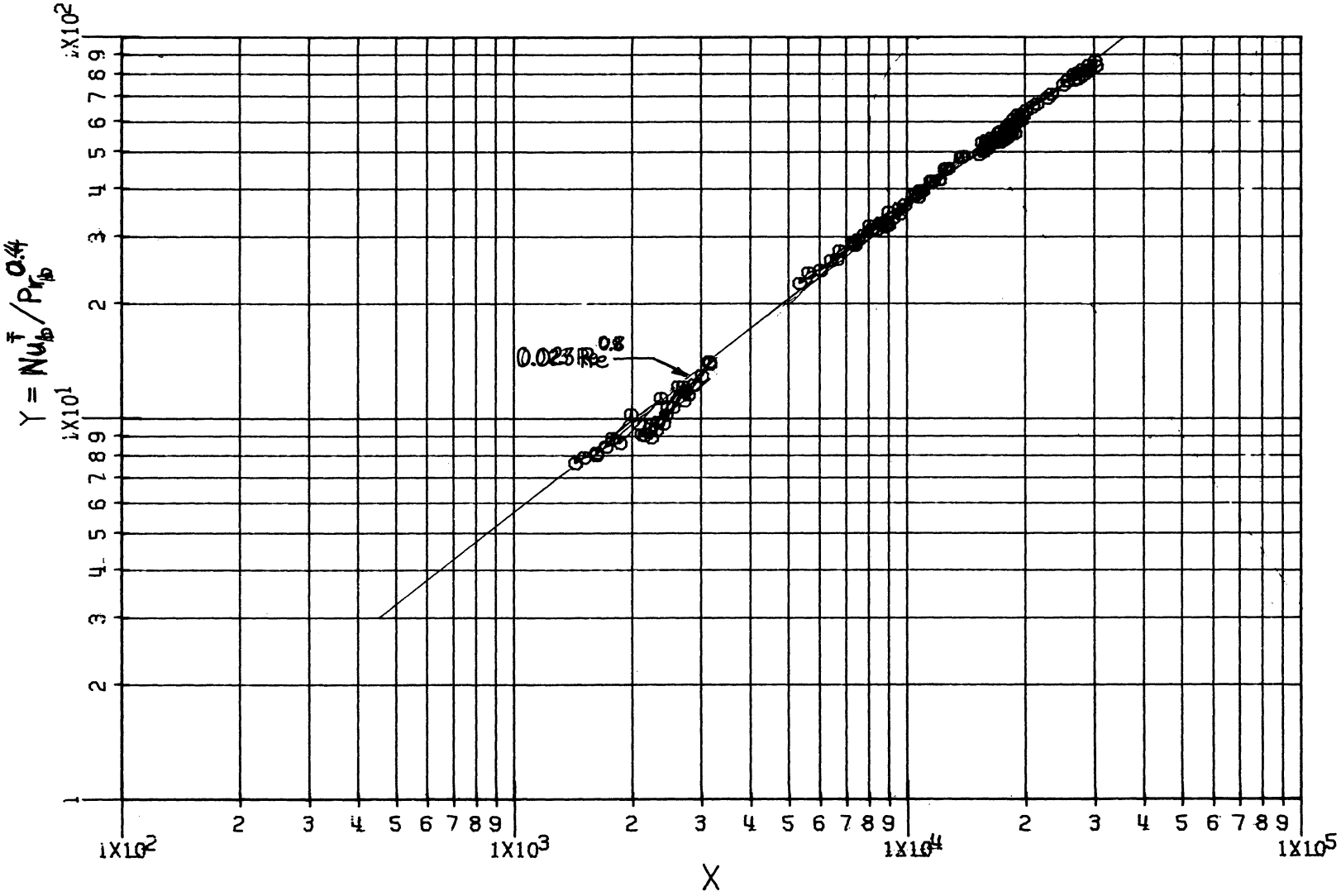

(b) 50 psia

Figure 11. (continued)

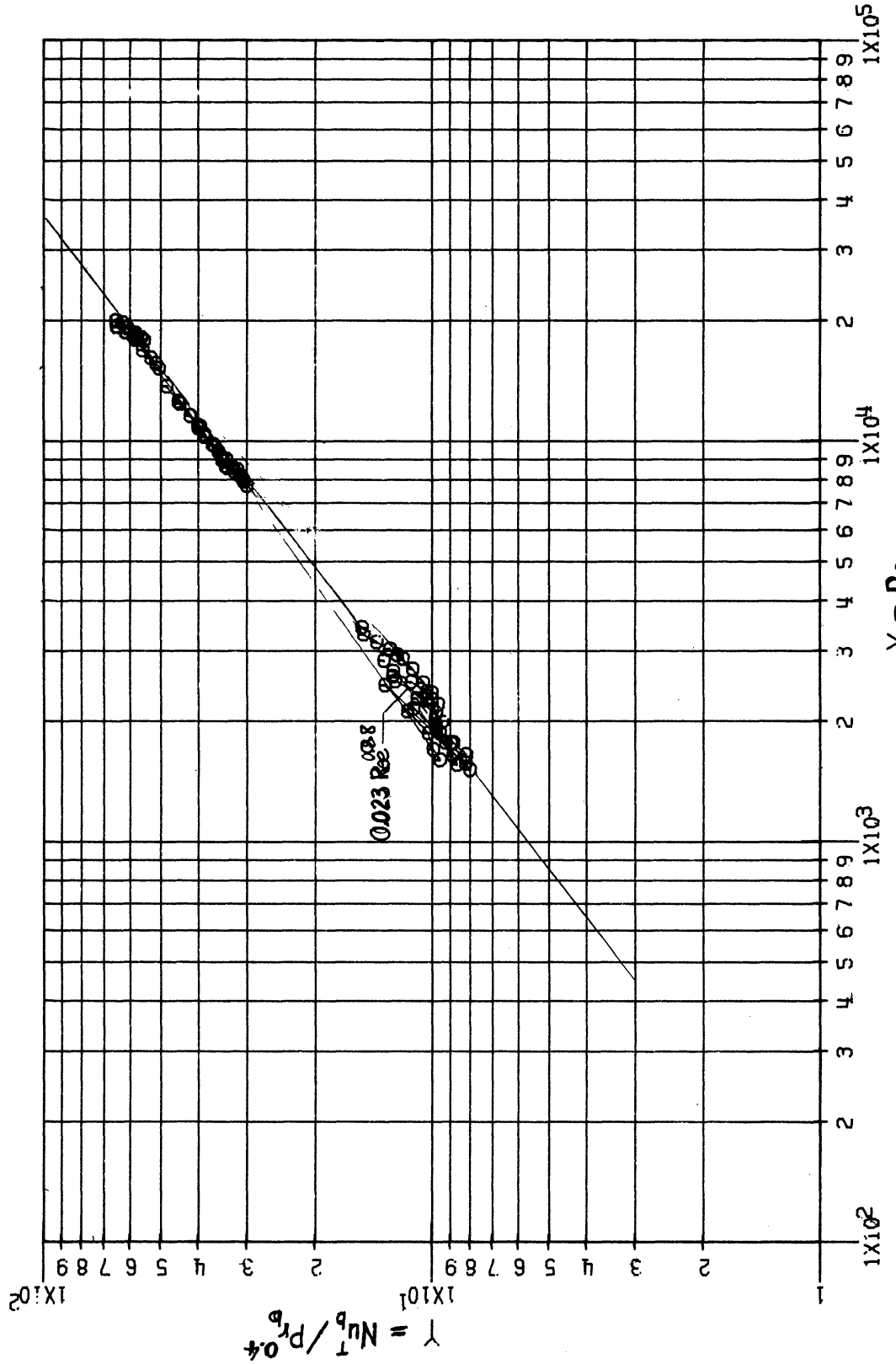

(c) 75 psia

Figure 11. (concluded)

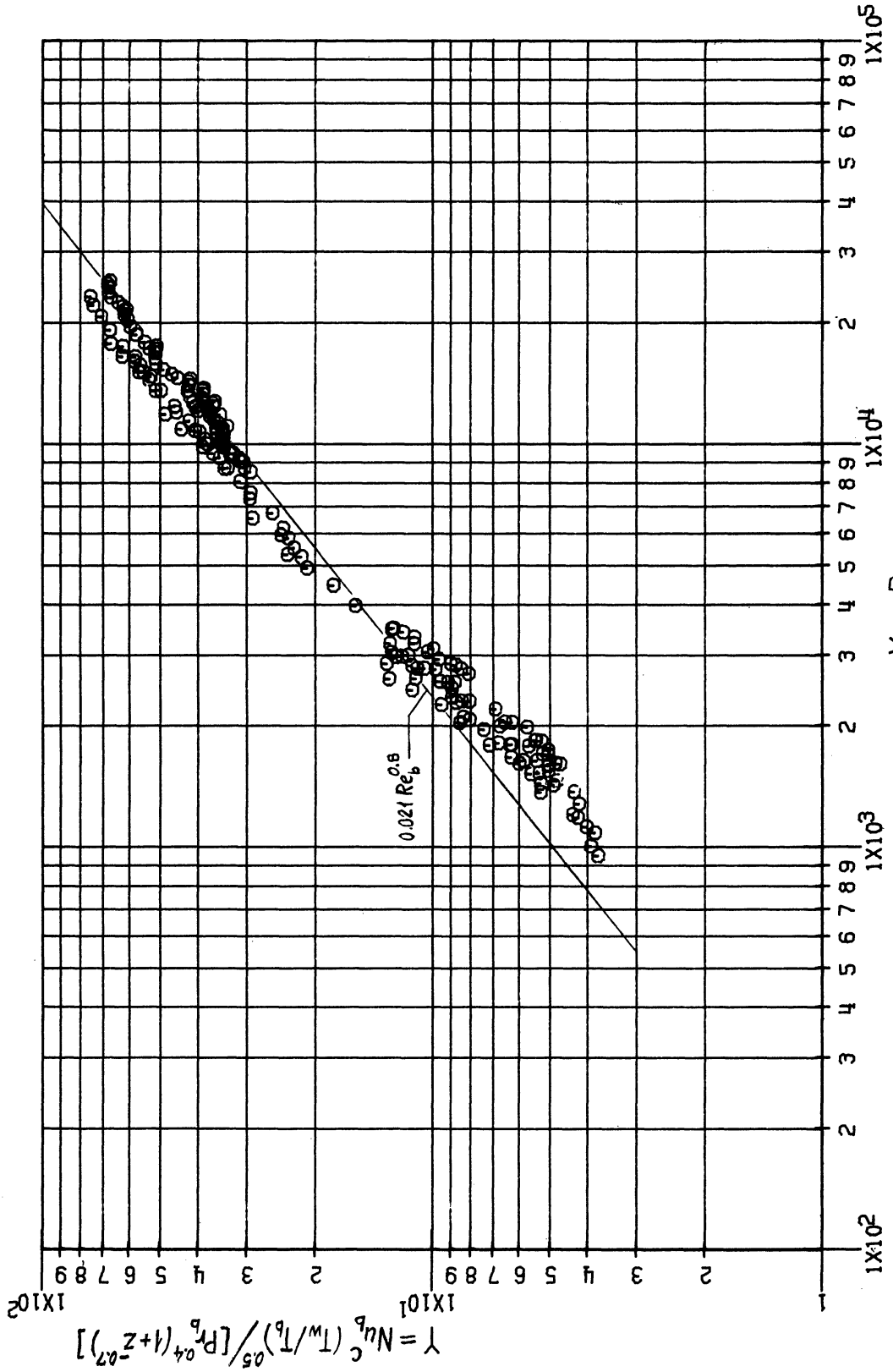

Figure 12. Steam data. Uniform flux SS-310 test section.

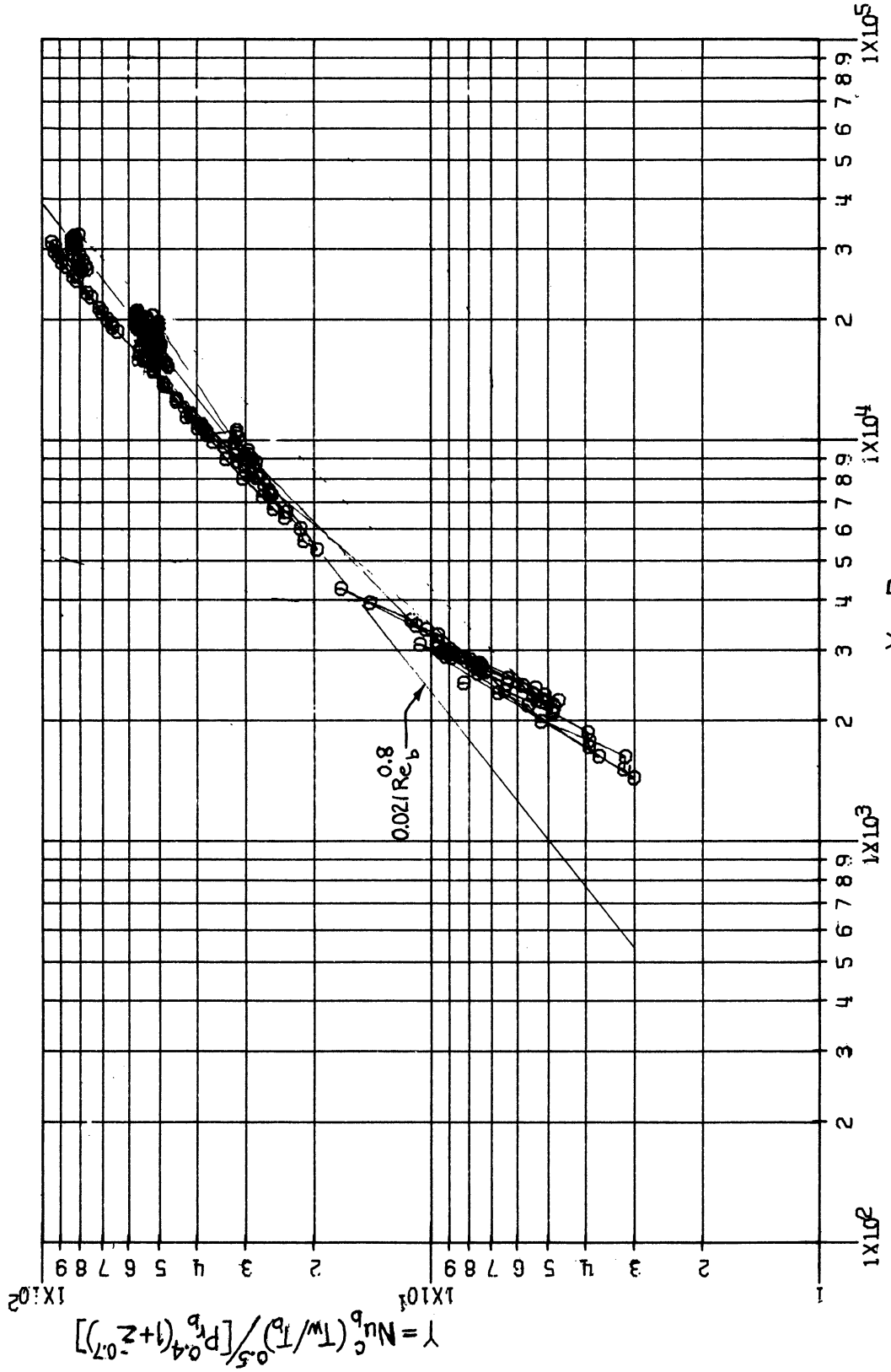

(b) 50 psia

Figure 12. (continued)

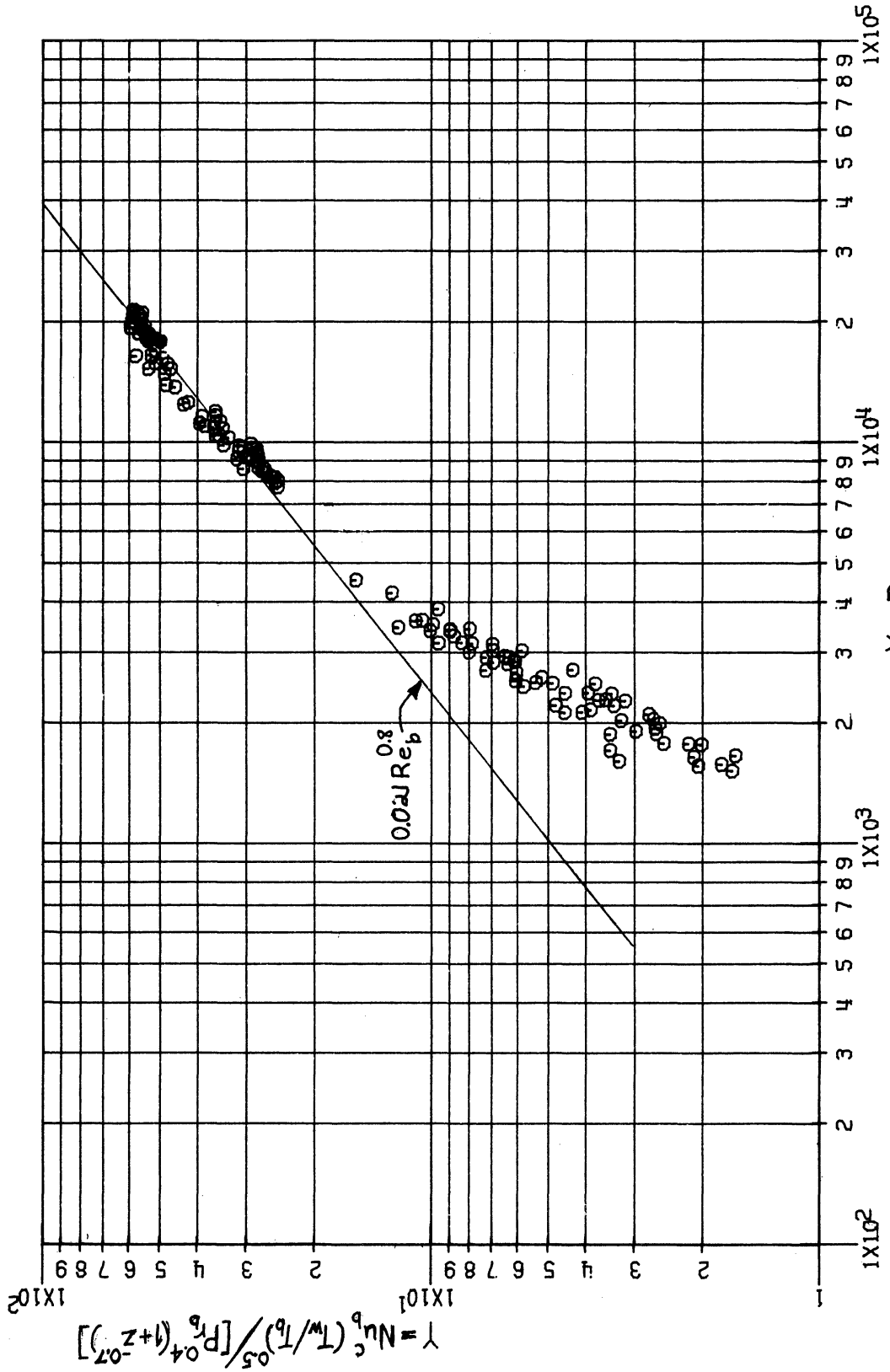

(c) 75 psia

Figure 12. (concluded)

Figures 13a, b, c show measured total local Nusselt number for $7.5 \leq Z \leq 60.2$ and $Re_b > 6000$ versus predicted total Nusselt numbers based on the McEligot correlation, Eq. (3-2), for convective heat transfer and Eq. (3-16) based on gas absorption coefficient data for the radiative heat transfer.

Figures 14a, b, c show similarly measured versus predicted total Nusselt numbers with the difference that radiation is predicted from Eq. (3-20) based the Hottel chart for gas emissivity.

For all pressures the first method gives best general agreement being rather conservative as compared to the second method which tends to overpredict the radiative transfer, particularly at the higher pressures. Neither method is totally satisfactory in accurately predicting the total heat transfer, although the first method based on absorption coefficient data appears to be most promising. The data suggest a pressure and optical thickness correction to the gas absorption coefficient, increasing its value at low temperatures and pressures. The correction is expected to be small at 75 psia (see Figure 13c).

The trend of the data indicated above may also be examined in light of the wall to bulk temperature ratio, T_w/T_b, used as variable property correction factor for the convective heat transfer according to Eq. (4-3). Dropping this factor from Eq. (4-3) would nearly collapse the fully turbulent data of Figures 12a, b, c. However, within the assumption of superposition there is no reason to believe that the variable property effect in convective heat transfer of steam should not follow Eq. (4-3). The magnitude of the factor, T_w/T_b, together with pressure also reflects the magnitude of the optical thickness and it is believed that the thin gas limit for absorption coefficient employed in the prediction of the radiative transfer is the approximation responsible for lack of agreement.

4.3.2. Uniform Flux Zr-2 Test Section

The test conditions for the steam data obtained with the uniform flux Zr-2 test section are listed in Table VIII of Appendix C. The first 10 data runs (105-114) were obtained for wall temperatures up to 900°F. Run 114 showed laminarization. The 8 data runs (115-122) obtained subsequently at maximum wall temperatures up to 1400°F are not considered to be reliable since considerable wall thickness reduction due to outside surface oxidation altered the heat flux distribution significantly.

The data from runs 105-114 is presented in Figures 15a-d in the manner described in Section 4.3.1 above, except that each graph presents all data at the three pressures 25, 50, and 75 psia.

Geometry and fluid being the same as for the steam data of the uniform flux SS-310 test section, only surface emissivity differs. Measurements presented in Appendix D indicate that the wall emissivity of Zr-2 depends on the

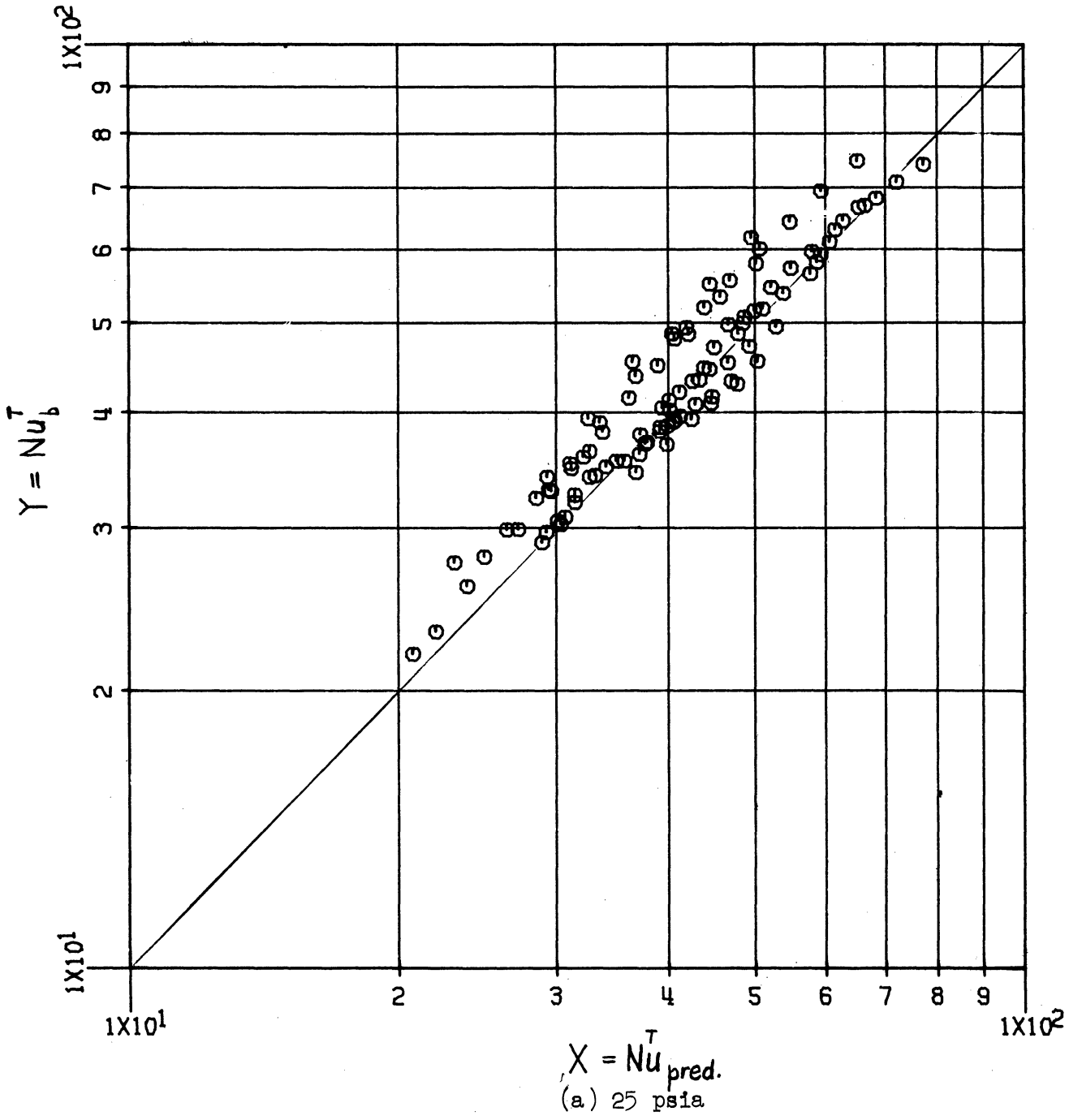

Figure 13. Steam data. Uniform flux SS-310 test section. Measured vs. predicted total bulk Nusselt number based on absorption coefficient.

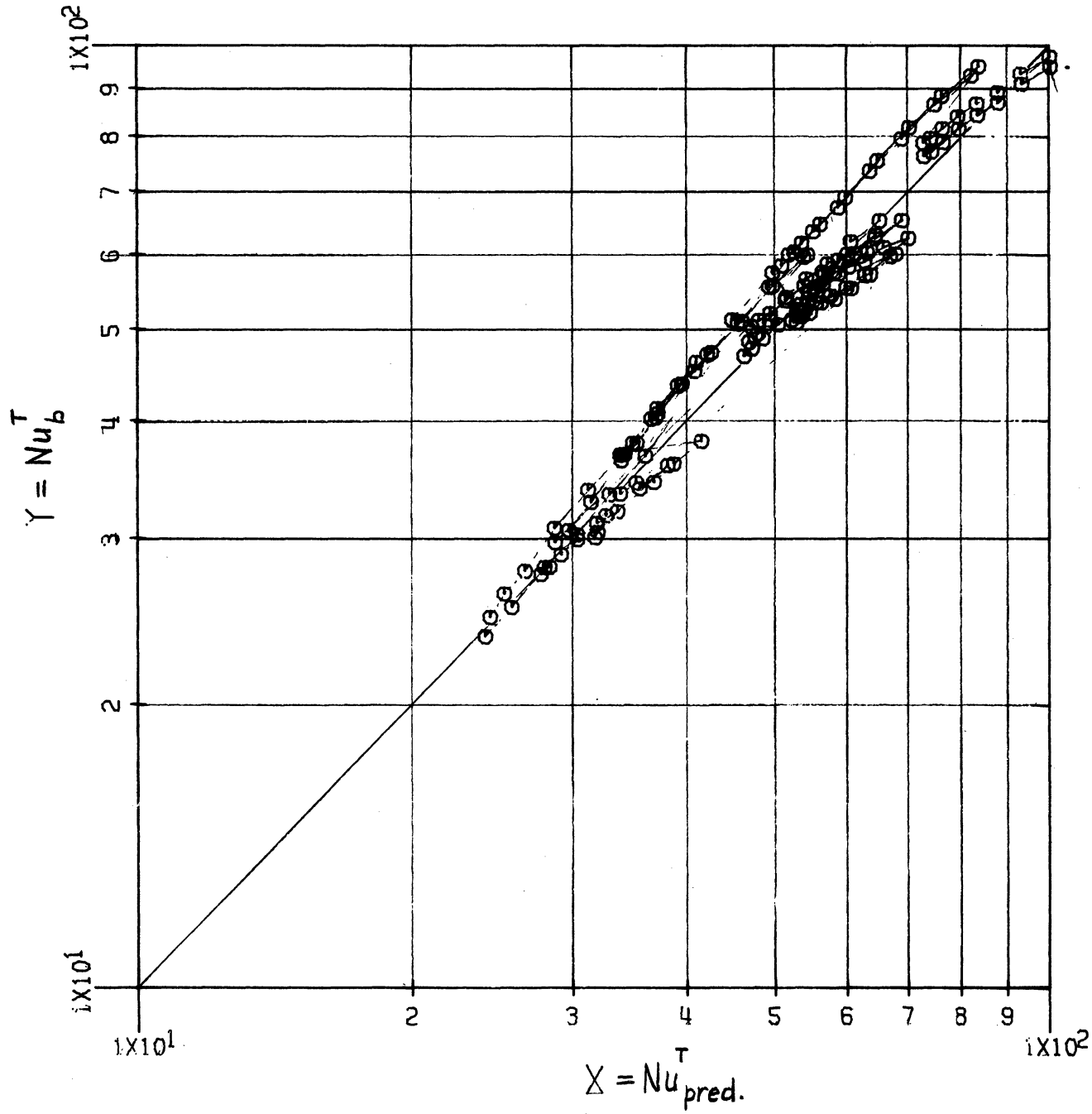

(b) 50 psia

Figure 13. (continued)

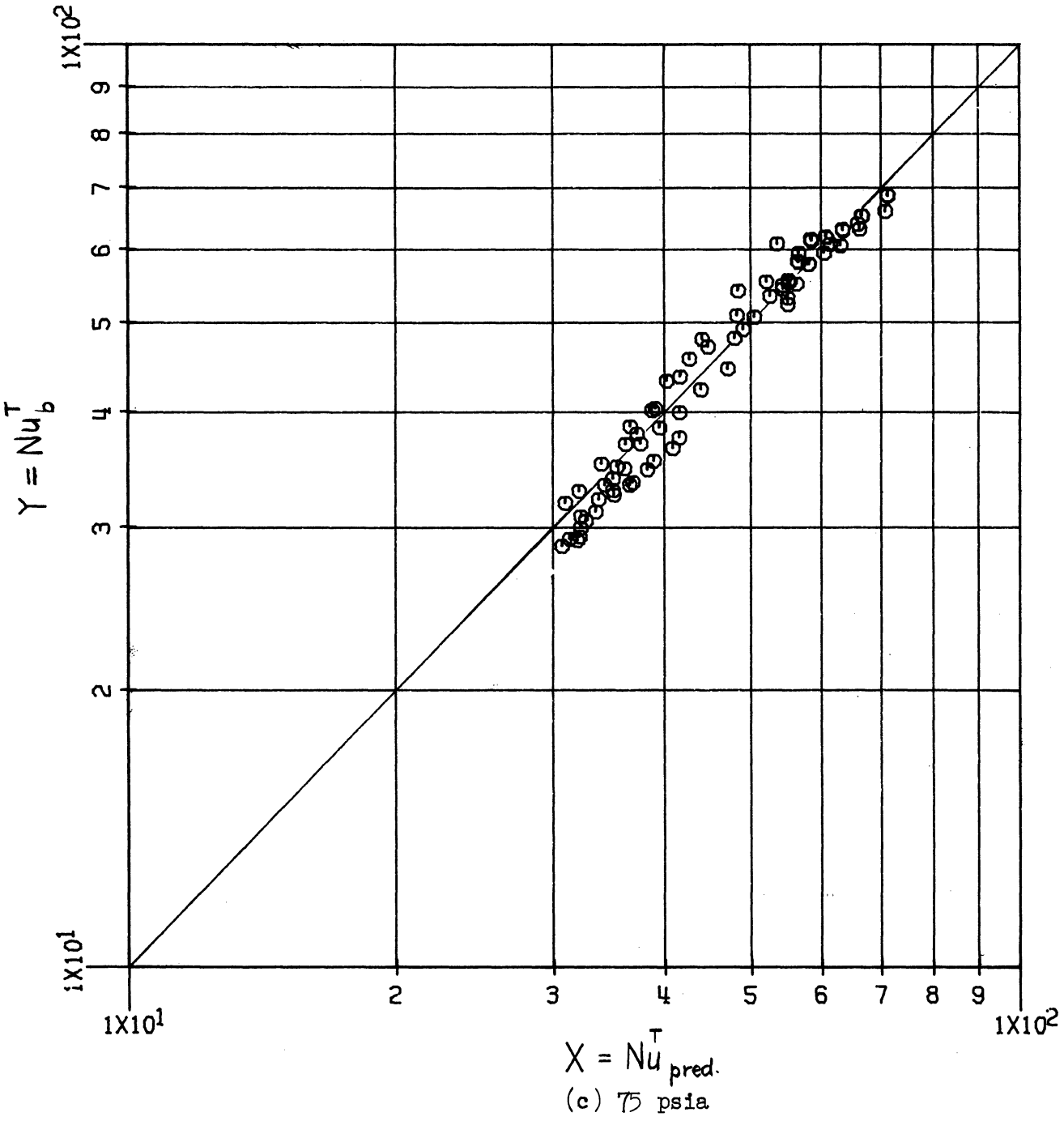

Figure 13. (concluded)

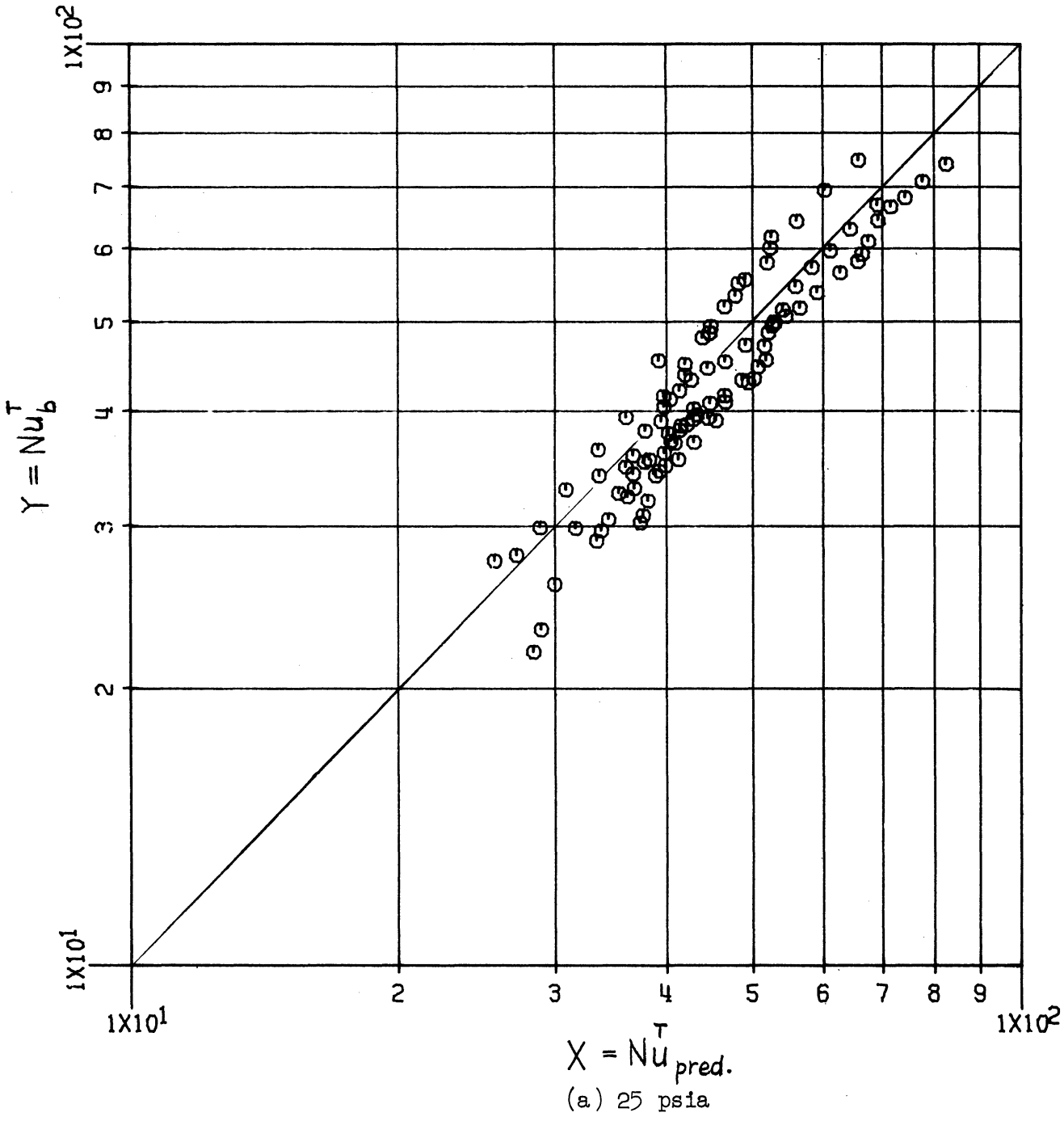

(a) 25 psia

Figure 14. Steam data. Uniform flux SS-310 test section. Measured vs. predicted total bulk Nusselt number based on emissivity.

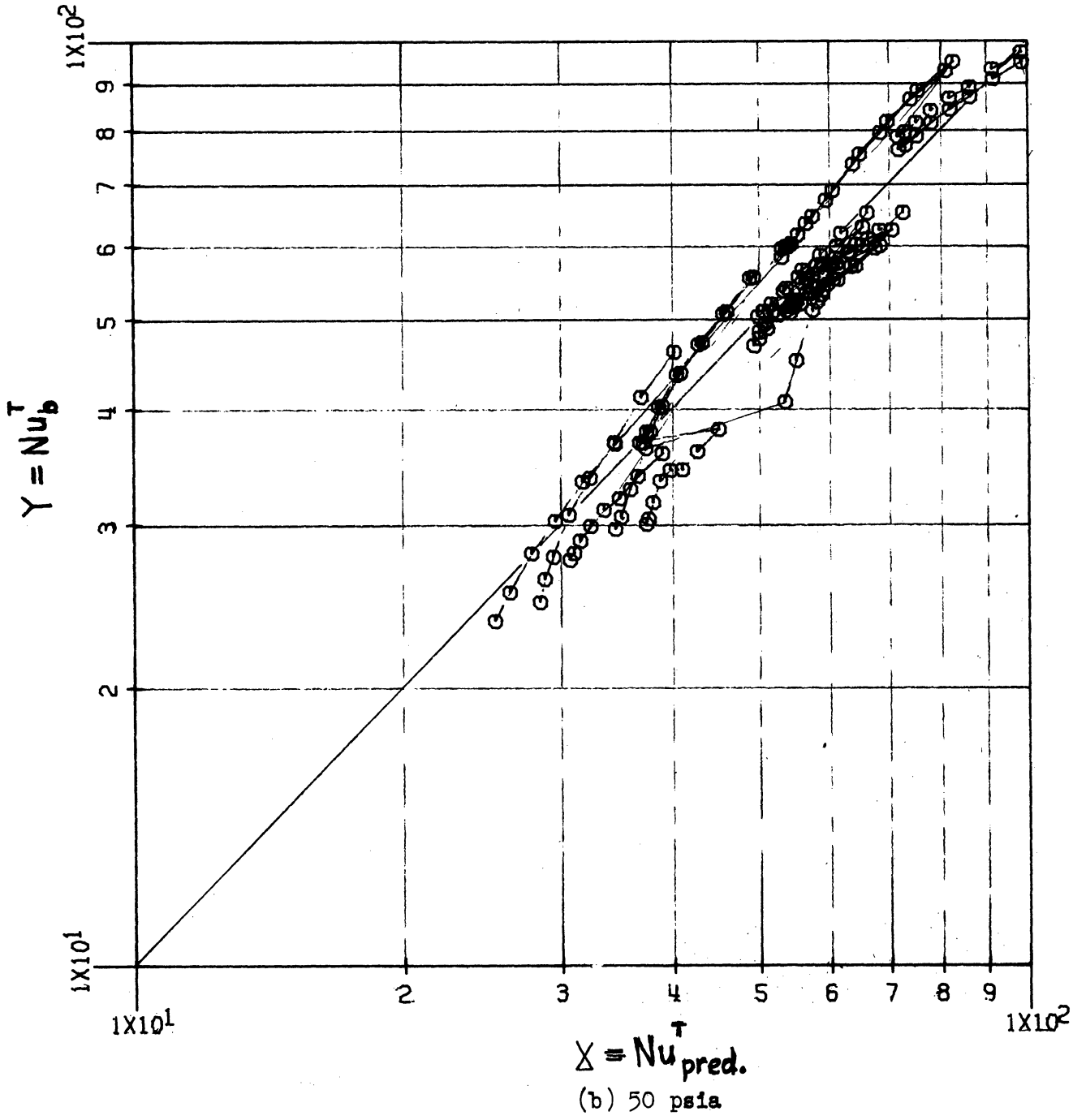

(b) 50 psia

Figure 14. (continued)

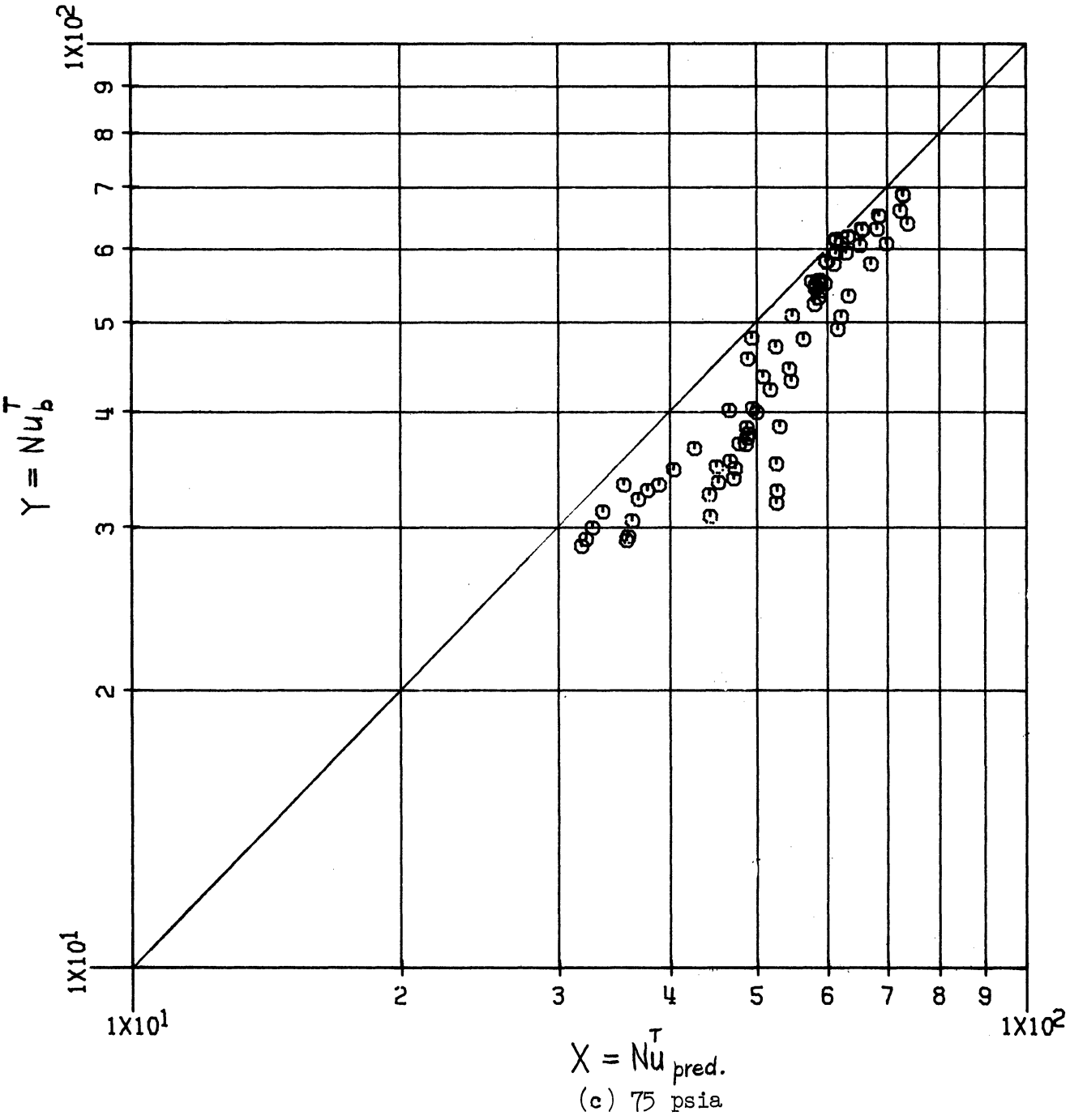

(c) 75 psia

Figure 14. (concluded)

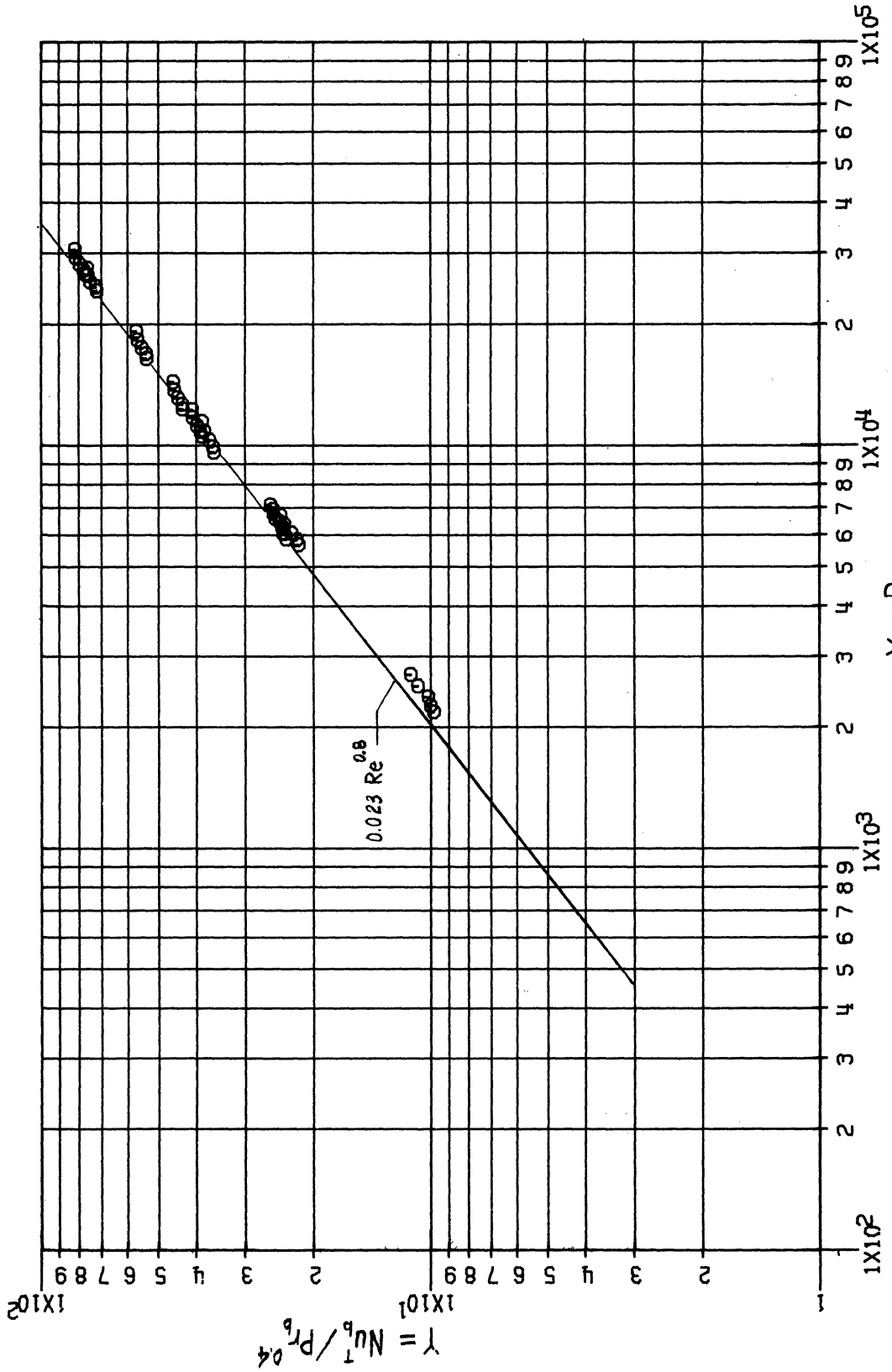

Figure 15. Steam data. Uniform flux Zr-2 test section. All pressures.

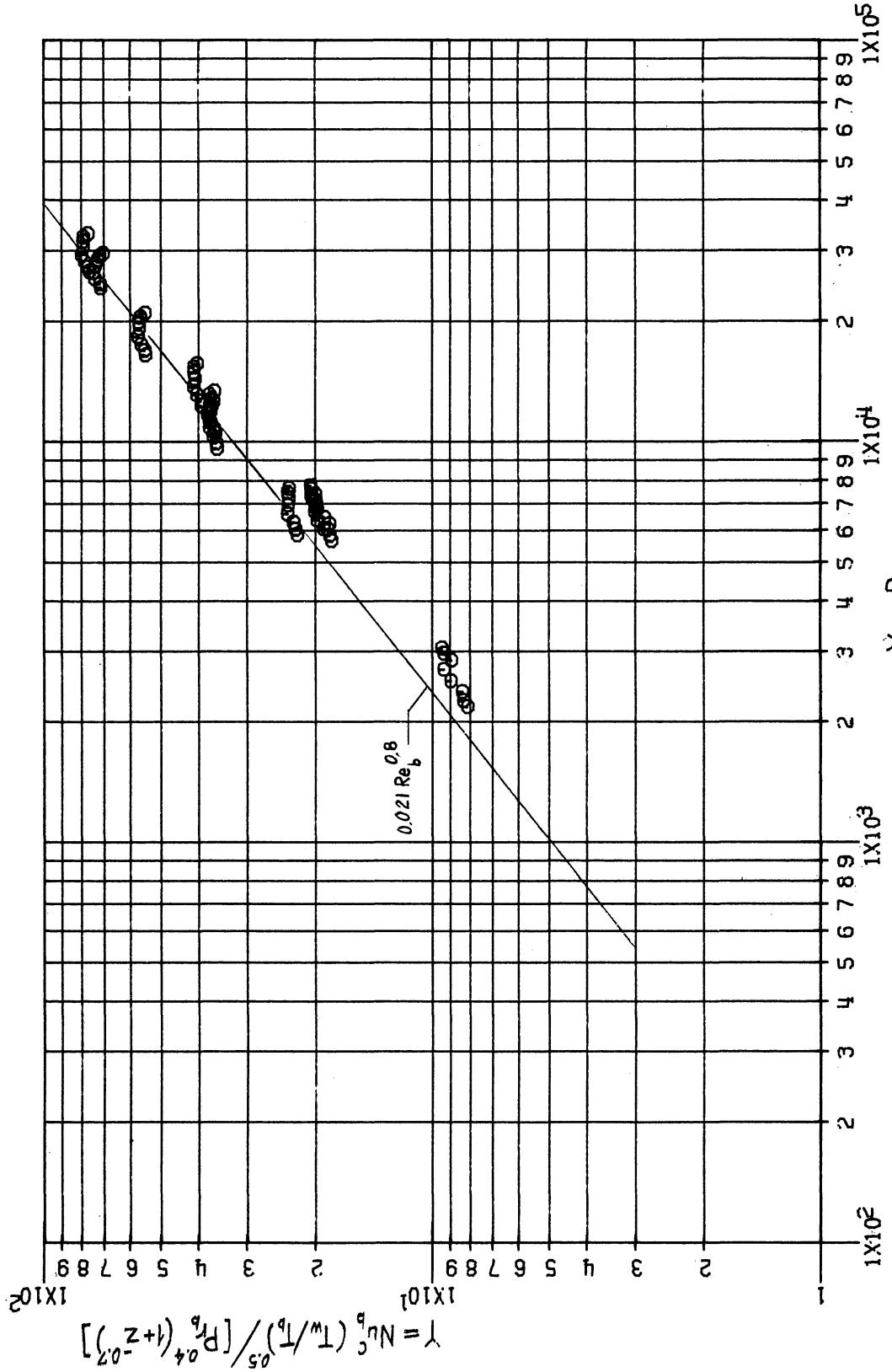

Figure 15. (continued)

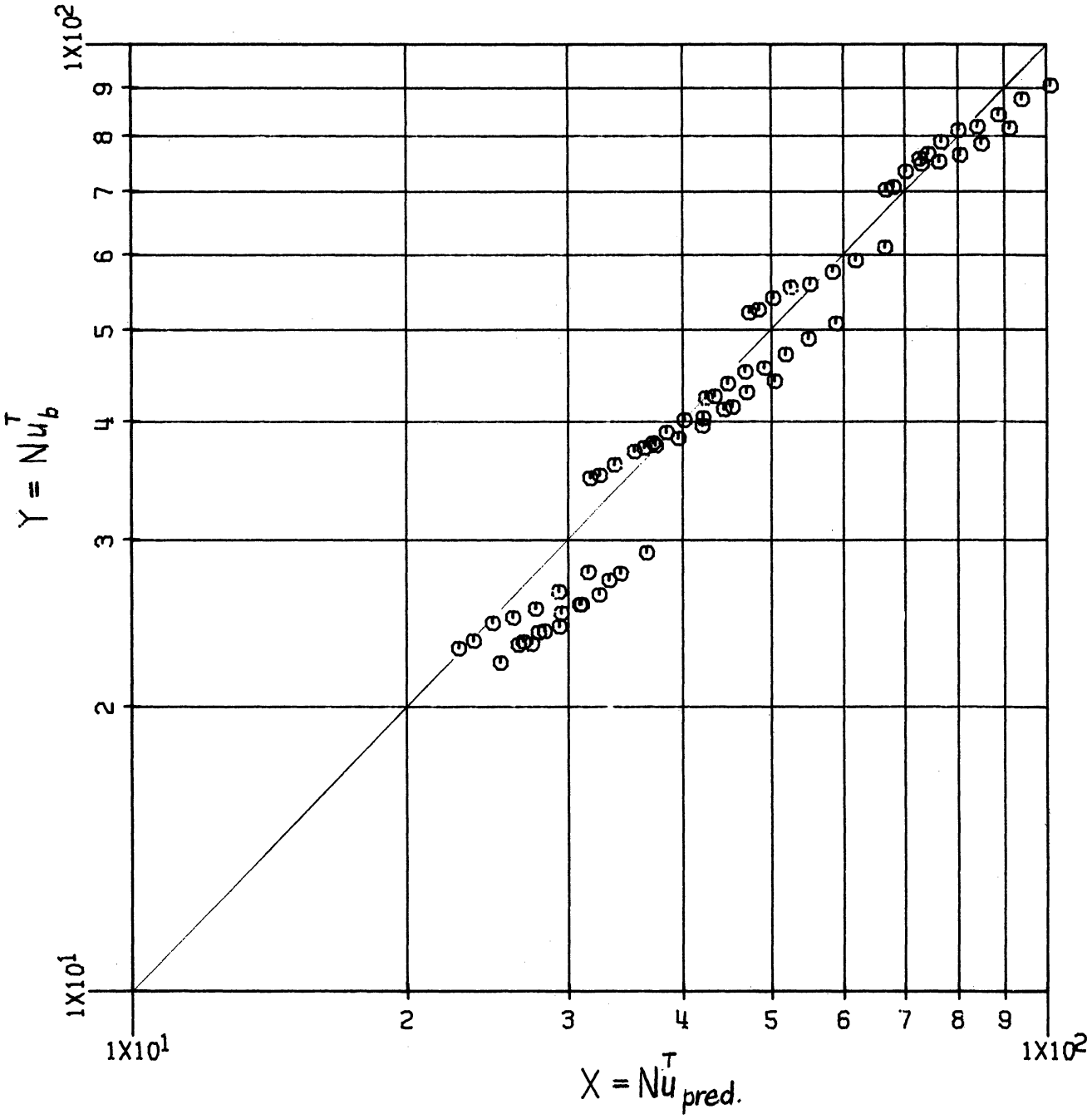

(c) Measured versus predicted total bulk Nusselt number based on absorption coefficient.

Figure 15. (continued)

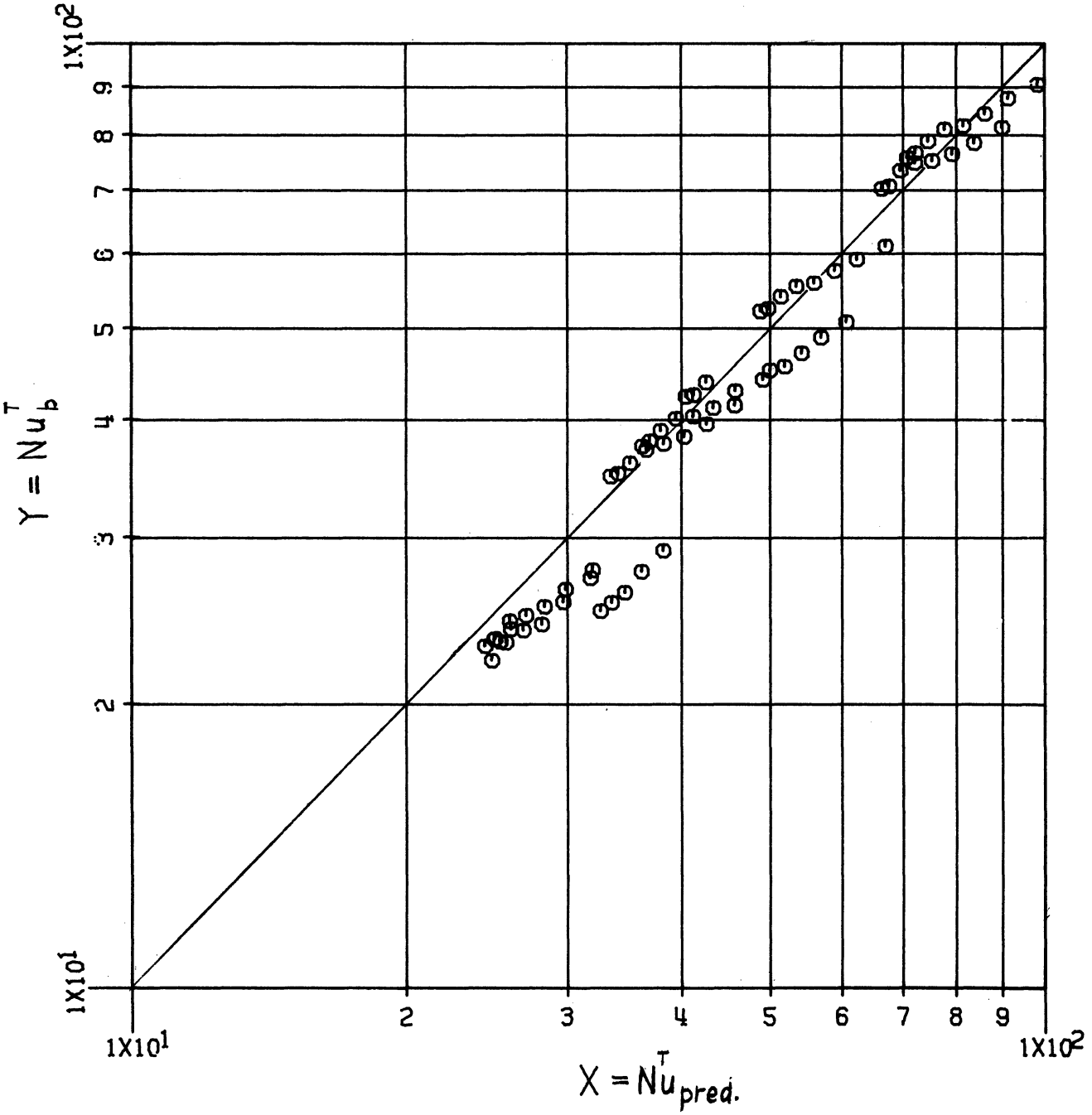

(d) Measured versus predicted total bulk Nusselt number based on emissivity.

Figure 15. (concluded)

nature of the oxide film formed on its surface. The dark oxide observed in the upstream section has a somewhat lower emissivity (0.87) than the light brown oxide found on the downstream section (0.92). The magnitude of the emissivity is approximately that of the SS-310 surface, however.

As for the uniform flux SS-310 test section the Dittus-Boelter correlation predicts total heat transfer to within ±5% for fully turbulent data (Figure 15a). The agreement between the convective heat transfer (obtained by subtracting the radiative heat transfer by Eq. (3-16) from the total measured heat transfer) and the McEligot correlation is less satisfactory for this data (Figure 15b), indicating that the radiative transfer is overpredicted upstream and underpredicted downstream. This is in conceptual agreement with the higher values of surface emissivity of the light brown oxide film observed in the downstream section as compared to the dark oxide film observed upstream. A mean value of effective surface emissivity was employed in the data reduction. The thin oxide film was considered to offer no resistance to heat transfer or to change the flow area.

For completeness the reduced data from the unreliable high wall temperature runs (115-122) is compared in Figure 16 to the Dittus-Boelter correlation. Since increasing run number indicates increased oxidation of the outside surface, particularly in the downstream portion of the test section, the associated wall thickness reduction is expected to yield actual heat fluxes in excess of those calculated assuming constant wall thickness. This trend is confirmed by Figure 16. Although the axial variation in electrical resistance along the test section could be inferred from voltage drop measurements the accuracy of these did not warrant an attempt to treat the data on the basis of specified nonuniform flux distribution.

4.3.3. Nonuniform Flux SS-310 Test Section

Test conditions for the 4 runs (206-209) obtained with the test section having a modified cosine heat flux distribution are listed in Table IX of Appendix C. All of the data except run 209 is considered to be reliable. Due to temperature dependency of electrical resistivity and minor guard heater correction the actual heat flux distribution differs slightly from that calculated for isothermal condition of the tapered wall thickness variation as shown in Figure 17.

All of the data represent fully turbulent flow ($Re_b > 6000$) throughout the test section length. Figures 18a, b show for each run the axial variation of wall and bulk temperatures, total measured Nusselt number, Nu_b^T, convective Nusselt number based on predicted radiative heat transfer by Eq. (3-16), $Nu_b^C = Nu_b^T - Nu_b^R$, and convective Nusselt number based on the McEligot correlation, Eq. (4-3). It is apparent that convective heat transfer cannot be predicted by a uniform flux correlation for large heat flux variations over relatively short test sections. As expected, the measured convective heat transfer

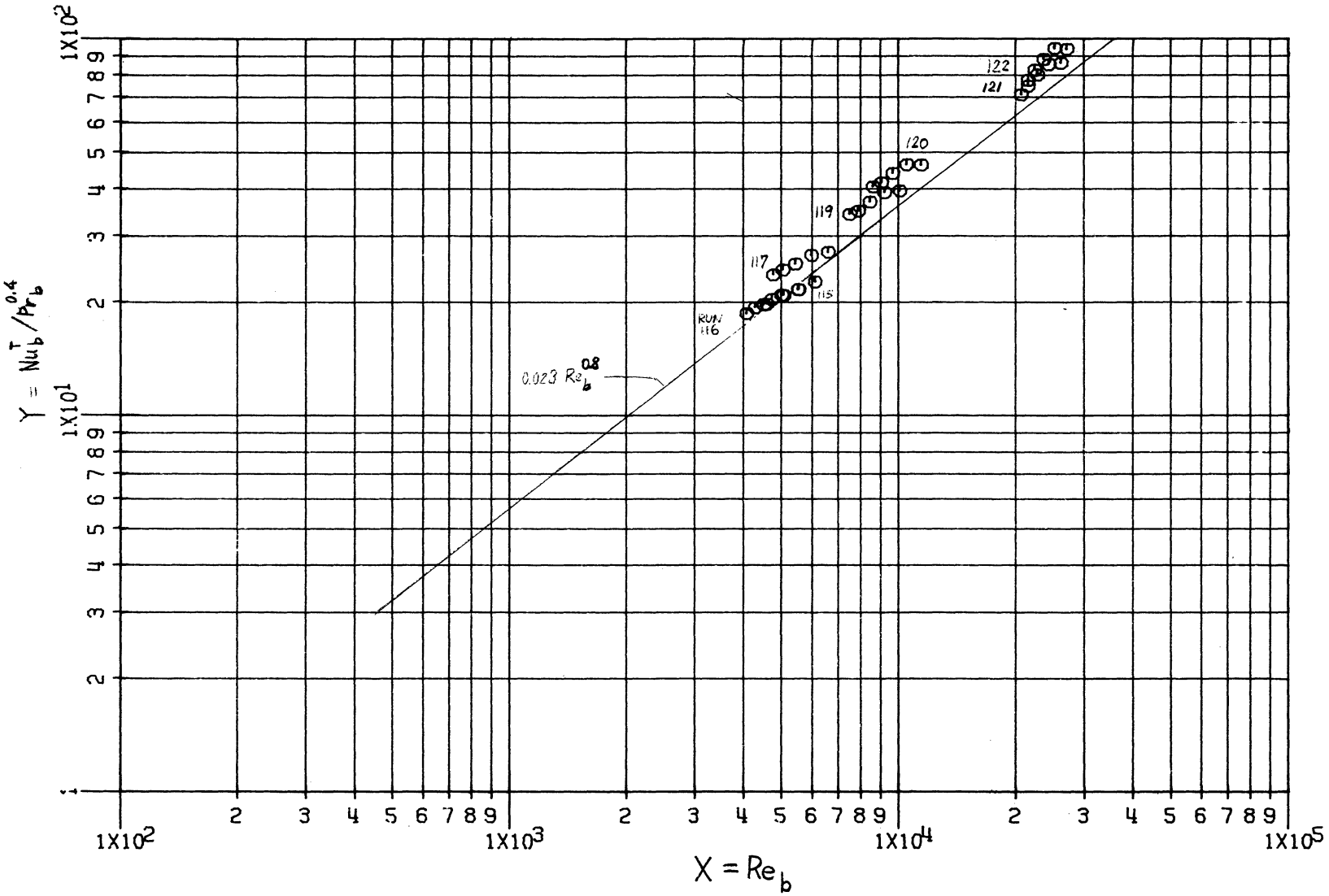

Figure 16. Steam data. Uniform flux Zr-2 test section. High wall temperature runs (nonuniformly oxidized outside surface).

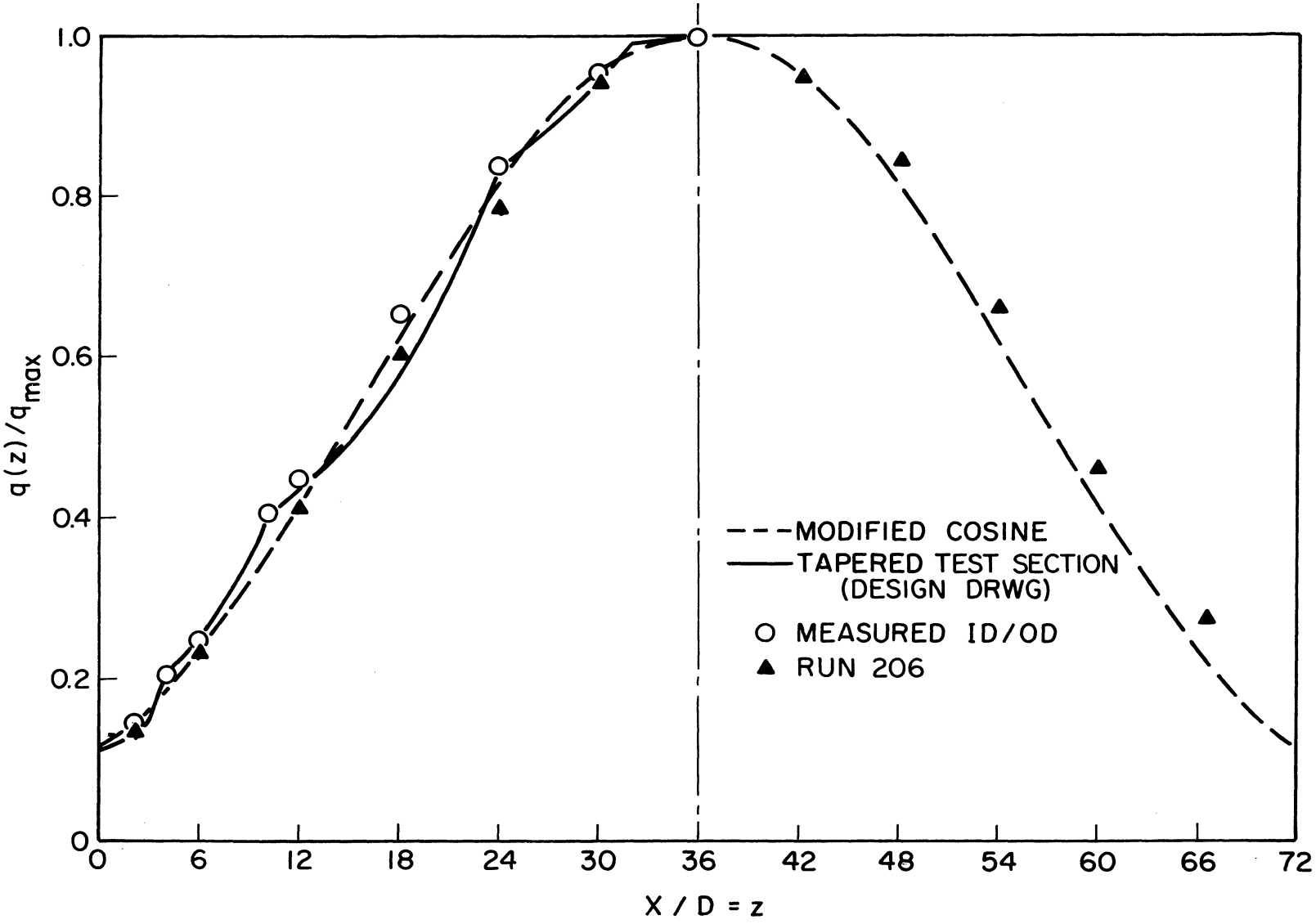

Figure 17. Nonuniform flux SS-310 test section. Theoretical and experimental heat flux distribution.

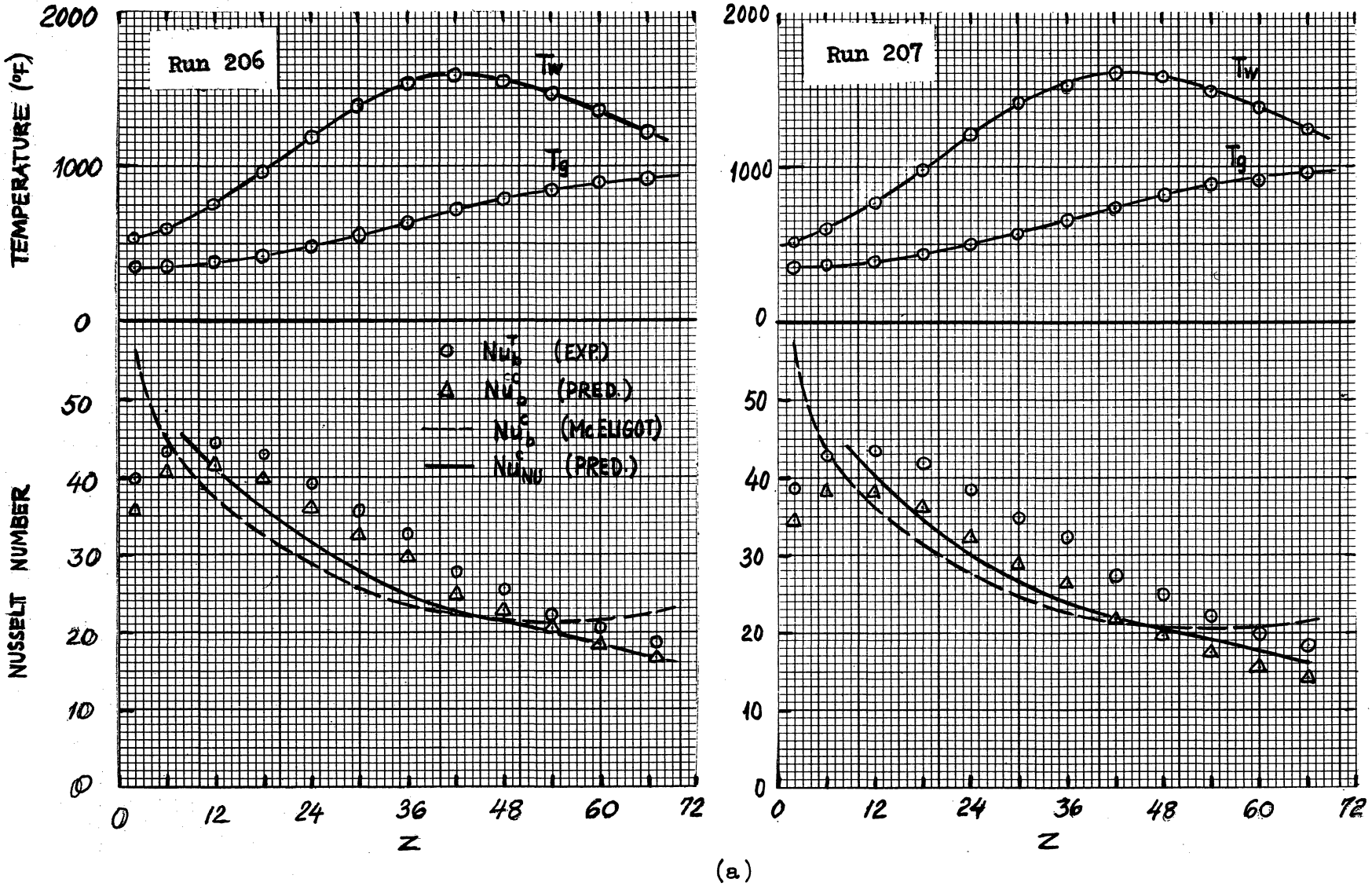

(a)

Figure 18. Steam data. Nonuniform flux SS-310 test section.

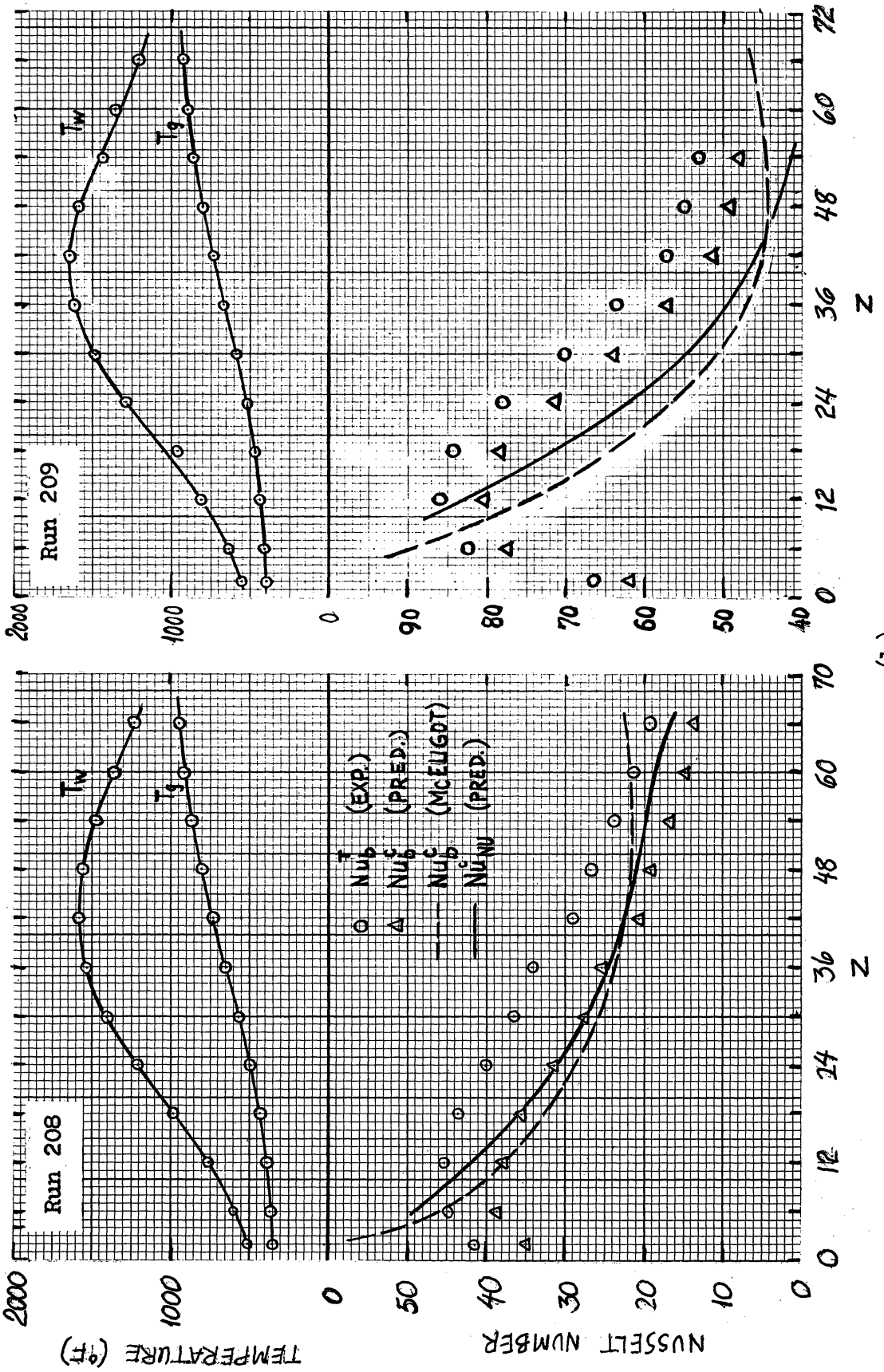

Figure 18. (concluded)

is greater for a downstream increasing heat flux and smaller for a downstream decreasing heat flux as compared to that predicted by a uniform flux correlation.

The equivalent uniform flux convective Nusselt number was evaluated according to the analysis of Section 3.3, Eq. (3-10), however, no satisfactory agreement was obtained with the McEligot correlation. Prediction of the nonuniform convective Nusselt number, Nu^{c}_{NU}, based on Eq. (3-11), however, shows improved agreement, although the convolution apparently does not weigh sufficiently the nonuniformity in heat flux.

The total Nusselt number is compared to the Dittus-Boelter correlation in Figure 19a for $26 \leq Z \leq 60.2$. Again, an increasing heat flux yields a greater and a decreasing heat flux a smaller Nusselt number than that obtained for a uniform flux.

Figure 19b shows measured total Nusselt number for $7.5 \leq Z \leq 60$ versus predicted total Nusselt number based on Eqs. (3-11) and (3-16).

4.4. LAMINARIZATION DATA

A number of runs at bulk Reynolds numbers less than about 6000 indicated retransition from turbulent to laminar flow. Among these runs the data for nitrogen, not obscured by radiative transfer, reveals the following characteristics when compared to fully turbulent data at higher Reynolds numbers or when compared to Eq. (4-3) (see Figure 10c). The measured Nu_b is greater in the entrance region. Beyond Z = 26 the measured Nu_b decreases rapidly downstream, taking values which deviate more and more from those expected for fully turbulent flow and approaching the laminar limit. The inlet bulk Reynolds number for these runs was 3200 to 5000, however, the modified wall-bulk Reynolds number, $Re_{wb} = (GD/\mu_w)(\rho_w/\rho_b)$, believed to be decisive for laminar stability, ranged from 850 to 2000. These characteristics agree qualitatively with the results of the study by Reynolds Jr.[12] for low Reynolds number flows, also denoted transitional or intermittantly laminar/turbulent flows. The beginning laminarization, promoted by the relatively high wall to bulk temperature ratios, reduces sharply the heat transfer coefficient. For the range of bulk inlet Reynolds numbers stated laminarization appears to take over in each case beyond Z = 26, approximately the point where turbulent flow would have become fully developed. The transitional effects upstream of this point are partly masked by the entrance effect. The correlation developed by Reynolds Jr., Eq. (4-5) does not correlate the present data (see Figure 10e), probably because of the present higher (T_w/T_b) - values.

A similar characteristic behavior is evident from the convective heat transfer of the steam data (Figures 12a, b, c). Note that as the pressure, hence the optical thickness, increases the convective laminar limit moves to smaller Nusselt numbers (see Figure 9).

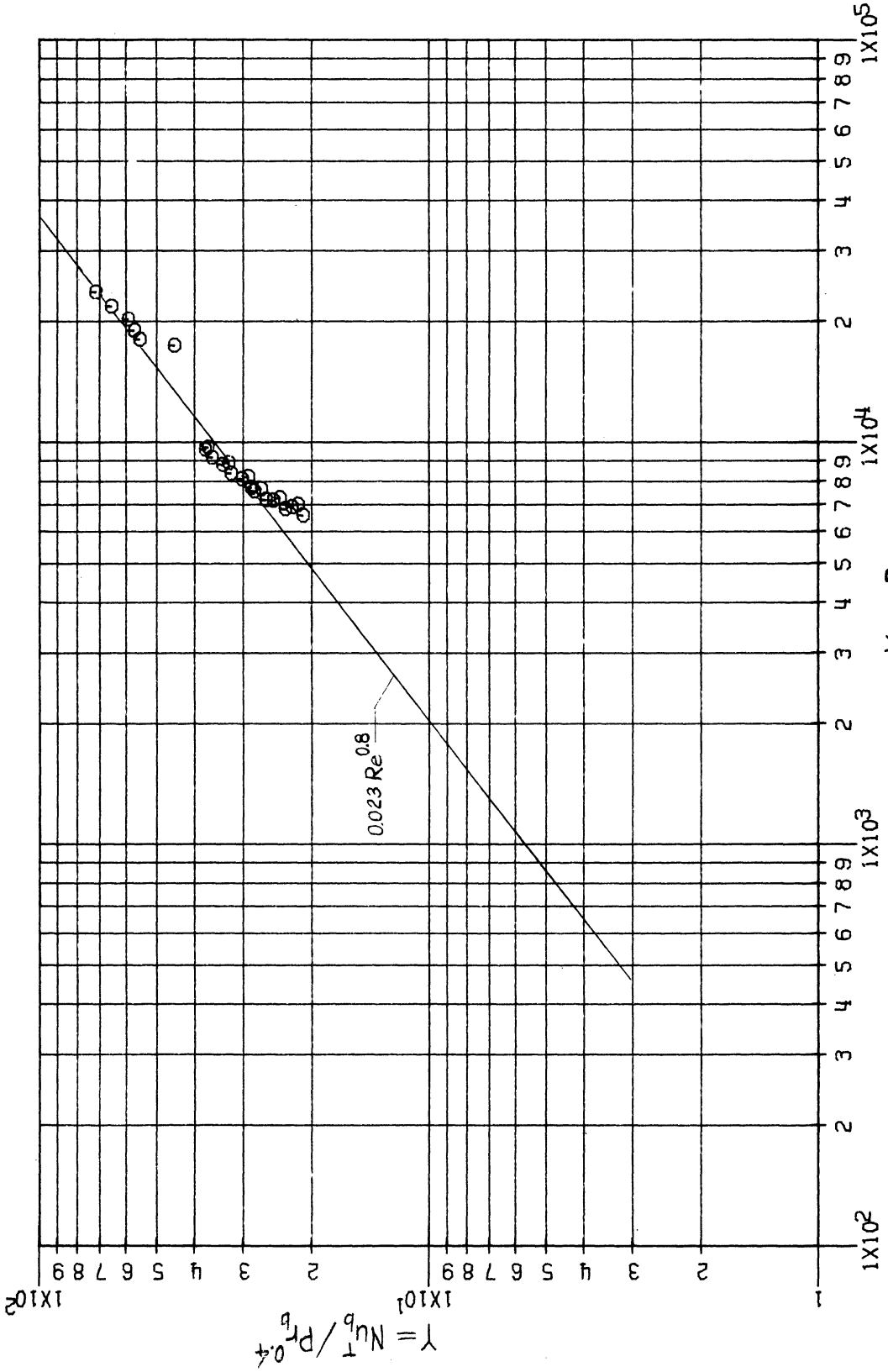

Figure 19. Steam data. Nonuniform flux SS-310 test section.

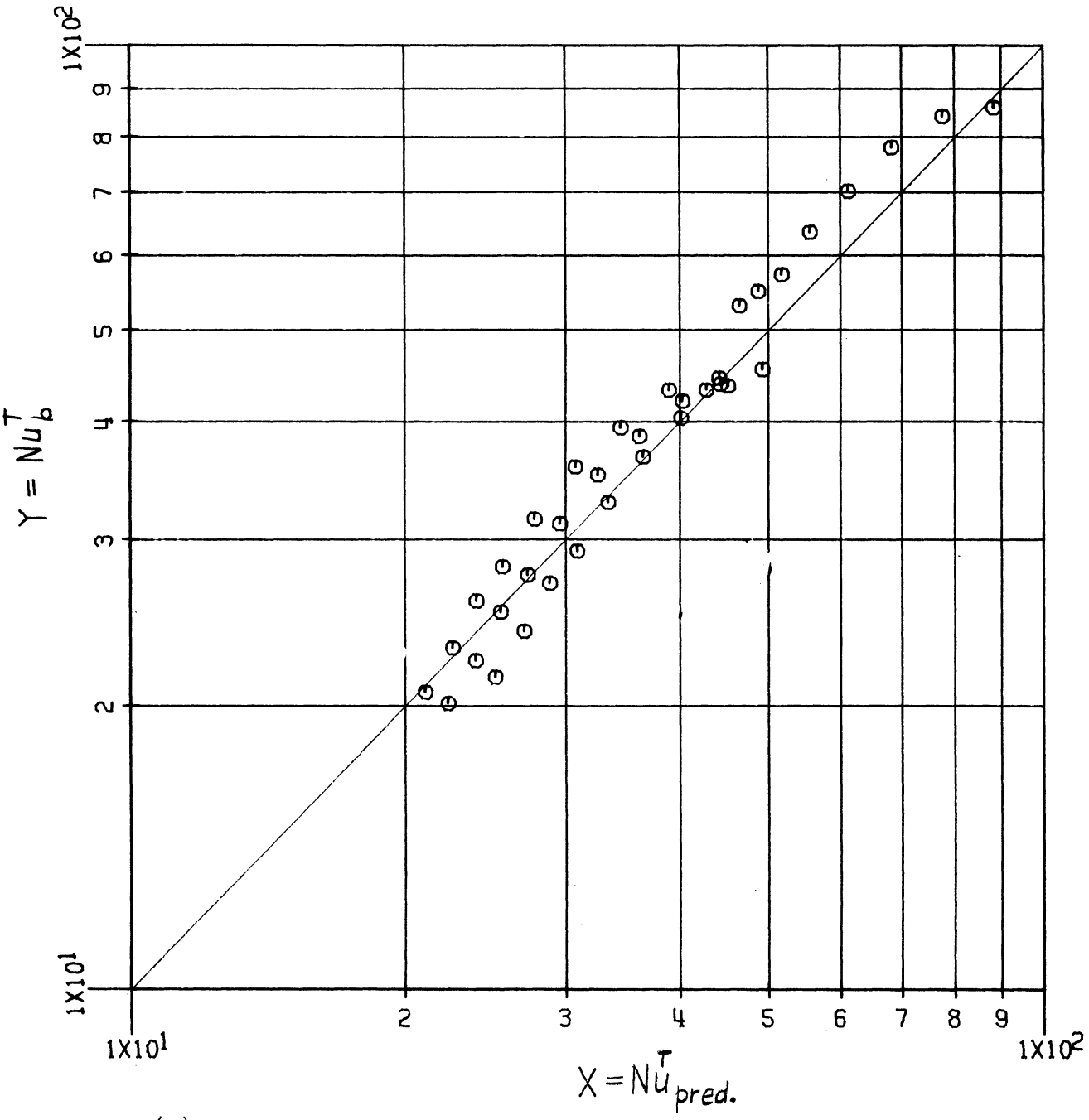

(b) Measured versus predicted total bulk Nusselt number based on absorption coefficient and convolution.

Figure 19. (concluded)

Laminarization appeared in 29 runs. These together with 11 of the lowest Reynolds number runs not showing sign of retransition as judged from consistency with fully turbulent data are listed in Table V. Figure 20 shows the laminar-

TABLE V

LAMINARIZATION DATA AT z = 26
(Run Number in Parentheses Signifies No Laminarization)

Run	Re_b	Re_{wb}	$A*10^6$
Steam—Uniform Flux SS-310			
(24)	7307	2593	0.77
(25)	7347	2660	0.75
(28)	8993	5376	0.27
(29)	8539	5144	0.30
31	2284	774	3.07
33	2300	810	2.75
34	2306	844	2.71
35	2364	860	2.84
36	2593	939	2.68
38	2621	1512	1.22
39	2699	1575	1.13
40	2666	1573	1.18
41	2483	884	2.52
42	2838	1061	2.25
45	1609	641	4.02
46	1985	863	2.86
47	1367	566	4.85
48	2153	943	2.68
49	1900	1055	2.04
72	3290	2210	0.69
73	3147	2054	0.76
74	3197	2054	0.73
(78)	8672	2336	0.82
(81)	8966	3131	0.65
82	2068	684	3.70
83	3147	1022	2.33
84	2462	857	3.31
88	3968	1256	1.74
89	3427	1176	1.98
Nitrogen—Uniform Flux SS-310			
52	3010	2079	3.14
(54)	8500	5860	0.965
55	3600	2654	2.49
92	5297	3255	2.51
93	2723	2327	5.73
Steam—Uniform Flux Zr-2			
(112)	6699	3807	0.37
114	2704	1446	1.19
(115)	6089	2428	0.76
(116)	5508	2261	0.86
(117)	6602	2646	0.78

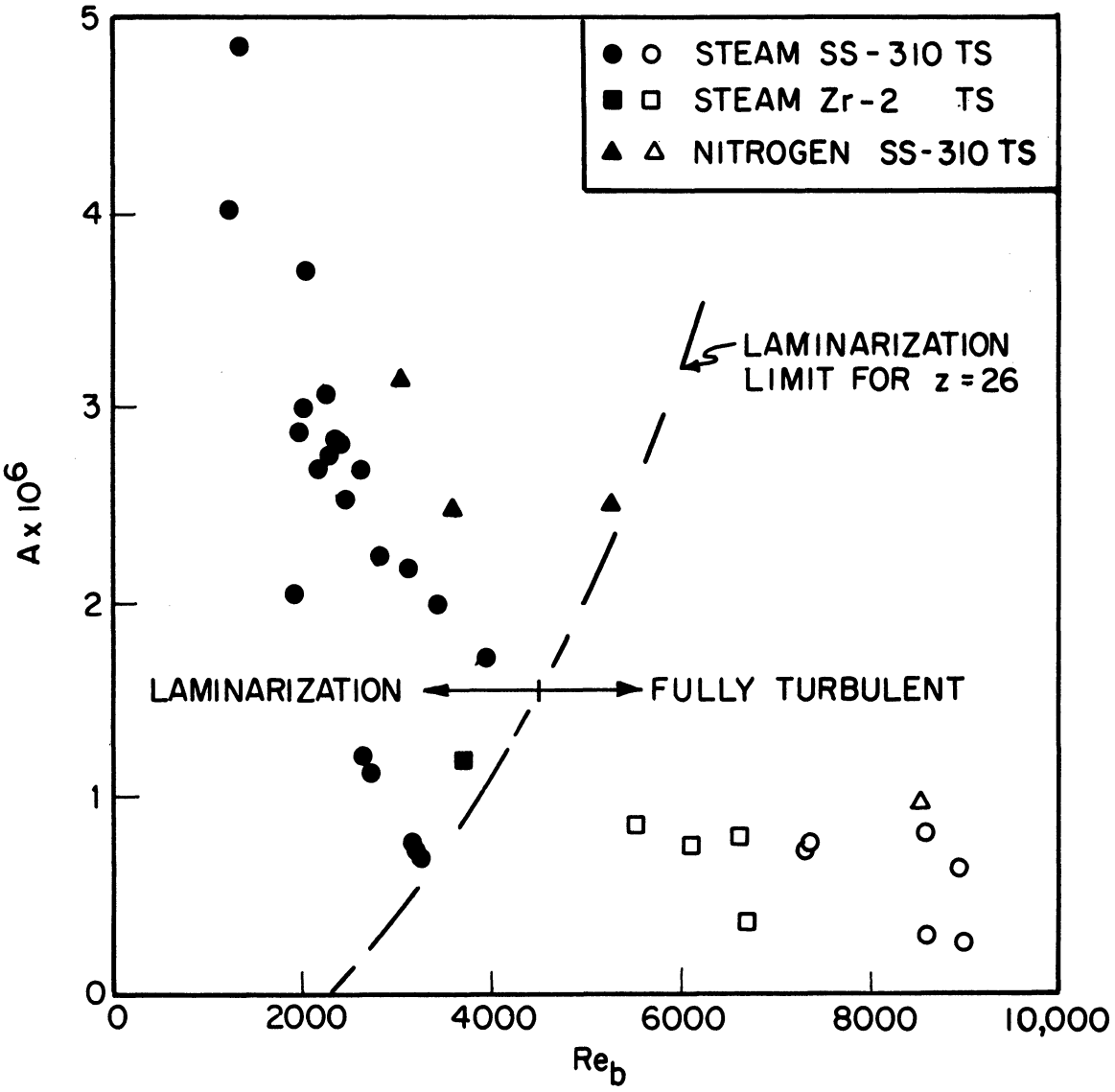

Figure 20. Laminarization parameter vs. bulk Reynolds number, z = 26.

ization parameter A, Eq. (3-31), versus bulk Reynolds number evaluated for each run at the axial position of Z = 26. Although the choice of axial position is somewhat arbitrary the nitrogen data discussed above suggest that laminarization can be expected to be detectable from heat transfer measurements beyond the point where fully turbulent flow would have become fully developed. The line drawn in Figure 20 represents a limit $A_c(Re_b)$,

$$A_c \simeq 0.7 \times 10^{-9} \, (Re_b - 2300) \tag{4-6}$$

below which laminarization may be expected to occur. Inspection of the reduced data shows that A varies less than 10% along the full length of the test section, $7.5 \leq Z \leq 60.2$, while of course the bulk Reynolds number is a steadily decreasing function of axial position. Hence, it is proposed that laminarization may be expected to develop in general from the point where the limit, A_c, of Figure 20 is passed if here $Z \gtrsim 20$.

An approximate evaluation of the heat transfer in the laminarization region for a transparent gas is proposed in the form

$$Nu_b = Nu_b^L + (Nu_b^T - Nu_b^L) \, f(Z,A,Re_b,\ldots) \tag{4-7}$$

where superscripts L and T refer to laminar and turbulent flow, respectively, and $f(Z,A,Re_b,\ldots)$ is a probability distribution function describing the likeliness that turbulent flow persists.[18] For large Re_b and small A f = 1, but for small Re_b and large A f is expected to asymptotically vanish with increasing Z. Figure 21 shows

$$f(z) = \frac{Nu_b - Nu_b^L}{Nu_b^T - Nu_b^L} \text{ vs. } z, \tag{4-8}$$

with $Nu_b^L = 48/11$, Nu_b^T from Eq. (4-3), and Nu_b equal to the measured Nusselt number for the nitrogen runs: 50, 51, 52, 55, 92, 92. Although there is considerable scatter, particularly in the entrance region and near the exit, Figure 21 suggests an exponential function

$$f \simeq \exp[- C_1 A \times 10^6 (z - z_o)].$$

Taking $z_o = 20$, runs 50, 51, 52 suggest $C_1 = 1.27$ while runs 55, 92 suggest $C_1 = 1.32$. The transparent gas data of the present study is insufficient to establish a firm correlation for the complex laminarization phenomenon.

The steam data, further complicated by the radiation-convection interaction, cannot be examined in the simple manner of Eq. (4-7). Fully laminar data, however, has been analyzed as discussed below. The asymptotic laminar limit for total Nusselt number is given in Figure 9.

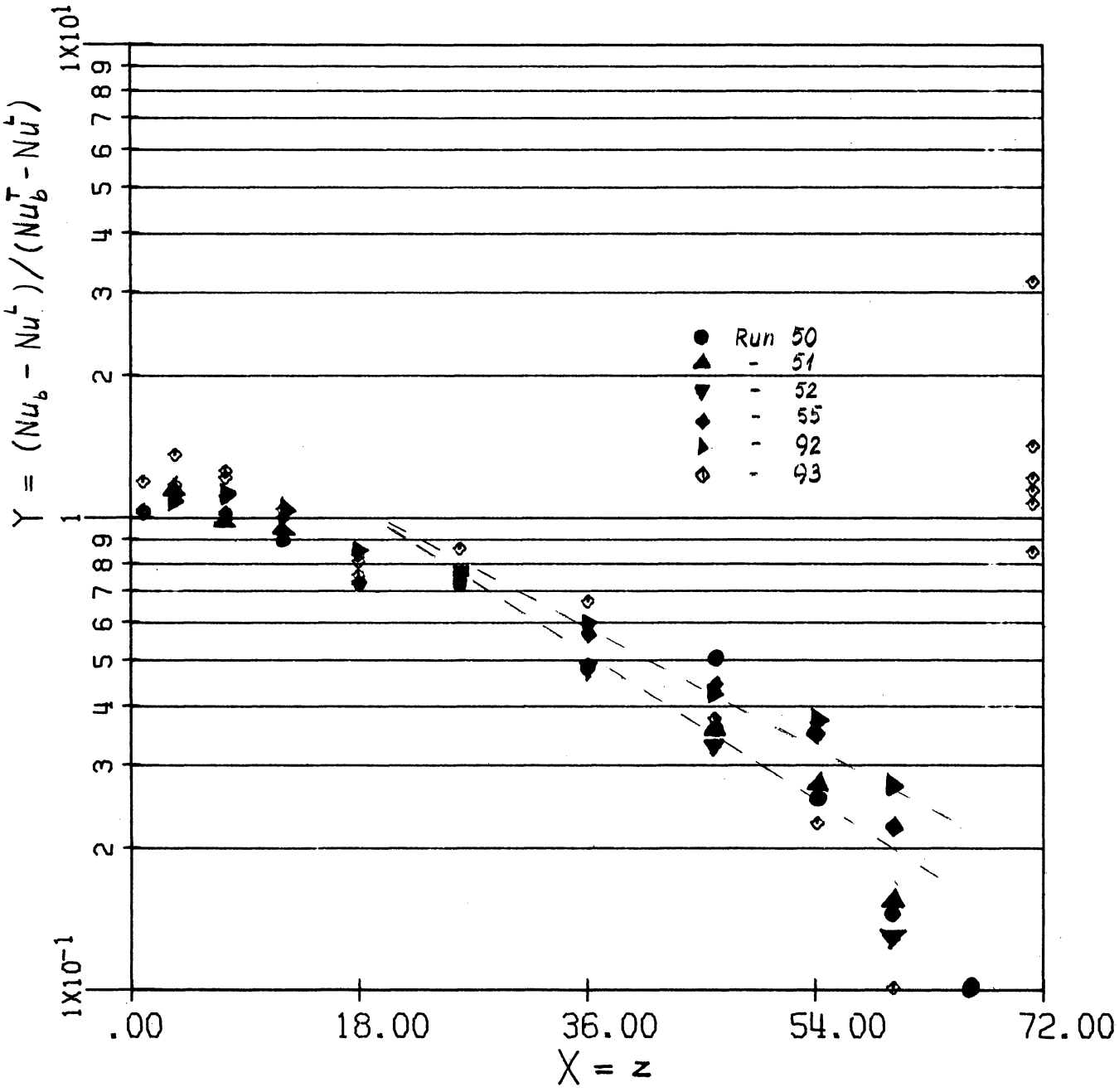

Figure 21. Nitrogen data. Uniform flux SS-310 test section. Function f(z).

4.5. LAMINAR DATA FOR STEAM

A total of three runs (45, 47, 49) obtained with the uniform flux SS-310 test section provided fully laminar data, the inlet Reynolds numbers being respectively 2173, 1873, and 2175. Because of the short test section a condition of fully developed laminar flow was only approached near the exit. The data is compared to Eq. (3-33) in Figure 22. The data appears to be 10-15% higher than the theory in the upstream region but approach the correct fully developed limit to within 5% further downstream. It should be noted that for the three runs the ratio of experimental to fully developed Nusselt number is respectively 1.37, 1.31, and 1.80. The theory therefore accounts well for the development region, too.

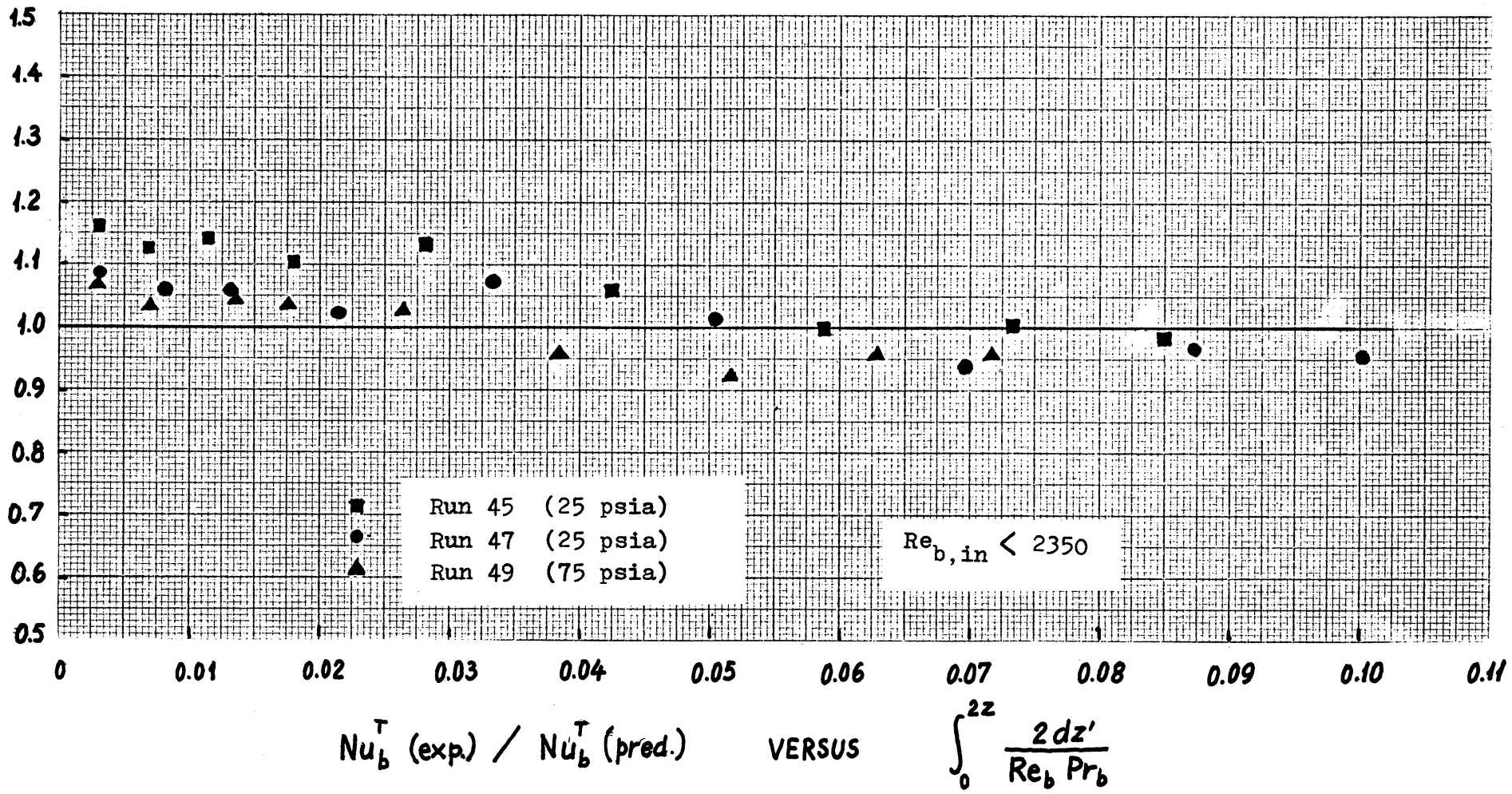

Figure 22. Laminar steam data. Uniform flux SS-310 test section. Ratio of experimental to theoretical total Nusselt number vs. nondimensional axial position.

5. SUMMARY AND CONCLUSIONS

An experimental facility was designed and constructed for the measurement of total convective and radiative heat transfer to steam at 12 local stations along 36-in. long by 0.5 in. I.D. uniformly and nonuniformly heated test sections. Data was obtained for three pressures (25, 50, 75 psia), three inlet temperatures (300, 700, 1100°F) and inlet bulk Reynolds numbers in the range 1900-35,000, with local bulk Reynolds numbers as low as 420. Wall to bulk temperature ratios ranged from 1.1 to 2.11 at heat fluxes from 2400 to 31,000 Btu/hr-ft^2 and at wall temperatures up to 1800°F.

Two uniform flux test sections (SS-310 and Zr-2) and one nonuniform flux test section (SS-310) having a modified cosine flux distribution of q_{max}/q_{mean} = 1.66 were employed. Data was obtained for fully turbulent flow, retransition flow with laminarization and fully laminar flow.

Fully turbulent convective heat transfer data for a transparent gas (nitrogen) was found to agree with the McEligot correlation

$$Nu_b = 0.021\ Re_b^{0.8}\ Pr_b^{0.4}\ (T_w/T_b)^{-0.5}(1 + z^{-0.7})$$

for $z \geq 5$ and $Re_b \geq 6000$.

Total convective and radiative heat transfer for fully turbulent flow of steam was found to agree to within $\pm 5\%$ with the Dittus-Boelter correlation

$$Nu_b^T = 0.023\ Re_b^{0.8}\ Pr_b^{0.4}$$

for $26 \leq z \leq 60.2$ and $Re_b \geq 6000$. The same equation correlates total heat transfer for steam at bulk Reynolds numbers of 1000 to 6000 to within +10% and -20% for all of the pressures investigated. It is concluded that radiative transfer to steam approximately makes up for the expected reduction in convective heat transfer due to variable properties for $Re_b > 6000$ and in addition makes up for the reduction due to laminarization in the range $1000 < Re_b < 6000$. Thermal radiation accounts for approximately 10-30% of the total heat transfer at Reynolds numbers above 6000 but may account for as much as 50-80% of the total at low Reynolds numbers.

Based on sample calculations axial wall-wall and wall-gas radiative transfer is found to be negligible for the present parameter ranges and may be ignored. Based on the assumption of superposition of convective and radiative

heat transfer in fully turbulent flow it is found that one-dimensional radiative heat transfer is well predicted based on the thin gas limit for the absorption coefficient of steam at the higher pressures and smaller optical depths. This procedure underpredicts the radiative heat transfer at lower pressures and higher optical depths. Use of steam emissivity data from the Hottel chart in a one-dimensional model overpredicts radiative heat transfer with an increasing amount as the pressure increases.

Resulting from high heat transfer rates to a gas with large property variation in the wall region retransition from turbulent to laminar flow appears at bulk Reynolds numbers in excess of 2300. The maximum observed value for nitrogen was 5300. Data indicates that retransition is a function of bulk Reynolds number and a laminarization parameter, A. Laminarization occurs if at $z \gtrsim 20$ a critical value is exceeded,

$$A = -\frac{1}{\rho_b}\left(\frac{\partial p}{\partial h}\right)_b \frac{4q''}{GRe_b} > A_c \cong 0.7 \times 10^{-9}\,(Re_b - 2300) \quad .$$

Nonuniform heat flux data shows that local correlations developed for a constant heat flux predict heat transfer in error by as much as 30% in the development range for large heat flux changes over a relatively short test section. Improved agreement results with use of superposition integral.

Fully laminar heat transfer to steam, including the thermal entrance length, is predicted to within 10-15% over the upstream 30 diameters and to within 5% downstream on the basis of a radiation-convection interaction analysis.

APPENDIX A

DATA REDUCTION ANALYSIS AND COMPUTER PROGRAM

I. INTRODUCTION

The experimental arrangement is shown on Figure 23, which is a schematic diagram of the loop, and on Figure 24 which is a sketch of the loop test section. The gas, either steam or nitrogen, is fed through a flow control valve, an orifice flow meter, a preheater, into the test section, and is discharged to the atmosphere through an aftercooler and a pressure control valve. Gas pressure, temperature, and manometer deflection are measured at the orifice, gas pressure and temperature are measured somewhat upstream of the test section, and gas temperature is measured somewhat downstream of the test section at the mixing chamber. Wall guard heater and lug heater temperatures are measured as indicated on Figure 24.

The purpose of the data reduction program is to calculate the following dimensionless quantities at each axial position along the test section where the wall temperature is measured:

$$\mathrm{Nu},\ \mathrm{Re},\ \mathrm{Pr},\ T_w/T_b, \mathcal{P},\ \tau_o \quad .$$

To accomplish this it is first necessary to obtain the following quantities:

$$q_{cor},\ T_b,\ T_w,\ \rho,\ \mu,\ C_p,\ k,\ \alpha \quad .$$

For the tube having uniform wall thickness, the experiment has been designed to approximate the case of uniform heat flux to the gas as closely as is practical. Thus as a first approximation q_{cor} = power/length, T_b simply increases linearly from T_{in} to T_{out}, and since the wall is thin, the inside wall temperature equals the outside (measured) wall temperature.

To be more accurate, however, q_{cor} differs from the nominal value given above due to the dependence of the electrical resistivity of the tube upon temperature, axial heat conduction in the tube wall, axial wall-to-wall radiant heat transfer, and heat transfer to and from the guard heaters. That is,

$$q_{cor} = q_{gen} + q_{con} + q_{rad} + q_{gh} \qquad \text{(A-1)}$$

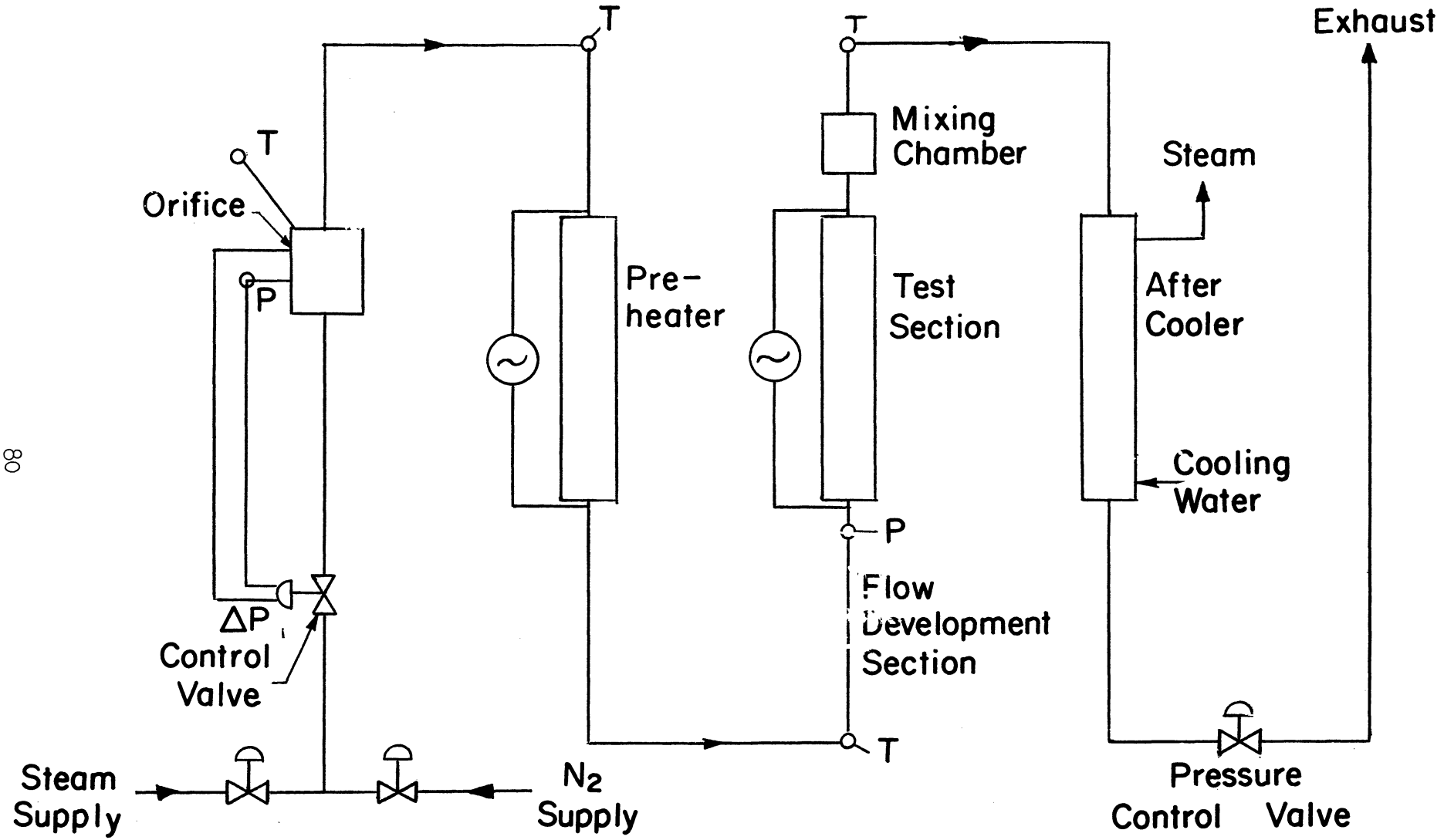

Figure 23. Loop schematic.

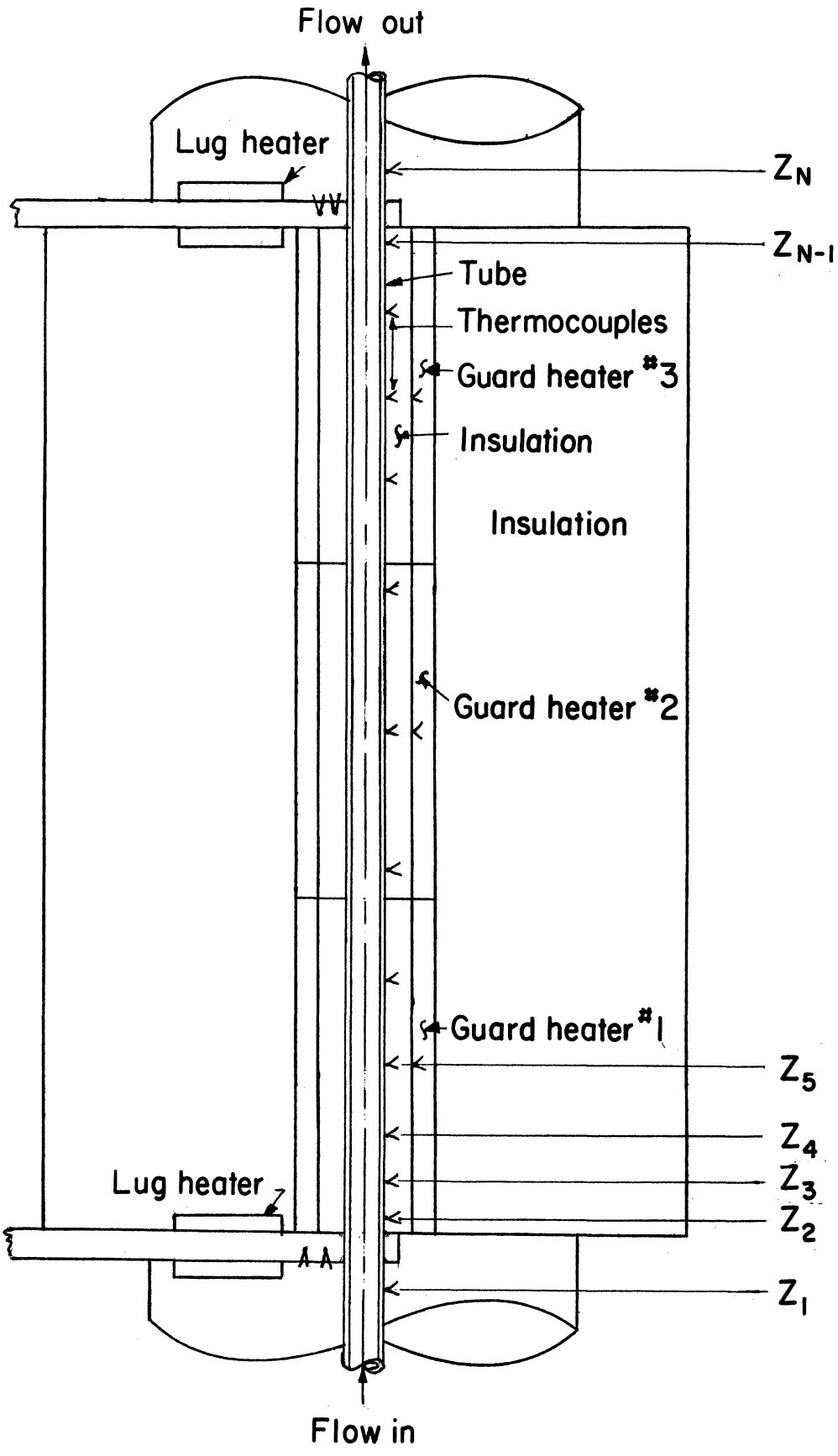

Figure 24. Test section schematic.

With q_{cor} a function of z, the temperature of the gas is obviously no longer a linear function of z. Note also that the inlet and outlet temperatures of the fluid are measured at a certain distance from the heated section, so that heat losses between the measurement points and the test section inlet and exit, respectively, must be accounted for. Heat conduction in the lugs also affects the gas temperature. Finally, the thermal resistance of the tube walls, although small, is not zero, so the inside wall temperature will differ slightly from the outside wall temperature.

A slight additional complication arises because, for an absorbing gas such as steam, in which the absorption coefficient depends upon temperature, the axial wall-to-wall heat transfer depends upon the gas temperature. Thus an iterative procedure is necessary in order to calculate this term. Since it has been found that the correction is not large, a single iteration is employed.

In the following sections the steps mentioned above will be examined in detail. The resulting digital computer program performing the calculations has been organized as a main program and a series of subprograms (functions and subroutines). In describing the main program the purpose of each subprogram called will be mentioned briefly. After the description of the main program has been completed, each of the subprograms will be considered in detail. A listing of the programs appears at the end of this appendix.

II. THE MAIN PROGRAM

A. Reading Data

The following data is supplied tc the program:

1. The number and axial location of the test section wall thermocouples, axial variation of wall area, length, diameter.
2. A key number indicating the type of fluid (steam or nitrogen).
3. The run number.
4. The emissivity of the tube walls.
5. Fluid inlet and outlet temperatures.
6. Test section power.
7. Wall thermocouple readings.

8. Guard heater and lug heater thermocouple readings.

9. Ambient temperature and pressure.

10. Test section pressure.

11. Orifice thermocouple reading and upstream pressure.

12. Specific gravity and deflection of the flow meter manometer fluid.

B. Geometrical Factors

Immediately after reading part (1) of Section A, the subroutine GEOM is called to calculate the ten arrays of geometrical view factors necessary for the calculation of the axial radiant heat transfer. Because these factors depend upon geometry alone, they are calculated before the remainder of the data is read. Any number of data sets may follow without causing repetition of this step.

C. Mass Flow Rate Calculation

First the type of gas is checked, and if it is steam corrections are made to the pressure readings due to the short column of water standing in the lines and the specific gravity of the water is subtracted from that of the manometer fluid. Next all of the measured thermocouple readings are converted to temperatures through the function TEMP. Now that the orifice temperature is known, the mass flow rate is calculated by calling the function FRATE.

D. Calculation of Local Heat Generation Rate

In order to calculate the local heat generation rate it is necessary to first approximate the test section wall temperatures at z = 0 and z = L/D. This is done by first calling the subroutine RGRN to obtain a polynomial fit to the wall temperature, and then substituting the above values of z into the resulting formulas. Next the nominal or average heat generation rate, expressed in the units of q_{cor} is calculated. Finally the subroutine Q is called to calculate the local heat generation rate at each value of z_i.

E. Correction for Axial Conduction in the Wall

The net heat conducted to a wall element per unit length is given by

$$q_{con} = \frac{d}{dx}\left(k_w A_w \frac{dT_w}{dx}\right) \quad . \qquad \text{(A-2)}$$

Considering variable wall thickness and thermal conductivity as a function of temperature, Eq. (A-2) becomes

$$q_{con} = k_w A_w \frac{d^2T_w}{dx^2} + k_w \frac{dT_w}{dx}\frac{dA_w}{dx} + A_w \frac{dk_w}{dT_w}\left(\frac{dT_w}{dx}\right)^2 \qquad \text{(A-3)}$$

For the temperature range of the present study thermal conductivity is approximated by linear functions

$$k_w = a + bT_w \qquad \text{(A-4)}$$

where

$$\text{SS-310} \quad \begin{matrix} a = 6.60 & (\text{Btu/hr ft } ^\circ\text{F}) \\ b = 0.00455 & (\text{Btu/hr ft } ^\circ\text{F}^2) \end{matrix} \qquad \text{(A-5)}$$

$$\text{Zr-2} \quad \begin{matrix} a = 6.53 & (\text{Btu/hr ft } ^\circ\text{F}) \\ b = 0.0074 & (\text{Btu/hr ft } ^\circ\text{F}^2) \end{matrix} \qquad \text{(A-6)}$$

Introducing $A'_w = A_w/D^2$ Eq. (A-3) becomes

$$q_{con}(z_i) = A'_w (a + bT_w)\left[\frac{d^2T_w(z_i)}{dz^2} + \frac{dT_w(z_i)}{dz}\frac{dA'_w(z_i)}{A'_w dz}\right] + bA'_w\left(\frac{dT(z_i)}{dz}\right)^2 \qquad \text{(A-7)}$$

The subroutine RGRN, called previously in part D, has computed the coefficients in a polynomial fit for $T_w(z)$. Thus dT_w/dz and d^2T_w/dz^2 can be readily eavluated, and q_{con_i} can thus be calculated from Eq. (A-7).

F. Guard Heater Correction

The system to be analyzed is sketched in Figure 25.

The power supplied to each guard heater is adjusted so as to keep the temperature at the center of the guard heater as close as possible to that of the wall at the same axial location. Since, however, it is not possible to maintain exact equality, and since the guard heater temperature will not exactly follow that of the wall away from the center, there will in general be heat

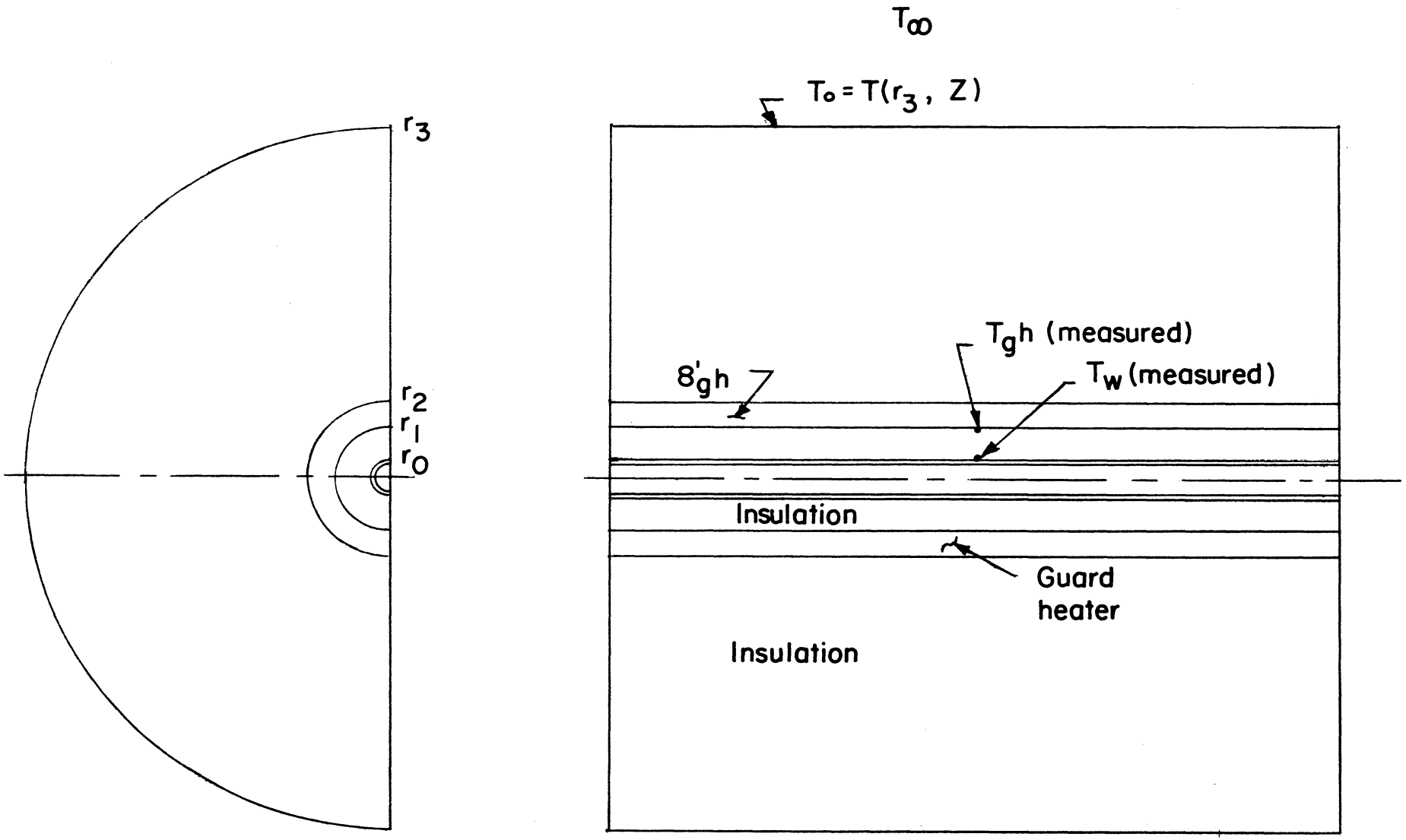

Figure 25. Schematic showing nomenclature for guard heater calculation.

transfer between the wall and the guard heater. If axial conduction in the guard heater and insulation is neglected, and if $\bar{U}_{in}$ and $\bar{U}_{out}$ are defined as the overall heat transfer coefficients between the guard heater and the wall and between the guard heater and the outside surface of the insulation respectively, then

$$q'_{gh} = \bar{U}_{in}(T_{gh} - T_w) + \bar{U}_{out}(T_{gh} - T_o) \tag{A-8}$$

Assuming for the moment that T_o is known, q'_{gh} can be evaluated in terms of $\bar{U}_{in}$ and $\bar{U}_{out}$ by substituting the known values of T_{gh} and T_w at the center of the guard heater. Since q'_{gh} is a constant the guard heater temperature at any other axial location, z_i, can thus be found by solving Eq. (A-8) for $T_{gh}(z_i)$

$$T_{gh}(z_i) = \frac{q'_{gh} + \bar{U}_{in}(z_i)\, T_{w_i}(z_i) + \bar{U}_{out}(z_i)\, T_o(z_i)}{\bar{U}_{in}(z_i) + \bar{U}_{out}(z_i)} \tag{A-9}$$

The heat transfer from the guard heater to the wall is then given by

$$q_{gh}(z_i) = \bar{U}_{in}(z_i)[T_{gh}(z_i) - T_w(z_i)] \tag{A-10}$$

Thus the problem is reduced to finding $\bar{U}_{in}$, $\bar{U}_{out}$, and T_o. Unfortunately the thermal conductivity of the insulation varies considerably with temperature. In the inner region the temperature difference will be quite small, so k will be evaluated at the measured wall temperature and assumed constant. Thus $\bar{U}_{in}$ is given by

$$\bar{U}_{in} = \frac{2\pi k(T_w)}{\ln(r_1/r_o)} \tag{A-11}$$

where for the nonuniform flux test section $r_o = f(z)$.

The temperature drop between the guard heater and the ambient is, of course, not small, so it is necessary to calculate some average value for k_{out}. A good approximation to k(T) for the insulation material in the temperature range of interest is given by

$$k(T) = a + bT + cT^2 \quad ; \qquad \begin{aligned} a &= 0.3233 \text{ Btu/hr ft } ^\circ\text{F} \\ b &= -0.0133 \times 10^{-3} \text{ Btu/hr ft } ^\circ\text{F}^2 \\ c &= 0.57 \times 10^{-6} \text{ Btu/hr ft } ^\circ\text{F}^3 \end{aligned} \tag{A-12}$$

Inserting this expression into the energy equation,

$$\frac{1}{r}\frac{\partial}{\partial r}\left(kr\frac{\partial T}{\partial r}\right) = 0 \qquad T(r_2) = T_{gh} \qquad T(r_3) = T_o \tag{A-13}$$

solving for T(r) and differentiating to obtain the heat transfer to the ambient, the result is

$$q_{gh-\infty} = \frac{2\pi}{\ln(\frac{r_3}{r_2})}\left[a(T_{gh} - T_o) + \frac{b}{2}(T_{gh}^2 - T_o^2) + \frac{c}{3}(T_{gh}^3 - T_o^3)\right] \tag{A-14}$$

In terms of a convective heat transfer coefficient, the heat transfer to the ambient is also given by

$$q_{gh-\infty} = 2\pi r_3 h(T_o - T_\infty) \tag{A-15}$$

The elimination of T_o from Eqs. (A-14) and (A-15) is unfortunately complicated due to the third power term. Actually, however, the bulk of the temperature drop occurs in the insulation for the range of parameters encountered in the experiment, so T_o is only moderately greater than T_∞, and the solution is relatively insensitive to a reasonable approximation of T_o. Based upon a calculation at a typical value of T_{gh}, the following expression is used to evaluate T_o.

$$T_{gh} - T_o = 0.8(T_{gh} - T_\infty) \tag{A-16}$$

For a known T_o, $\bar{U}_{out}$ can be evaluated from Eq. (A-14)

$$\bar{U}_{out} = \frac{2\pi}{\ln(\frac{r_3}{r_2})}\left[a + \frac{b}{2}(T_{gh} + T_o) + \frac{c}{3}(T_{gh}^2 + T_{gh}T_o + T_o^2)\right] \tag{A-17}$$

$\bar{U}_{out}$ is evaluated at the center of the guard heater, where T_{gh} is known, and assumed independent of axial position in order to avoid the solution of a cubic equation to find $T_{gh}(z_i)$. $T_{gh}(z_i)$ is then calculated using Eq. (A-9), and $q_{gh}(z_i)$ is calculated from Eq. (A-10).

G. Corrected Heat Flux

Because the correction for radiant axial heat transfer depends upon the gas temperature, an iteration procedure is necessary. Thus, in the first

iteration it will be assumed that q_{rad} is zero. Based upon this assumption the corrected heat flux will be computed. The result is

$$q_{cor} = q_{gen} + q_{gh} + q_{con} \tag{A-18}$$

Based upon this heat flux, the gas temperature will be calculated, and based upon this temperature q_{rad} will be determined. Then q_{rad} will be added to q_{cor} of Eq. (A-18) to obtain a value of heat flux which includes axial radiant transfer. On the basis of this improved corrected heat flux a more accurate gas temperature will subsequently be determined. In the present analysis the iteration is terminated at this point because experience has shown satisfactory convergence at this level. The detailed description of these steps is given in parts I and K below. First, however, the inlet gas temperature will be determined.

H. Corrected Inlet Temperature

Because of the desire for fully developed velocity field at the inlet to the heated section the fluid temperature is measured well upstream of the test section. Hence evaluation of the actual inlet temperature requires careful calculation of the heat loss to the ambient from the inlet flow development section. The term inlet temperature will be used to refer to the gas temperature at the axial location of the first wall thermocouple. The control volume to be analyzed is sketched in Figure 26. Applying the conservation of thermal energy,

$$q_{wall} - q_{loss} = \dot{m}(h_1 - h_{in}) \tag{A-19}$$

or

$$h_1 = h_{in} + \frac{q_{wall} - q_{loss}}{\dot{m}} \tag{A-20}$$

The heat loss in the inlet and outlet sections can be determined either by an overall heat balance or by a calculation based upon the known temperatures, thermal conductivity of the insulation, and geometry. The method based upon an overall heat balance is preferred, but gives only the total heat loss, not the separate losses in the inlet and outlet sections. Therefore the following procedure is used. First the overall heat loss is computed by means of a heat balance. This quantity is referred to as the experimental heat loss and is given by

$$q_{loss_{ex}} = \text{power} - \dot{m}(h_{out} - h_{in}) \tag{A-21}$$

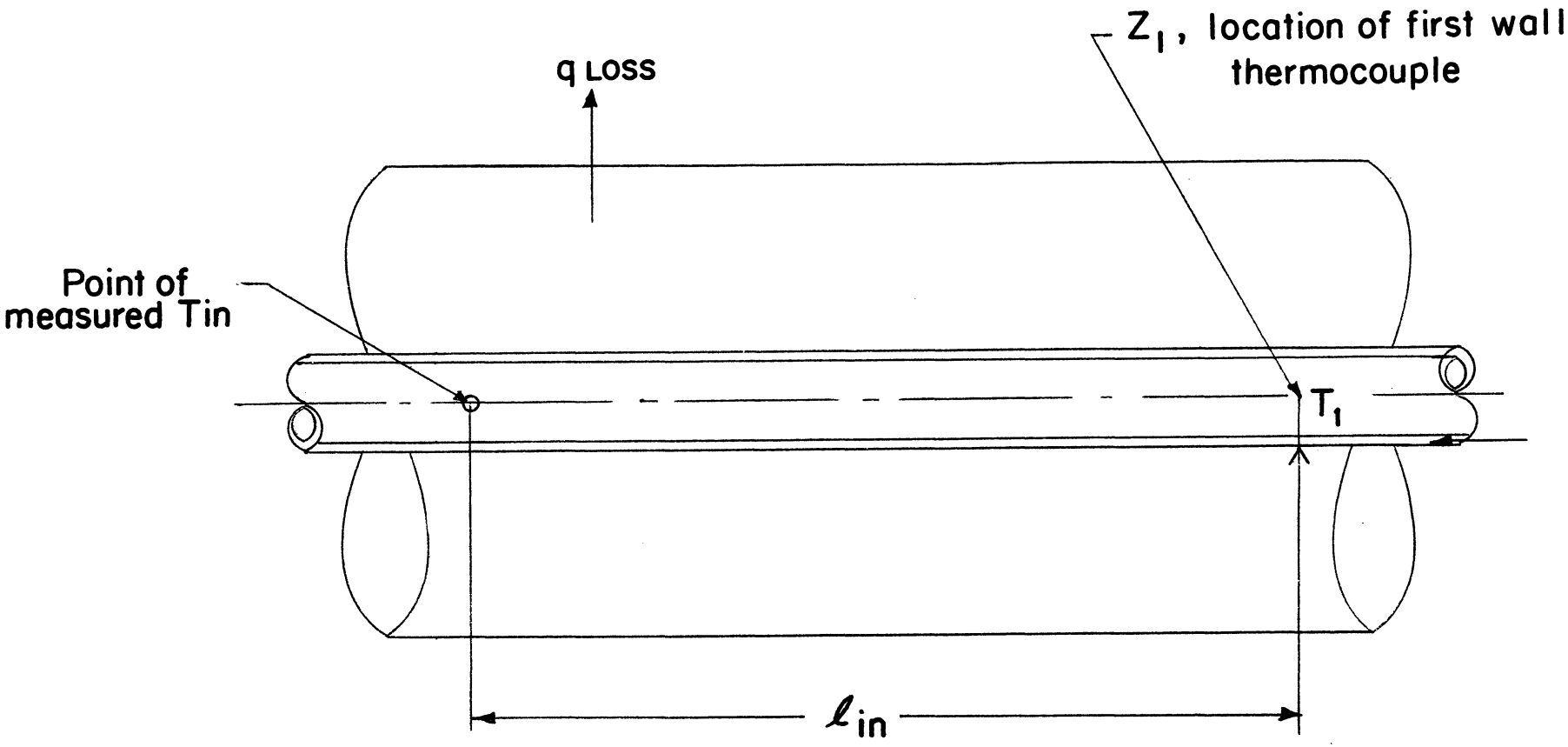

Figure 26. Flow development section.

Then, independent of the preceding, the calculated heat losses in the inlet and outlet sections are computed, following the method outlined in the section on guard heater corrections.

$$T_{o_i} = .8T_\infty + .2T_{in} \tag{A-22}$$

$$q_{loss_i} = \frac{2\pi \ell_{in}}{\ln(\frac{r_{out}}{r_{in}})}\left[a(T_{in} - T_{o_i}) + \frac{b}{2}(T_{in}^2 - T_o^2) + \frac{c}{3}(T_{in}^3 - T_o^3)\right] \tag{A-23}$$

$$T_{o_o} = .8T_\infty + .2T_{out} \tag{A-24}$$

$$q_{loss_o} = \frac{2\pi \ell_{out}}{\ln(\frac{r_{out}}{r_{in}})}\left[a(T_{out} - T_{o_o}) + \frac{b}{2}(T_{out}^2 - T_{o_o}^2) + \frac{c}{3}(T_{out}^3 - T_{o_o}^3)\right] \tag{A-25}$$

If the calculations were to agree perfectly, $q_{loss_{ex}}$ would equal the sum of q_{los_i} and q_{los_o}. The three quantities are printed out for the purpose of comparison. Since perfect agreement is not anticipated, the inlet heat loss used is taken to be

$$q_{loss} = q_{loss_{ex}} \frac{q_{los_i}}{q_{los_i} + q_{los_o}} \tag{A-26}$$

Heat conducted into the control volume through the wall is given by

$$q_{wall} = -k_w A_w \frac{dT_w(x_1)}{dx} \tag{A-27}$$

and can thus be readily computed, as all of these factors are known.

I. Calculation of the Bulk Gas Temperature

Between z_1 and z_2 the electrical power lug crosses the control volume (Figure 27) (see also Figure 24 for location of z_1 to z_n). The first law for this control volume is given by

$$\dot{m}(h_2 - h_1) = k_{lug} A_{lug} \frac{dT_{lug}}{dx_{lug}} + k_w A_w^{(o)} \frac{dT_w(o)}{dx} - k_w A_w^{(x_1)} \frac{dT_w(x_1)}{dx} - q_{los_{1-2}}$$

$$+ \int_o^{x_2} q_{cor}(x)\, dx \tag{A-28}$$

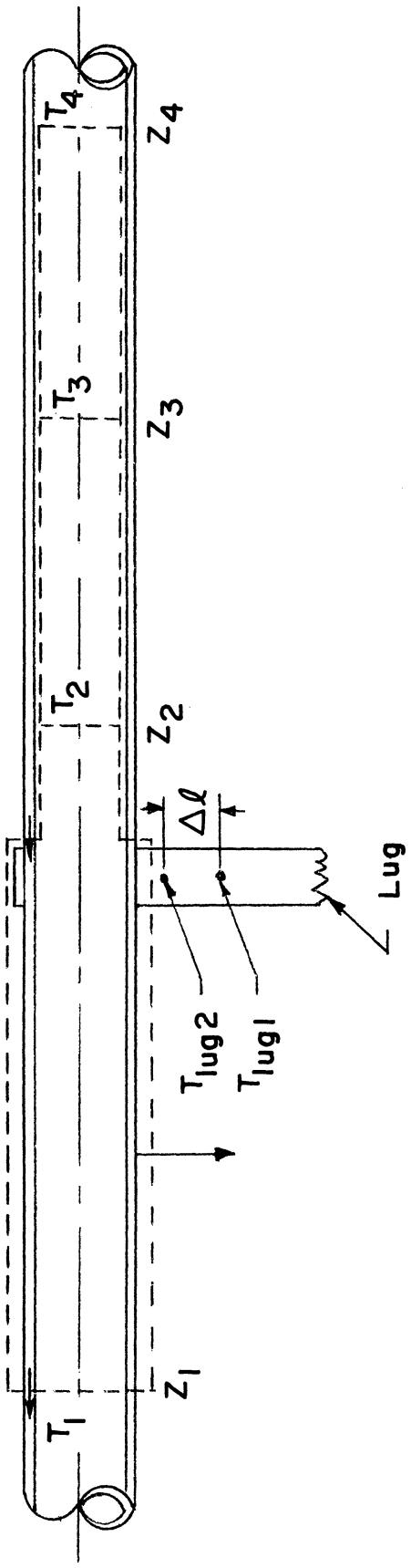

Figure 27. Gas temperature calculation.

In evaluating the enthalpy rise in Eq. (A-28) the following approximations are employed

$$\frac{dT_{lug}}{dx_{lug}} \simeq \frac{T_{lug_1} - T_{lug_2}}{\Delta x_{lug}}$$

$$\int_0^{x_2} q_{cor}(x)\, dx \simeq q_{cor}(x_2) \times x_2$$

$q_{los_{1-2}}$ is a portion of the heat loss in the inlet section calculated in Section H above. dT_w/dx is evaluated using the polynomial fit for T(z) found by the regression analysis.

From z_2 to z_{n-1} the first law for each interval is given by

$$\dot{m}(h_{i+1} - h_i) = \int_{x_i}^{x_{i+1}} q_{cor}(x)\, dx \qquad \text{(A-29)}$$

The integral is approximated by the following expression

$$\int_{x_i}^{x_{i+1}} q_{cor}(x)\, dx \simeq \frac{1}{2}(q_{cor_{i+1}} + q_{cor_i})(x_{i+1} - x_i) \qquad \text{(A-30)}$$

Between z_{n-1} and z_n the control volume and the resulting expressions are similar to those for the range z_1 to z_2. Finally, a calculated outlet enthalpy is evaluated by considering the heat loss from z_n to the thermocouple location. Temperatures are calculated by calling the function TPHD(P,H).

J. Calculation of the Inside Wall Temperature

The radial temperature distribution in the tube wall may be obtained by solving the one-dimensional energy equation

$$\frac{1}{r}\frac{\partial}{\partial r}\left(rk_w \frac{\partial T_w}{\partial r}\right) = -q''' \qquad \text{(A-31)}$$

with the boundary conditions

$$T_w(r_o) = T_{w_o} \qquad \text{(A-32)}$$

$$2\pi r_i k_w \frac{\partial T_w(r_i)}{\partial r} = q_{cor} \tag{A-33}$$

where k_w is taken to be constant and evaluated at the local outside wall temperature. Due to axial conduction the effective heat generation rate may be increased or decreased from the actual value. Thus rather than using the previously calculated value of q_{gen} it is possible to use the alternate condition

$$2\pi r_o k_w \frac{\partial T_w(r_o)}{\partial r} = q_{gh} \tag{A-34}$$

and solve for q'''. Employing this procedure c is defined such that

$$\frac{1}{r}\frac{\partial}{\partial r}\left(2\pi r k_w \frac{\partial T}{\partial r}\right) = -\frac{2c}{r_o^2} \tag{A-35}$$

Integrating once from r_i to r, the result is

$$2\pi r k_w \frac{\partial T}{\partial r} - 2\pi r_i k_w \frac{\partial T(r_i)}{\partial r} = -\frac{c}{r_o^2}(r^2 - r_i^2) \tag{A-36}$$

Letting $r = r_o$, employing Eqs. (A-33) and (A-34), and solving for c, the result is

$$c = \frac{q_{cor} - q_{gh}}{1 - (r_i/r_o)^2} \tag{A-37}$$

Integrating Eq. (A-36) again from r_i to r_o, substituting Eq. (A-32), and solving for T_{w_i}, the result is

$$T_{w_i} = T_{w_o} + \frac{1}{2\pi k_w}\left\{q_{cor}\ln\left(\frac{r_i}{r_o}\right) + c\left[\frac{1}{2}\left(1 - \frac{r_i^2}{r_o^2}\right) + \frac{r_i^2}{r_o^2}\ln\left(\frac{r_i}{r_o}\right)\right]\right\} \tag{A-38}$$

where $r_o = f(z)$ for the nonuniform flux test section.

K. Axial Radiant Heat Transfer

The correction for axial radiant heat transfer is discussed in detail in Ref. 15. The correction has been found to be small enough that only a single iteration is required, and that the optical thickness of the gas is sometimes too large to permit the use of the thin gas model. Summarizing briefly, first

the optical thicknesses based upon the wall and gas temperatures are calculated. If the optical thickness based upon the wall temperature exceeds 0.5 at any point the thin gas approximation is considered to be too much in error and no correction for axial radiant transfer is attempted. The radiosity is calculated assuming the axial transfer is zero. Note that in fact the relatively high rate of absorption will decrease axial radiation transfer under these circumstances. If the optical thickness is less than 0.5 everywhere, the matrix described in detail in Ref. 15 is constructed and solved for the radiosity by calling the subroutines ARRAY and SIMQ of the IBM Scientific Subroutine Package. Once the radiosity is known, the axial radiant transfer q_{rad} is calculated, the resulting total heat flux is calculated and the gas enthalpy, and consequently its temperature is modified to account for the axial radiant heat transfer.

L. Wall-to-Gas Radiant Heat Transfer

Ignoring axial transfer the local radiant heat flux from the wall to the gas is given by

$$q_{rr} = \alpha_g B - \epsilon_g \sigma T_g^4 \quad . \tag{A-39}$$

For the circular tube geometry, the emissivity of the gas can be very closely approximated at small to moderate optical thicknesses by the expression

$$\epsilon_g = 1 - e^{-\tau_o} \tag{A-40}$$

The absorptivity, of course, is approximated by the same expression except that in evaluating α_g, τ_o is evaluated at T_w, while in evaluating ϵ_g, τ_o is evaluated at T_g. The thin gas approximation produces the leading terms in the expansion of the above, but at moderate optical thicknesses Eq. (A-40) is more accurate. The results are expressed in terms of a radiant heat transfer coefficient defined by

$$h^R = \frac{q_{rr}}{T_{w_i} - T_g} \tag{A-41}$$

M. Total Heat Transfer Coefficient

A total heat transfer coefficient, including the effects of combined conduction and radiation to the gas, defined as

$$h^T = \frac{q_{cor}}{T_{w_i} - T_g}$$

is calculated.

N. Gas Properties at Bulk, Film, and Wall Temperatures

In order to evaluate the important parameters and to facilitate attempts to correlate the data in different ways, gas properties ρ, μ, k, and C_p are evaluated at the bulk, film, and wall temperatures, through the use of the functions VPTD, VIS, CDT, and SPHT, respectively.

O. Local Nusselt, Reynolds, Prandtl, and Planck Numbers

Local Nusselt, Reynolds, and Prandtl numbers are evaluated based upon wall, film, and bulk properties. For comparison to data for nonabsorbing gases, a bulk Nusselt number based upon conductive heat transfer alone, and defined as

$$Nu_{BC} \equiv \frac{(h^T - h^R)D}{k}$$

is computed. Two Reynolds numbers based upon a combination of properties evaluated at different temperatures are also computed. The Planck number, $\mathcal{P} = k\tau_o/4\sigma DT_g^3$, is computed based upon bulk properties.

In addition, the radiant heat flux using the method of Hottel is evaluated, based on steam emissivity from the Hottel chart (see Section 3.4.2). A corresponding conductive Nusselt number is evaluated for comparison with data for transparent gases. The Nusselt number based on the McEligot correlation and the laminarization parameter, A, of Section 3.5 are calculated. A nonuniform flux analysis is made by calling subroutine CNUHF. This produces according to Section 3.3 an equivalent uniform flux conductive Nusselt number for comparison with constant flux correlations and, if KPUNCH = 5, in addition a predicted nonuniform flux conductive Nusselt number.

P. Output Specifications

For each point z_i along the tube where the wall thermocouples are located, cards are punched giving the local values of the most important dimensionless parameters. In addition two copies of printed output are produced giving detailed information about the run. Sample output is included at the end of this appendix. All symbols appearing on the output are defined in the program output nomenclature.

III. FUNCTIONS AND SUBROUTINES

A. Geometric Factors, GEOM

A detailed discussion of the necessity of calculating the various geometrical factors needed in the axial radiant transfer calculation and a derivation of their formulas appears in Ref. 15. All of these factors tend rapidly to zero for large Δz, so they have been calculated for Δz less than 10 and they are equated to zero for $\Delta z > 10$. This subroutine carries out the computation of the 10 arrays of factors required according to the formulas of Ref. 15.

B. Millivolt to Temperature Conversion, TEMP

The thermocouples attached to the outer wall, guard heaters, lug heaters, and orifice plate are identical couples purchased in one batch. A sample of five couples was calibrated and compared to standard tables, and a deviation curve was constructed. All five couples produced substantially the same deviation curve. A regression analysis was performed to determine the best cubic function T(mv), and it was found that by breaking the range of 100°F to 2000°F into five smaller ranges the error in prediction could be reduced to about .1°F, which was deemed adequate. The function TEMP selects the proper equation for the range of the emf supplied and computes the temperature.

C. Mass Flow Rate, FRATE

Calibration runs were made with the orifice plate used and the discharge coefficient C_d was found to be constant for $Re > 5000$ and to vary with the logarithm of the Reynolds number for $Re < 5000$. The function FRATE assumes $Re > 5000$, calculates the flow rate and Reynolds number based upon this assumption and checks to see if $Re > 5000$. If so, the calculation is complete. If not, a new discharge coefficient is calculated based upon the current value of Re, and the flow rate and Reynolds number are recalculated. This iteration is repeated until the Reynolds number changes by less than 50 from one iteration to the next.

D. Regression Analysis, RGRN

In order to calculate the axial conduction correction at each point it is necessary to compute the first and second derivatives of the wall temperature. A polynomial approximation based on the measured discrete values of wall temperature facilitates accurate evaluation of derivatives. It would be possible to construct a 13th order polynomial which intersects all of the 14 known points, but such high order polynomials frequently exhibit oscillations which do not correspond to the physical behavior. Also, even if the order of the polynomial

is reduced by considering fewer points, forcing the polynomial to be exactly correct at the known points can lead to unreal behavior. Thus it was felt that a regression analysis where the polynomial is forced to be the best fit to more points than it can actually intersect was the best solution. It was decided to fit a cubic to five points. In the interior of the heated section, this means the third order polynomial upon which the calculation of the second derivative at a point is based is the best fit to the point in question and the two points to either side of it. At the entrance and exit, since there is only one point beyond the heated length at each end, the polynomial must be based on one point to one side and the three on the other side.

Details of the method of least squares are presented in Ref. 19. The subroutine first considers the first five pairs, z_i and T_i, calculates the coefficients of the four simultaneous linear equations resulting from the analysis, and calls the IBM subroutine SIMQ. The solution of these equations is a vector containing the four coefficients a_o, a_1, a_2, a_3 in the equation

$$T_w(z) = a_o + a_1 z + a_2 z^2 + a_3 z^3 \qquad \text{(A-42)}$$

These values are stored in a two-dimensional array SOL, and in order to allow checking of the results the temperatures predicted by Eq. (A-42) are calculated and may be printed along with the measured values. The subroutine then considers the points 2 through 6, repeats the above procedure, and continues to move along one point at a time until it reaches point z_n. At this time, all of the desired coefficients are stored in SOL, and control returns to the main program.

E. Heat Generation Rate, Q

The electrical resistivity of type 310 stainless steel and Zr-2 varies moderately with temperature and can be closely approximated by an equation of the form

$$\rho_e = a + bT + cT^2$$

where

	SS-310	Zr-2
$a(\Omega - cm \times 10^6)$	103.0	72.0
$b(\Omega - cm \times 10^6/°F)$	0.0165	0.09
$c(\Omega - cm \times 10^6/°F^2)$	0	0.27×10^{-4}

The local heat generation rate is directly proportional to $I^2\rho_e$, and since T_w is known at the points where q_{gen} is desired, it is possible to calculate q_{gen} directly for known I and T_w. However the most important quantity, and the one that is most accurately measured is the total power, not I, and ρ_e may vary slightly depending upon composition. Thus it is desirable to ascertain that the total power, which is given by

$$P_T = \int_o^L (I^2\rho_e/A_w)\, dx$$

agrees with the measured power.

The nominal heat generation per unit length is defined by

$$q_{nom} = \frac{P_T}{L}$$

hence the actual local heat generation is

$$q_{gen} = q_{nom} \frac{[a + bT(z) + cT^2(z)]/A_w(z)}{\overline{[a + bT + cT^2]/A_w}} \qquad \text{(A-43)}$$

where

$$\overline{[a + bT + cT^2]/A_w} = \frac{1}{L}\int_o^L \frac{a + bT(z) + cT^2(z)}{A_w(z)}\, dz$$

The main program calculates the temperature at z = 0 and z = L/D based on the regression analysis performed earlier and provides these values to the subroutine Q. The subroutine performs an integration of ρ/A_w by a trapezoidal method to obtain $\overline{\rho/A_w}$, and then calculates q_{gen} at each point z_i by Eq. (A-43).

IV. STEAM PROPERTIES

A. Enthalpy HPTD(P,T)

B. Temperature TPHD(P,H)

C. Specific Volume VPTD(P,T)

These functions were supplied in a Fortran-IV subroutine by the Argonne National Laboratory and have been checked and found to be in good agreement with

the 1967 ASME Steam Tables in the range of interest.

D. Specific Heat, SPHT

This function is based on a finite difference approximation of the expression

$$C_p \equiv \left.\frac{\partial h}{\partial T}\right|_p \cong \left.\frac{\Delta h}{\Delta T}\right|_p$$

The actual formula used is

$$C_p(P,T) = \frac{h(P,T + 5°) - h(P,T - 5°)}{10°}$$

E. Viscosity, VIS(T)

The viscosity of steam is independent of pressure in the temperature and pressure range encountered in the experiment. An equation of the form

$$\mu = a + bT$$

has been found to fit the data presented in the 1967 ASME Steam Tables adequately.

F. Thermal Conductivity, CDT(P,T)

The data presented in the 1967 ASME Steam Tables can be represented adequately by a series of straight lines to account for variation with temperature, and the small correction for pressure can be simply accounted for by multiplying the temperature expression by a factor close to one. Five temperature ranges are used and in each range the function is of the form:

$$k(P,T) = (a + bT)(1 + c(P - 50))$$

G. Optical Thicknesses, TAU

While measurements of the absorptivity of steam are in progress, an expression of the form

$$\tau_o(P,T) = P\left(\frac{a}{T^2} + \frac{b}{T^4}\right)$$

which fits the data for the Planck mean absorption coefficient as presented in Ref. 16, is being used (see Eq. (3-19) of Section 3.4.1).

V. NITROGEN PROPERTIES

Nitrogen properties are taken from Refs. 20 and 21. Although some of the properties are not pressure dependent in the range considered, the function calls specify P as a parameter in order to be able to use the same calling program as for steam.

A. Specific Heat SPHT(P,T)

The specific heat is calculated by a linear interpolation in a table of values taken from Ref. 21.

B. Enthalpy HPTD(P,T)

A numerical integration of the form

$$h - h_o = \int_{T_o}^{T} C_p(T)\, dT$$

was performed using the values of specific heat taken in 100° increments from Ref. 20, and a table of h vs. T was thus constructed. Enthalpy values are obtained by interpolating within this table.

C. Temperature TPHD(P,H)

The temperature is obtained by interpolation in the above mentioned h vs. T table.

D. Thermal Conductivity CDT(P,T)

A table of values of k vs. T given in Ref. 21 was fed into the machine, and values of k are obtained by interpolation in this table.

E. Specific Volume VPTD(P,T)

The specific volume is calculated from the perfect gas equation of state.

F. Viscosity VIS(T)

Viscosity is obtained by linear interpolation in a table of μ vs. T taken from Ref. 21.

G. Optical Thickness TAU(P,T)

The absorption coefficient, and hence the optical thickness for nitrogen is equal to zero.

VI. NOMENCLATURE

A_w	Cross sectional area of the tube wall
B	Wall radiosity
C_p	Constant pressure specific heat
D	Tube inside diameter
h	Enthalpy
h^T	Total heat transfer coefficient
h^R	Radiant heat transfer coefficient
I	Electrical current
k	Thermal conductivity
ℓ_{in}	Length of inlet section
ℓ_{out}	Length ofoutlet section
L	Length of heated section
$\dot{m}$	Mass flow rate
Nu	Local Nusselt number
P	Gas pressure

Pr	Local Prandtl number
Π_T	Test section power
$\mathcal{P}$	Local Planck number, $\kappa k/4\sigma T_g^3$
q_{cor}	Local heat flux to the gas per unit length
q_{con}	Local heat flux to the gas per unit length due to axial conduction in the tube walls
q_{gen}	Local heat flux to the gas per unit length due to heat generation in the tube walls
q_{gh}	Local heat flux to the gas per unit length due to heat transfer from the guard heater
q_{rad}	Local heat flux to the gas per unit length due to axial radiant wall-to-wall heat transfer
$q_{gh-\infty}$	Local heat flux per unit length from guard heater to ambient
q_{los_i}	Heat loss to ambient in inlet section
q_{los_o}	Heat loss to ambient in outlet section
$q_{loss_{ex}}$	Experimental heat loss to ambient computed by an energy balance
q_{rr}	Local radiant heat flux per unit area from the wall to the gas
q'_{gh}	Heat generated in the guard heater per unit length
r	Radial coordinate
Re	Local Reynolds number
T_w	Wall temperature
T_{w_i}	Inside wall temperature
T_{w_o}	Outside wall temperature
T_g	Bulk temperature of gas
T_{gh}	Guard heater temperature
T_o	Outside temperature of test section insulation

T_{o_i} Outside temperature of inlet section insulation

T_{o_o} Outside temperature of outlet section insulation

T_∞ Ambient temperature

$\bar{U}_{in}, \bar{U}_{out}$ Overall heat transfer coefficients between guard heater and tube and guard heater and outside of insulation, respectively

x Axial coordinate

z Dimensionless axial coordinate, x/D

α_g Absorptivity of gas volume

ϵ_g Emissivity of gas volume

κ Gas absorption coefficient

ρ Gas density

ρ_e Electrical resistivity

τ_o Optical thickness of gas, κD

μ Gas viscosity

VII. PROGRAM OUTPUT NOMENCLATURE

KS An output digit produced by the subroutine SIMQ. A normal solution results in KS = 0

MDOT Mass flow rate, lbm/hr

TSKW Test section power, kilowatts

PABS Absolute pressure in test section, $lbf/in.^2$

TIN Gas inlet temperature, °F

QNOM "Nominal" or average heat flux to the gas, $Btu/hr\text{-}ft^2$

QLOSEX Experimental heat loss, Btu/hr

QLOSI Calculated heat loss in inlet section, Btu/hr

QLOSO Calculated heat loss in outlet section, Btu/hr

TOUT	Gas outlet temperature, measured, °F
TINF	Ambient temperature, °F
PINF	Ambient pressure, lbf/in.^{2}
PTS	Test section gage pressure reading, lbf/in.^{2}
G	Mass velocity, lbm/hr-ft^2
RATING	The ratio of the experimental heat loss over heat input
TOUTC	Calculated outlet temperature, °F
TGH(I)	Measured temperatures at the center of the three guard heaters, °F
TLH(I)	Measured temperatures at the lugs, °F
I	The number of the axial location
Z(I)	Dimensionless axial coordinate, x/D
TWO(I)	Measured outside wall temperature, °F
TWI(I)	Calculated inside wall temperature, °F
QCON(I)	Addition to local heat flux due to axial conduction in the wall, Btu/hr-ft^2
EPSA	Coefficient in wall emissivity expression, Eq. (3-17)
EPSB	Coefficient in wall emissivity expression, Eq. (3-17)
TAULIM	Below this value axial radiant transfer is included
QGH(I)	Addition to local heat flux due to heat transfer between the wall and the guard heater, Btu/hr-ft^2
QRAD(I)	Addition to local heat flux due to axial radiant heat transfer between wall elements, Btu/hr-ft^2
QGEN(I)	Local heat flux due to heat generated in the wall, Btu/hr-ft^2
QCOR(I)	Corrected total heat flux, the sum of the previous four quantities, Btu/hr-ft^2
TG(I)	Bulk temperature of the gas, °F

HZ(I) Local total heat transfer coefficient, Btu/(hr-ft^2-°F)

HZR(I) Local radiant heat transfer coefficient, Btu/(hr-ft^2-°F)

RHOW(I) Gas density evaluated at wall temperature, lbm/ft^3

RHOB(I) Gas density evaluated at bulk temperature, lbm/ft^3

RHOF(I) Gas density evaluated at film temperature, lbm/ft^3

MUW(I) Gas viscosity evaluated at wall temperature, lbf-sec/ft^2

MUB(I) Gas viscosity evaluated at bulk temperature, lbf-sec/ft^2

MUF(I) Gas viscosity evaluated at film temperature, lbf-sec/ft^2

KGW(I) Thermal conductivity of the gas evaluated at wall temperature, Btu/hr-ft-°F

KGB(I) Thermal conductivity of the gas evaluated at the bulk temperature, Btu/hr-ft-°F

KGF(I) Thermal conductivity of the gas evaluated at the film temperature, Btu/hr-ft-°F

CP(I) Constant pressure specific heat of the gas evaluated at the bulk temperature, Btu/lbm-°F

TAW(I) Optical thickness of the gas evaluated at the wall temperature, dimensionless

TAG(I) Optical thickness of the gas evaluated at the bulk temperature, dimensionless

REW(I) Reynolds number based on viscosity evaluated at the wall temperature

REF(I) Reynolds number based upon viscosity evaluated at the film temperature

REFB(I) Reynolds number based upon mixed properties, $Re_f(\rho_f/\rho_b)$

REWB(I) Reynolds number based upon mixed properties, $Re_w(\rho_w/\rho_b)$

PRW(I) Prandtl number based upon wall properties

PRB(I) Prandtl number based upon bulk properties

PRF(I) Prandtl number based upon film properties

NUW(I) Total Nusselt number based upon wall properties

NUB(I) Total Nusselt number based upon bulk properties

NUF(I) Total Nusselt number based upon film properties

NUBC(I) Conductive Nusselt number based upon bulk properties

REB(I) Reynolds number based upon bulk properties

TRAT(I) Absolute temperature ratio, T_w/T_b

TGNR(I) Gas temperature before correction to account for axial radiant transfer

B(I) Radiosity, Btu/hr-ft^2

BBK(I) Radiosity for black walled case, σT_w^4

PLNKB(I) Planck number based upon bulk temperature, dimensionless

UFNUBC(I) Equivalent uniform flux convective Nusselt number

NUMCEL(I) Convective Nusselt number based on McEligot correlation

PLNKW(I) Planck number based on wall temperature

ACCPAR(I) Laminarization parameter

```
C          MAIN PROGRAM
      DIMENSION TGNR(14),Z(14),TWO(14),TWI(14),QCON(14),UFNUBC(14),
     1QGH(14),UBC(14),B(14),BBK(14),VW(14),VGH(3),VLH(4),ACCPAR(14),
     2QRAD(14),QCOR(14),TG(14),ENTH(14),HZ(14),CW(14),RHOW(14),RHOB(14),
     3RHOF(14),VSW(14),VSB(14),VSF(14),CGW(14),CGB(14),CGF(14),CP(14),
     4REW(14),REB(14),REF(14),REWB(14),REFB(14),PRW(14),PRB(14),PRF(14),
     5UW(14),UB(14),UF(14),TRAT(14),TGH(3),TLH(4),UMCEL(14),
     6TO(3),QPGH(3),SOL(14,4),TG4(14),TW4(14),TAW(14),TAG(14),HZR(14),
     7PLNKB(14),PLNKW(14),QGEN(14),UIN(14),UOUT(14),CPW(14),CPF(14)
      DIMENSION X(75),F1(75,74),F2(75,74),PHI1(75,74),PHI2(75,74),
     1G1(75,74),G2(75,74),F3(75),F4(75),H1(75),H2(75),UBCHOT(14)
      DIMENSION AW(14),DAW(14),RR(14)
      REAL L
      SIG=.1714E-8
C
C          READING GENERAL DATA
 4    READ 5,AWP,AKT,BKT,RI
 5    FORMAT (4F10.5)
      READ 10,N,(Z(I),I=1,N)
 10   FORMAT (I10/7F10.3/7F10.3)
      READ 11,KEY
 11   FORMAT (I1)
      N1=N-1
      N2=N-2
      IF (AWP) 7,6,7
 6    READ 161,(AW(I),I=1,N)
 161  FORMAT (7F10.5/7F10.5)
      GO TO 9
 7    DO 8 I=1,N
 8    AW(I) = AWP
 9    DO 901 I=1,N
 901  RR(I) = 1./SQRT(12.*4.*AW(I)/3.14159+1.)
      DAW(1) = 0.
      DO 111 I=2,N2
 111  DAW(I) = (AW(I+1)-AW(I))/(Z(I+1)-Z(I))
      DAW(N1) = -DAW(3)
      DAW(N) = 0.
C
C          GEOMETRICAL FACTORS
      READ 13,IND,KPUNCH,L,FILIM
 13   FORMAT (2I2,F10.5,F10.5)
      IND2=IND+2
      IND3=IND+3
      FIND=IND
      DX=L/FIND
      X(1)=-DX
      DO 2 I=2,IND3
 2    X(I)=X(I-1)+DX
      CALL GEOM(X,IND3,F3,F4,H1,H2,F1,F2,G1,G2,PHI1,PHI2)
C
C          WALL EMISSIVITY CONSTANTS AND THICK GAS LIMIT TAULIM
      READ 17,EPSA,EPSB,TAULIM
C
C          READING DATA FOR INDIVIDUAL RUN
 15   READ 12,M,EPS,TIN,TOUT,TSKW
 12   FORMAT (I10,4F10.3)
      IF (M) 152,151,152
 151  GO TO 4
 152  CONTINUE
      READ 16, (VW(I),I=1,N)
 16   FORMAT (7F10.3/7F10.3)
      READ 17, (VGH(I),I=1,3), (VLH(I),I=1,4)
 17   FORMAT (7F10.3)
      READ 17,TINF,PINF,PTS,POR,VOR,SG,DH
C
C          MASS FLOW RATE CALCULATION
      IF (KEY-1) 18,19,21
 18    CALL ERROR
 19   PABS=PTS+PINF+.433
      POR=POR+.433
      SG=SG-1.
      GO TO 22
 21   PABS=PTS+PINF
 22   DO 30 I=1,N
 30   TWO(I)=TEMP(VW(I))
      DO 40 I=1,4
 40   TLH(I)=TEMP(VLH(I))
      DO 50 I=1,3
 50   TGH(I)=TEMP(VGH(I))
      TOR=TEMP(VOR)
      TWI(1)=TWO(1)
      TWI(N)=TWO(N)
      FLRT=FRATE(POR,PINF,DH,SG,TOR)
      G=737.*FLRT
C
C          LOCAL HEAT GENERATION RATE
      PRINT 20,M
      CALL RGRN(Z,TWO,N,SOL)
      QNOM=3413.*TSKW/36.0
      TO=SOL(1,1)
      TL=POLY(N-4,L,SOL)
      CALL Q(TWO,TO,TL,N,QNOM,QGEN,Z,L,AW)
C
C          CORRECTION FOR WALL CONDUCTION
      DO 60 I=1,N
 60   CW(I)=AKT+BKT*TWO(I)
      D2TDZ2=2.*SOL(1,3)+6.*SOL(1,4)*Z(2)
      DTDZ2=(SOL(1,2)+2.*SOL(1,3)*Z(2)+3.*SOL(1,4)*Z(2)*Z(2))**2
      QCON(2) = AW(2)*(CW(2)*D2TDZ2+BKT*DTDZ2) + CW(2)*SQRT(DTDZ2)*
     1          DAW(2)
      DO 70 I=3,N2
      D2TDZ2=2.*SOL(I-2,3)+6.*SOL(I-2,4)*Z(I)
      DTDZ2=(SOL(I-2,2)+2.*SOL(I-2,3)*Z(I)+3.*SOL(I-2,4)*Z(I)*Z(I))**2
 70   QCON(I) = AW(I)*(CW(I)*D2TDZ2+BKT*DTDZ2) + CW(I)*SQRT(DTDZ2)*
     1          DAW(I)
      D2TDZ2=2.*SOL(N-4,3)+6.*SOL(N-4,4)*Z(N-1)
      DTDZ2=(SOL(N-4,2)+2.*SOL(N-4,3)*Z(N-1)+3.*SOL(N-4,4)*Z(N-1)*
     1 Z(N-1))**2
      QCON(N1) = AW(N1)*(CW(N1)*D2TDZ2+BKT*DTDZ2) + CW(N1)*SQRT(DTDZ2)*
     1          DAW(N1)
```

```
C
C                    CORRECTION FOR GUARD HEATERS
      DO 80 J=1,3
      TO(J)=.8*TINF+.2*TGH(J)
80    UOUT(J)=3.93*(.3233-.00667E-3*(TGH(J)+TO(J))+.19E-6*
     1 (TGH(J)*TGH(J)+TGH(J)*TO(J)+TO(J)*TO(J)))
      DO 801 I=2,N1
801   UIN(I) = 2.*3.14159*(.3233-.0133E-3*TWO(I)+.57E-6*TWO(I)*TWO(I))/
     1         ALOG(.827*RR(I)/RI)
      DO 805 J=1,3
      IF (J-2) 802,803,804
802   I=5
      GO TO 805
803   I=8
      GO TO 805
804   I=11
805   QPGH(J)=UIN(I)*(TGH(J)-TWO(I))+UOUT(J)*(TGH(J)-TO(J))
      DO 92 I=2,N1
      IF (I-7) 81,84,82
81    J=1
      GO TO 90
82    IF (I-9) 84,84,83
83    J=3
      GO TO 90
84    J=2
90    TH=(QPGH(J)+UIN(I)*TWO(I)+UOUT(J)*TO(J))/(UIN(I)+UOUT(J))
92    QGH(I)=UIN(I)*(TH-TWO(I))/144.
C
C          CALCULATION OF CORRECTED HEAT FLUX
      DO 110 I=2,N1
110   QCOR(I)=QGEN(I)+QCON(I)+QGH(I)
C
C          CALCULATION OF CORRECTED INLET TEMPERATURE
      QLOSEX=3413.*TSKW-FLRT*(HPTD(PABS,TOUT)-HPTD(PABS,TIN))
      TOI=0.8*TINF+0.2*TIN
      QLOSI=1.65*(.197*(TIN-TOI)-.585E-5*(TIN*TIN-TOI*TOI)+.115E-6*
     1 (TIN**3-TOI**3) )
      TOO=0.8*TINF+0.2*TOUT
      QLOSO=.29*(.197*(TOUT-TOO)-.585E-5*(TOUT*TOUT-TOO*TOO)+.115E-6*
     1 (TOUT*TOUT*TOUT-TOO*TOO*TOO))
      QLOSS=QLOSI*QLOSEX/(QLOSI+QLOSO)
      QC1 = .499*CW(1)*AW(1)*(SOL(1,2)+2.*SOL(1,3)*Z(1)+
     1       3.*SOL(1,4)*Z(1)*Z(1))
      ENTH(1)=HPTD(PABS,TIN)+(QC1-QLOSS)/FLRT
      TG(1)=TPHD(PABS,ENTH(1))
C
C          CALCULATION OF BULK GAS TEMPERATURE
      QCO = .499*(6.6+.0074*TO)*AW(2)*SOL(1,2)
      QLUG=0.075*(7.4+.00512*TLH(1))*(TLH(1)-TLH(2))
      ENTH(2)=ENTH(1)+(QCO-QC1+QLUG+.499*QCOR(2)*Z(2))/FLRT
      DO 130 I=3,N1
130   ENTH(I)=ENTH(I-1)+.2495*(QCOR(I)+QCOR(I-1))*(Z(I)-Z(I-1))/FLRT
      QCL = .499*(6.6+.0074*TL)*AW(N1)*(SOL(N-4,2) +
     1      2.*SOL(N-4,3)*L + 3.*SOL(N-4,4)*L*L)
      QCN = .499*CW(N)*AW(N)*(SOL(N-4,2) + 2.*SOL(N-4,3)*Z(N) +
     1      3.*SOL(N-4,4)*Z(N)*Z(N))
      QLUG=0.075*(7.4+.00512*TLH(3))*(TLH(3)-TLH(4))
      ENTH(N)=ENTH(N-1)+(QCN-QCL+QLUG+.499*QCOR(N-1)*(72.2-Z(N-1)))/FLRT
      DO 140 I=2,N
140   TG(I)=TPHD(PABS,ENTH(I))
      QLOSS=QLOSEX-QLOSS
      ENTHO=ENTH(N)-(QLOSS+QCN)/FLRT
      TOUTC=TPHD(PABS,ENTHO)
      RATING=QLOSEX/(3413.*TSKW)
C
C          CALCULATION OF INSIDE WALL TEMPERATURE
      DO 120 I=2,N1
      C = (QCOR(I) - QGH(I))/(1.-RR(I)**2.)
120   TWI(I) = TWO(I) + (QCOR(I)*ALOG(RR(I))+C*(.5*(1.-RR(I)**2.) +
     1         RR(I)**2.*ALOG(RR(I))))*1.91/CW(I)
C
C          CORRECTION FOR AXIAL RADIANT TRANSFER
      DO 141 I=1,N
      TGNR(I)=TG(I)
      X1=TG(I)+459.6
      X2=TWI(I)+459.6
      TG4(I)=X1*X1*X1*X1
      TW4(I)=X2*X2*X2*X2
      BBK(I)=SIG*TW4(I)
      TAW(I)=TAU(PABS,X2)
141   TAG(I)=TAU(PABS,X1)
      IF (TAW(1)-TAULIM) 165,165,162
162   PRINT 163
163   FORMAT ('0THE GAS IS NOT OPTICALLY THIN. NO CORRECTION FOR AXIAL
     1RADIANT HEAT TRANSFER WILL BE ATTEMPTED.')
      KS=0
      DO 164 I=1,N
      QRAD(I)=0.0
      EPS = EPSA + EPSB*ALOG(TWI(I) + 459.6)
164   B(I)=SIG*(EPS*TW4(I)+(1.-EPS)*TG4(I)*(1.-EXP(-TAG(I))))/
     1 (1.-(1.-EPS)*EXP(-TAW(I)))
      GO TO 230
165   CALL AXRAD(Z,N,X,IND,TG,SOL,PABS,EPS,F3,F4,H1,H2,F1,F2,G1,G2,
     1PHI1,PHI2,FLRT,KS,ENTH,QRAD,QCOR,KPUNCH,B,EPSA,EPSB)
C
C          WALL TO GAS RADIANT HEAT TRANSFER
230   DO 240 I=2,N1
      QRR=(1.-EXP(-TAW(I)))*B(I)-(1.-EXP(-TAG(I)))*SIG*TG4(I)
240   HZR(I)=QRR/(TWI(I)-TG(I))
C
C          TOTAL HEAT TRANSFER COEFFICIENT
      DO 250 I=2,N1
      UNITC = 144./(3.14159*2.*RI)
250   HZ(I)=UNITC*QCOR(I)/(TWI(I)-TG(I))
C
C          GAS PROPERTIES AT BULK, FILM, AND WALL TEMPERATURES
      DO 260 I=1,N
      TFLM=0.5*(TG(I)+TWI(I))
      RHOW(I)=1./VPTD(PABS,TWI(I))
      RHOB(I)=1./VPTD(PABS,TG(I))
```

```
      RHOF(I)=1./VPTD(PABS,TFLM)
      VSW(I)=VIS(TWI(I))
      VSB(I)=VIS(TG(I))
      VSF(I)=VIS(TFLM)
      CGW(I)=CDT(PABS,TWI(I))
      CGB(I)=CDT(PABS,TG(I))
      CGF(I)=CDT(PABS,TFLM)
      CPW(I)=SPHT(PABS,TWI(I))
      CPF(I)=SPHT(PABS,TFLM)
  260 CP(I)=SPHT(PABS,TG(I))
C
C         LOCAL NUSSELT, REYNOLDS, PRANDTL, AND PLANCK NUMBERS
      UN=116000.
      EM=.264E-3*FLRT
      DO 270 I=1,N
      PLNKB(I)=6.012*CGB(I)*TAG(I)*(TG(I)+459.6)/(SIG*TG4(I))
      PLNKW(I)=6.012*CGW(I)*TAW(I)*(TWI(I)+459.6)/(SIG*TW4(I))
      REW(I)=EM/VSW(I)
      REB(I)=EM/VSB(I)
      REF(I)=EM/VSF(I)
      REWB(I)=REW(I)*RHOW(I)/RHOB(I)
      REFB(I)=REF(I)*RHOF(I)/RHOB(I)
      PRW(I)=UN*CPW(I)*VSW(I)/CGW(I)
      PRB(I)=UN*CP(I)*VSB(I)/CGB(I)
  270 PRF(I)=UN*CPF(I)*VSF(I)/CGF(I)
      DO 280 I=2,N1
      H=.0416*HZ(I)
      UB(I)=H/CGB(I)
      UW(I)=H/CGW(I)
      UF(I)=H/CGF(I)
      UBC(I) = UB(I) - 2.*RI*HZR(I)/(12.*CGB(I))
      TRAT(I)=(TWI(I)+459.6)/(TG(I)+459.6)
      CALL QHOTF(QHOT,PABS,TWI(I),TG(I),TRAT(I),EPSA,EPSB,KEY)
      UBCHOT(I) = UB(I)*(1. - QHOT/QCOR(I)/UNITC)
  280 UMCEL(I)=.021*REB(I)**.8*PRB(I)**.4*(1.+Z(I)**(-.7))/SQRT(TRAT(I))
C
C           UNIT CONVERSION
      QNOM=UNITC*QNOM
      DO 290 I=2,N1
      QGH(I)=UNITC*QGH(I)
      QCON(I)=UNITC*QCON(I)
      QGEN(I)=UNITC*QGEN(I)
      QCOR(I)=UNITC*QCOR(I)
  290 ACCPAR(I)=-4.*QCOR(I)*(1./VPTD(PABS,TG(I)+5.)-1./VPTD(PABS,
     1TG(I)-.5))/(10.*RHOB(I)*CP(I)*G*REB(I))
      CALL CNUHF(Z,L,N,TWI,TG,QCOR,HZR,KPUNCH,UBC,UFNUBC,FILIM,
     1   UMCEL,UBCHOT)
C
C           OUTPUT SPECIFICATIONS
      DO 294 I=2,N1
      J=1
      PUNCH 292,M,KEY,J,UB(I),UBC(I),UFNUBC(I),Z(I),REB(I),REWB(I),
     1 PRB(I),TAG(I),PLNKB(I),TRAT(I),UBCHOT(I)
  292 FORMAT (I3,2I2,3F6.2,F5.1,2F7.0,2F6.3,F7.4,F6.3,F7.2)
      J=2
  294 PUNCH 296,M,KEY,J,UW(I),Z(I),REW(I),REWB(I),PRW(I),TAW(I),PLNKW(I)
     1 ,TRAT(I),ACCPAR(I)
  296 FORMAT (I3,2I2,F8.2,F6.1,2F8.0,2F7.3,F7.4,F7.3,E11.3)
      DO 485 LP=1,2
      PRINT 20,M
   20 FORMAT ('1                              RUN NUMBER 'I3)
      PRINT 201,KS
  201 FORMAT ('0KS = ',I3)
      PRINT 300,FLRT,TSKW,PABS,TIN
  300 FORMAT ('0MDOT = ',F10.3,'          TSKW = ',F10.4,'          PABS = '
     1,F10.2,'          TIN = ',F10.2)
      PRINT 310,QNOM,QLOSEX,QLOSI,QLOSO
  310 FORMAT ('0QNOM = ',F10.2,'          QLOSEX = ',F10.2,'          QLOSI =
     1',F10.2,'          QLOSO = ',F10.2)
      PRINT 320, TOUT,TINF,PINF,PTS
  320 FORMAT ('0TOUT = ',F10.1,'          TINF = ',F10.1,'          PINF = '
     1,F10.0,'          PTS = ',F10.1)
      PRINT 330,G,RATING,TOUTC
  330 FORMAT ('0    G = ',F10.0,'          RATING = ',F10.4,'          TOUTC ='
     1,F10.1)
      PRINT 331,EPSA,EPSB,TAULIM
  331 FORMAT ('0          EPSA = ',F10.3,'          EPSB = ',F10.3,'
     1          TAULIM = ',F10.3)
      PRINT 340, (TGH(I),I=1,3),(TLH(I),I=1,4)
  340 FORMAT ('0TGH(I) = ',3F10.2,'          TLH(I) = ',4F10.2)
      PRINT 350
  350 FORMAT ('1 I       Z(I)      TWO(I)      TWI(I)      QCON(I)      QGH(I
     1)     QRAD(I)     QGEN(I)     QCOR(I)      TG(I)      HZ(I)      HZR(I)
     2')
      I=1
      PRINT 360,I,Z(I),TWO(I),TWI(I),TG(I)
  360 FORMAT ('0',I2,3F11.2,55X,F11.2)
      DO 370 I=2,N1
  370 PRINT 380,I,Z(I),TWO(I),TWI(I),QCON(I),QGH(I),QRAD(I),QGEN(I),
     1QCOR(I),TG(I),HZ(I),HZR(I)
  380 FORMAT ('0@',I2,11F11.2)
      I=N
      PRINT 360,I,Z(I),TWO(I),TWI(I),TG(I)
      PRINT 390
  390 FORMAT ('0 I    RHOW(I)     RHOB(I)     RHOF(I)      MUW(I)      MUB(I)
     1     MUF(I)     KGW(I)     KGB(I)     KGF(I)     CP(I)  TAW(I) TAG(I
     2)')
      DO 400 I=1,N
  400 PRINT 410,I,RHOW(I),RHOB(I),RHOF(I),VSW(I),VSB(I),VSF(I),CGW(I),
     1 CGB(I),CGF(I),CP(I),TAW(I),TAG(I)
  410 FORMAT ('0@',I2,9E11.3,3F7.3)
      PRINT 420
  420 FORMAT ('1 I       REW(I)      REB(I)      REF(I)      REWB(I)      REFB(I
     1)      PRW(I)      PRB(I)      PRF(I)       B(I)      BBK(I)     TGNR(I)
     2')
      I=1
      PRINT 430,I,REW(I),REB(I),REF(I),REWB(I),REFB(I)
  430 FORMAT ('0',I2,5F11.0)
      DO 440 I=2,N1
  440 PRINT 450,I,REW(I),REB(I),REF(I),REWB(I),REFB(I),PRW(I),PRB(I),
```

```
     1PRF(I),B(I),BBK(I),TGNR(I)
450  FORMAT ('0',I2,5F11.0,3F11.3,2F11.0,F11.2)
     I=N
     PRINT 430,I,REW(I),REB(I),REF(I),REWB(I),REFB(I)
     PRINT 460
460  FORMAT ('0 I      NUW(I)      NUF(I)      NUB(I)      NUBC(I)    UFNUBC
    1(I)  NUMCEL(I)   PLNKB(I)    PLNKW(I)     TRAT(I)    ACCPAR(I)  NUBCHO
    2T')
     DO 470 I=2,N1
470  PRINT 480,I,UW(I),UF(I),UB(I),UBC(I),UFNUBC(I),UMCEL(I),PLNKB(I),
    1 PLNKW(I),TRAT(I),ACCPAR(I),UBCHOT(I)
480  FORMAT ('0',I2,6F11.2,2E11.3,F11.3,E11.3,F11.2)
485  CONTINUE
     GO TO 15
     END
```

```
     SUBROUTINE GEOM(Z,N,F3,F4,H1,H2,F1,F2,G1,G2,PHI1,PHI2)
     DIMENSION Z(75),F1(75,74),F2(75,74),F3(75),F4(75),H1(75),H2(75),
    1G1(75,74),G2(75,74),PHI1(75,74),PHI2(75,74)
     N1=N-1
     DO 500 I=1,N
          V=Z(I)-Z(1)
     IF (V-10.) 20,20,30
20   V2=V*V
     F3(I)=(1.+2.*V2)/(2.*SQRT(1.+V2))-V
     H1(I)=1.+2.*V2-2.*V*SQRT(1.+V2)
     GO TO 40
30   F3(I)=0.0
          H1(I)=0.0
40   V=Z(N)-Z(I)
     IF (V-10.) 50,50,60
50   V2=V*V
     F4(I)=(1.+2.*V2)/(2.*SQRT(1.+V2))-V
     H2(I)=1.+2.*V2-2.*V*SQRT(1.+V2)
     GO TO 70
60   F4(I)=0.0
          H2(I)=0.0
70   DO 500 J=1,N1
     IF (J-1) 75,80,90
75   CALL ERROR
80   ZIJ=Z(I)-Z(1)
     SZIJ=SQRT(ZIJ*ZIJ+1.)
     GO TO 100
90   ZIJ=ZIJ1
          SZIJ=SZIJ1
100  ZIJ1=Z(I)-Z(J+1)
     SZIJ1=SQRT(ZIJ1*ZIJ1+1.)
          ZJ1J=Z(J+1)-Z(J)
     IF (ABS(ZIJ)-10.)  130,110,110
110  IF (ABS(ZIJ1)-10.) 130,120,120
120  F1(I,J)=0.0
          F2(I,J)=0.
          G1(I,J)=0.0
          G2(I,J)=0.0
          PHI1(I,J)=0.0
          PHI2(I,J)=0.0
     GO TO 500
130  IF (J-I) 140,170,170
140       F1(I,J)=ZJ1J+SZIJ1-SZIJ+0.5*(1.0/SZIJ-1.0/SZIJ1)
          F2(I,J)=0.5*(ZJ1J+(ZIJ/ZJ1J+1.0)*SZIJ1-(ZIJ/ZJ1J)*SZIJ-
    1      1.0/SZIJ1)
          G1(I,J)=0.3927*(ZIJ1*SZIJ1-ZIJ*SZIJ-ZIJ1*ZIJ1+ZIJ*ZIJ)
          G2(I,J)=(0.3927/ZJ1J)*(-0.66667*(SZIJ1*SZIJ1*SZIJ1-SZIJ*
    1     SZIJ*SZIJ)+SZIJ1-SZIJ+ZIJ*ZIJ1*SZIJ1-ZIJ*ZIJ*SZIJ+0.66667*
    2     ZIJ1*ZIJ1*ZIJ1+0.33333*ZIJ*ZIJ*ZIJ-ZIJ*ZIJ1*ZIJ1)
     IF (J+1-I) 150,160,75
150       PHI1(I,J)=0.75*(1.0/(ZIJ1*ZIJ1)-1.0/(ZIJ*ZIJ))
          PHI2(I,J)=(0.75/ZJ1J)*(1.0/ZIJ-1.0/ZIJ1-0.5*ZIJ*
    1     (1.0/(ZIJ*ZIJ)-1.0/(ZIJ1*ZIJ1)))
     GO TO 500
160  PHI1(I,J)=(1.414214*ZIJ)/(SQRT(2.*ZIJ*ZIJ+1.))
```

```
            PHI2(I,J)=1.0-2.66667/(3.14159*ZIJ)+0.75/(ZIJ*ZIJ)
      GO TO 500
170         F1(I,J)=ZJ1J-SZIJ1+SZIJ-0.5*(1.0/SZIJ-1.0/SZIJ1)
            F2(I,J)=0.5*(ZJ1J-(ZIJ/ZJ1J+1.0)*SZIJ1+(ZIJ/ZJ1J)*SZIJ+
     1 1.0/SZIJ1)
            G1(I,J)=0.3927*(ZIJ*SZIJ-ZIJ1*SZIJ1-ZIJ1*ZIJ1+ZIJ*ZIJ)
            G2(I,J)=(0.3927/ZJ1J)*(0.66667*(SZIJ1*SZIJ1*SZIJ1-SZIJ*SZIJ
     1      *SZIJ)-SZIJ1+SZIJ-ZIJ*ZIJ1*SZIJ1+ZIJ*ZIJ*SZIJ+0.66667*ZIJ1*
     2      ZIJ1*ZIJ1+0.33333*ZIJ*ZIJ*ZIJ-ZIJ*ZIJ1*ZIJ1)
      IF (I-J) 190,180,75
180   PHI1(I,J)=-1.414214*ZIJ1/(SQRT(2.*ZIJ1*ZIJ1+1.))
            PHI2(I,J)=-2.66667/(3.14159*ZIJ1)-0.75/(ZIJ1*ZIJ1)
      GO TO 500
190         PHI1(I,J)=0.75*(1.0/(ZIJ*ZIJ)-1.0/(ZIJ1*ZIJ1))
      PHI2(I,J)=(.75/ZJ1J)*(1./ZIJ1-1./ZIJ+0.5*ZIJ*(1./
     1      (ZIJ*ZIJ)-1.0/(ZIJ1*ZIJ1)))
500   CONTINUE
      RETURN
      END

      FUNCTION FRATE(POR,PINF,DH,SG,TOR)
           PORA=POR+PINF
           CD=0.6604
      M=0
      DP=.0361*DH*SG
           Y=1.-.325*DP/PORA
5     FRATE=16.51*CD*Y*SQRT(DH*SG/VPTD(PORA,TOR))
      RE=.263E-3*FRATE/VIS(TOR)
      IF (RE-5000.) 10,30,30
10     IF (M) 42,20,50
20    CD=.6604+.03855*ALOG(5000./RE)
      REO=RE
      M=M+1
      IF (M-10) 5,40,40
40    PRINT 41
41    FORMAT ('OFLOW RATE ITERATION IS DIVERGING')
42     CALL ERROR
50    IF (ABS(REO-RE)-50.) 30,30,20
30    RETURN
      END

      FUNCTION TEMP(V)
           IF (V-10.503) 40, 40, 2
2     IF (V-17.42) 30, 30, 3
3     IF (V-25.915) 20, 20, 4
4     IF (V-34.729) 10, 5, 5
5     TEMP=-2.922553E-4 +48.71800*V-.2441477*V*V+.003399242*V*V*V
      GO TO 50
10    TEMP=-1.619159E-4 + 50.10753*V-.3220169*V*V+.004488756*V*V*V
      GO TO 50
20    TEMP=-2.3413E-4+50.88013*V-.3836926*V*V+.00570383*V*V*V
      GO TO 50
30    TEMP=-2.906128E-4+51.71265*V-.4811362*V*V+.008547176*V*V*V
      GO TO 50
40    TEMP=-1.0269E-3+54.38010*V-1.0079*V*V+.03474082*V*V*V
50    RETURN
      END
```

```
      SUBROUTINE RGRN(Z,T,N,SOL)
      DIMENSION Z2(14),Z3(14),Z4(14),Z5(14),Z6(14),ZT(14),Z2T(14),
     1 Z3T(14),TP(14,14),C(4),A(4,4),Z(14),T(14),SOL(14,4)
           K=0
       N4=N-4
      DO 10 I=1,N
           Z2(I)=Z(I)*Z(I)
           Z3(I)=Z(I)*Z2(I)
           Z4(I)=Z(I)*Z3(I)
           Z5(I)=Z(I)*Z4(I)
           Z6(I)=Z(I)*Z5(I)
           ZT(I)=Z(I)*T(I)
           Z2T(I)=Z2(I)*T(I)
10    Z3T(I)=Z3(I)*T(I)
           SZ=0.0
           SZ2=0.0
           SZ3=0.0
           SZ4=0.0
           SZ5=0.0
           SZ6=0.0
           ST=0.0
           SZT=0.0
           SZ2T=0.0
           SZ3T=0.0
      DO 20 I=1,5
           SZ=SZ+Z(I)
           SZ2=SZ2+Z2(I)
           SZ3=SZ3+Z3(I)
           SZ4=SZ4+Z4(I)
           SZ5=SZ5+Z5(I)
           SZ6=SZ6+Z6(I)
           ST=ST+T(I)
           SZT=SZT+ZT(I)
           SZ2T=SZ2T+Z2T(I)
20    SZ3T=SZ3T+Z3T(I)
30    DO 50 I=1,4
      DO 50 J=1,4
      IF (I+J-2) 31,32,33
31     CALL ERROR
32    A(I,J)=5.0
      GO TO 50
33    IF (I+J-3) 31,34,35
34         A(I,J)=SZ
      GO TO 50
35    IF (I+J-4) 31,36,37
36         A(I,J)=SZ2
      GO TO 50
37    IF (I+J-5) 31,38,39
38         A(I,J)=SZ3
      GO TO 50
39    IF (I+J-6) 31,40,41
40         A(I,J)=SZ4
      GO TO 50
41    IF (I+J-7) 31,42,43
42         A(I,J)=SZ5
```

```
      GO TO 50
43    IF (I+J-8) 31,44,31
44          A(I,J)=SZ6
50    CONTINUE
            C(1)=ST
            C(2)=SZT
            C(3)=SZ2T
            C(4)=SZ3T
      CALL SIMQ(A,C,4,KS)
      DO 60 I=1,4
60    SOL(K+1,I)=C(I)
      K=K+1
      K4=K+4
      DO 70 I=K,K4
70    TP(K,I)=POLY(K,Z(I),SOL)
      IF (K+4-N) 80,85,85
80          SZ=SZ-Z(K)+Z(K+5)
            SZ2=SZ2-Z2(K)+Z2(K+5)
            SZ3=SZ3-Z3(K)+Z3(K+5)
            SZ4=SZ4-Z4(K)+Z4(K+5)
            SZ5=SZ5-Z5(K)+Z5(K+5)
            SZ6=SZ6-Z6(K)+Z6(K+5)
            ST=ST-T(K)+T(K+5)
            SZT=SZT-ZT(K)+ZT(K+5)
            SZ2T=SZ2T-Z2T(K)+Z2T(K+5)
            SZ3T=SZ3T-Z3T(K)+Z3T(K+5)
      GO TO 30
85    PRINT 90
90    FORMAT ('0 I         T(I)      TP(I-4,I)    TP(I-3,I)    TP(I-2,I)    T
     1P(I-1,I)     TP(I,I)')
          I=1
      PRINT 100,I,T(I),TP(I,I)
100    FORMAT ('0',I2,F12.1,48X,F12.1)
          I=2
      PRINT 110,I,T(I),TP(I-1,I),TP(I,I)
110   FORMAT ('0',I2,F12.1,36X,2F12.1)
          I=3
      PRINT 120,I,T(I),TP(I-2,I),TP(I-1,I),TP(I,I)
120   FORMAT ('0',I2,F12.1,24X,3F12.1)
          I=4
      PRINT 130,I,T(I),TP(I-3,I),TP(I-2,I),TP(I-1,I),TP(I,I)
130   FORMAT ('0',I2,F12.1,12X,4F12.1)
      DO 140 I=5,N4
140   PRINT 141,I,T(I),TP(I-4,I),TP(I-3,I),TP(I-2,I),TP(I-1,I),TP(I,I)
141   FORMAT ('0',I2,6F12.1)
          I=N-3
      PRINT 141,I,T(I),TP(I-4,I),TP(I-3,I),TP(I-2,I),TP(I-1,I)
          I=N-2
      PRINT 141,I,T(I),TP(I-4,I),TP(I-3,I),TP(I-2,I)
          I=N-1
      PRINT 141,I,T(I),TP(I-4,I),TP(I-3,I)
          I=N
      PRINT 141,I,T(I),TP(I-4,I)
      RETURN
      END
```

```
      SUBROUTINE CNUHE(Z,L,N,TWI,TG,QCOR,HZR,KPUNCH,UBC,UFNUBC,FILIM,
     1  UMCEL,UBCHOT)
      DIMENSION Z(14),TWI(14),TG(14),QCOR(14),HZR(14),UBC(14),DT(14),
     1UFNUBC(14),QWC(14),SOLT(14,4),SOLQ(14,4),ZTQ(73),DTP(73),QWCP(73),
     2FI(73),FIO(73),FIZ(14),FIZO(14)
      DIMENSION VF(73),UMCEL(14),UBCHOT(14)
      REAL L
      N1=N-1
      N2=N-2
      DO 10 I=1,N
10    DT(I)=TWI(I)-TG(I)
      QWC(1)=0.0
      DO 15 I=2,N1
15    QWC(I)=QCOR(I)-HZR(I)/DT(I)
      QWC(N)=0.0
      CALL RGRN(Z,DT,N,SOLT)
      CALL RGRN(Z,QWC,N,SOLQ)
      DZTQ=L/72.
      ZTQ(1)=0.0
      DO 50 J=1,73
      IF (J-1) 21,22,21
22    ZTQ(J)=ZTQ(J)
      GO TO 25
21    ZTQ(J)=ZTQ(J-1)+DZTQ
25    DO 24 I=3,N2
      IF (ZTQ(J)-Z(I)) 23,23,24
23    K=I-2
      GO TO 40
24    CONTINUE
      K=N-4
40    DTP(J)=POLY(K,ZTQ(J),SOLT)
      QWCP(J)=POLY(K,ZTQ(J),SOLQ)
      FI(J)=DTP(J)/QWCP(J)
50    FIO(J)=FI(J)
      IM=0
53    IF (IM-10) 54,54,60
54    IM=IM+1
      SUMFI=0.0
      DO 56 IR=2,73
      SUM=0.0
       DO 55 I=2,IR
55    SUM=SUM+(QWCP(I)-QWCP(I-1))*FI(IR-I+1)
      FI1=(DTP(IR)-SUM)/QWCP(1)
      SUMFI = SUMFI + (1.-FI1/FI(IR))**2
56    FI(IR)=FI1
      RMSFI=SQRT(SUMFI/71.)
      IF (RMSFI-FILIM) 58,58,53
58    IF (KPUNCH-1) 65,60,65
60    PRINT 61,IM,RMSFI
61    FORMAT ('0IM=',I2,20X,'RMSFI=',F6.3)
      PRINT 62
62     FORMAT ('0 J',8X,'ZTQ(J)',15X,'FI(J)',14X,'DTP(J)',14X,'QWCP(J)')
      DO 63 J=1,73
63    PRINT 64,J,ZTQ(J),FI(J),DTP(J),QWCP(J)
64    FORMAT (' ',I2,4F20.8)
```

```
 65   CONTINUE
C              CONVOLUTION WITH MCELIGOT (FOR KPUNCH = 5)
      IF (KPUNCH-5) 93,90,93
 90   DO 92 IR=2,73
      SUM = 0.
      DO 91 I=2,IR
 91   SUM = SUM + (QWCP(I)-QWCP(I-1))/(1.+((IR-I+1)*DZTQ)**(-.7))
 92   VF(IR) = QWCP(IR)/(QWCP(1)/(1.+(IR*DZTQ)**(-.7))+SUM)
 93   CONTINUE
      DO 75 I=2,N1
      DO 70 J=2,73
      IF (ZTQ(J)-Z(I)) 70,72,72
 70    CONTINUE
 72   FIZ(I)=FI(J-1)+(FI(J)-FI(J-1))*(Z(I)-ZTQ(J-1))/(ZTQ(J)-ZTQ(J-1))
      IF (KPUNCH-5) 95,94,95
 94   UBCHOT(I) = (UMCEL(I)/(1.+Z(I)**(-.7)))*
     1   (VF(J-1)+(VF(J)-VF(J-1))*(Z(I)-ZTQ(J-1))/(ZTQ(J)-ZTQ(J-1)))
 95   CONTINUE
 75   FIZO(I)=FIO(J-1)+(FIO(J)-FIO(J-1))*(Z(I)-ZTQ(J-1))/(ZTQ(J)-
     1 ZTQ(J-1))
      DO 80 I=2,N1
 80   UFNUBC(I)=UBC(I)*FIZO(I)/FIZ(I)
      RETURN
      END

      FUNCTION POLY(K,X,SOL)
      DIMENSION SOL(14,4)
      POLY=SOL(K,1)+SOL(K,2)*X+SOL(K,3)*X*X+SOL(K,4)*X*X*X
      RETURN
      END

      SUBROUTINE AXRAD(Z,N,X,IND,TG,SOL,PABS,EPS,F3,F4,H1,H2,F1,F2,
     1G1,G2,PHI1,PHI2,FLRT,KS,ENTH,QRAD,QCOR,KPUNCH,B,EPSA,EPSB)
      DIMENSION Z(14),X(75),TG(14),SOL(14,4),F3(75),F4(75),H1(75),H2(75)
     1,F1(75,74),F2(75,74),G1(75,74),G2(75,74),PHI1(75,74),PHI2(75,74),
     2ENTH(14),QRAD(14),QCOR(14),TGX(75),TWX(75),C1(75),QRADX(75),
     3ENTHX(75),TAWX(75),TAGX(75),TWX4(75),TGX4(75),ALFA(75,74),
     4BETA(75,74),GAMA(75,74),A(75,75),AA(5625),B(14)
      SIG=.1714E-8
      IND2=IND+2
      IND3=IND+3
      N1=N-1
      DO 160 I=1,IND3
      JZ=1
142   JZ=JZ+1
      IF (Z(JZ)-X(I)) 142,143,143
143   TGX(I)=TG(JZ-1)+(TG(JZ)-TG(JZ-1))*(X(I)-Z(JZ-1))/(Z(JZ)-Z(JZ-1))
      IF (JZ-3) 144,145,146
144   TWX(I)=POLY(JZ-1,X(I),SOL)
      GO TO 154
145   TWX(I)=(POLY(JZ-1,X(I),SOL)+POLY(JZ-2,X(I),SOL))/2.
      GO TO 154
146   IF (JZ-5) 147,148,148
147   TWX(I)=(POLY(JZ-1,X(I),SOL)+POLY(JZ-2,X(I),SOL)+POLY(JZ-3,X(I),
     1 SOL))/3.
      GO TO 154
148   IF (N-JZ-1) 149,150,151
149   TWX(I)= POLY(JZ-4,X(I),SOL)
      GO TO 154
150   TWX(I)=(POLY(JZ-4,X(I),SOL)+POLY(JZ-3,X(I),SOL))/2.
      GO TO 154
151   IF (N-JZ-3) 152,153,153
152   TWX(I)=(POLY(JZ-4,X(I),SOL)+POLY(JZ-3,X(I),SOL)+POLY(JZ-2,X(I),SOL
     1 ))/3.
      GO TO 154
153   TWX(I)=(POLY(JZ-4,X(I),SOL)+POLY(JZ-3,X(I),SOL)+POLY(JZ-2,X(I),SOL
     1 )+POLY(JZ-1,X(I),SOL))/4.
154   XX1=TGX(I)+459.6
      XX2=TWX(I)+459.6
      TGX4(I)=XX1**4
      TWX4(I)=XX2**4
      TAWX(I)=TAU(PABS,XX2)
160   TAGX(I)=TAU(PABS,XX1)
      DO 200 I=1,IND3
      EPS = EPSA + EPSB*ALOG(TWX(I) + 459.6)
      C1(I)=SIG*(EPS*TWX4(I)+(1.-EPS)*(TGX4(1)*F3(I)+TGX4(IND3)*F4(I)+
     1 TAGX(I)*(1.-F3(I)-F4(I))*TGX4(I)))
      DO 180 J=1,IND2
      ALFA(I,J)=F1(I,J)-0.5*TAWX(I)*PHI1(I,J)
      BETA(I,J)=F2(I,J)-0.5*TAWX(I)*PHI2(I,J)
180   GAMA(I,J)=ALFA(I,J)-BETA(I,J)
      A(I,1)=-(1.-EPS)*GAMA(I,1)
      DO 190 J=2,IND2
190   A(I,J)=-(1.-EPS)*(BETA(I,J-1)+GAMA(I,J))
       A(I,IND3)=-(1.-EPS)*BETA(I,IND2)
200   A(I,I)=1.+A(I,I)
      CALL ARRAY(2,IND3,IND3,75,75,AA,A)
      CALL SIMQ(AA,C1,IND3,KS)
      DO 220 I=1,IND3
      QRA=0.0
      QRC=0.0
      DO 210 J=1,IND2
      QRA=QRA+C1(J)*G1(I,J)+(C1(J+1)-C1(J))*G2(I,J)
210   QRC=QRC+C1(J)*GAMA(I,J)+C1(J+1)*BETA(I,J)
      QRA=.001356*(QRA+SIG*(TGX4(IND3)*H2(I)-TGX4(I)*H1(I)))
      QRADX(I)=QRC+SIG*(TGX4(1)*F3(I)+TGX4(IND3)*F4(I))-C1(I)*(1.-
     1 TAWX(I))
220   ENTHX(I)=HPTD(PABS,TGX(I))+QRA/FLRT
      DO 223 J=2,N1
      I=1
221   I=I+1
      IF (X(I)-Z(J)) 221,222,222
222   ENTH(J)=ENTHX(I-1)+(ENTHX(I)-ENTHX(I-1))*(Z(J)-X(I-1))/(X(I)-
     1 X(I-1))
      B(J)=C1(I-1)+(C1(I)-C1(I-1))*(Z(J)-X(I-1))/(X(I)-X(I-1))
      QRAD(J)=QRADX(I-1)+(QRADX(I)-QRADX(I-1))*(Z(J)-X(I-1))/(X(I)-
     1 X(I-1))
      QCOR(J)=QCOR(J)+QRAD(J)/91.86
223   TG(J)=TPHD(PABS,ENTH(J))
      IF (KPUNCH-1) 224,225,224
224   RETURN
225   PRINT 980
980   FORMAT ('1 I',10X,'X(I)',10X,'TGX(I)',9X,'TWX(I)',12X,'B(I)',9X,
     1 'QRADX(I)')
      DO 990 I=1,IND3
990   PRINT 1000,I,X(I),TGX(I),TWX(I),C1(I),QRADX(I)
1000  FORMAT (' ',I2,3F15.2,F15.0,F15.2)
      RETURN
      END
```

```
C
C           LOCAL RADIANT FLUX BASED ON HOTTEL
      SUBROUTINE QHOTE(QHOT,PABS,TWI,TG,TRAT,EPSA,EPSB,KEY)
      IF (KEY-2) 10,20,10
   10 PL = PABS*TRAT/24./14.696
      CALL EPSHOT(ESTEAM,TWI,PL)
      IF (PABS - 14.696*2.) 1,2,2
    1 CW = .4*(PABS/14.696+3.)
      GO TO 3
    2 CW = 2.
    3 AGW = ESTEAM*CW*TRAT**(-.45)
      EPS = EPSA + EPSB*ALOG(TWI + 459.6)
      QHOT = .171E-8*((TWI+459.6)**4. - (TG+459.6)**4.)/
     1          (1./EPS + 1./AGW - 1.)
      GO TO 30
   20 QHOT = 0.
   30 CONTINUE
      RETURN
      END
C
C           STEAM EMISSIVITY FROM HOTTEL CHART, T(F), PL(ATM-FT)
      SUBROUTINE EPSHOT(ESTEAM,T,PL)
      IF (T-940.4) 1,2,2
    1 K2 = 56.E-5 - 44.E-5*SQRT(PL-.05)
      GO TO 3
    2 K2 = 76.8E-5 - 55.E-5*SQRT(PL-.033)
    3 K3 = - 3.34 + 2.75*SQRT(PL-.033)
      ESTEAM = EXP(K3 - K2*(T-940.4))
      RETURN
      END
C           TAU BASED ON SPECTRAL DATA (ABU-ROMIA&TIEN) - OVERRIDE
      FUNCTION TAU(P,T)
      TT=1.E-6*T*T
      TAU=0.00283*P*(5.6/TT-.3/(TT*TT))
      RETURN
      END

      SUBROUTINE Q(TWO,TO,TL,N,QNOM,QGEN,Z,L,AW)
C           SUBROUTINE FOR UNIFORM AND NONUNIFORM 310-SS TEST SECTION
      DIMENSION TWO(14),QGEN(14),Z(14),AW(14)
      REAL L
      N1=N-1
      N2=N-2
      RA = 103.0
      RB = .0165
      RABAR = Z(2)*(RA+RB*(TO+TWO(2))/2.)/AW(2) + (L-Z(N1))*
     1(RA+RB*(TWO(N1)+TL)/2.)/AW(N1)
      DO 10 I=2,N2
      T=TWO(I)
      T1=TWO(I+1)
   10 RABAR = RABAR + ((RA+RB*T)/AW(I) + (RA+RB*T1)/AW(I+1))
     1      *(Z(I+1)-Z(I))/2.
      X = QNOM*L/RABAR
      DO 20 I=2,N1
   20 QGEN(I) = X*(RA+RB*TWO(I))/AW(I)
      RETURN
      END
```

```
      FUNCTION VPTD(P,T)                                                VPTD0010
C-----------------------------------------------------------------------VPTD0020
C     SPECIFIC VOLUME AS A FUNCTION OF PRESSURE AND                     VPTD0030
C     TEMPERATURE IN THE DRY REGION                                     VPTD0040
C-----------------------------------------------------------------------VPTD0050
      COMMON/UUU/STPRS(22)                                              VPTD0060
C-----------------------------------------------------------------------VPTD0070
      TT1=STPRD(P,T)                                                    VPTD0080
      STPRS(15)=((STPRS(9)*STPRS(5)*STPRS(13)*STPRS(10)                 VPTD0090
     1+STPRS(14))*STPRS(10)+1.0)*STPRS(9)                               VPTD0100
      VPTD=(STPRS(6)/STPRS(5)*4.55504+STPRS(15))*1.60185E-2             VPTD0110
     1-0.0160185*STPRS(19)*STPRS(5)**12                                 VPTD0120
      RETURN                                                            VPTD0130
      END                                                               VPTD0140
```

```
      FUNCTION STPRD(P,T)                                               STRD0010
C-----------------------------------------------------------------------STRD0020
C     CALCULATES COMMON TERMS FOR ALL DRY PROPERTIES                    STRD0030
C-----------------------------------------------------------------------STRD0040
      COMMON/UUU/STPRS(22)                                              STRD0050
C-----------------------------------------------------------------------STRD0060
      IF(P.GT.5500.0)CALL ERROR(1)                                      STRD0070
      IF(T.LE.0.0)CALL ERROR(2)                                         STRD0080
      STPRS(1)=P                                                        STRD0090
      STPRS(2)=T                                                        STRD0100
      STPRS(5)=STPRS(1)/14.6959                                         STRD0110
      STPRS(6)=STPRS(2)*0.55555556+255.38                               STRD0120
      STPRS(7)=STPRS(6)*STPRS(6)                                        STRD0130
      STPRS(8)=268644.325/STPRS(7)                                      STRD0140
      STPRS(8)=EXP(STPRS(8)*0.693147)/STPRS(6)*(-2641.62)               STRD0150
      STPRS(9)=STPRS(8)+1.89                                            STRD0160
      STPRS(10)=STPRS(9)/STPRS(7)*STPRS(5)                              STRD0170
      STPRS(11)=162460./STPRS(6)                                        STRD0180
      STPRS(12)=126970./STPRS(6)                                        STRD0190
      STPRS(13)=0.21828*STPRS(6)-STPRS(12)                              STRD0200
      STPRS(14)=82.546-STPRS(11)                                        STRD0210
      STPRS(17)=(1.0/STPRS(6))**6  *1.0E-16                             STRD0220
      STPRS(17)=3.635E-04-(STPRS(17)*STPRS(17)*STPRS(17)                STRD0230
     1*STPRS(17)*6.768)                                                 STRD0240
      STPRS(18)=(STPRS(9)/STPRS(6))**12                                 STRD0250
      STPRS(19)=STPRS(18)*STPRS(9)*STPRS(17)                            STRD0260
      STPRS(18)=-STPRS(18)*( (37.0*STPRS(17)-0.008724)*                 STRD0270
     1STPRS(9)+13.0*STPRS(17)*(STPRS(9)-1.89)*(1.0                      STRD0280
     2+372420.0/STPRS(7)))                                              STRD0290
      STPRD=1.0                                                         STRD0300
      RETURN                                                            STRD0310
      END                                                               STRD0320
```

```
      FUNCTION STPRE(X)                                                 STRE0010
C-----------------------------------------------------------------------STRE0020
C     CALCULATES ADDITIONAL COMMON TERMS FOR SOME OF                    STRE0030
C     THE DRY PROPERTIES                                                STRE0040
C-----------------------------------------------------------------------STRE0050
      COMMON/UUU/STPRS(22)                                              STRE0060
C-----------------------------------------------------------------------STRE0070
      STPRS(8)=372420./STPRS( 7)*STPRS(8)+STPRS(8)+STPRS(8)+1.89        STRE0080
      STPRS(10)=STPRS(10)/2.0*STPRS(5)                                  STRE0090
      STPRS(11)=STPRS(11)*STPRS(9)                                      STRE0100
      STPRS(11)=(-STPRS(14)-STPRS(14))*STPRS(8)+STPRS(11)               STRE0110
      STPRS(12)=STPRS(9)*STPRS(12)                                      STRE0120
      STPRS(12)=((STPRS(13)*STPRS(8)*2.0)-STPRS(12))*2.0                STRE0130
      STPRE=2.0                                                         STRE0140
      RETURN                                                            STRE0150
      END                                                               STRE0160
```

```
      FUNCTION CDT(P,T)
      IF (T-400.) 10,20,20
10    CDT=(.00865+2.75E-5*T)*(1.0+6.0E-6*(P-50.))
      GO TO 100
20     IF (T-500.) 30,40,40
30    CDT=(.00705+3.15E-5*T)*(1.0+5.0E-6*(P-50.))
      GO TO 100
40    IF (T-700.) 50,60,60
50    CDT=(.00505+3.55E-5*T)*(1.0+4.0E-6*(P-50.))
      GO TO 100
60    IF (T-1000.) 70,80,80
70    CDT=(.0019+4.0E-5*T)*(1.0+4.0E-6*(P-50.))
      GO TO 100
80    CDT=(-.0019+4.38E-5*T)*(1.+4.0E-6*(P-50.))
100   RETURN
      END
```

```
      FUNCTION TERPL(X,Y,ARG)                                           TERP0010
C-----------------------------------------------------------------------TERP0020
C     DOES FIFTH ORDER LAGRANGE INTERPOLATION                           TERP0030
C-----------------------------------------------------------------------TERP0040
      DIMENSION X(1),Y(1)                                               TERP0050
C-----------------------------------------------------------------------TERP0060
   10 SUM=0.0                                                           TERP0070
      DO 115 I=1,6                                                      TERP0080
      P=1.0                                                             TERP0090
      PK=1.0                                                            TERP0100
      DO 114 IP=1,6                                                     TERP0110
      IF(IP-I)113,114,113                                               TERP0120
  113 P=P*(ARG-X(IP))                                                   TERP0130
      PK=PK*(X(I) -X(IP))                                               TERP0140
  114 CONTINUE                                                          TERP0150
      SUM=SUM+P*Y(I)/PK                                                 TERP0160
  115 CONTINUE                                                          TERP0170
      TERPL=SUM                                                         TERP0180
      RETURN                                                            TERP0190
      END                                                               TERP0200
```

```
      FUNCTION VIS(T)
      VIS=1.0E-7*(1.53+4.74E-3*T)
      RETURN
      END
```

```
      FUNCTION SPHT(P,T)
      TPLS=T+5.0
      TMNS=T-5.0
      SPHT=0.1*(HPTD(P,TPLS)-HPTD(P,TMNS))
      RETURN
      END
```

```
      FUNCTION TAU(P,T)
      TT=1.E-6*T*T
      TAU=0.00283*P*(5.6/TT-1./(TT*TT))
      RETURN
      END
```

NITROGEN PROPERTIES

```
      FUNCTION HPTD(P,T)
      DIMENSION H1(20),T1(20)
      T1(1)=0.
      T1(2)=100.
      T1(3)=300.
      DO 10 I=4,20
10    T1(I)=T1(I-1)+100.
      H1(1)=-62.2
      H1(2)=-37.3
      H1(3)=12.495
      H1(4)=37.57
      H1(5)=62.825
      H1(6)=88.325
      H1(7)=114.105
      H1(8)=140.18
      H1(9)=166.56
      H1(10)=193.26
      H1(11)=220.29
      H1(12)=247.64
      H1(13)=275.28
      H1(14)=303.195
      H1(15)=331.375
      H1(16)=359.79
      H1(17)=388.435
      H1(18)=417.335
      H1(19)=446.365
      H1(20)=475.665
      IF (T) 20,30,15
15    IF (2000.-T) 20,30,30
20      PRINT 21
21    FORMAT ('0TEMPERATURE IS NOT WITHIN THE RANGE ALLOWING THE USE OF
     1HPTD@)
      CALL ERROR
30    I=0
35    I=I+1
      IF (T-T1(I+1)) 50,40,35
40    HPTD=H1(I+1)
      GO TO 100
50    HPTD=H1(I)+(H1(I+1)-H1(I))*(T-T1(I))/(T1(I+1)-T1(I))
100   RETURN
      END
```

```
      FUNCTION TPHD(P,H)
      DIMENSION H1(20),T1(20)
      T1(1)=0.
      T1(2)=100.
      T1(3)=300.
      DO 10 I=4,20
10    T1(I)=T1(I-1)+100.
      H1(1)=-62.2
      H1(2)=-37.3
      H1(3)=12.495
      H1(4)=37.57
      H1(5)=62.825
      H1(6)=88.325
      H1(7)=114.105
      H1(8)=140.18
      H1(9)=166.56
      H1(10)=193.26
      H1(11)=220.29
      H1(12)=247.64
      H1(13)=275.28
      H1(14)=303.195
      H1(15)=331.375
      H1(16)=359.79
      H1(17)=388.435
      H1(18)=417.335
      H1(19)=446.365
      H1(20)=475.665
      IF (H+62.2) 20,30,15
15    IF (475.665-H) 20,30,30
20    PRINT 21
21    FORMAT (' ENTHALPY IS NOT WITHIN THE RANGE ALLOWING THE USE OF
     1TPHD.@)
      CALL ERROR
30    I=0
35    I=I+1
      IF (H-H1(I+1)) 50,40,35
40    TPHD=T1(I+1)
      GO TO 100
50    TPHD=T1(I)+(T1(I+1)-T1(I))*(H-H1(I))/(H1(I+1)-H1(I))
100   RETURN
      END
```

```
      FUNCTION VPTD(P,T)
      VPTD=0.383*(T+459.6)/P
      RETURN
      END
```

```
      FUNCTION SPHT(P,T)
      DIMENSION T1(13),C(13)
      T1(1)=-100.
      DO 10 I=2,13
 10   T1(I)=T1(I-1)+180.
      C(1)=.2491
      C(2)=.2486
      C(3)=.2498
      C(4)=.2521
      C(5)=.2569
      C(6)=.2620
      C(7)=.2681
      C(8)=.2738
      C(9)=.2789
      C(10)=.2832
      C(11)=.2875
      C(12)=.2915
      C(13)=.2952
      IF (T+100.) 20,30,15
 15   IF (2060.-T) 20,30,30
 20   PRINT 21
 21   FORMAT (' TEMPERATURE IS NOT WITHIN THE RANGE ALLOWING THE USE OF
     1SPHT.@)
       CALL ERROR
 30   I=0
 35   I=I+1
      IF (T-T1(I+1)) 50,40,35
 40   SPHT=C(I+1)
      GO TO 100
 50   SPHT=C(I)+(C(I+1)-C(I))*(T-T1(I))/(T1(I+1)-T1(I))
 100  RETURN
      END
```

```
      FUNCTION CDT(P,T)
      DIMENSION T1(13),C(13)
      T1(1)=-100.
      DO 10 I=2,13
 10   T1(I)=T1(I-1)+180.
      C(1)=0.01054
      C(2)=.01514
      C(3)=.01927
      C(4)=.02302
      C(5)=.02646
      C(6)=.02960
      C(7)=.03241
      C(8)=.03507
      C(9)=.03741
      C(10)=.03958
      C(11)=.04151
      C(12)=.04335
      C(13)=.04500
      IF (T+100.) 20,30,15
 15   IF (2060.-T) 20,30,30
 20   PRINT 21
 21   FORMAT (' TEMPERATURE IS NOT WITHIN THE RANGE ALLOWING THE USE
     1OF CDT.@)
      CALL ERROR
 30   I=0
 35   I=I+1
      IF (T-T1(I+1)) 50,40,35
 40   CDT=C(I+1)
      GO TO 100
 50    CDT=C(I)+(C(I+1)-C(I))*(T-T1(I))/(T1(I+1)-T1(I))
 100  RETURN
      END
```

```
      FUNCTION VIS(T)
      DIMENSION V(13),T1(13)
      T1(1)=-100.
      DO 10 I=2,13
   10 T1(I)=T1(I-1)+180.
      V(1)=0.870
      V(2)=1.199
      V(3)=1.477
      V(4)=1.727
      V(5)=1.956
      V(6)=2.159
      V(7)=2.341
      V(8)=2.519
      V(9)=2.688
      V(10)=2.841
      V(11)=2.990
      V(12)=3.140
      V(13)=3.260
      IF (T+100.) 20,30,15
   15 IF (2060.-T) 20,30,30
   20 PRINT 21
   21 FORMAT (' TEMPERATURE IS NOT WITHIN THE RANGE ALLOWING THE USE
     1OF VIS%T< a)
      CALL SYSTEM
   30 I=0
   35 I=I+1
      IF (T-T1(I+1)) 50,40,35
   40 VIS=V(I+1)*1.E-5
      GO TO 100
   50 VIS=(V(I)+(V(I+1)-V(I))*(T-T1(I))/(T1(I+1)-T1(I)))*1.E-5
  100 VIS=VIS/32.2
      RETURN
      END


      FUNCTION TAU(P,T)
      TAU=0.0
      RETURN
      END
```

SAMPLE DATA INPUT

(Uniform flux and nonuniform flux data set)

```
$RUN MAIN+-LOAD#+FUN+STPROP+*SSP
                GENERAL DATA
 .0390      6.60       .00455     .2495
          14
 -4.26      1.00       3.51       7.51       12.02      18.03      26.05
 36.10      46.10      54.20      60.20      66.20      71.20      76.40
1
20 0 72.2
       .371       .066       .500
                DATA FOR INDIVIDUAL RUN
         19 0.8       297.3      478.7      1.02
 6.02       9.53       10.73      11.34      11.75      12.22      12.73
 13.32      13.90      14.38      14.69      14.96      14.70      10.73
 11.62      13.25      14.77      9.64       8.99       13.58      13.40
 78.0       14.31      35.9       38.85      8.18       13.55      9.00
C              STOP CARD - PROGRAM EXPECTS NEW GENERAL DATA
        000 0.8       297.3      478.7      1.02
C
C               GENERAL DATA
 .0         6.60       .00455     .2505
          14
 -4.24      1.996      5.988      11.976     17.964     23.952      29.94
 35.928     41.916     47.904     53.892     59.88      65.868     75.8
1
 .039       .15143     .09108     .05164     .03537     .02748     .02426
 .02306     .02426     .02748     .03537     .05164     .09108     .039
20 5 71.856     .00001
       .371       .066       .500
                DATA FOR INDIVIDUAL RUN
         206 0.8       343.0      931.3      1.31
 7.12       10.57      12.43      16.45      21.18      26.52      31.17
34.48      35.65      34.97      33.12      30.50      27.3       21.74
 20.96      34.18      33.57      11.62      11.87      24.21      24.15
 76.0       14.3       10.1       10.9       6.37       13.55      2.85
$ENDFILE
$RUN *STATUS
$SIGNOFF
```

OUTPUT PRINT SAMPLE

(In this case NUBCHOT contains output for $Nu^{c}_{b,NU}$ of Eq. (3-11))

RUN NUMBER 208

I	T(I)	TP(I-4,I)	TP(I-3,I)	TP(I-2,I)	TP(I-1,I)	TP(I,I)
1	364.9					365.9
2	516.2				510.6	515.5
3	600.1			607.8	602.1	600.7
4	778.6		774.8	776.3	776.3	778.3
5	983.4	984.3	984.9	987.0	984.4	983.2
6	1207.4	1207.0	1204.9	1206.0	1208.2	1206.9
7	1401.8	1402.4	1402.5	1400.2	1402.7	1396.8
8	1533.3	1533.1	1534.4	1532.6	1543.3	1545.2
9	1586.3	1586.0	1586.3	1582.6	1563.4	1589.3
10	1553.6	1553.6	1550.0	1555.4	1547.5	1560.3
11	1478.6	1480.7	1496.3	1478.7	1467.6	
12	1369.8	1361.2	1375.4	1365.3		
13	1232.9	1230.2	1245.3			
14	988.9	985.2				

THE GAS IS NOT OPTICALLY THIN. NO CORRECTION FOR AXIAL RADIANT HEAT TRANSFER WILL BE ATTEMPTED.

I	T(I)	TP(I-4,I)	TP(I-3,I)	TP(I-2,I)	TP(I-1,I)	TP(I,I)
1	13.8					14.8
2	157.8				152.2	157.1
3	231.5			239.1	233.6	232.0
4	383.7		379.9	381.2	381.5	383.4
5	546.5	547.4	548.1	549.8	547.7	546.4
6	711.7	711.4	709.5	710.0	712.5	711.1
7	832.4	833.0	833.5	830.6	833.7	827.6
8	881.5	881.2	883.0	881.0	891.2	893.5
9	852.2	851.7	851.7	848.6	829.2	854.4
10	744.3	744.6	740.9	746.4	739.9	748.1
11	607.2	609.2	624.7	607.6	601.1	
12	452.5	444.0	456.1	449.7		

13	285.5	283.7	292.6			
14	18.8	16.7				
I	T(I)	TP(I-4,I)	TP(I-3,I)	TP(I-2,I)	TP(I-1,I)	TP(I,I)
1	0.0					10.4
2	2858.3				2797.9	2856.8
3	4693.5			4775.3	4697.7	4695.5
4	8139.8		8098.4	8134.5	8131.9	8146.1
5	11929.2	11938.7	11932.6	11941.2	11902.4	11916.4
6	15587.2	15586.3	15578.9	15628.1	15638.3	15532.5
7	18498.2	18500.3	18470.5	18419.7	18624.2	18441.8
8	19570.3	19577.4	19624.0	19491.2	19628.8	19751.4
9	18628.3	18614.5	18621.3	18736.3	18346.5	18880.3
10	16488.2	16502.2	16311.8	16330.0	15990.3	16551.7
11	12837.8	12903.1	13284.6	12892.2	12706.0	
12	8980.2	8792.8	9363.0	8998.8		
13	5371.1	5180.0	5450.3			
14	0.0	-29.9				

RUN NUMBER 208

KS = 0

MDOT = 15.307 TSKW = 1.3750 PABS = 75.13 TIN = 360.50

QNOM = 11926.47 QLOSEX = 146.95 QLOSI = 81.34 QLOSO = 67.12

TOUT = 954.0 TINF = 76.0 PINF = 14. PTS = 60.4

G = 11281. RATING = 0.0313 TOUTC = 962.5

EPSA = 0.371 EPSB = 0.066 TAULIM = 0.500

TGH(I) = 988.89 1522.29 1491.21 TLH(I) = 562.97 571.74 1082.34 1081.92

I	Z(I)	TWO(I)	TWI(I)	QCON(I)	QGH(I)	QRAD(I)	QGEN(I)	QCOR(I)	TG(I)	HZ(I)	HZR(I)
1	-4.24	364.91	364.91						351.08		
2	2.00	516.24	513.59	-220.30	471.81	0.0	2606.77	2858.27	355.75	18.11	2.52
3	5.99	600.14	597.37	-67.93	373.58	0.0	4387.82	4693.48	365.90	20.28	2.78
4	11.98	778.64	775.91	-13.21	212.09	0.0	7940.89	8139.77	392.20	21.21	3.33
5	17.96	983.39	980.78	-21.85	19.32	0.0	11931.77	11929.24	434.30	21.83	3.98
6	23.95	1207.35	1204.89	-27.92	-218.51	0.0	15833.60	15587.18	493.16	21.90	4.69
7	29.94	1401.76	1399.27	-45.22	140.18	0.0	18403.20	18498.16	566.89	22.22	5.34
8	35.93	1533.27	1530.89	-54.63	-68.99	0.0	19693.95	19570.33	649.40	22.20	5.84
9	41.92	1586.27	1583.96	-61.23	-157.90	0.0	18847.42	18628.29	731.78	21.86	6.14
10	47.90	1553.56	1551.22	-40.63	-40.56	0.0	16569.41	16488.22	806.88	22.15	6.23
11	53.89	1478.56	1476.22	8.41	80.03	0.0	12749.43	12837.86	869.05	21.14	6.19
12	59.88	1369.85	1367.46	119.07	251.62	0.0	8609.56	8980.25	914.94	19.84	6.03
13	65.87	1232.89	1230.45	106.67	470.87	0.0	4793.58	5371.13	944.96	18.81	5.76
14	75.80	988.89	988.89						970.12		

I	RHOW(I)	RHOB(I)	RHOF(I)	MUW(I)	MUB(I)	MUF(I)	KGW(I)	KGB(I)	KGF(I)	CP(I)	TAW(I)	TAG(I)
1	0.158E 00	0.161E 00	0.160E 00	0.326E-06	0.319E-06	0.323E-06	0.187E-01	0.183E-01	0.185E-01	0.535	1.613	1.664
2	0.132E 00	0.160E 00	0.144E 00	0.396E-06	0.322E-06	0.359E-06	0.233E-01	0.184E-01	0.207E-01	0.532	1.186	1.647
3	0.121E 00	0.158E 00	0.136E 00	0.436E-06	0.326E-06	0.381E-06	0.263E-01	0.187E-01	0.222E-01	0.526	1.015	1.610
4	0.103E 00	0.152E 00	0.122E 00	0.521E-06	0.339E-06	0.430E-06	0.329E-01	0.194E-01	0.258E-01	0.515	0.753	1.520
5	0.879E-01	0.144E 00	0.109E 00	0.618E-06	0.359E-06	0.488E-06	0.411E-01	0.207E-01	0.302E-01	0.503	0.559	1.390
6	0.759E-01	0.135E 00	0.969E-01	0.724E-06	0.387E-06	0.555E-06	0.509E-01	0.226E-01	0.359E-01	0.495	0.421	1.234
7	0.679E-01	0.124E 00	0.877E-01	0.816E-06	0.422E-06	0.619E-06	0.594E-01	0.252E-01	0.412E-01	0.492	0.339	1.073
8	0.634E-01	0.115E 00	0.816E-01	0.879E-06	0.461E-06	0.670E-06	0.652E-01	0.281E-01	0.459E-01	0.493	0.296	0.926
9	0.618E-01	0.107E 00	0.781E-01	0.904E-06	0.500E-06	0.702E-06	0.675E-01	0.312E-01	0.488E-01	0.497	0.281	0.807
10	0.628E-01	0.100E 00	0.771E-01	0.888E-06	0.535E-06	0.712E-06	0.661E-01	0.342E-01	0.497E-01	0.501	0.291	0.718
11	0.652E-01	0.954E-01	0.774E-01	0.853E-06	0.565E-06	0.709E-06	0.628E-01	0.367E-01	0.495E-01	0.505	0.313	0.654
12	0.691E-01	0.921E-01	0.790E-01	0.801E-06	0.587E-06	0.694E-06	0.580E-01	0.385E-01	0.481E-01	0.509	0.351	0.612
13	0.748E-01	0.901E-01	0.817E-01	0.736E-06	0.601E-06	0.669E-06	0.520E-01	0.397E-01	0.457E-01	0.511	0.409	0.587
14	0.874E-01	0.885E-01	0.879E-01	0.622E-06	0.613E-06	0.617E-06	0.415E-01	0.407E-01	0.411E-01	0.513	0.553	0.567

I	REW(I)	REB(I)	REF(I)	REWB(I)	REFB(I)	PRW(I)	PRB(I)	PRF(I)	B(I)	BBK(I)	TGNR(I)
1	12397.	12652.	12523.	12155.	12399.						
2	10193.	12565.	11255.	8383.	10141.	0.975	1.077	1.010	1453.	1537.	355.75
3	9265.	12379.	10598.	7086.	9163.	0.948	1.065	0.988	2008.	2139.	365.90
4	7760.	11924.	9401.	5235.	7551.	0.915	1.042	0.951	3752.	3994.	392.20
5	6540.	11261.	8275.	3982.	6245.	0.896	1.011	0.929	6997.	7378.	434.30
6	5581.	10449.	7275.	3146.	5233.	0.880	0.984	0.905	12615.	13156.	493.16
7	4951.	9583.	6529.	2703.	4603.	0.878	0.956	0.896	19788.	20465.	566.89
8	4599.	8769.	6034.	2541.	4289.	0.880	0.938	0.886	26153.	26906.	649.40
9	4471.	8084.	5758.	2590.	4220.	0.882	0.924	0.882	29138.	29892.	731.78
10	4549.	7547.	5677.	2851.	4372.	0.881	0.911	0.881	27348.	28023.	806.88
11	4739.	7153.	5701.	3240.	4629.	0.879	0.903	0.881	23511.	24070.	869.05
12	5044.	6888.	5823.	3784.	4991.	0.878	0.899	0.883	18680.	19100.	914.94
13	5489.	6725.	6044.	4552.	5480.	0.879	0.897	0.886	13719.	13983.	944.96
14	6500.	6594.	6546.	6414.	6503.						

I	NUW(I)	NUF(I)	NUB(I)	NUBC(I)	UFNUBC(I)	NUMCEL(I)	PLNKB(I)	PLNKW(I)	TRAT(I)	ACCPAR(I)	NUBCHOT
2	32.35	36.31	40.86	35.15	36.00	60.89	0.196E 00	0.105E 00	1.194	0.118E-06	58.70
3	32.12	37.95	45.07	38.87	42.17	46.01	0.188E 00	0.791E-01	1.280	0.155E-06	49.61
4	26.79	34.22	45.40	38.24	43.04	38.02	0.168E 00	0.461E-01	1.450	0.340E-06	42.08
5	22.08	30.06	43.80	35.79	38.01	32.79	0.142E 00	0.270E-01	1.611	0.501E-06	36.28
6	17.91	25.40	40.33	31.67	32.42	28.71	0.113E 00	0.163E-01	1.747	0.657E-06	31.48
7	15.57	22.42	36.72	27.87	27.31	25.65	0.876E-01	0.110E-01	1.811	0.779E-06	27.63
8	14.17	20.14	32.86	24.19	21.19	23.57	0.669E-01	0.859E-02	1.795	0.821E-06	24.71
9	13.48	18.63	29.17	20.94	19.85	22.29	0.522E-01	0.781E-02	1.715	0.777E-06	22.64
10	13.95	18.52	26.96	19.35	19.60	21.67	0.423E-01	0.828E-02	1.588	0.683E-06	21.21
11	14.01	17.78	23.99	16.94	17.69	21.49	0.359E-01	0.950E-02	1.457	0.529E-06	19.96
12	14.23	17.17	21.44	14.91	15.69	21.70	0.318E-01	0.117E-01	1.329	0.368E-06	18.60
13	15.05	17.11	19.71	13.66	16.06	22.28	0.295E-01	0.155E-01	1.203	0.219E-06	16.83

APPENDIX B

REDUCED STEAM DATA

Notes: 1. Uniform Flux SS-310 Test Section Data arranged by pressure.

2. For Nonuniform Flux SS-310 Test Section Data UBCHOT contains Nu^{c}_{NU} from Eq. (3-11).

M	P	Z	QW	TW	TG	NUB	NUBC	REB	PRB	NUMCEL	A E6	TAW	TAG	PLNKW	PLNKB	TRAT	UBCHOT
1	29.51	1.00	5850.	777.	666.	76.10	73.15	12959.	0.923	75.66	0.11	0.295	0.355	0.0181	0.0253	1.099	72.05
1	29.51	3.50	5832.	840.	670.	49.33	46.84	12886.	0.922	52.09	0.11	0.268	0.351	0.0152	0.0246	1.151	45.02
1	29.51	7.50	5810.	874.	681.	42.86	40.12	12740.	0.922	45.00	0.11	0.255	0.344	0.0139	0.0238	1.169	38.38
1	29.51	12.00	5877.	896.	695.	40.90	38.22	12579.	0.921	41.98	0.11	0.247	0.337	0.0131	0.0229	1.174	36.32
1	29.51	18.00	5876.	917.	712.	39.27	36.60	12370.	0.918	39.83	0.11	0.240	0.328	0.0124	0.0217	1.175	34.58
1	29.51	26.00	6084.	941.	734.	39.18	36.56	12096.	0.914	38.05	0.11	0.232	0.316	0.0117	0.0203	1.173	34.36
1	29.51	36.10	6099.	966.	763.	38.53	35.91	11766.	0.909	36.54	0.11	0.224	0.301	0.0110	0.0187	1.166	33.56
1	29.51	46.10	6098.	997.	794.	37.13	34.59	11456.	0.906	35.35	0.11	0.215	0.287	0.0102	0.0172	1.162	32.00
1	29.51	54.20	6114.	1022.	817.	35.98	33.32	11218.	0.903	34.51	0.11	0.208	0.277	0.0096	0.0161	1.160	30.71
1	29.51	60.20	6095.	1044.	835.	34.42	31.51	11048.	0.901	33.91	0.11	0.202	0.270	0.0091	0.0154	1.161	29.04
1	29.51	66.20	6068.	1044.	852.	36.60	34.16	10884.	0.899	33.58	0.11	0.202	0.263	0.0091	0.0147	1.146	31.19
1	29.51	71.20	6196.	1025.	865.	44.05	43.27	10765.	0.898	33.55	0.11	0.207	0.258	0.0095	0.0141	1.121	38.70
2	29.81	1.00	6377.	750.	616.	73.31	69.75	13975.	0.928	79.61	0.11	0.311	0.391	0.0197	0.0299	1.125	69.44
2	29.81	3.50	6195.	802.	621.	52.67	50.12	13887.	0.927	55.04	0.11	0.287	0.386	0.0170	0.0290	1.167	48.58
2	29.81	7.50	6048.	835.	634.	45.40	42.57	13717.	0.926	47.51	0.11	0.273	0.378	0.0156	0.0280	1.184	41.15
2	29.81	12.00	6089.	855.	645.	43.18	40.39	13531.	0.925	44.28	0.11	0.265	0.369	0.0147	0.0268	1.190	38.83
2	29.81	18.00	6116.	878.	665.	41.55	38.81	13291.	0.923	42.01	0.11	0.256	0.358	0.0139	0.0254	1.190	37.08
2	29.81	26.00	6158.	901.	687.	40.77	38.04	12983.	0.921	40.16	0.11	0.248	0.345	0.0131	0.0236	1.186	36.17
2	29.81	36.10	6143.	927.	715.	39.60	36.91	12616.	0.917	38.54	0.11	0.239	0.328	0.0122	0.0216	1.180	34.85
2	29.81	46.10	6151.	954.	746.	38.66	36.01	12272.	0.912	37.28	0.11	0.230	0.313	0.0114	0.0199	1.173	33.77
2	29.81	54.20	6241.	977.	768.	38.11	35.38	12007.	0.909	36.38	0.11	0.223	0.302	0.0108	0.0186	1.170	33.09
2	29.81	60.20	6153.	994.	786.	36.91	32.82	11817.	0.906	35.77	0.11	0.218	0.294	0.0104	0.0177	1.167	31.80
2	29.81	66.20	6123.	1004.	803.	37.26	34.87	11635.	0.904	35.30	0.11	0.215	0.286	0.0101	0.0169	1.159	32.09
2	29.81	71.20	6639.	987.	818.	47.26	49.05	11500.	0.903	35.28	0.11	0.220	0.280	0.0106	0.0162	1.132	42.16
23	25.24	1.00	16306.	653.	271.	110.16	107.21	24931.	1.010	112.47	0.22	0.309	0.674	0.0222	0.0976	1.523	107.23
23	25.24	3.50	16565.	778.	289.	84.85	81.71	24237.	0.998	74.35	0.22	0.252	0.647	0.0154	0.0899	1.654	81.36
23	25.24	7.50	16740.	853.	317.	74.79	71.59	23182.	0.983	61.96	0.23	0.225	0.606	0.0126	0.0790	1.691	70.93
23	25.24	12.00	16891.	904.	348.	69.37	66.18	22075.	0.973	56.13	0.23	0.209	0.563	0.0110	0.0683	1.688	65.23
23	25.24	18.00	16959.	957.	391.	64.22	61.07	20732.	0.965	51.59	0.23	0.194	0.511	0.0096	0.0565	1.665	59.77
23	25.24	26.00	17254.	1013.	450.	60.08	57.03	19152.	0.953	47.56	0.24	0.180	0.452	0.0084	0.0447	1.619	55.33
23	25.24	36.10	17380.	1075.	525.	55.47	52.56	17467.	0.941	43.95	0.24	0.166	0.390	0.0073	0.0339	1.559	50.39
23	25.24	46.10	17415.	1130.	599.	51.84	49.07	16063.	0.928	41.15	0.24	0.155	0.340	0.0064	0.0264	1.502	46.47
23	25.24	54.20	17574.	1179.	657.	49.35	46.67	15082.	0.922	39.21	0.24	0.146	0.306	0.0058	0.0218	1.467	43.70
23	25.24	60.20	17702.	1215.	705.	48.01	45.40	14431.	0.919	38.04	0.24	0.140	0.284	0.0054	0.0190	1.437	42.17
23	25.24	66.20	17644.	1240.	749.	46.95	44.43	13838.	0.911	36.93	0.24	0.136	0.265	0.0051	0.0168	1.406	40.99
23	25.24	71.20	17924.	1197.	786.	54.43	52.02	13379.	0.906	36.79	0.24	0.143	0.250	0.0056	0.0151	1.330	48.68
24	25.14	1.00	8520.	624.	271.	62.37	59.50	10128.	1.010	55.44	0.69	0.324	0.671	0.0243	0.0972	1.483	59.57
24	25.14	3.50	8584.	776.	294.	44.29	41.17	9769.	0.994	36.03	0.70	0.252	0.637	0.0155	0.0875	1.640	40.81
24	25.14	7.50	8583.	885.	328.	36.30	33.10	9237.	0.978	29.49	0.71	0.214	0.586	0.0115	0.0743	1.706	32.27
24	25.14	12.00	8693.	954.	368.	32.86	29.66	8692.	0.968	26.42	0.73	0.194	0.535	0.0096	0.0619	1.708	28.44
24	25.14	18.00	8766.	1022.	425.	29.86	26.73	8048.	0.958	24.05	0.73	0.177	0.475	0.0082	0.0492	1.676	25.06
24	25.14	26.00	9186.	1101.	501.	27.88	24.87	7307.	0.947	21.91	0.77	0.160	0.407	0.0069	0.0368	1.624	22.66
24	25.14	36.10	9183.	1127.	597.	27.48	24.73	6539.	0.929	20.30	0.77	0.155	0.340	0.0065	0.0265	1.501	22.14
24	25.14	46.10	9177.	1242.	692.	23.41	20.75	5926.	0.920	18.61	0.77	0.135	0.288	0.0050	0.0196	1.478	17.42
24	25.14	54.20	9261.	1310.	771.	21.81	19.27	5511.	0.908	17.59	0.77	0.125	0.255	0.0044	0.0157	1.438	15.48
24	25.14	60.20	9170.	1348.	824.	20.89	18.44	5242.	0.901	16.96	0.76	0.120	0.234	0.0041	0.0135	1.408	14.33
24	25.14	66.20	9100.	1379.	881.	20.45	18.07	5002.	0.897	16.46	0.75	0.116	0.215	0.0038	0.0117	1.372	13.71
24	25.14	71.20	9398.	1296.	928.	27.22	24.99	4819.	0.894	16.58	0.76	0.127	0.202	0.0045	0.0104	1.265	20.88
31	24.95	1.00	3249.	542.	217.	28.42	25.58	3421.	1.083	23.94	2.71	0.373	0.763	0.0316	0.1263	1.481	25.98
31	24.95	3.50	3187.	674.	242.	20.06	17.01	3267.	1.040	15.39	2.71	0.295	0.715	0.0206	0.1111	1.615	17.08
31	24.95	7.50	3104.	794.	283.	15.37	12.20	3046.	1.000	12.31	2.69	0.243	0.647	0.0145	0.0909	1.688	11.81
31	24.95	12.00	3143.	886.	331.	13.27	10.09	2825.	0.977	10.81	2.75	0.212	0.579	0.0114	0.0730	1.702	9.25
31	24.95	18.00	3116.	980.	394.	11.36	8.21	2572.	0.964	9.65	2.77	0.186	0.502	0.0089	0.0550	1.686	6.79
31	24.95	26.00	3459.	1110.	487.	10.31	7.27	2284.	0.948	8.56	3.07	0.157	0.416	0.0067	0.0386	1.658	5.05
31	24.95	36.10	3360.	1230.	603.	8.43	5.59	1995.	0.928	7.63	2.98	0.136	0.334	0.0051	0.0258	1.590	2.55
31	24.95	46.10	3279.	1318.	714.	7.41	4.75	1780.	0.917	7.02	2.90	0.123	0.276	0.0043	0.0182	1.515	1.01
31	24.95	54.20	3511.	1413.	809.	7.05	4.52	1636.	0.903	6.56	3.07	0.111	0.239	0.0036	0.0141	1.477	0.17
31	24.95	60.20	3404.	1449.	871.	6.67	4.24	1543.	0.897	6.31	2.98	0.107	0.216	0.0033	0.0118	1.434	-0.47
31	24.95	66.20	3320.	1467.	940.	6.63	4.30	1463.	0.893	6.13	2.88	0.105	0.196	0.0032	0.0099	1.377	-0.61

M	P	Z	QW	TW	TG	NUB	NUBC	REB	PRB	NUMCEL	A E6	TAW	TAG	PLNKW	PLNKB	TRAT	UBCHOT
31	24.95	71.20	3525.	1326.	993.	10.59	8.45	1402.	0.891	6.25	3.04	0.122	0.182	0.0042	0.0087	1.229	4.02
33	25.23	1.00	2925.	537.	237.	26.76	23.97	3299.	1.049	23.37	2.47	0.381	0.733	0.0326	0.1154	1.430	24.32
33	25.23	3.50	2871.	657.	261.	19.05	16.06	3167.	1.020	15.21	2.45	0.307	0.692	0.0220	0.1028	1.550	16.12
33	25.23	7.50	2805.	768.	298.	14.74	11.64	2976.	0.992	12.29	2.44	0.256	0.632	0.0158	0.0859	1.621	11.29
33	25.23	12.00	2836.	859.	342.	12.64	9.51	2783.	0.974	10.85	2.48	0.223	0.572	0.0124	0.0705	1.645	8.74
33	25.23	18.00	2807.	953.	399.	10.74	7.62	2560.	0.964	9.73	2.48	0.195	0.503	0.0097	0.0548	1.645	6.31
33	25.23	26.00	3095.	1070.	480.	9.84	6.80	2300.	0.949	8.69	2.75	0.167	0.425	0.0073	0.0399	1.628	4.77
33	25.23	36.10	3012.	1185.	584.	8.09	5.22	2034.	0.930	7.79	2.68	0.145	0.348	0.0057	0.0277	1.575	2.42
33	25.23	46.10	2946.	1272.	686.	7.11	4.40	1831.	0.920	7.19	2.60	0.131	0.292	0.0048	0.0201	1.512	0.95
33	25.23	54.20	3165.	1359.	767.	6.83	4.23	1692.	0.908	6.74	2.79	0.119	0.256	0.0040	0.0158	1.482	0.19
33	25.23	60.20	3099.	1399.	831.	6.46	3.96	1601.	0.901	6.49	2.71	0.114	0.233	0.0037	0.0133	1.440	-0.39
33	25.23	66.20	2998.	1407.	888.	6.42	4.03	1522.	0.896	6.32	2.62	0.113	0.213	0.0036	0.0114	1.385	-0.51
33	25.23	71.20	3175.	1279.	940.	9.87	7.66	1462.	0.893	6.44	2.76	0.130	0.198	0.0047	0.0100	1.242	3.57
34	25.63	1.00	2928.	534.	247.	27.47	24.68	3285.	1.037	23.38	2.42	0.389	0.725	0.0333	0.1111	1.406	25.02
34	25.63	3.50	2881.	649.	270.	19.66	16.67	3156.	1.012	15.27	2.41	0.316	0.684	0.0228	0.0991	1.519	16.73
34	25.63	7.50	2834.	758.	309.	15.30	12.21	2965.	0.987	12.38	2.40	0.264	0.626	0.0165	0.0830	1.585	11.87
34	25.63	12.00	2860.	845.	352.	13.15	10.03	2780.	0.972	10.96	2.44	0.231	0.567	0.0131	0.0683	1.608	9.28
34	25.63	18.00	2830.	939.	409.	11.14	8.03	2561.	0.962	9.83	2.44	0.202	0.500	0.0102	0.0534	1.610	6.75
34	25.63	26.00	3142.	1059.	490.	10.21	7.18	2306.	0.948	8.78	2.72	0.172	0.424	0.0077	0.0390	1.599	5.18
34	25.63	36.10	3056.	1175.	594.	8.37	5.50	2042.	0.929	7.87	2.64	0.149	0.348	0.0059	0.0272	1.551	2.73
34	25.63	46.10	2979.	1266.	695.	7.30	4.58	1840.	0.920	7.26	2.57	0.134	0.292	0.0049	0.0198	1.495	1.13
34	25.63	54.20	3222.	1358.	778.	7.00	4.39	1702.	0.907	6.80	2.75	0.121	0.256	0.0041	0.0156	1.468	0.34
34	25.63	60.20	3146.	1397.	839.	6.61	4.09	1611.	0.900	6.55	2.67	0.116	0.233	0.0038	0.0132	1.430	-0.28
34	25.63	66.20	3077.	1414.	903.	6.59	4.18	1532.	0.895	6.38	2.59	0.114	0.213	0.0037	0.0113	1.375	-0.38
34	25.63	71.20	3266.	1293.	952.	9.98	7.75	1472.	0.893	6.48	2.73	0.130	0.199	0.0047	0.0099	1.241	3.59
41	25.56	1.00	2940.	530.	225.	27.02	24.18	3541.	1.071	24.80	2.23	0.391	0.765	0.0338	0.1240	1.445	24.60
41	25.56	3.50	2892.	640.	247.	19.80	16.77	3404.	1.037	16.18	2.23	0.320	0.724	0.0234	0.1111	1.557	16.93
41	25.56	7.50	2852.	742.	283.	15.71	12.58	3203.	1.002	13.10	2.23	0.270	0.663	0.0172	0.0934	1.619	12.37
41	25.56	12.00	2883.	824.	325.	13.67	10.52	2999.	0.981	11.58	2.28	0.238	0.602	0.0138	0.0770	1.636	9.93
41	25.56	18.00	2869.	913.	381.	11.73	8.58	2761.	0.967	10.39	2.29	0.209	0.531	0.0109	0.0601	1.633	7.50
41	25.56	26.00	3126.	1026.	459.	10.65	7.58	2483.	0.952	9.28	2.51	0.179	0.450	0.0083	0.0438	1.618	5.81
41	25.56	36.10	3034.	1140.	558.	8.72	5.79	2199.	0.935	8.32	2.45	0.155	0.370	0.0063	0.0305	1.572	3.26
41	25.56	46.10	2969.	1232.	656.	7.57	4.80	1981.	0.922	7.66	2.39	0.139	0.311	0.0052	0.0222	1.516	1.61
41	25.56	54.20	3141.	1311.	734.	7.24	4.58	1833.	0.913	7.19	2.52	0.127	0.273	0.0044	0.0175	1.484	0.83
41	25.56	60.20	3095.	1355.	795.	6.82	4.26	1736.	0.905	6.93	2.46	0.121	0.249	0.0041	0.0149	1.446	0.19
41	25.56	66.20	3010.	1371.	854.	6.72	4.26	1651.	0.899	6.74	2.37	0.119	0.228	0.0040	0.0128	1.393	-0.0
41	25.56	71.20	3211.	1250.	902.	10.09	7.82	1586.	0.895	6.84	2.53	0.136	0.213	0.0051	0.0112	1.256	3.96
43	24.85	1.00	3181.	379.	280.	81.15	78.85	14811.	1.002	85.62	0.12	0.517	0.650	0.0585	0.0922	1.135	79.19
43	24.85	3.50	3181.	427.	285.	56.47	54.08	14677.	0.998	58.66	0.12	0.467	0.642	0.0481	0.0898	1.191	54.36
43	24.85	7.50	3177.	454.	294.	49.45	47.02	14468.	0.993	50.40	0.12	0.442	0.628	0.0434	0.0862	1.212	47.25
43	24.85	12.00	3208.	471.	304.	47.10	44.66	14238.	0.987	46.79	0.12	0.427	0.614	0.0407	0.0822	1.218	44.83
43	24.85	18.00	3213.	487.	317.	45.21	42.76	13938.	0.981	44.18	0.12	0.413	0.595	0.0382	0.0773	1.219	42.86
43	24.85	26.00	3248.	505.	335.	44.48	42.04	13553.	0.975	42.03	0.12	0.399	0.570	0.0358	0.0711	1.214	42.05
43	24.85	36.10	3250.	528.	358.	43.16	40.72	13094.	0.969	40.13	0.12	0.382	0.541	0.0331	0.0642	1.207	40.62
43	24.85	46.10	3236.	549.	381.	42.03	39.60	12667.	0.966	38.70	0.12	0.367	0.514	0.0307	0.0580	1.199	39.38
43	24.85	54.20	3275.	568.	400.	41.18	38.75	12338.	0.964	37.65	0.12	0.354	0.494	0.0288	0.0536	1.196	38.43
43	24.85	60.20	3278.	582.	414.	40.41	37.99	12104.	0.960	36.93	0.12	0.345	0.480	0.0276	0.0506	1.192	37.60
43	24.85	66.20	3244.	592.	428.	40.18	37.77	11880.	0.957	36.33	0.12	0.339	0.466	0.0267	0.0479	1.184	37.32
43	24.85	71.20	3345.	573.	440.	50.01	47.66	11697.	0.955	36.32	0.13	0.351	0.454	0.0284	0.0458	1.148	47.20
45	25.78	1.00	2551.	611.	277.	19.53	16.63	2349.	1.008	17.38	3.78	0.340	0.679	0.0260	0.0969	1.454	16.75
45	25.78	3.50	2484.	730.	305.	14.28	11.23	2246.	0.990	11.39	3.72	0.278	0.635	0.0180	0.0850	1.556	10.98
45	25.78	7.50	2412.	838.	348.	11.24	8.10	2100.	0.974	9.28	3.63	0.235	0.575	0.0134	0.0698	1.606	7.39
45	25.78	12.00	2426.	919.	397.	9.88	6.75	1957.	0.965	8.24	3.71	0.209	0.516	0.0108	0.0564	1.610	5.59
45	25.78	18.00	2409.	1004.	463.	8.56	5.51	1794.	0.952	7.42	3.68	0.186	0.450	0.0088	0.0436	1.586	3.83
45	25.78	26.00	2629.	1101.	554.	8.08	5.17	1609.	0.936	6.68	4.02	0.164	0.378	0.0070	0.0315	1.540	2.84
45	25.78	36.10	2540.	1197.	667.	6.94	4.22	1422.	0.922	6.04	3.87	0.146	0.308	0.0057	0.0216	1.470	1.15
45	25.78	46.10	2459.	1278.	776.	6.19	3.64	1280.	0.907	5.57	3.73	0.133	0.257	0.0048	0.0157	1.406	-0.05
45	25.78	54.20	2630.	1356.	865.	6.11	3.67	1184.	0.898	5.24	3.95	0.122	0.225	0.0041	0.0124	1.370	-0.57
45	25.78	60.20	2557.	1395.	932.	5.87	3.52	1121.	0.894	5.06	3.82	0.117	0.205	0.0038	0.0104	1.332	-1.06
45	25.78	66.20	2486.	1411.	999.	6.00	3.74	1067.	0.891	4.93	3.67	0.115	0.188	0.0037	0.0089	1.282	-1.05

M	P	Z	QW	TW	TG	NUB	NUBC	REB	PRB	NUMCEL	A B6	TAW	TAG	PLNKW	PLNKB	TRAT	UBCHOT
45	25.78	71.20	2672.	1284.	1053.	10.86	8.77	1026.	0.886	5.02	3.91	0.132	0.175	0.0048	0.0079	1.153	4.39
47	25.36	1.00	2509.	656.	311.	17.59	14.75	2011.	0.985	15.24	4.60	0.309	0.615	0.0221	0.0810	1.447	14.62
47	25.36	3.50	2431.	779.	341.	12.82	9.82	1919.	0.974	10.01	4.49	0.253	0.574	0.0154	0.0705	1.546	9.28
47	25.36	7.50	2349.	894.	389.	10.00	6.94	1792.	0.966	8.17	4.37	0.213	0.516	0.0113	0.0573	1.595	5.87
47	25.36	12.00	2364.	976.	442.	8.78	5.75	1668.	0.955	7.26	4.41	0.190	0.462	0.0092	0.0463	1.593	4.22
47	25.36	18.00	2341.	1060.	513.	7.65	4.71	1527.	0.944	6.55	4.38	0.170	0.401	0.0076	0.0356	1.563	2.64
47	25.36	26.00	2605.	1161.	611.	7.37	4.58	1367.	0.927	5.89	4.84	0.150	0.335	0.0060	0.0256	1.514	1.83
47	25.36	36.10	2532.	1263.	738.	6.38	3.79	1205.	0.913	5.32	4.64	0.133	0.271	0.0049	0.0174	1.439	0.28
47	25.36	46.10	2429.	1340.	852.	5.75	3.34	1084.	0.899	4.92	4.46	0.122	0.226	0.0041	0.0126	1.372	-0.81
47	25.36	54.20	2598.	1420.	948.	5.74	3.43	1002.	0.893	4.64	4.74	0.112	0.197	0.0035	0.0098	1.336	-1.32
47	25.36	60.20	2528.	1465.	1022.	5.54	3.31	949.	0.889	4.47	4.56	0.107	0.179	0.0033	0.0083	1.299	-1.79
47	25.36	66.20	2430.	1474.	1090.	5.74	3.61	903.	0.883	4.36	4.35	0.106	0.164	0.0032	0.0071	1.248	-1.69
47	25.36	71.20	2585.	1333.	1147.	11.94	9.97	868.	0.880	4.45	4.60	0.123	0.153	0.0042	0.0062	1.116	5.13
57	25.13	1.00	10688.	914.	698.	68.85	66.23	11329.	0.919	65.27	0.24	0.205	0.287	0.0107	0.0196	1.187	64.44
57	25.13	3.50	10711.	1022.	709.	47.01	44.71	11206.	0.918	44.30	0.24	0.177	0.280	0.0082	0.0187	1.268	42.12
57	25.13	7.50	10701.	1086.	730.	40.21	37.74	10962.	0.914	37.72	0.24	0.163	0.270	0.0071	0.0175	1.299	35.00
57	25.13	12.00	10828.	1126.	756.	37.82	35.39	10698.	0.910	34.81	0.24	0.155	0.259	0.0064	0.0162	1.305	32.41
57	25.13	18.00	10932.	1175.	794.	35.42	33.04	10365.	0.905	32.63	0.24	0.146	0.245	0.0058	0.0147	1.304	29.78
57	25.13	26.00	11045.	1217.	837.	34.17	31.83	9949.	0.900	30.80	0.25	0.139	0.229	0.0053	0.0130	1.293	28.27
57	25.13	36.10	11142.	1275.	899.	32.53	30.24	9472.	0.895	29.17	0.25	0.130	0.210	0.0047	0.0111	1.277	26.32
57	25.13	46.10	11085.	1332.	955.	30.46	28.23	9045.	0.893	27.86	0.25	0.122	0.194	0.0042	0.0096	1.267	23.89
57	25.13	54.20	11282.	1379.	1002.	29.65	27.37	8726.	0.891	26.96	0.25	0.116	0.182	0.0038	0.0086	1.258	22.79
57	25.13	60.20	11122.	1403.	1034.	28.88	26.35	8505.	0.887	26.37	0.24	0.113	0.174	0.0036	0.0079	1.247	21.86
57	25.13	66.20	11064.	1429.	1071.	28.55	26.65	8296.	0.885	25.88	0.24	0.110	0.166	0.0035	0.0073	1.234	21.39
57	25.13	71.20	11403.	1371.	1093.	37.13	36.24	8148.	0.883	26.01	0.25	0.117	0.160	0.0039	0.0068	1.179	30.23
61	25.46	1.00	18451.	938.	676.	101.04	98.42	22099.	0.921	109.52	0.11	0.201	0.300	0.0101	0.0211	1.230	96.53
61	25.46	3.50	18622.	1041.	687.	74.42	72.01	21872.	0.920	74.55	0.11	0.175	0.294	0.0079	0.0201	1.308	69.43
61	25.46	7.50	18818.	1096.	710.	66.88	64.28	21429.	0.918	63.84	0.12	0.163	0.284	0.0070	0.0189	1.330	61.62
61	25.46	12.00	18880.	1132.	731.	62.97	60.46	20946.	0.913	58.97	0.12	0.156	0.273	0.0064	0.0176	1.336	57.52
61	25.46	18.00	19071.	1175.	767.	59.64	57.14	20334.	0.909	55.43	0.12	0.148	0.260	0.0059	0.0161	1.333	53.98
61	25.46	26.00	19207.	1216.	808.	57.21	54.77	19569.	0.903	52.41	0.12	0.141	0.243	0.0054	0.0143	1.322	51.33
61	25.46	36.10	19321.	1267.	861.	54.53	52.14	18690.	0.898	49.73	0.12	0.133	0.225	0.0049	0.0124	1.307	48.36
61	25.46	46.10	19406.	1322.	914.	51.44	49.10	17894.	0.895	47.58	0.12	0.125	0.208	0.0044	0.0108	1.297	44.96
61	25.46	54.20	19735.	1367.	959.	49.93	47.56	17297.	0.893	46.10	0.12	0.119	0.196	0.0040	0.0097	1.288	43.18
61	25.46	60.20	19529.	1391.	987.	48.61	45.89	16880.	0.891	45.15	0.12	0.116	0.188	0.0038	0.0090	1.279	41.69
61	25.46	66.20	19339.	1407.	1016.	48.26	46.19	16484.	0.889	44.35	0.12	0.114	0.180	0.0036	0.0084	1.265	41.20
61	25.46	71.20	19775.	1367.	1040.	57.62	56.85	16205.	0.887	44.43	0.12	0.119	0.174	0.0039	0.0078	1.218	50.76
65	24.93	1.00	16648.	788.	382.	88.95	86.09	17774.	0.966	85.41	0.32	0.245	0.516	0.0148	0.0582	1.483	85.35
65	24.93	3.50	16853.	933.	403.	66.92	63.88	17253.	0.963	56.51	0.32	0.198	0.493	0.0101	0.0532	1.615	62.61
65	24.93	7.50	17020.	1025.	437.	57.87	54.80	16473.	0.955	47.11	0.33	0.175	0.458	0.0081	0.0464	1.655	53.07
65	24.93	12.00	17176.	1085.	475.	53.24	50.21	15665.	0.949	42.69	0.33	0.162	0.423	0.0070	0.0399	1.652	48.11
65	24.93	18.00	17338.	1152.	529.	48.57	45.61	14698.	0.940	39.18	0.34	0.149	0.382	0.0061	0.0330	1.630	43.09
65	24.93	26.00	17710.	1223.	601.	44.91	42.07	13573.	0.928	36.10	0.34	0.137	0.335	0.0052	0.0260	1.586	39.07
65	24.93	36.10	17838.	1296.	691.	41.46	38.76	12383.	0.920	33.43	0.34	0.126	0.288	0.0045	0.0197	1.526	35.21
65	24.93	46.10	17915.	1371.	778.	38.04	35.49	11397.	0.907	31.22	0.34	0.116	0.250	0.0039	0.0153	1.479	31.40
65	24.93	54.20	18197.	1439.	849.	35.77	33.31	10708.	0.899	29.68	0.34	0.108	0.224	0.0034	0.0126	1.451	28.74
65	24.93	60.20	18218.	1476.	901.	34.76	32.36	10250.	0.895	28.78	0.34	0.104	0.208	0.0032	0.0110	1.422	27.51
65	24.93	66.20	17945.	1495.	947.	34.26	31.93	9834.	0.893	28.05	0.34	0.102	0.193	0.0030	0.0097	1.389	26.83
65	24.93	71.20	18354.	1430.	995.	42.08	39.87	9513.	0.891	28.15	0.34	0.109	0.182	0.0035	0.0087	1.299	35.00
68	29.20	1.00	29486.	1318.	1075.	111.86	109.25	25841.	0.884	125.84	0.07	0.144	0.192	0.0050	0.0084	1.158	104.86
68	29.20	3.50	29769.	1420.	1089.	81.60	79.23	25668.	0.884	86.55	0.07	0.129	0.189	0.0041	0.0082	1.214	74.07
68	29.20	7.50	29851.	1466.	1106.	74.07	71.52	25324.	0.882	74.66	0.07	0.123	0.184	0.0038	0.0078	1.230	66.26
68	29.20	12.00	30104.	1499.	1126.	70.85	68.37	24945.	0.881	69.54	0.07	0.119	0.180	0.0035	0.0075	1.235	62.83
68	29.20	18.00	30105.	1533.	1155.	68.05	65.59	24458.	0.880	65.92	0.07	0.115	0.173	0.0033	0.0070	1.234	59.81
68	29.20	26.00	30746.	1578.	1199.	66.55	64.12	23835.	0.878	62.93	0.07	0.110	0.165	0.0031	0.0065	1.229	58.05
68	29.20	36.10	30518.	1617.	1241.	64.37	61.97	23099.	0.877	60.37	0.07	0.106	0.156	0.0028	0.0058	1.221	55.54
68	29.20	46.10	30912.	1679.	1295.	61.04	58.68	22414.	0.876	58.26	0.07	0.100	0.148	0.0026	0.0053	1.219	51.83
68	29.20	54.20	31299.	1724.	1334.	59.13	56.72	21888.	0.876	56.82	0.07	0.096	0.142	0.0024	0.0049	1.217	49.61
68	29.20	60.20	31010.	1747.	1363.	58.05	55.32	21515.	0.876	55.95	0.07	0.094	0.138	0.0023	0.0046	1.211	48.34
68	29.20	66.20	30689.	1759.	1386.	58.20	56.08	21156.	0.876	55.22	0.07	0.093	0.133	0.0022	0.0044	1.202	48.33

M	P	Z	QW	TW	TG	NUB	NUBC	REB	PRB	NUMCEL	A E6	TAW	TAG	PLNKW	PLNKB	TRAT	UBCHOT
68	29.20	71.20	31322.	1712.	1408.	71.60	70.72	20899.	0.877	55.48	0.07	0.097	0.130	0.0024	0.0042	1.163	61.97
69	25.69	1.00	14658.	1255.	1047.	66.70	64.32	11196.	0.886	65.07	0.18	0.136	0.175	0.0050	0.0080	1.138	60.34
69	25.69	3.50	14611.	1360.	1058.	45.28	43.23	11107.	0.886	44.60	0.18	0.121	0.172	0.0040	0.0077	1.199	38.42
69	25.69	7.50	14659.	1424.	1081.	39.06	36.85	10930.	0.884	38.27	0.18	0.113	0.167	0.0036	0.0073	1.223	31.85
69	25.69	12.00	14905.	1468.	1109.	36.98	34.82	10737.	0.882	35.53	0.18	0.108	0.162	0.0033	0.0069	1.229	29.54
69	25.69	18.00	14895.	1505.	1142.	35.42	33.27	10489.	0.880	33.58	0.18	0.104	0.156	0.0031	0.0064	1.227	27.74
69	25.69	26.00	15115.	1545.	1185.	34.92	32.82	10174.	0.879	31.99	0.18	0.100	0.147	0.0029	0.0058	1.219	26.97
69	25.69	36.10	15191.	1598.	1245.	34.03	31.95	9806.	0.877	30.60	0.18	0.095	0.138	0.0026	0.0051	1.207	25.75
69	25.69	46.10	15100.	1655.	1296.	31.94	29.89	9468.	0.876	29.42	0.18	0.090	0.129	0.0023	0.0046	1.204	23.24
69	25.69	54.20	15336.	1704.	1339.	30.79	28.70	9211.	0.876	28.60	0.18	0.086	0.123	0.0021	0.0042	1.203	21.74
69	25.69	60.20	15332.	1743.	1384.	30.22	27.99	9030.	0.876	28.12	0.18	0.083	0.119	0.0020	0.0039	1.195	20.97
69	25.69	66.20	15071.	1757.	1411.	30.25	28.52	8857.	0.877	27.73	0.18	0.082	0.115	0.0020	0.0037	1.185	20.83
69	25.69	71.20	15387.	1679.	1433.	42.74	41.65	8734.	0.877	28.01	0.18	0.088	0.111	0.0023	0.0035	1.130	33.68
74	25.25	1.00	5467.	1152.	975.	31.50	29.08	3601.	0.892	26.51	0.74	0.151	0.190	0.0061	0.0093	1.123	25.75
74	25.25	3.50	5307.	1259.	991.	19.80	17.78	3565.	0.891	18.12	0.71	0.133	0.186	0.0049	0.0089	1.185	13.55
74	25.25	7.50	5165.	1336.	1015.	15.70	13.52	3493.	0.889	15.43	0.69	0.122	0.179	0.0042	0.0083	1.218	9.04
74	25.25	12.00	5269.	1399.	1047.	14.14	12.00	3416.	0.887	14.22	0.70	0.114	0.172	0.0037	0.0078	1.234	7.15
74	25.25	18.00	5200.	1451.	1083.	12.89	10.76	3320.	0.884	13.34	0.70	0.108	0.164	0.0033	0.0071	1.239	5.57
74	25.25	26.00	5479.	1517.	1140.	12.57	10.48	3197.	0.880	12.59	0.73	0.101	0.153	0.0030	0.0063	1.236	4.88
74	25.25	36.10	5416.	1591.	1210.	11.58	9.54	3055.	0.878	11.94	0.71	0.094	0.141	0.0026	0.0054	1.228	3.44
74	25.25	46.10	5400.	1660.	1275.	10.81	8.80	2928.	0.876	11.42	0.70	0.088	0.131	0.0023	0.0047	1.222	2.21
74	25.25	54.20	5418.	1724.	1324.	10.05	7.91	2833.	0.876	11.04	0.70	0.083	0.123	0.0020	0.0043	1.224	0.99
74	25.25	60.20	5327.	1765.	1370.	9.65	7.67	2767.	0.876	10.82	0.68	0.080	0.118	0.0019	0.0039	1.216	0.34
74	25.25	66.20	5173.	1779.	1411.	9.75	8.32	2705.	0.876	10.68	0.66	0.079	0.113	0.0019	0.0037	1.197	0.31
74	25.25	71.20	5343.	1602.	1437.	22.07	19.73	2661.	0.877	11.03	0.68	0.093	0.110	0.0026	0.0034	1.087	13.48
77	25.95	1.00	26098.	959.	362.	97.76	94.43	19832.	0.971	86.60	0.43	0.199	0.561	0.0099	0.0660	1.726	93.27
77	25.95	3.50	26518.	1163.	392.	73.60	70.02	18979.	0.966	56.21	0.44	0.153	0.525	0.0061	0.0578	1.906	67.89
77	25.95	7.50	27070.	1311.	444.	61.75	58.15	17738.	0.955	45.94	0.44	0.129	0.472	0.0046	0.0473	1.959	55.16
77	25.95	12.00	27388.	1409.	500.	54.96	51.43	16504.	0.948	40.98	0.45	0.116	0.421	0.0037	0.0381	1.947	47.73
77	25.95	18.00	27741.	1506.	579.	48.62	45.26	15094.	0.932	37.02	0.45	0.105	0.364	0.0031	0.0293	1.893	40.87
77	25.95	26.00	28497.	1608.	683.	43.73	40.58	13540.	0.921	33.62	0.46	0.095	0.304	0.0026	0.0210	1.810	35.40
77	25.95	36.10	28672.	1702.	812.	38.96	36.08	11995.	0.903	30.65	0.46	0.087	0.247	0.0022	0.0145	1.700	30.17
77	25.95	46.10	28627.	1796.	935.	35.19	32.51	10788.	0.893	28.40	0.46	0.080	0.205	0.0019	0.0104	1.617	25.79
77	25.95	54.20	29270.	1886.	1039.	32.94	30.39	9980.	0.888	26.88	0.46	0.074	0.179	0.0016	0.0082	1.565	22.99
77	25.95	60.20	29300.	1919.	1116.	32.29	29.85	9459.	0.882	26.04	0.46	0.072	0.163	0.0016	0.0069	1.510	22.16
77	25.95	66.20	28928.	1953.	1183.	31.29	28.94	8996.	0.878	25.22	0.45	0.070	0.149	0.0015	0.0059	1.469	20.86
77	25.95	71.20	29520.	1810.	1252.	41.55	39.37	8647.	0.877	25.65	0.45	0.079	0.139	0.0019	0.0052	1.326	32.06
78	25.45	1.00	18012.	903.	305.	73.53	70.17	13512.	0.989	63.16	0.74	0.211	0.627	0.0111	0.0838	1.782	69.39
78	25.45	3.50	18280.	1106.	338.	55.17	51.57	12828.	0.975	40.65	0.76	0.161	0.580	0.0068	0.0718	1.962	49.87
78	25.45	7.50	18527.	1266.	393.	45.35	41.68	11846.	0.965	32.86	0.78	0.133	0.514	0.0049	0.0565	2.024	39.02
78	25.45	12.00	18773.	1382.	455.	39.36	35.77	10888.	0.953	28.96	0.79	0.117	0.450	0.0038	0.0440	2.013	32.30
78	25.45	18.00	18946.	1496.	541.	34.02	30.60	9819.	0.938	25.89	0.80	0.104	0.381	0.0031	0.0324	1.955	26.30
78	25.45	26.00	19612.	1621.	657.	29.81	26.64	8672.	0.923	23.22	0.82	0.092	0.310	0.0025	0.0222	1.864	21.40
78	25.45	36.10	19696.	1733.	800.	25.91	23.03	7565.	0.904	20.95	0.82	0.083	0.246	0.0021	0.0147	1.741	16.92
78	25.45	46.10	19614.	1832.	936.	23.13	20.48	6728.	0.893	19.32	0.81	0.076	0.201	0.0017	0.0102	1.642	13.53
78	25.45	54.20	20397.	1930.	1055.	21.89	19.39	6177.	0.886	18.22	0.82	0.070	0.173	0.0015	0.0078	1.577	11.76
78	25.45	60.20	20066.	1947.	1130.	21.46	19.08	5825.	0.881	17.63	0.81	0.069	0.156	0.0014	0.0064	1.514	11.15
78	25.45	66.20	20020.	1983.	1215.	21.12	18.84	5517.	0.878	17.12	0.80	0.067	0.141	0.0014	0.0054	1.459	10.59
78	25.45	71.20	20220.	1788.	1280.	30.56	28.48	5287.	0.876	17.52	0.80	0.079	0.131	0.0019	0.0047	1.292	21.18
82	25.88	1.00	4946.	739.	307.	27.87	24.79	3294.	0.989	21.80	3.42	0.275	0.636	0.0177	0.0847	1.564	24.52
82	25.88	3.50	4879.	902.	343.	20.09	16.81	3111.	0.975	14.08	3.39	0.215	0.583	0.0113	0.0715	1.696	15.92
82	25.88	7.50	4806.	1058.	402.	15.46	12.11	2857.	0.965	11.29	3.38	0.174	0.512	0.0078	0.0553	1.761	10.41
82	25.88	12.00	4834.	1183.	469.	12.90	9.58	2617.	0.951	9.87	3.43	0.149	0.446	0.0059	0.0426	1.769	7.13
82	25.88	18.00	4808.	1315.	559.	10.62	7.44	2354.	0.935	8.74	3.38	0.128	0.376	0.0045	0.0312	1.743	4.13
82	25.88	26.00	5292.	1466.	680.	9.59	6.59	2068.	0.921	7.74	3.70	0.109	0.303	0.0033	0.0210	1.690	2.21
82	25.88	36.10	5183.	1605.	837.	7.93	5.20	1790.	0.901	6.91	3.59	0.095	0.237	0.0026	0.0135	1.593	-0.21
82	25.88	46.10	5020.	1738.	983.	6.71	4.16	1589.	0.892	6.32	3.43	0.084	0.192	0.0021	0.0093	1.523	-2.27
82	25.88	54.20	5449.	1867.	1104.	6.39	3.97	1456.	0.883	5.90	3.66	0.075	0.165	0.0017	0.0070	1.488	-3.39
82	25.88	60.20	5213.	1916.	1184.	5.93	3.61	1370.	0.878	5.66	3.51	0.072	0.148	0.0015	0.0058	1.445	-4.26
82	25.88	66.20	5042.	1933.	1270.	5.89	3.68	1298.	0.876	5.52	3.36	0.071	0.134	0.0015	0.0049	1.383	-4.43

M	P	Z	QW	TW	TG	NUB	NUBC	REB	PRB	NUMCEL	A E6	TAW	TAG	PLNKW	PLNKB	TRAT	UBCHOT
82	25.88	71.20	5363.	1663.	1342.	12.23	10.25	1243.	0.876	5.76	3.52	0.090	0.124	0.0023	0.0042	1.178	3.41
85	24.96	1.00	22035.	1276.	1050.	91.85	89.52	17907.	0.887	94.29	0.11	0.129	0.171	0.0047	0.0078	1.150	85.49
85	24.96	3.50	21996.	1380.	1057.	63.75	61.73	17774.	0.886	64.59	0.11	0.115	0.168	0.0038	0.0075	1.213	56.87
85	24.96	7.50	22197.	1440.	1080.	56.45	54.26	17508.	0.884	55.53	0.11	0.108	0.163	0.0034	0.0071	1.234	49.26
85	24.96	12.00	22399.	1477.	1103.	53.72	51.59	17215.	0.883	51.65	0.11	0.104	0.159	0.0032	0.0068	1.239	46.32
85	24.96	18.00	22528.	1516.	1137.	51.67	49.55	16840.	0.881	48.87	0.11	0.100	0.152	0.0030	0.0063	1.237	44.04
85	24.96	26.00	22508.	1546.	1173.	50.63	48.56	16363.	0.879	46.60	0.11	0.097	0.145	0.0027	0.0058	1.229	42.75
85	24.96	36.10	22596.	1590.	1224.	49.72	47.67	15803.	0.877	44.64	0.11	0.093	0.136	0.0025	0.0051	1.217	41.54
85	24.96	46.10	22972.	1660.	1286.	46.96	44.95	15286.	0.876	42.98	0.11	0.087	0.128	0.0023	0.0046	1.214	38.40
85	24.96	54.20	23172.	1711.	1327.	44.62	42.54	14892.	0.876	41.79	0.11	0.083	0.122	0.0021	0.0042	1.215	35.70
85	24.96	60.20	22924.	1738.	1355.	43.33	41.05	14612.	0.876	41.06	0.11	0.081	0.118	0.0020	0.0040	1.211	34.20
85	24.96	66.20	22820.	1766.	1389.	42.70	41.01	14344.	0.876	40.43	0.11	0.079	0.114	0.0019	0.0037	1.204	33.37
85	24.96	71.20	23241.	1685.	1410.	58.73	57.80	14154.	0.876	40.88	0.11	0.085	0.111	0.0022	0.0035	1.147	49.79
88	25.16	1.00	7061.	695.	282.	43.32	40.33	6014.	1.002	35.55	1.58	0.287	0.655	0.0195	0.0925	1.557	40.21
88	25.16	3.50	7058.	854.	312.	31.44	28.23	5729.	0.985	22.99	1.59	0.224	0.610	0.0125	0.0803	1.703	27.57
88	25.16	7.50	7028.	990.	360.	25.02	21.73	5321.	0.970	18.57	1.60	0.185	0.546	0.0088	0.0645	1.768	20.42
88	25.16	12.00	7131.	1102.	417.	21.46	18.17	4920.	0.960	16.35	1.63	0.160	0.484	0.0069	0.0510	1.782	16.22
88	25.16	18.00	7156.	1218.	492.	18.18	14.98	4468.	0.948	14.59	1.64	0.139	0.415	0.0053	0.0382	1.762	12.29
88	25.16	26.00	7611.	1356.	595.	15.89	12.85	3968.	0.929	12.96	1.74	0.119	0.342	0.0040	0.0269	1.721	9.24
88	25.16	36.10	7516.	1494.	724.	13.15	10.33	3476.	0.915	11.61	1.71	0.103	0.274	0.0031	0.0179	1.651	5.70
88	25.16	46.10	7433.	1656.	851.	10.68	8.01	3104.	0.899	10.52	1.67	0.088	0.226	0.0023	0.0127	1.614	2.31
88	25.16	54.20	8008.	1804.	955.	9.78	7.20	2855.	0.893	9.79	1.78	0.077	0.195	0.0018	0.0097	1.600	0.49
88	25.16	60.20	7804.	1866.	1028.	8.98	6.50	2692.	0.888	9.39	1.73	0.073	0.176	0.0016	0.0081	1.563	-0.75
88	25.16	66.20	7653.	1899.	1104.	8.62	6.25	2552.	0.883	9.11	1.67	0.071	0.160	0.0016	0.0068	1.508	-1.26
88	25.16	71.20	7948.	1632.	1166.	14.41	12.29	2447.	0.879	9.49	1.73	0.090	0.148	0.0024	0.0060	1.287	6.11
14	50.67	1.00	8795.	810.	686.	100.57	96.41	20791.	0.926	110.13	0.06	0.482	0.588	0.0284	0.0404	1.108	96.37
14	50.67	3.50	8781.	866.	691.	70.55	66.26	20658.	0.926	76.08	0.06	0.443	0.581	0.0243	0.0396	1.152	66.09
14	50.67	7.50	8802.	898.	703.	62.45	58.12	20450.	0.925	65.82	0.06	0.423	0.572	0.0225	0.0383	1.168	57.85
14	50.67	12.00	8860.	912.	713.	61.08	56.76	20220.	0.922	61.53	0.06	0.415	0.561	0.0216	0.0371	1.169	56.40
14	50.67	18.00	8888.	931.	729.	58.94	54.63	19920.	0.919	58.45	0.06	0.404	0.547	0.0206	0.0355	1.170	54.16
14	50.67	26.00	8963.	950.	750.	58.22	53.95	19533.	0.915	56.02	0.06	0.393	0.529	0.0196	0.0334	1.166	53.34
14	50.67	36.10	8977.	973.	776.	57.38	53.14	19067.	0.911	53.94	0.06	0.381	0.507	0.0185	0.0311	1.160	52.37
14	50.67	46.10	8961.	999.	803.	55.95	51.75	18626.	0.908	52.36	0.06	0.368	0.487	0.0174	0.0289	1.155	50.81
14	50.67	54.20	9097.	1020.	823.	55.32	51.14	18283.	0.905	51.21	0.06	0.358	0.472	0.0166	0.0273	1.153	50.06
14	50.67	60.20	9099.	1035.	840.	54.69	50.54	18036.	0.903	50.47	0.06	0.351	0.461	0.0161	0.0262	1.150	49.35
14	50.67	66.20	9016.	1046.	855.	54.47	50.34	17797.	0.902	49.85	0.06	0.346	0.450	0.0156	0.0251	1.145	49.05
14	50.67	71.20	9172.	1035.	869.	62.68	58.61	17602.	0.901	49.70	0.06	0.351	0.442	0.0161	0.0243	1.125	57.30
15	50.17	1.00	8820.	811.	684.	98.45	94.31	20036.	0.926	106.78	0.07	0.476	0.583	0.0280	0.0401	1.111	94.23
15	50.17	3.50	8833.	875.	691.	67.46	63.19	19902.	0.926	73.59	0.07	0.433	0.576	0.0236	0.0393	1.160	62.97
15	50.17	7.50	8844.	906.	702.	60.03	55.72	19693.	0.925	63.64	0.07	0.414	0.566	0.0218	0.0380	1.176	55.39
15	50.17	12.00	8898.	927.	715.	57.12	52.80	19462.	0.922	59.37	0.07	0.402	0.555	0.0206	0.0367	1.181	52.38
15	50.17	18.00	8943.	947.	730.	55.18	50.88	19161.	0.919	56.38	0.07	0.391	0.540	0.0196	0.0350	1.182	50.34
15	50.17	26.00	8919.	968.	752.	53.76	49.49	18775.	0.915	53.99	0.07	0.380	0.522	0.0187	0.0329	1.178	48.81
15	50.17	36.10	8918.	989.	779.	53.28	49.06	18315.	0.911	52.01	0.07	0.369	0.500	0.0177	0.0305	1.170	48.20
15	50.17	46.10	8904.	1014.	806.	51.98	47.80	17880.	0.907	50.44	0.07	0.357	0.480	0.0166	0.0284	1.165	46.77
15	50.17	54.20	8939.	1034.	828.	51.55	47.40	17543.	0.905	49.40	0.07	0.348	0.465	0.0159	0.0268	1.160	46.22
15	50.17	60.20	8950.	1049.	843.	50.72	46.58	17301.	0.903	48.65	0.07	0.341	0.454	0.0153	0.0256	1.158	45.30
15	50.17	66.20	8900.	1063.	859.	49.96	45.84	17067.	0.901	47.98	0.07	0.335	0.443	0.0148	0.0246	1.155	44.46
15	50.17	71.20	9040.	1047.	871.	58.21	54.16	16876.	0.900	47.89	0.07	0.342	0.434	0.0154	0.0237	1.132	52.76
16	50.05	1.00	8678.	822.	698.	97.60	93.48	19638.	0.925	105.22	0.07	0.467	0.568	0.0271	0.0383	1.107	93.32
16	50.05	3.50	8687.	883.	705.	67.38	63.15	19511.	0.924	72.59	0.07	0.427	0.562	0.0230	0.0375	1.153	62.84
16	50.05	7.50	8709.	915.	716.	59.67	55.40	19311.	0.922	62.76	0.07	0.408	0.552	0.0213	0.0364	1.169	54.98
16	50.05	12.00	8753.	934.	729.	57.02	52.75	19091.	0.919	58.59	0.07	0.397	0.541	0.0202	0.0352	1.173	52.24
16	50.05	18.00	8770.	953.	744.	55.27	51.02	18803.	0.916	55.67	0.07	0.387	0.527	0.0193	0.0336	1.173	50.39
16	50.05	26.00	8825.	974.	766.	54.18	49.95	18432.	0.913	53.34	0.07	0.376	0.510	0.0183	0.0316	1.170	49.18
16	50.05	36.10	8846.	998.	793.	53.31	49.13	17986.	0.909	51.35	0.07	0.364	0.489	0.0172	0.0294	1.164	48.18
16	50.05	46.10	8868.	1023.	820.	52.26	48.11	17565.	0.905	49.81	0.07	0.352	0.469	0.0163	0.0273	1.159	46.99
16	50.05	54.20	8895.	1043.	841.	51.59	47.47	17239.	0.903	48.77	0.07	0.343	0.454	0.0156	0.0257	1.155	46.21
16	50.05	60.20	8885.	1057.	857.	51.07	46.97	17005.	0.902	48.09	0.07	0.337	0.444	0.0151	0.0247	1.152	45.60
16	50.05	66.20	8834.	1068.	872.	50.98	46.90	16778.	0.900	47.47	0.07	0.332	0.433	0.0146	0.0237	1.147	45.43

M	P	Z	QW	TW	TG	NUB	NUBC	REB	PRB	NUMCEL	A B6	TAW	TAG	PLNKW	PLNKB	TRAT	UBCHOT
16	50.05	71.20	8923.	1052.	886.	59.99	55.98	16594.	0.899	47.41	0.07	0.339	0.425	0.0152	0.0229	1.123	54.51
17	50.47	1.00	16628.	926.	675.	95.00	90.53	20237.	0.927	102.72	0.12	0.405	0.595	0.0208	0.0415	1.221	90.30
17	50.47	3.50	16742.	1025.	688.	70.03	65.37	19982.	0.926	69.90	0.12	0.354	0.583	0.0163	0.0399	1.294	64.85
17	50.47	7.50	16844.	1077.	709.	62.87	58.18	19586.	0.923	59.87	0.12	0.331	0.563	0.0145	0.0375	1.315	57.43
17	50.47	12.00	16966.	1109.	731.	59.97	55.30	19156.	0.919	55.45	0.13	0.318	0.542	0.0135	0.0351	1.317	54.35
17	50.47	18.00	17033.	1146.	763.	57.10	52.47	18611.	0.913	52.12	0.13	0.304	0.516	0.0125	0.0322	1.313	51.28
17	50.47	26.00	17186.	1182.	804.	55.54	51.00	17928.	0.907	49.38	0.13	0.291	0.484	0.0115	0.0287	1.299	49.52
17	50.47	36.10	17265.	1227.	856.	53.57	49.12	17141.	0.902	46.94	0.13	0.276	0.448	0.0105	0.0250	1.282	47.27
17	50.47	46.10	17277.	1269.	906.	51.90	47.54	16426.	0.898	45.03	0.13	0.263	0.416	0.0096	0.0218	1.266	45.33
17	50.47	54.20	17488.	1307.	949.	51.00	46.69	15890.	0.895	43.70	0.13	0.252	0.393	0.0089	0.0197	1.254	44.19
17	50.47	60.20	17508.	1332.	980.	50.26	46.00	15515.	0.894	42.83	0.13	0.245	0.376	0.0084	0.0182	1.245	43.28
17	50.47	66.20	17432.	1351.	1010.	50.21	46.00	15160.	0.892	42.08	0.13	0.240	0.361	0.0081	0.0169	1.232	43.09
17	50.47	71.20	17654.	1325.	1035.	58.31	54.22	14876.	0.889	41.94	0.13	0.247	0.350	0.0086	0.0159	1.194	51.31
18	49.77	1.00	16655.	949.	707.	95.00	90.64	19694.	0.923	100.91	0.12	0.387	0.557	0.0194	0.0371	1.207	90.16
18	49.77	3.50	16817.	1055.	721.	68.15	63.61	19453.	0.921	68.56	0.12	0.336	0.545	0.0151	0.0358	1.283	62.81
18	49.77	7.50	16884.	1111.	741.	60.22	55.63	19081.	0.917	58.64	0.12	0.313	0.528	0.0133	0.0338	1.308	54.59
18	49.77	12.00	17025.	1145.	763.	57.20	52.63	18676.	0.913	54.29	0.12	0.300	0.509	0.0123	0.0316	1.312	51.38
18	49.77	18.00	17082.	1182.	793.	54.38	49.86	18162.	0.909	51.08	0.12	0.287	0.485	0.0113	0.0291	1.310	48.36
18	49.77	26.00	17289.	1224.	837.	52.46	48.01	17517.	0.904	48.41	0.13	0.273	0.456	0.0104	0.0260	1.299	46.20
18	49.77	36.10	17267.	1266.	886.	50.52	46.16	16771.	0.899	46.04	0.13	0.260	0.422	0.0095	0.0227	1.283	43.98
18	49.77	46.10	17339.	1312.	938.	48.86	44.57	16092.	0.896	44.22	0.12	0.247	0.393	0.0086	0.0199	1.268	42.03
18	49.77	54.20	17492.	1350.	978.	47.66	43.43	15583.	0.894	42.92	0.13	0.237	0.371	0.0080	0.0180	1.259	40.58
18	49.77	60.20	17510.	1378.	1010.	46.80	42.61	15227.	0.892	42.07	0.13	0.230	0.357	0.0076	0.0167	1.250	39.55
18	49.77	66.20	17482.	1398.	1040.	46.48	42.35	14888.	0.889	41.30	0.12	0.225	0.343	0.0073	0.0156	1.239	39.09
18	49.77	71.20	17654.	1365.	1064.	54.45	50.43	14617.	0.887	41.25	0.13	0.233	0.332	0.0078	0.0147	1.198	47.21
19	50.64	1.00	8639.	454.	296.	135.48	131.23	33271.	1.084	163.57	0.06	0.900	1.273	0.0883	0.1736	1.209	133.14
19	50.64	3.50	8686.	507.	302.	103.83	99.35	32952.	1.075	111.80	0.06	0.809	1.255	0.0724	0.1688	1.269	101.28
19	50.64	7.50	8732.	535.	312.	94.76	90.20	32448.	1.062	95.83	0.06	0.768	1.227	0.0659	0.1613	1.288	92.11
19	50.64	12.00	8796.	553.	323.	90.86	86.26	31889.	1.049	88.70	0.06	0.742	1.195	0.0620	0.1533	1.293	88.13
19	50.64	18.00	8798.	573.	338.	86.86	82.22	31161.	1.034	83.35	0.06	0.715	1.155	0.0578	0.1431	1.294	84.02
19	50.64	26.00	8877.	596.	359.	84.22	79.56	30222.	1.019	78.87	0.06	0.686	1.102	0.0537	0.1306	1.289	81.26
19	50.64	36.10	8892.	621.	384.	81.39	76.71	29102.	1.005	74.91	0.06	0.656	1.040	0.0494	0.1165	1.280	78.29
19	50.64	46.10	8919.	647.	412.	78.79	74.11	28055.	0.993	71.82	0.06	0.627	0.983	0.0455	0.1044	1.270	75.56
19	50.64	54.20	8963.	667.	433.	77.06	72.40	27251.	0.983	69.63	0.06	0.606	0.939	0.0427	0.0958	1.262	73.72
19	50.64	60.20	8973.	681.	450.	76.17	71.53	26680.	0.977	68.23	0.06	0.592	0.908	0.0409	0.0900	1.254	72.76
19	50.64	66.20	8953.	692.	465.	75.71	71.09	26132.	0.972	66.98	0.06	0.581	0.879	0.0395	0.0846	1.245	72.23
19	50.64	71.20	9126.	681.	479.	84.99	80.46	25687.	0.969	66.62	0.07	0.592	0.855	0.0409	0.0803	1.215	81.55
20	50.44	1.00	8735.	455.	298.	137.53	133.29	33173.	1.081	163.14	0.06	0.895	1.263	0.0878	0.1716	1.207	135.18
20	50.44	3.50	8771.	505.	304.	106.40	101.95	32851.	1.072	111.62	0.06	0.809	1.245	0.0725	0.1668	1.264	103.86
20	50.44	7.50	8822.	532.	314.	97.21	92.68	32344.	1.059	95.70	0.06	0.768	1.217	0.0661	0.1594	1.282	94.57
20	50.44	12.00	8871.	550.	325.	93.17	88.60	31781.	1.046	88.56	0.06	0.743	1.185	0.0622	0.1513	1.287	90.44
20	50.44	18.00	8888.	571.	340.	89.07	84.47	31048.	1.032	83.23	0.06	0.715	1.144	0.0580	0.1412	1.288	86.24
20	50.44	26.00	8963.	593.	361.	86.64	82.01	30104.	1.017	78.77	0.06	0.687	1.092	0.0539	0.1287	1.282	83.69
20	50.44	36.10	8979.	618.	387.	83.97	79.34	28979.	1.003	74.83	0.06	0.657	1.030	0.0497	0.1147	1.272	80.89
20	50.44	46.10	8990.	643.	414.	81.50	76.86	27928.	0.991	71.76	0.06	0.629	0.973	0.0459	0.1027	1.261	78.28
20	50.44	54.20	9051.	663.	436.	79.62	75.00	27122.	0.982	69.56	0.07	0.607	0.929	0.0430	0.0942	1.254	76.30
20	50.44	60.20	9043.	677.	453.	78.62	74.01	26551.	0.976	68.15	0.06	0.593	0.899	0.0411	0.0884	1.246	75.22
20	50.44	66.20	9042.	690.	469.	77.90	73.31	26003.	0.971	66.87	0.06	0.580	0.869	0.0396	0.0831	1.238	74.43
20	50.44	71.20	9193.	679.	483.	87.56	83.06	25559.	0.967	66.49	0.07	0.591	0.846	0.0410	0.0789	1.208	84.12
21	50.14	1.00	26041.	762.	305.	138.94	133.39	33586.	1.069	142.55	0.17	0.513	1.235	0.0319	0.1650	1.598	135.31
21	50.14	3.50	26463.	909.	323.	107.07	101.02	32645.	1.047	93.53	0.18	0.412	1.184	0.0215	0.1518	1.749	102.67
21	50.14	7.50	26811.	993.	353.	94.88	88.69	31199.	1.022	77.64	0.18	0.367	1.106	0.0175	0.1326	1.787	89.99
21	50.14	12.00	27123.	1049.	389.	88.34	82.14	29669.	1.003	70.13	0.18	0.341	1.024	0.0154	0.1139	1.778	83.11
21	50.14	18.00	27286.	1104.	436.	81.75	75.67	27807.	0.982	64.18	0.19	0.318	0.925	0.0136	0.0940	1.745	76.20
21	50.14	26.00	27596.	1168.	501.	75.37	69.47	25620.	0.964	58.96	0.19	0.294	0.812	0.0118	0.0735	1.694	69.44
21	50.14	36.10	27767.	1234.	583.	68.93	63.34	23299.	0.941	54.22	0.19	0.272	0.696	0.0103	0.0555	1.624	62.66
21	50.14	46.10	27841.	1290.	664.	64.60	59.27	21371.	0.928	50.78	0.19	0.255	0.603	0.0091	0.0427	1.557	57.99
21	50.14	54.20	28201.	1341.	730.	61.69	56.55	20027.	0.919	48.37	0.19	0.241	0.540	0.0082	0.0350	1.514	54.77
21	50.14	60.20	28281.	1372.	779.	59.95	54.97	19134.	0.911	46.82	0.19	0.233	0.500	0.0077	0.0305	1.479	52.86
21	50.14	66.20	28315.	1405.	829.	58.29	53.45	18323.	0.904	45.43	0.19	0.225	0.464	0.0073	0.0267	1.447	51.02

M	P	Z	QW	TW	TG	NUB	NUBC	REB	PRB	NUMCEL	A B6	TAW	TAG	PLNKW	PLNKB	TRAT	UBCHOT
21	50.14	71.20	28749.	1368.	870.	65.35	60.72	17698.	0.900	45.13	0.19	0.234	0.437	0.0078	0.0239	1.375	58.28
22	49.84	1.00	25464.	766.	307.	134.92	129.39	32759.	1.065	139.49	0.18	0.507	1.221	0.0314	0.1623	1.599	131.27
22	49.84	3.50	25873.	908.	325.	104.86	98.86	31842.	1.044	91.73	0.18	0.410	1.170	0.0214	0.1493	1.743	100.46
22	49.84	7.50	26189.	993.	355.	92.75	86.60	30434.	1.019	76.11	0.18	0.365	1.093	0.0174	0.1305	1.783	87.86
22	49.84	12.00	26448.	1047.	390.	86.46	80.31	28945.	1.001	68.80	0.19	0.340	1.012	0.0153	0.1121	1.773	81.23
22	49.84	18.00	26650.	1107.	438.	79.51	73.46	27133.	0.980	62.88	0.19	0.315	0.915	0.0134	0.0925	1.745	73.93
22	49.84	26.00	27069.	1171.	503.	73.53	67.67	25002.	0.962	57.77	0.19	0.291	0.803	0.0116	0.0724	1.694	67.58
22	49.84	36.10	27258.	1238.	586.	67.24	61.68	22736.	0.940	53.15	0.19	0.269	0.688	0.0101	0.0547	1.624	60.94
22	49.84	46.10	27397.	1292.	668.	63.49	58.20	20855.	0.928	49.86	0.19	0.253	0.596	0.0091	0.0420	1.553	56.87
22	49.84	54.20	27648.	1343.	734.	60.35	55.25	19546.	0.918	47.46	0.20	0.239	0.534	0.0082	0.0345	1.511	53.43
22	49.84	60.20	27621.	1375.	782.	58.38	53.43	18678.	0.910	45.93	0.20	0.231	0.494	0.0076	0.0300	1.478	51.27
22	49.84	66.20	27567.	1404.	830.	56.92	52.11	17890.	0.904	44.60	0.19	0.224	0.459	0.0072	0.0263	1.445	49.64
22	49.84	71.20	27996.	1371.	873.	63.49	58.89	17282.	0.900	44.30	0.20	0.232	0.432	0.0077	0.0236	1.374	56.40
25	50.64	1.00	8758.	643.	294.	62.31	57.19	9986.	1.089	56.86	0.68	0.631	1.282	0.0461	0.1762	1.464	59.24
25	50.64	3.50	8806.	789.	314.	44.59	38.94	9666.	1.060	36.95	0.69	0.497	1.222	0.0300	0.1601	1.614	40.83
25	50.64	7.50	8818.	896.	347.	36.71	30.80	9180.	1.027	30.14	0.70	0.424	1.131	0.0225	0.1374	1.681	32.37
25	50.64	12.00	8954.	965.	386.	33.38	27.42	8671.	1.004	26.94	0.71	0.385	1.037	0.0189	0.1157	1.684	28.64
25	50.64	18.00	9019.	1032.	441.	30.30	24.43	8058.	0.980	24.44	0.72	0.352	0.925	0.0161	0.0931	1.656	25.18
25	50.64	26.00	9235.	1104.	514.	27.93	22.24	7347.	0.959	22.24	0.75	0.321	0.798	0.0137	0.0706	1.606	22.38
25	50.64	36.10	9261.	1179.	609.	25.34	19.97	6605.	0.936	20.31	0.74	0.293	0.670	0.0116	0.0514	1.533	19.40
25	50.64	46.10	9250.	1245.	701.	23.60	18.48	6006.	0.925	18.91	0.74	0.271	0.572	0.0101	0.0384	1.469	17.23
25	50.64	54.20	9437.	1292.	776.	23.08	18.19	5594.	0.911	17.95	0.75	0.257	0.507	0.0092	0.0310	1.418	16.45
25	50.64	60.20	9407.	1347.	831.	21.60	16.83	5324.	0.904	17.25	0.74	0.242	0.465	0.0082	0.0266	1.399	14.65
25	50.64	66.20	9298.	1378.	887.	21.09	16.46	5083.	0.899	16.74	0.73	0.234	0.429	0.0077	0.0230	1.364	13.94
25	50.64	71.20	9529.	1296.	934.	27.94	23.60	4898.	0.896	16.85	0.75	0.256	0.402	0.0091	0.0205	1.259	21.21
29	49.94	1.00	9075.	877.	676.	64.68	60.37	9770.	0.927	58.43	0.29	0.430	0.589	0.0234	0.0411	1.177	60.20
29	49.94	3.50	9067.	988.	688.	42.67	38.14	9631.	0.926	39.49	0.29	0.368	0.575	0.0176	0.0393	1.261	37.66
29	49.94	7.50	9049.	1057.	712.	35.86	31.26	9419.	0.922	33.57	0.29	0.336	0.554	0.0150	0.0367	1.295	30.50
29	49.94	12.00	9157.	1096.	738.	33.87	29.30	9189.	0.917	30.99	0.29	0.320	0.531	0.0137	0.0341	1.299	28.32
29	49.94	18.00	9199.	1137.	773.	32.04	27.52	8900.	0.912	29.08	0.29	0.304	0.503	0.0126	0.0309	1.295	26.27
29	49.94	26.00	9350.	1179.	818.	31.15	26.71	8539.	0.906	27.45	0.30	0.289	0.468	0.0115	0.0273	1.282	25.13
29	49.94	36.10	9369.	1230.	878.	29.90	25.55	8125.	0.900	26.00	0.29	0.272	0.430	0.0103	0.0234	1.263	23.57
29	49.94	46.10	9341.	1276.	932.	28.82	24.56	7755.	0.896	24.87	0.29	0.258	0.396	0.0093	0.0202	1.247	22.18
29	49.94	54.20	9468.	1323.	980.	27.96	23.76	7479.	0.894	24.06	0.29	0.245	0.372	0.0085	0.0180	1.238	21.02
29	49.94	60.20	9474.	1353.	1016.	27.47	23.32	7287.	0.891	23.53	0.29	0.237	0.355	0.0080	0.0165	1.228	20.35
29	49.94	66.20	9363.	1373.	1048.	27.28	23.20	7107.	0.888	23.07	0.29	0.232	0.340	0.0077	0.0153	1.215	20.02
29	49.94	71.20	9533.	1323.	1077.	35.63	31.70	6964.	0.886	23.15	0.29	0.245	0.328	0.0085	0.0143	1.160	28.60
35	49.73	1.00	3584.	575.	258.	29.83	24.93	3438.	1.161	25.05	2.58	0.699	1.370	0.0563	0.2046	1.442	27.08
35	49.73	3.50	3522.	708.	282.	20.94	15.55	3301.	1.104	16.10	2.58	0.555	1.292	0.0370	0.1820	1.574	17.58
35	49.73	7.50	3437.	825.	322.	16.23	10.55	3097.	1.047	12.88	2.56	0.462	1.176	0.0267	0.1511	1.643	12.27
35	49.73	12.00	3482.	914.	369.	14.14	8.37	2889.	1.011	11.31	2.63	0.406	1.059	0.0212	0.1227	1.657	9.70
35	49.73	18.00	3457.	1008.	432.	12.09	6.34	2645.	0.982	10.07	2.64	0.357	0.923	0.0167	0.0942	1.645	7.10
35	49.73	26.00	3729.	1115.	523.	11.09	5.51	2364.	0.956	8.98	2.84	0.311	0.772	0.0131	0.0675	1.603	5.49
35	49.73	36.10	3657.	1223.	638.	9.38	4.12	2080.	0.932	8.05	2.78	0.273	0.625	0.0104	0.0460	1.533	3.17
35	49.73	46.10	3577.	1311.	748.	8.30	3.35	1864.	0.915	7.39	2.71	0.247	0.520	0.0086	0.0329	1.466	1.57
35	49.73	54.20	3815.	1393.	841.	8.08	3.34	1718.	0.903	6.94	2.86	0.226	0.452	0.0074	0.0256	1.425	0.87
35	49.73	60.20	3735.	1432.	907.	7.75	3.17	1623.	0.897	6.68	2.79	0.217	0.409	0.0068	0.0214	1.384	0.27
35	49.73	66.20	3638.	1450.	974.	7.78	3.38	1541.	0.894	6.50	2.69	0.213	0.373	0.0066	0.0182	1.332	0.15
35	49.73	71.20	3834.	1334.	1029.	12.11	8.04	1478.	0.890	6.59	2.82	0.241	0.347	0.0083	0.0159	1.205	5.06
38	50.73	1.00	3249.	783.	594.	27.41	23.00	3111.	0.939	23.49	1.21	0.503	0.689	0.0306	0.0540	1.179	23.43
38	50.73	3.50	3172.	878.	612.	18.53	13.93	3053.	0.936	15.90	1.19	0.436	0.668	0.0237	0.0510	1.248	14.12
38	50.73	7.50	3095.	955.	640.	14.70	10.01	2966.	0.932	13.42	1.15	0.391	0.637	0.0195	0.0468	1.287	9.91
38	50.73	12.00	3137.	1004.	670.	13.54	8.84	2875.	0.928	12.31	1.17	0.366	0.605	0.0172	0.0425	1.296	8.49
38	50.73	18.00	3125.	1060.	709.	12.22	7.54	2762.	0.923	11.43	1.16	0.340	0.565	0.0151	0.0375	1.301	6.84
38	50.73	26.00	3309.	1129.	766.	11.66	7.06	2621.	0.913	10.64	1.22	0.312	0.517	0.0130	0.0321	1.296	5.93
38	50.73	36.10	3252.	1207.	835.	10.31	5.81	2463.	0.904	9.93	1.20	0.284	0.464	0.0110	0.0265	1.287	4.14
38	50.73	46.10	3193.	1277.	903.	9.35	4.94	2326.	0.898	9.40	1.17	0.262	0.420	0.0095	0.0222	1.274	2.75
38	50.73	54.20	3360.	1344.	959.	9.00	4.64	2226.	0.895	9.01	1.22	0.243	0.389	0.0083	0.0193	1.272	1.98
38	50.73	60.20	3295.	1379.	1000.	8.62	4.32	2156.	0.893	8.78	1.19	0.234	0.368	0.0077	0.0174	1.260	1.36
38	50.73	66.20	3211.	1400.	1041.	8.52	4.31	2093.	0.889	8.60	1.15	0.229	0.349	0.0074	0.0159	1.239	1.13

M	P	Z	QW	TW	TG	NUB	NUBC	REB	PRB	NUMCEL	A B6	TAW	TAG	PLNKW	PLNKB	TRAT	UBCHOT
38	50.73	71.20	3357.	1304.	1074.	13.44	9.46	2043.	0.886	8.72	1.21	0.254	0.334	0.0090	0.0147	1.150	6.50
39	50.53	1.00	3236.	789.	609.	28.08	23.73	3174.	0.936	23.95	1.12	0.496	0.668	0.0299	0.0511	1.168	24.06
39	50.53	3.50	3155.	882.	626.	18.84	14.30	3118.	0.933	16.24	1.10	0.432	0.648	0.0233	0.0484	1.235	14.39
39	50.53	7.50	3092.	958.	653.	14.94	10.31	3035.	0.930	13.73	1.07	0.388	0.619	0.0192	0.0445	1.274	10.13
39	50.53	12.00	3124.	1009.	681.	13.54	8.89	2946.	0.927	12.58	1.08	0.362	0.589	0.0169	0.0407	1.288	8.44
39	50.53	18.00	3113.	1064.	720.	12.25	7.62	2837.	0.921	11.71	1.07	0.337	0.553	0.0149	0.0362	1.292	6.85
39	50.53	26.00	3290.	1131.	773.	11.66	7.11	2699.	0.912	10.92	1.13	0.310	0.508	0.0129	0.0312	1.290	5.91
39	50.53	36.10	3232.	1209.	841.	10.27	5.80	2544.	0.903	10.20	1.10	0.282	0.458	0.0109	0.0260	1.283	4.07
39	50.53	46.10	3176.	1280.	906.	9.26	4.87	2409.	0.898	9.66	1.08	0.260	0.417	0.0094	0.0219	1.274	2.64
39	50.53	54.20	3337.	1345.	958.	8.92	4.58	2309.	0.895	9.27	1.13	0.242	0.387	0.0082	0.0192	1.273	1.89
39	50.53	60.20	3283.	1384.	1000.	8.49	4.21	2240.	0.893	9.04	1.10	0.232	0.367	0.0077	0.0174	1.263	1.22
39	50.53	66.20	3188.	1400.	1038.	8.40	4.19	2177.	0.889	8.86	1.07	0.228	0.349	0.0074	0.0159	1.242	1.00
39	50.53	71.20	3328.	1301.	1070.	13.33	9.36	2127.	0.886	9.00	1.11	0.254	0.335	0.0090	0.0148	1.151	6.42
46	51.78	1.00	2532.	546.	296.	25.02	20.27	2701.	1.089	20.94	2.67	0.768	1.303	0.0647	0.1780	1.332	22.34
46	51.78	3.50	2472.	651.	317.	17.71	12.56	2610.	1.059	13.77	2.63	0.636	1.239	0.0458	0.1611	1.430	14.58
46	51.78	7.50	2402.	745.	351.	13.87	8.48	2477.	1.026	11.24	2.59	0.545	1.146	0.0347	0.1379	1.485	10.29
46	51.78	12.00	2414.	824.	391.	11.95	6.42	2341.	1.004	9.99	2.62	0.482	1.051	0.0279	0.1163	1.509	7.94
46	51.78	18.00	2403.	890.	444.	10.64	5.15	2179.	0.980	9.04	2.62	0.437	0.939	0.0234	0.0939	1.494	6.28
46	51.78	26.00	2623.	981.	519.	10.05	4.64	1985.	0.958	8.15	2.86	0.385	0.809	0.0186	0.0711	1.472	5.18
46	51.78	36.10	2559.	1074.	616.	8.63	3.44	1780.	0.936	7.38	2.79	0.341	0.677	0.0150	0.0514	1.426	3.26
46	51.78	46.10	2492.	1151.	708.	7.75	2.78	1619.	0.924	6.84	2.71	0.310	0.577	0.0126	0.0384	1.379	1.91
46	51.78	54.20	2639.	1218.	784.	7.60	2.80	1508.	0.910	6.45	2.85	0.286	0.511	0.0109	0.0310	1.349	1.38
46	51.78	60.20	2586.	1255.	841.	7.31	2.65	1434.	0.903	6.22	2.77	0.274	0.469	0.0101	0.0266	1.318	0.87
46	51.78	66.20	2507.	1268.	897.	7.43	2.93	1370.	0.898	6.06	2.68	0.270	0.433	0.0098	0.0230	1.274	0.88
46	51.78	71.20	2686.	1167.	944.	12.63	8.45	1320.	0.895	6.15	2.85	0.304	0.406	0.0122	0.0204	1.159	6.54
60	50.76	1.00	18613.	954.	683.	97.59	93.06	20751.	0.927	104.12	0.13	0.392	0.591	0.0195	0.0407	1.237	92.76
60	50.76	3.50	18802.	1058.	697.	72.66	67.94	20469.	0.925	70.74	0.13	0.341	0.577	0.0152	0.0390	1.312	67.31
60	50.76	7.50	18928.	1114.	720.	65.11	60.35	20033.	0.921	60.47	0.13	0.318	0.557	0.0134	0.0366	1.334	59.47
60	50.76	12.00	19121.	1150.	745.	61.92	57.19	19560.	0.916	55.90	0.13	0.304	0.535	0.0124	0.0340	1.336	56.09
60	50.76	18.00	19156.	1189.	778.	58.66	53.98	18964.	0.911	52.49	0.13	0.290	0.507	0.0114	0.0310	1.332	52.61
60	50.76	26.00	19359.	1232.	823.	56.55	51.95	18220.	0.905	49.60	0.13	0.276	0.473	0.0104	0.0274	1.319	50.25
60	50.76	36.10	19479.	1284.	879.	54.02	49.52	17367.	0.900	47.02	0.13	0.260	0.436	0.0094	0.0236	1.302	47.40
60	50.76	46.10	19467.	1337.	933.	51.07	46.65	16597.	0.896	44.94	0.13	0.245	0.402	0.0084	0.0205	1.290	44.10
60	50.76	54.20	19721.	1384.	981.	49.45	45.09	16023.	0.894	43.52	0.13	0.233	0.378	0.0077	0.0183	1.280	42.19
60	50.76	60.20	19762.	1413.	1013.	48.45	44.14	15623.	0.892	42.59	0.13	0.226	0.362	0.0072	0.0169	1.271	41.00
60	50.76	66.20	19668.	1392.	1047.	53.93	49.75	15244.	0.888	42.24	0.13	0.231	0.346	0.0075	0.0156	1.229	46.57
60	50.76	71.20	19922.	1396.	1075.	57.14	53.03	14943.	0.886	41.78	0.13	0.230	0.334	0.0075	0.0147	1.209	49.73
63	50.53	1.00	16937.	781.	382.	92.11	86.82	18089.	1.006	88.30	0.32	0.502	1.045	0.0306	0.1179	1.474	88.32
63	50.53	3.50	17163.	927.	403.	68.99	63.25	17577.	0.997	58.29	0.32	0.405	1.000	0.0208	0.1080	1.608	64.44
63	50.53	7.50	17353.	1015.	437.	59.92	54.09	16805.	0.982	48.53	0.32	0.359	0.932	0.0167	0.0947	1.646	54.89
63	50.53	12.00	17533.	1071.	474.	55.55	49.75	15999.	0.970	43.96	0.33	0.334	0.862	0.0147	0.0817	1.640	50.19
63	50.53	18.00	17656.	1133.	526.	50.97	45.28	15025.	0.955	40.31	0.33	0.309	0.780	0.0128	0.0678	1.616	45.26
63	50.53	26.00	17995.	1200.	596.	47.24	41.75	13884.	0.939	37.09	0.34	0.285	0.685	0.0111	0.0536	1.573	41.16
63	50.53	36.10	18077.	1270.	683.	43.74	38.50	12671.	0.927	34.30	0.34	0.263	0.588	0.0096	0.0405	1.513	37.24
63	50.53	46.10	18089.	1341.	769.	40.29	35.29	11662.	0.912	32.02	0.34	0.243	0.511	0.0083	0.0315	1.465	33.38
63	50.53	54.20	18366.	1408.	840.	37.86	33.02	10957.	0.903	30.43	0.34	0.226	0.459	0.0073	0.0260	1.437	30.55
63	50.53	60.20	18453.	1447.	894.	36.82	32.11	10488.	0.899	29.50	0.34	0.217	0.425	0.0068	0.0227	1.409	29.29
63	50.53	66.20	18324.	1470.	944.	36.52	31.93	10061.	0.895	28.73	0.33	0.212	0.395	0.0065	0.0199	1.375	28.81
63	50.53	71.20	18615.	1413.	988.	44.04	39.68	9733.	0.893	28.76	0.34	0.225	0.373	0.0072	0.0179	1.293	36.63
64	50.53	1.00	16997.	786.	381.	91.10	85.78	17911.	1.007	87.37	0.32	0.498	1.048	0.0301	0.1185	1.483	87.29
64	50.53	3.50	17201.	932.	401.	68.42	62.66	17397.	0.998	57.67	0.33	0.402	1.002	0.0205	0.1085	1.617	63.85
64	50.53	7.50	17402.	1020.	435.	59.64	53.79	16621.	0.982	48.00	0.33	0.357	0.933	0.0166	0.0949	1.653	54.59
64	50.53	12.00	17621.	1076.	474.	55.40	49.58	15811.	0.970	43.49	0.34	0.332	0.862	0.0146	0.0817	1.644	50.02
64	50.53	18.00	17701.	1138.	526.	50.66	44.96	14835.	0.955	39.84	0.34	0.307	0.778	0.0127	0.0676	1.621	44.92
64	50.53	26.00	17988.	1203.	596.	47.00	41.51	13694.	0.938	36.64	0.35	0.284	0.683	0.0110	0.0533	1.575	40.90
64	50.53	36.10	18082.	1273.	686.	43.55	38.31	12483.	0.926	33.88	0.35	0.262	0.585	0.0095	0.0401	1.513	37.02
64	50.53	46.10	18218.	1348.	775.	40.17	35.18	11480.	0.911	31.62	0.34	0.241	0.507	0.0082	0.0311	1.464	33.23
64	50.53	54.20	18431.	1413.	846.	37.85	33.02	10779.	0.903	30.06	0.35	0.225	0.455	0.0072	0.0256	1.434	30.52
64	50.53	60.20	18498.	1452.	900.	36.78	32.08	10313.	0.898	29.12	0.35	0.216	0.421	0.0067	0.0223	1.406	29.21
64	50.53	66.20	18390.	1479.	952.	36.26	31.68	9891.	0.895	28.36	0.34	0.210	0.392	0.0064	0.0196	1.374	28.49

M	P	Z	QW	TW	TG	NUB	NUBC	REB	PRB	NUMCEL	A E6	TAW	TAG	PLNKW	PLNKB	TRAT	UBCHOT
64	50.53	71.20	18675.	1417.	996.	44.22	39.87	9565.	0.893	28.40	0.35	0.224	0.369	0.0072	0.0176	1.289	36.78
67	50.10	1.00	24377.	1297.	1077.	101.93	97.54	21444.	0.886	109.21	0.08	0.253	0.330	0.0090	0.0146	1.143	95.04
67	50.10	3.50	24423.	1392.	1086.	72.68	68.75	21302.	0.885	75.09	0.08	0.228	0.325	0.0075	0.0141	1.198	65.28
67	50.10	7.50	24461.	1439.	1103.	65.23	61.01	21020.	0.884	64.78	0.08	0.217	0.318	0.0068	0.0135	1.215	57.56
67	50.10	12.00	24778.	1476.	1128.	62.39	58.26	20708.	0.882	60.34	0.08	0.209	0.309	0.0064	0.0129	1.219	54.51
67	50.10	18.00	24700.	1504.	1153.	60.13	56.03	20306.	0.881	57.20	0.08	0.203	0.299	0.0060	0.0121	1.218	52.04
67	50.10	26.00	24917.	1540.	1191.	59.16	55.11	19793.	0.879	54.67	0.08	0.196	0.285	0.0056	0.0112	1.211	50.83
67	50.10	36.10	25147.	1588.	1241.	57.47	53.46	19186.	0.878	52.43	0.08	0.187	0.270	0.0052	0.0101	1.204	48.82
67	50.10	46.10	25130.	1640.	1288.	54.55	50.60	18621.	0.877	50.63	0.08	0.178	0.255	0.0047	0.0091	1.201	45.53
67	50.10	54.20	25437.	1683.	1329.	53.07	49.06	18188.	0.877	49.41	0.08	0.171	0.245	0.0044	0.0085	1.198	43.76
67	50.10	60.20	25175.	1702.	1352.	52.22	47.71	17880.	0.877	48.64	0.08	0.168	0.237	0.0042	0.0080	1.193	42.73
67	50.10	66.20	25097.	1722.	1381.	52.30	48.77	17585.	0.877	47.99	0.08	0.165	0.230	0.0041	0.0076	1.185	42.65
67	50.10	71.20	25494.	1676.	1403.	65.05	63.49	17374.	0.877	48.19	0.08	0.172	0.224	0.0044	0.0072	1.147	55.61
71	49.13	1.00	14130.	1269.	1069.	65.37	61.00	10820.	0.886	63.51	0.18	0.256	0.327	0.0093	0.0146	1.131	58.62
71	49.13	3.50	14084.	1374.	1081.	44.03	40.25	10737.	0.886	43.57	0.18	0.228	0.322	0.0076	0.0141	1.190	36.75
71	49.13	7.50	14097.	1434.	1101.	38.06	33.96	10572.	0.884	37.41	0.18	0.214	0.313	0.0067	0.0134	1.213	30.43
71	49.13	12.00	14210.	1471.	1124.	36.01	32.00	10391.	0.882	34.75	0.18	0.206	0.303	0.0063	0.0127	1.219	28.14
71	49.13	18.00	14230.	1510.	1157.	34.41	30.44	10159.	0.881	32.87	0.18	0.198	0.291	0.0058	0.0118	1.218	26.29
71	49.13	26.00	14679.	1551.	1201.	34.36	30.44	9863.	0.879	31.31	0.19	0.190	0.276	0.0054	0.0107	1.211	25.95
71	49.13	36.10	14703.	1601.	1258.	33.46	29.59	9512.	0.878	29.96	0.19	0.181	0.259	0.0049	0.0095	1.200	24.69
71	49.13	46.10	14715.	1662.	1315.	31.73	27.92	9190.	0.877	28.85	0.18	0.171	0.243	0.0045	0.0085	1.195	22.56
71	49.13	54.20	14959.	1714.	1359.	30.44	26.54	8945.	0.877	28.04	0.19	0.163	0.231	0.0041	0.0078	1.195	20.89
71	49.13	60.20	14825.	1741.	1394.	30.05	25.91	8772.	0.877	27.58	0.18	0.159	0.223	0.0039	0.0073	1.187	20.29
71	49.13	66.20	14720.	1762.	1428.	30.20	27.03	8606.	0.877	27.19	0.18	0.156	0.216	0.0038	0.0068	1.177	20.26
71	49.13	71.20	14979.	1674.	1451.	45.21	42.97	8489.	0.878	27.55	0.18	0.169	0.210	0.0044	0.0065	1.117	35.70
73	49.75	1.00	5393.	1145.	966.	31.02	26.46	3557.	0.894	26.25	0.76	0.300	0.380	0.0123	0.0188	1.125	24.98
73	49.75	3.50	5253.	1249.	981.	19.80	15.92	3520.	0.894	17.95	0.73	0.265	0.371	0.0099	0.0179	1.186	13.25
73	49.75	7.50	5121.	1323.	1006.	15.95	11.76	3448.	0.892	15.30	0.72	0.244	0.357	0.0084	0.0168	1.216	8.98
73	49.75	12.00	5200.	1381.	1039.	14.50	10.40	3370.	0.889	14.11	0.72	0.229	0.343	0.0076	0.0156	1.228	7.21
73	49.75	18.00	5169.	1432.	1079.	13.40	9.31	3272.	0.886	13.24	0.72	0.217	0.326	0.0068	0.0142	1.230	5.79
73	49.75	26.00	5484.	1497.	1135.	13.17	9.16	3147.	0.882	12.49	0.76	0.203	0.304	0.0061	0.0126	1.227	5.16
73	49.75	36.10	5392.	1564.	1203.	12.23	8.30	3003.	0.879	11.83	0.74	0.190	0.279	0.0053	0.0108	1.217	3.74
73	49.75	46.10	5367.	1632.	1275.	11.58	7.69	2874.	0.877	11.33	0.72	0.178	0.258	0.0048	0.0094	1.206	2.64
73	49.75	54.20	5510.	1701.	1327.	10.91	6.84	2777.	0.877	10.94	0.74	0.167	0.242	0.0042	0.0084	1.209	1.47
73	49.75	60.20	5436.	1741.	1373.	10.54	6.75	2709.	0.877	10.71	0.72	0.161	0.232	0.0040	0.0077	1.201	0.83
73	49.75	66.20	5267.	1755.	1412.	10.66	7.85	2645.	0.877	10.55	0.70	0.159	0.222	0.0039	0.0071	1.183	0.77
73	49.75	71.20	5435.	1592.	1440.	24.32	19.59	2601.	0.878	10.87	0.72	0.185	0.214	0.0051	0.0066	1.080	15.26
76	53.95	1.00	24215.	958.	366.	90.84	84.45	17730.	1.021	80.97	0.49	0.414	1.155	0.0205	0.1347	1.718	86.14
76	53.95	3.50	24715.	1163.	397.	68.53	61.55	16981.	1.005	52.40	0.50	0.318	1.081	0.0128	0.1181	1.895	53.17
76	53.95	7.50	25101.	1308.	447.	57.37	50.27	15878.	0.981	42.60	0.51	0.269	0.973	0.0095	0.0969	1.949	39.57
76	53.95	12.00	25421.	1406.	504.	51.10	44.09	14770.	0.965	37.88	0.52	0.242	0.867	0.0078	0.0779	1.935	31.59
76	53.95	18.00	25704.	1503.	584.	45.14	38.43	13496.	0.943	34.11	0.52	0.219	0.749	0.0065	0.0597	1.881	24.20
76	53.95	26.00	26317.	1600.	687.	40.71	34.40	12087.	0.927	30.90	0.54	0.199	0.623	0.0054	0.0426	1.796	18.18
76	53.95	36.10	26524.	1695.	821.	36.31	30.52	10685.	0.906	28.12	0.53	0.182	0.505	0.0046	0.0293	1.683	27.12
76	53.95	46.10	26658.	1798.	951.	32.77	27.36	9593.	0.895	26.01	0.53	0.166	0.418	0.0039	0.0209	1.600	22.93
76	53.95	54.20	27072.	1885.	1053.	30.59	25.44	8863.	0.888	24.56	0.53	0.154	0.364	0.0034	0.0163	1.550	20.14
76	53.95	60.20	27222.	1933.	1134.	29.67	24.72	8393.	0.882	23.73	0.53	0.148	0.330	0.0031	0.0137	1.501	18.94
76	53.95	66.20	26983.	1958.	1206.	29.32	24.56	7976.	0.879	23.06	0.52	0.145	0.301	0.0030	0.0116	1.451	18.37
76	53.95	71.20	27285.	1805.	1272.	39.55	35.16	7662.	0.877	23.44	0.52	0.165	0.280	0.0039	0.0102	1.308	29.58
81	51.20	1.00	14381.	791.	350.	74.18	68.64	12595.	1.026	65.07	0.60	0.501	1.138	0.0302	0.1375	1.545	70.37
81	51.20	3.50	14552.	954.	376.	55.09	49.06	12130.	1.010	42.44	0.61	0.395	1.074	0.0197	0.1228	1.693	50.41
81	51.20	7.50	14668.	1072.	417.	46.13	39.91	11439.	0.991	34.76	0.62	0.338	0.981	0.0148	0.1030	1.747	40.75
81	51.20	12.00	14892.	1157.	467.	41.22	35.04	10733.	0.972	30.98	0.63	0.304	0.887	0.0123	0.0852	1.746	35.34
81	51.20	18.00	14999.	1239.	533.	36.85	30.83	9905.	0.954	28.05	0.64	0.276	0.780	0.0104	0.0671	1.712	30.50
81	51.20	26.00	15433.	1323.	622.	33.73	28.01	8966.	0.934	25.47	0.65	0.251	0.662	0.0087	0.0498	1.649	26.90
81	51.20	36.10	15498.	1404.	735.	30.77	25.42	8008.	0.918	23.31	0.65	0.230	0.547	0.0074	0.0353	1.560	23.47
81	51.20	46.10	15506.	1497.	845.	27.70	22.66	7245.	0.903	21.54	0.65	0.209	0.461	0.0062	0.0260	1.500	19.85
81	51.20	54.20	15908.	1578.	935.	26.19	21.34	6727.	0.896	20.36	0.66	0.193	0.405	0.0054	0.0205	1.461	17.80
81	51.20	60.20	15909.	1639.	1002.	24.73	20.00	6388.	0.893	19.60	0.65	0.182	0.370	0.0048	0.0174	1.436	15.93
81	51.20	66.20	15835.	1687.	1071.	23.73	19.16	6087.	0.886	18.95	0.64	0.174	0.339	0.0045	0.0150	1.403	14.65

M	P	Z	QW	TW	TG	NUB	NUBC	REB	PRB	NUMCEL	A E6	TAW	TAG	PLNKW	PLNKB	TRAT	UBCHOT
81	51.20	71.20	15998.	1541.	1125.	33.72	29.51	5858.	0.883	19.30	0.64	0.200	0.317	0.0058	0.0133	1.263	25.48
83	50.88	1.00	6962.	752.	325.	38.53	33.06	4837.	1.047	30.52	2.11	0.529	1.195	0.0333	0.1525	1.544	34.93
83	50.88	3.50	6957.	918.	358.	27.94	21.99	4602.	1.020	19.68	2.13	0.413	1.108	0.0214	0.1314	1.684	23.48
83	50.88	7.50	6947.	1063.	413.	22.17	15.99	4264.	0.993	15.80	2.14	0.340	0.986	0.0151	0.1045	1.745	16.85
83	50.88	12.00	7014.	1183.	475.	18.72	12.54	3932.	0.970	13.82	2.17	0.293	0.867	0.0116	0.0821	1.758	12.68
83	50.88	18.00	6982.	1314.	557.	15.45	9.42	3559.	0.947	12.22	2.17	0.252	0.738	0.0088	0.0611	1.744	8.62
83	50.88	26.00	7543.	1468.	673.	13.64	7.87	3147.	0.928	10.82	2.33	0.214	0.602	0.0065	0.0420	1.702	5.86
83	50.88	36.10	7483.	1610.	822.	11.36	6.05	2742.	0.905	9.66	2.28	0.186	0.476	0.0051	0.0276	1.615	2.78
83	50.88	46.10	7348.	1739.	961.	9.74	4.75	2440.	0.894	8.84	2.21	0.165	0.388	0.0040	0.0192	1.547	0.30
83	50.88	54.20	7818.	1863.	1079.	9.14	4.38	2240.	0.886	8.27	2.32	0.148	0.334	0.0033	0.0146	1.510	-1.10
83	50.88	60.20	7680.	1921.	1164.	8.60	4.03	2112.	0.881	7.96	2.25	0.141	0.301	0.0030	0.0121	1.466	-2.03
83	50.88	66.20	7503.	1947.	1247.	8.46	4.08	2001.	0.878	7.74	2.17	0.138	0.273	0.0029	0.0102	1.410	-2.38
83	50.88	71.20	7768.	1712.	1312.	14.52	10.56	1918.	0.877	8.00	2.24	0.169	0.253	0.0042	0.0089	1.226	5.05
28	75.14	1.00	9491.	882.	693.	70.42	64.37	10235.	0.932	61.11	0.27	0.642	0.861	0.0347	0.0585	1.164	65.89
28	75.14	3.50	9492.	999.	707.	44.85	38.44	10096.	0.929	41.24	0.27	0.546	0.841	0.0259	0.0561	1.250	39.78
28	75.14	7.50	9449.	1066.	728.	37.52	31.00	9882.	0.924	35.07	0.27	0.500	0.811	0.0221	0.0527	1.284	23.77
28	75.14	12.00	9562.	1105.	754.	35.36	28.84	9652.	0.919	32.39	0.27	0.476	0.779	0.0203	0.0490	1.289	21.07
28	75.14	18.00	9619.	1145.	788.	33.54	27.07	9359.	0.914	30.40	0.27	0.453	0.739	0.0186	0.0447	1.286	18.69
28	75.14	26.00	9783.	1188.	833.	32.51	26.12	8993.	0.907	28.70	0.27	0.430	0.690	0.0169	0.0395	1.275	17.00
28	75.14	36.10	9772.	1237.	889.	31.17	24.89	8573.	0.901	27.21	0.27	0.406	0.635	0.0152	0.0340	1.258	24.78
28	75.14	46.10	9810.	1288.	945.	29.96	23.79	8194.	0.897	26.03	0.27	0.383	0.587	0.0137	0.0295	1.244	23.26
28	75.14	54.20	9965.	1334.	992.	29.11	22.99	7911.	0.895	25.19	0.27	0.364	0.552	0.0125	0.0263	1.236	22.11
28	75.14	60.20	9970.	1362.	1025.	28.60	22.56	7713.	0.892	24.64	0.27	0.353	0.528	0.0119	0.0243	1.227	21.42
28	75.14	66.20	9900.	1384.	1059.	28.49	22.53	7526.	0.889	24.18	0.27	0.345	0.505	0.0114	0.0225	1.214	21.17
28	75.14	71.20	10069.	1339.	1086.	36.19	30.43	7378.	0.887	24.22	0.27	0.362	0.487	0.0124	0.0212	1.164	29.06
36	75.53	1.00	4169.	600.	274.	32.91	26.30	3749.	1.274	27.85	2.40	1.016	2.002	0.0791	0.2879	1.443	25.68
36	75.53	3.50	4103.	735.	297.	23.15	15.72	3609.	1.192	17.80	2.40	0.807	1.894	0.0519	0.2579	1.579	14.28
36	75.53	7.50	4025.	853.	337.	18.09	10.14	3396.	1.106	14.15	2.40	0.673	1.731	0.0376	0.2156	1.649	7.63
36	75.53	12.00	4080.	939.	383.	15.90	7.74	3172.	1.050	12.36	2.46	0.595	1.560	0.0301	0.1757	1.660	4.15
36	75.53	18.00	4072.	1031.	448.	13.73	5.56	2905.	1.003	10.95	2.48	0.526	1.360	0.0241	0.1351	1.642	0.62
36	75.53	26.00	4390.	1145.	540.	12.45	4.44	2593.	0.965	9.70	2.68	0.455	1.134	0.0187	0.0964	1.605	-2.34
36	75.53	36.10	4314.	1252.	659.	10.63	3.02	2277.	0.936	8.67	2.63	0.401	0.914	0.0148	0.0650	1.530	-5.78
36	75.53	46.10	4254.	1344.	776.	9.46	2.28	2035.	0.915	7.95	2.57	0.362	0.755	0.0123	0.0462	1.459	-8.30
36	75.53	54.20	4443.	1422.	873.	9.14	2.25	1873.	0.903	7.47	2.65	0.333	0.655	0.0106	0.0358	1.412	-9.82
36	75.53	60.20	4379.	1463.	943.	8.83	2.17	1769.	0.898	7.20	2.59	0.319	0.593	0.0098	0.0299	1.371	-10.86
36	75.53	66.20	4263.	1482.	1009.	8.86	2.44	1679.	0.894	6.99	2.51	0.313	0.540	0.0094	0.0253	1.322	-11.27
36	75.53	71.20	4480.	1380.	1067.	13.27	7.32	1610.	0.888	7.05	2.62	0.348	0.502	0.0115	0.0222	1.205	5.95
40	75.23	1.00	3191.	782.	598.	27.46	21.39	3144.	0.948	23.83	1.17	0.747	1.015	0.0454	0.0791	1.174	23.48
40	75.23	3.50	3125.	872.	614.	18.77	12.40	3088.	0.944	16.16	1.14	0.652	0.985	0.0356	0.0749	1.240	14.38
40	75.23	7.50	3056.	944.	641.	15.10	8.57	3004.	0.939	13.66	1.11	0.589	0.941	0.0297	0.0689	1.275	3.07
40	75.23	12.00	3093.	993.	671.	13.84	7.27	2915.	0.935	12.53	1.12	0.551	0.895	0.0263	0.0628	1.285	1.13
40	75.23	18.00	3087.	1044.	710.	12.70	6.14	2804.	0.929	11.67	1.12	0.515	0.838	0.0233	0.0557	1.285	-0.74
40	75.23	26.00	3264.	1107.	763.	12.15	5.66	2666.	0.918	10.87	1.18	0.475	0.769	0.0202	0.0479	1.282	-2.18
40	75.23	36.10	3213.	1181.	831.	10.86	4.48	2509.	0.908	10.16	1.15	0.434	0.693	0.0172	0.0397	1.271	-4.55
40	75.23	46.10	3156.	1249.	897.	9.88	3.60	2373.	0.901	9.62	1.13	0.401	0.629	0.0149	0.0334	1.259	3.43
40	75.23	54.20	3334.	1313.	951.	9.58	3.35	2273.	0.897	9.22	1.18	0.373	0.583	0.0131	0.0291	1.257	2.74
40	75.23	60.20	3276.	1348.	992.	9.21	3.06	2203.	0.895	8.99	1.15	0.359	0.552	0.0122	0.0264	1.245	2.14
40	75.23	66.20	3189.	1363.	1030.	9.20	3.17	2139.	0.891	8.81	1.12	0.353	0.524	0.0118	0.0240	1.224	2.01
40	75.23	71.20	3341.	1273.	1063.	14.80	9.11	2088.	0.888	8.93	1.17	0.390	0.502	0.0142	0.0223	1.138	8.03
42	75.65	1.00	3702.	572.	271.	31.76	25.33	3919.	1.290	29.32	1.96	1.070	2.022	0.0867	0.2931	1.412	24.83
42	75.65	3.50	3660.	686.	290.	23.11	15.97	3794.	1.214	18.98	1.97	0.876	1.929	0.0601	0.2670	1.528	14.86
42	75.65	7.50	3610.	785.	323.	18.52	10.91	3602.	1.130	15.23	1.98	0.747	1.786	0.0452	0.2292	1.591	8.97
42	75.65	12.00	3655.	861.	362.	16.36	8.52	3395.	1.070	13.36	2.04	0.666	1.634	0.0369	0.1922	1.607	5.74
42	75.65	18.00	3643.	945.	418.	14.21	6.26	3142.	1.023	11.90	2.05	0.591	1.450	0.0297	0.1523	1.601	2.35
42	75.65	26.00	3974.	1048.	496.	13.20	5.28	2838.	0.983	10.59	2.25	0.515	1.234	0.0232	0.1123	1.577	-0.19
42	75.65	36.10	3952.	1115.	602.	12.12	4.66	2515.	0.947	9.58	2.23	0.473	1.013	0.0200	0.0785	1.483	-2.17
42	75.65	46.10	3870.	1239.	705.	10.02	2.72	2263.	0.930	8.71	2.17	0.408	0.849	0.0153	0.0568	1.458	-6.17
42	75.65	54.20	3945.	1311.	788.	9.39	2.36	2095.	0.914	8.19	2.20	0.376	0.744	0.0132	0.0450	1.419	-7.84
42	75.65	60.20	3888.	1348.	849.	9.04	2.22	1986.	0.906	7.89	2.16	0.361	0.679	0.0123	0.0381	1.381	-8.78
42	75.65	66.20	3792.	1363.	907.	9.05	2.48	1891.	0.900	7.68	2.09	0.355	0.623	0.0119	0.0327	1.334	-9.09

M	P	Z	QW	TW	TG	NUB	NUBC	REB	PRB	NUMCEL	A B6	TAW	TAG	PLNKW	PLNKB	TRAT	UBCHOT
42	75.65	71.20	3979.	1260.	957.	13.58	7.48	1817.	0.897	7.76	2.19	0.398	0.581	0.0146	0.0288	1.214	7.00
48	76.26	1.00	3666.	692.	384.	25.78	19.04	2956.	1.051	21.92	2.55	0.875	1.573	0.0596	0.1768	1.365	17.23
48	76.26	3.50	3599.	811.	409.	18.68	11.36	2853.	1.030	14.46	2.51	0.724	1.488	0.0425	0.1588	1.463	8.63
48	76.26	7.50	3531.	913.	450.	14.93	7.32	2702.	1.003	11.85	2.48	0.623	1.366	0.0325	0.1352	1.509	3.51
48	76.26	12.00	3580.	985.	497.	13.42	5.75	2548.	0.983	10.59	2.52	0.564	1.244	0.0271	0.1133	1.511	0.95
48	76.26	18.00	3564.	1068.	560.	11.70	4.11	2366.	0.959	9.56	2.50	0.506	1.104	0.0224	0.0911	1.498	-1.91
48	76.26	26.00	3829.	1170.	647.	10.87	3.43	2153.	0.938	8.63	2.68	0.446	0.944	0.0179	0.0685	1.472	-4.24
48	76.26	36.10	3744.	1270.	757.	9.44	2.32	1932.	0.919	7.83	2.60	0.397	0.786	0.0144	0.0492	1.421	-7.19
48	76.26	46.10	3683.	1355.	865.	8.56	1.76	1757.	0.904	7.26	2.53	0.361	0.667	0.0122	0.0368	1.370	-9.39
48	76.26	54.20	3873.	1428.	951.	8.45	1.85	1637.	0.897	6.87	2.63	0.334	0.590	0.0105	0.0294	1.338	-10.75
48	76.26	60.20	3794.	1467.	1017.	8.22	1.81	1558.	0.893	6.65	2.57	0.321	0.540	0.0098	0.0251	1.305	-11.69
48	76.26	66.20	3713.	1488.	1080.	8.33	2.14	1488.	0.887	6.47	2.48	0.314	0.498	0.0094	0.0217	1.265	-11.96
48	76.26	71.20	3892.	1373.	1132.	14.04	8.29	1434.	0.883	6.55	2.60	0.354	0.467	0.0117	0.0194	1.152	6.67
49	75.76	1.00	2914.	798.	567.	20.85	14.53	2342.	0.956	18.49	2.05	0.734	1.081	0.0438	0.0883	1.225	16.84
49	75.76	3.50	2834.	896.	588.	14.75	8.11	2287.	0.950	12.47	1.99	0.634	1.040	0.0337	0.0823	1.294	3.41
49	75.76	7.50	2753.	978.	621.	11.84	5.04	2207.	0.943	10.47	1.94	0.566	0.981	0.0274	0.0739	1.330	-0.58
49	75.76	12.00	2793.	1034.	659.	10.87	4.04	2124.	0.937	9.55	1.96	0.525	0.920	0.0240	0.0657	1.336	-2.35
49	75.76	18.00	2776.	1095.	707.	9.87	3.08	2023.	0.929	8.83	1.94	0.486	0.847	0.0209	0.0565	1.332	-4.25
49	75.76	26.00	2929.	1168.	774.	9.41	2.75	1900.	0.916	8.17	2.04	0.444	0.761	0.0178	0.0468	1.319	-5.74
49	75.76	36.10	2863.	1246.	858.	8.46	1.98	1765.	0.905	7.59	1.97	0.405	0.670	0.0151	0.0372	1.295	-7.90
49	75.76	46.10	2800.	1317.	939.	7.81	1.49	1651.	0.898	7.15	1.91	0.374	0.597	0.0131	0.0302	1.270	-9.71
49	75.76	54.20	2954.	1378.	1006.	7.83	1.62	1570.	0.894	6.86	2.01	0.350	0.546	0.0116	0.0257	1.254	0.58
49	75.76	60.20	2892.	1411.	1054.	7.61	1.52	1513.	0.889	6.66	1.96	0.338	0.512	0.0108	0.0229	1.236	0.13
49	75.76	66.20	2813.	1422.	1101.	7.86	1.93	1463.	0.885	6.53	1.89	0.334	0.482	0.0106	0.0206	1.206	0.27
49	75.76	71.20	2958.	1322.	1142.	14.24	8.67	1423.	0.883	6.63	1.98	0.372	0.459	0.0129	0.0189	1.112	7.12
58	76.13	1.00	11816.	911.	680.	72.80	66.51	12362.	0.934	69.97	0.23	0.624	0.891	0.0326	0.0617	1.203	68.16
58	76.13	3.50	11906.	1021.	694.	51.04	44.41	12184.	0.932	47.38	0.24	0.537	0.869	0.0249	0.0589	1.283	37.91
58	76.13	7.50	11943.	1082.	718.	44.53	37.81	11909.	0.927	40.38	0.24	0.496	0.837	0.0216	0.0550	1.309	30.57
58	76.13	12.00	12048.	1119.	744.	42.25	35.56	11613.	0.921	37.27	0.24	0.474	0.801	0.0199	0.0510	1.311	27.78
58	76.13	18.00	12109.	1161.	780.	39.94	33.30	11238.	0.915	34.92	0.24	0.450	0.758	0.0182	0.0462	1.307	24.88
58	76.13	26.00	12232.	1205.	827.	38.45	31.91	10774.	0.908	32.93	0.24	0.427	0.705	0.0165	0.0406	1.294	22.70
58	76.13	36.10	12268.	1257.	888.	36.93	30.52	10243.	0.902	31.19	0.24	0.402	0.646	0.0148	0.0347	1.274	20.37
58	76.13	46.10	12284.	1316.	947.	34.73	28.41	9768.	0.898	29.75	0.24	0.376	0.594	0.0131	0.0298	1.263	17.20
58	76.13	54.20	12534.	1364.	995.	33.85	27.60	9414.	0.895	28.75	0.24	0.357	0.557	0.0120	0.0265	1.254	15.52
58	76.13	60.20	12509.	1390.	1029.	33.32	27.16	9166.	0.892	28.11	0.24	0.347	0.531	0.0113	0.0244	1.243	25.98
58	76.13	66.20	12451.	1415.	1065.	33.01	26.94	8934.	0.888	27.54	0.24	0.338	0.507	0.0108	0.0225	1.230	25.52
58	76.13	71.20	12562.	1364.	1094.	42.01	36.15	8750.	0.886	27.63	0.24	0.357	0.489	0.0119	0.0211	1.174	34.74
59	75.06	1.00	18438.	966.	701.	96.72	90.40	20103.	0.931	102.06	0.13	0.570	0.847	0.0280	0.0569	1.228	91.81
59	75.06	3.50	18655.	1073.	716.	71.13	64.51	19835.	0.927	69.25	0.13	0.495	0.828	0.0218	0.0547	1.304	57.30
59	75.06	7.50	18750.	1126.	737.	63.86	57.19	19421.	0.923	59.24	0.13	0.463	0.799	0.0193	0.0513	1.325	49.30
59	75.06	12.00	18924.	1162.	763.	60.75	54.09	18973.	0.918	54.79	0.13	0.443	0.768	0.0179	0.0478	1.327	45.68
59	75.06	18.00	19000.	1201.	796.	57.78	51.18	18405.	0.912	51.44	0.13	0.423	0.729	0.0164	0.0436	1.323	42.14
59	75.06	36.10	19237.	1294.	897.	53.29	46.89	16877.	0.901	46.14	0.14	0.380	0.627	0.0135	0.0333	1.293	36.16
59	75.06	46.10	19312.	1348.	952.	50.66	44.36	16141.	0.897	44.12	0.14	0.358	0.580	0.0121	0.0289	1.281	32.64
59	75.06	54.20	19517.	1394.	998.	49.09	42.86	15591.	0.895	42.75	0.14	0.341	0.546	0.0111	0.0259	1.271	30.31
59	75.06	60.20	19529.	1422.	1031.	48.05	41.90	15207.	0.891	41.81	0.14	0.331	0.522	0.0105	0.0239	1.262	40.54
59	75.06	66.20	19521.	1445.	1066.	47.74	41.67	14844.	0.888	41.02	0.13	0.323	0.500	0.0101	0.0222	1.249	40.08
59	75.06	71.20	19684.	1405.	1091.	56.91	51.04	14555.	0.886	41.02	0.14	0.337	0.483	0.0109	0.0208	1.202	49.44
62	75.03	1.00	16645.	770.	389.	94.00	86.89	17709.	1.044	88.90	0.32	0.759	1.527	0.0468	0.1695	1.448	84.50
62	75.03	3.50	16864.	921.	409.	68.65	60.81	17233.	1.028	58.41	0.32	0.606	1.464	0.0313	0.1562	1.590	57.12
62	75.03	7.50	17015.	1010.	441.	59.38	51.31	16507.	1.006	48.51	0.33	0.537	1.369	0.0251	0.1376	1.632	46.57
62	75.03	12.00	17235.	1065.	478.	55.26	47.18	15742.	0.989	43.93	0.33	0.500	1.269	0.0221	0.1194	1.625	41.62
62	75.03	18.00	17364.	1126.	529.	50.77	42.80	14811.	0.969	40.24	0.33	0.463	1.151	0.0194	0.0996	1.603	36.26
62	75.03	26.00	17688.	1193.	597.	47.04	39.29	13709.	0.948	36.96	0.34	0.427	1.014	0.0167	0.0791	1.564	31.56
62	75.03	36.10	17780.	1262.	684.	43.62	36.16	12528.	0.933	34.17	0.34	0.394	0.872	0.0145	0.0600	1.505	27.07
62	75.03	46.10	17846.	1333.	770.	40.32	33.18	11542.	0.916	31.89	0.34	0.364	0.759	0.0125	0.0468	1.458	22.74
62	75.03	54.20	18160.	1402.	839.	37.86	30.90	10849.	0.906	30.27	0.34	0.338	0.682	0.0109	0.0387	1.433	19.20
62	75.03	60.20	18153.	1436.	891.	36.88	30.09	10386.	0.901	29.35	0.34	0.326	0.632	0.0102	0.0338	1.404	17.65
62	75.03	66.20	18135.	1466.	944.	36.41	29.78	9965.	0.898	28.58	0.34	0.316	0.588	0.0097	0.0296	1.372	16.67
62	75.03	71.20	18396.	1402.	985.	44.49	38.20	9640.	0.895	28.62	0.34	0.338	0.555	0.0110	0.0267	1.288	25.63

M	P	Z	QW	TW	TG	NUB	NUBC	REB	PRB	NUMCEL	A E6	TAW	TAG	PLNKW	PLNKB	TRAT	UBCHOT
66	75.10	1.00	25130.	1307.	1082.	102.12	95.77	21419.	0.887	109.01	0.08	0.375	0.492	0.0132	0.0216	1.146	95.16
66	75.10	3.50	25192.	1402.	1091.	73.27	67.53	21274.	0.886	74.95	0.08	0.338	0.484	0.0109	0.0209	1.201	65.81
66	75.10	7.50	25332.	1452.	1110.	65.92	59.75	20985.	0.885	64.64	0.08	0.321	0.472	0.0099	0.0200	1.218	58.18
66	75.10	12.00	25559.	1486.	1132.	63.03	56.99	20665.	0.883	60.19	0.08	0.310	0.460	0.0093	0.0191	1.222	55.08
66	75.10	18.00	25585.	1522.	1163.	60.47	54.48	20255.	0.882	57.04	0.08	0.299	0.443	0.0087	0.0179	1.221	52.29
66	75.10	26.00	25925.	1560.	1203.	59.41	53.47	19730.	0.880	54.46	0.08	0.288	0.423	0.0082	0.0164	1.215	50.97
66	75.10	36.10	25896.	1604.	1251.	57.73	51.86	19111.	0.879	52.25	0.08	0.276	0.399	0.0075	0.0148	1.206	48.97
66	75.10	46.10	26046.	1659.	1302.	54.97	49.14	18534.	0.878	50.42	0.08	0.262	0.378	0.0069	0.0134	1.203	45.84
66	75.10	54.20	26297.	1701.	1338.	53.10	47.24	18092.	0.878	49.14	0.08	0.252	0.362	0.0063	0.0124	1.202	43.64
66	75.10	60.20	26214.	1728.	1368.	52.20	45.59	17778.	0.878	48.36	0.08	0.246	0.350	0.0061	0.0117	1.197	42.54
66	75.10	66.20	26167.	1751.	1398.	51.98	46.76	17476.	0.878	47.67	0.08	0.241	0.340	0.0059	0.0110	1.190	42.14
66	75.10	71.20	26553.	1701.	1419.	65.00	62.53	17261.	0.878	47.90	0.08	0.252	0.331	0.0064	0.0105	1.150	55.40
70	76.23	1.00	13073.	1289.	1105.	63.33	56.90	9780.	0.885	58.89	0.20	0.388	0.485	0.0139	0.0208	1.118	56.42
70	76.23	3.50	12959.	1386.	1115.	42.36	36.75	9707.	0.884	40.47	0.19	0.349	0.476	0.0114	0.0201	1.172	34.95
70	76.23	7.50	12965.	1445.	1137.	36.51	30.46	9563.	0.883	34.80	0.19	0.328	0.464	0.0102	0.0191	1.193	28.76
70	76.23	12.00	13124.	1485.	1164.	34.61	28.68	9405.	0.882	32.37	0.19	0.315	0.450	0.0095	0.0181	1.198	26.63
70	76.23	18.00	13128.	1520.	1196.	33.33	27.42	9202.	0.880	30.63	0.19	0.304	0.433	0.0089	0.0169	1.196	25.12
70	76.23	26.00	13351.	1561.	1238.	32.87	27.07	8943.	0.879	29.21	0.20	0.292	0.411	0.0083	0.0154	1.190	24.37
70	76.23	36.10	13305.	1608.	1294.	32.16	26.40	8639.	0.878	27.99	0.19	0.279	0.386	0.0076	0.0138	1.179	23.31
70	76.23	46.10	13329.	1667.	1349.	30.46	24.77	8359.	0.878	26.97	0.19	0.264	0.364	0.0069	0.0123	1.176	21.20
70	76.23	54.20	13546.	1718.	1392.	29.27	23.40	8145.	0.878	26.24	0.19	0.252	0.347	0.0063	0.0113	1.176	19.64
70	76.23	60.20	13463.	1744.	1426.	29.02	22.93	7993.	0.878	25.81	0.19	0.246	0.335	0.0060	0.0106	1.169	19.18
70	76.23	66.20	13295.	1763.	1458.	29.27	24.54	7849.	0.879	25.47	0.19	0.242	0.324	0.0058	0.0100	1.159	19.26
70	76.23	71.20	13545.	1679.	1481.	45.17	41.36	7746.	0.879	25.79	0.19	0.261	0.316	0.0067	0.0095	1.102	35.57
72	75.73	1.00	5445.	1135.	982.	35.96	30.26	3698.	0.896	27.33	0.69	0.462	0.562	0.0191	0.0271	1.106	29.94
72	75.73	3.50	5367.	1237.	1000.	22.40	16.51	3651.	0.895	18.67	0.68	0.409	0.550	0.0154	0.0260	1.163	15.87
72	75.73	7.50	5299.	1312.	1025.	17.88	11.91	3581.	0.892	15.93	0.67	0.376	0.531	0.0132	0.0245	1.193	10.96
72	75.73	12.00	5339.	1367.	1055.	16.06	10.08	3506.	0.889	14.70	0.67	0.354	0.512	0.0118	0.0229	1.206	8.83
72	75.73	18.00	5309.	1419.	1092.	14.69	8.74	3411.	0.886	13.80	0.67	0.335	0.487	0.0107	0.0210	1.211	7.14
72	75.73	26.00	5550.	1482.	1145.	14.20	8.31	3290.	0.883	13.04	0.69	0.314	0.457	0.0095	0.0187	1.210	6.27
72	75.73	36.10	5467.	1547.	1209.	13.15	7.34	3150.	0.880	12.37	0.68	0.294	0.422	0.0084	0.0163	1.203	4.75
72	75.73	46.10	5406.	1616.	1273.	12.16	6.42	3024.	0.878	11.85	0.66	0.275	0.393	0.0074	0.0143	1.198	3.29
72	75.73	54.20	5703.	1689.	1326.	11.64	5.93	2929.	0.878	11.45	0.69	0.257	0.370	0.0066	0.0128	1.203	2.29
72	75.73	60.20	5612.	1724.	1366.	11.26	5.60	2861.	0.878	11.22	0.68	0.249	0.355	0.0062	0.0119	1.196	1.64
72	75.73	66.20	5483.	1741.	1403.	11.30	5.72	2798.	0.878	11.05	0.66	0.245	0.341	0.0060	0.0110	1.182	1.51
72	75.73	71.20	5612.	1590.	1433.	24.40	19.14	2748.	0.878	11.35	0.67	0.282	0.330	0.0078	0.0104	1.083	15.37
75	75.55	1.00	26574.	985.	375.	95.51	87.03	18312.	1.057	83.93	0.49	0.559	1.588	0.0269	0.1819	1.731	83.08
75	75.55	3.50	27038.	1191.	405.	72.24	62.87	17536.	1.032	54.14	0.50	0.431	1.485	0.0169	0.1595	1.909	56.40
75	75.55	7.50	27511.	1334.	457.	60.82	51.23	16384.	0.999	43.92	0.51	0.366	1.335	0.0126	0.1305	1.957	42.54
75	75.55	12.00	27885.	1434.	516.	54.05	44.57	15220.	0.974	38.90	0.52	0.329	1.186	0.0104	0.1047	1.940	34.06
75	75.55	18.00	28155.	1528.	598.	47.91	38.82	13881.	0.948	34.97	0.53	0.299	1.021	0.0087	0.0796	1.880	26.52
75	75.55	26.00	28804.	1626.	707.	43.20	34.64	12405.	0.929	31.66	0.53	0.272	0.845	0.0073	0.0564	1.787	20.28
75	75.55	36.10	28998.	1721.	845.	38.56	30.71	10942.	0.906	28.76	0.53	0.249	0.682	0.0062	0.0385	1.671	14.36
75	75.55	46.10	29156.	1820.	981.	35.11	27.76	9806.	0.896	26.63	0.53	0.228	0.563	0.0053	0.0272	1.583	9.22
75	75.55	54.20	29923.	1917.	1090.	32.82	25.81	9048.	0.886	25.08	0.53	0.210	0.488	0.0045	0.0211	1.534	5.27
75	75.55	60.20	29810.	1958.	1168.	31.86	25.13	8559.	0.881	24.23	0.53	0.203	0.442	0.0042	0.0177	1.485	3.53
75	75.55	66.20	29798.	1995.	1250.	31.47	24.99	8126.	0.879	23.53	0.52	0.197	0.403	0.0040	0.0150	1.436	2.47
75	75.55	71.20	29913.	1841.	1314.	42.43	36.44	7801.	0.878	23.89	0.52	0.224	0.374	0.0051	0.0131	1.297	15.98
84	75.28	1.00	6500.	758.	307.	35.08	27.58	3985.	1.163	26.88	3.04	0.776	1.844	0.0486	0.2452	1.588	25.91
84	75.28	3.50	6476.	924.	343.	25.64	17.32	3774.	1.095	17.07	3.08	0.606	1.699	0.0312	0.2087	1.724	14.15
84	75.28	7.50	6429.	1072.	402.	20.24	11.49	3465.	1.035	13.48	3.11	0.497	1.491	0.0219	0.1613	1.778	6.42
84	75.28	12.00	6488.	1190.	471.	17.15	8.40	3161.	0.992	11.66	3.15	0.430	1.291	0.0169	0.1229	1.772	1.49
84	75.28	18.00	6474.	1314.	567.	14.32	5.83	2824.	0.956	10.24	3.14	0.373	1.075	0.0131	0.0878	1.728	-3.21
84	75.28	26.00	6877.	1445.	698.	12.83	4.81	2462.	0.931	9.05	3.31	0.324	0.856	0.0101	0.0578	1.646	-6.77
84	75.28	36.10	6800.	1562.	863.	11.10	3.80	2117.	0.904	8.07	3.23	0.288	0.661	0.0081	0.0365	1.529	-10.22
84	75.28	46.10	6685.	1687.	1021.	9.75	2.93	1867.	0.892	7.37	3.12	0.256	0.530	0.0065	0.0245	1.450	-13.74
84	75.28	54.20	7196.	1806.	1152.	9.42	2.94	1703.	0.882	6.87	3.30	0.230	0.450	0.0054	0.0183	1.406	-16.11
84	75.28	60.20	7061.	1863.	1248.	9.05	2.82	1598.	0.879	6.61	3.21	0.219	0.401	0.0049	0.0149	1.360	-17.61
84	75.28	66.20	6871.	1890.	1340.	9.14	3.17	1509.	0.877	6.41	3.09	0.214	0.362	0.0047	0.0123	1.306	-18.26
84	75.28	71.20	7072.	1678.	1417.	18.73	13.32	1442.	0.878	6.61	3.14	0.258	0.333	0.0066	0.0106	1.139	9.26

M	P	Z	QW	TW	TG	NUB	NUBC	REB	PRB	NUMCEL	A E6	TAW	TAG	PLNKW	PLNKB	TRAT	UBCHOT
86	75.36	1.00	26237.	1293.	1061.	105.28	99.52	21773.	0.889	110.21	0.08	0.382	0.505	0.0136	0.0224	1.153	98.41
86	75.36	3.50	26343.	1392.	1073.	76.19	70.25	21575.	0.888	75.65	0.08	0.343	0.497	0.0112	0.0218	1.208	68.80
86	75.36	7.50	26534.	1443.	1094.	68.62	62.65	21266.	0.886	65.18	0.09	0.325	0.484	0.0102	0.0208	1.225	60.94
86	75.36	12.00	26722.	1480.	1117.	65.14	59.18	20927.	0.884	60.63	0.09	0.313	0.470	0.0095	0.0198	1.230	57.25
86	75.36	18.00	26749.	1512.	1147.	63.06	57.14	20491.	0.883	57.46	0.09	0.303	0.453	0.0089	0.0185	1.227	54.95
86	75.36	26.00	27013.	1549.	1187.	61.89	56.03	19936.	0.881	54.83	0.09	0.292	0.431	0.0083	0.0169	1.220	53.51
86	75.36	36.10	27088.	1589.	1239.	61.47	55.71	19282.	0.879	52.62	0.09	0.281	0.406	0.0077	0.0152	1.206	52.81
86	75.36	46.10	27262.	1647.	1290.	58.19	52.48	18676.	0.878	50.71	0.09	0.266	0.383	0.0070	0.0137	1.204	49.13
86	75.36	54.20	27499.	1696.	1331.	55.50	49.82	18213.	0.878	49.36	0.09	0.254	0.366	0.0064	0.0126	1.204	46.09
86	75.36	60.20	27504.	1723.	1360.	54.74	49.10	17884.	0.877	48.53	0.09	0.248	0.354	0.0061	0.0119	1.199	45.12
86	75.36	66.20	27440.	1745.	1390.	54.47	48.87	17569.	0.878	47.84	0.08	0.243	0.343	0.0059	0.0112	1.192	44.66
86	75.36	71.20	27592.	1684.	1419.	71.91	66.49	17316.	0.878	48.21	0.09	0.257	0.334	0.0066	0.0107	1.141	62.43
87	75.46	1.00	25998.	1287.	1054.	104.73	98.95	21820.	0.889	110.35	0.08	0.385	0.509	0.0138	0.0228	1.154	97.89
87	75.46	3.50	26307.	1388.	1068.	76.31	70.35	21622.	0.888	75.75	0.08	0.345	0.501	0.0113	0.0221	1.209	68.95
87	75.46	7.50	26379.	1439.	1089.	68.47	62.48	21311.	0.886	65.26	0.08	0.327	0.488	0.0103	0.0211	1.226	60.82
87	75.46	12.00	26616.	1475.	1112.	65.14	59.16	20971.	0.885	60.73	0.09	0.315	0.474	0.0096	0.0201	1.231	57.28
87	75.46	18.00	26604.	1507.	1140.	62.83	56.89	20534.	0.883	57.51	0.09	0.305	0.457	0.0090	0.0188	1.229	54.74
87	75.46	26.00	26833.	1544.	1181.	61.74	55.87	19978.	0.881	54.90	0.09	0.294	0.435	0.0084	0.0172	1.221	53.41
87	75.46	36.10	26859.	1583.	1233.	61.21	55.43	19323.	0.879	52.69	0.09	0.283	0.409	0.0078	0.0154	1.207	52.59
87	75.46	46.10	26993.	1640.	1284.	58.05	52.32	18717.	0.878	50.80	0.08	0.268	0.387	0.0071	0.0139	1.204	49.04
87	75.46	54.20	27215.	1689.	1324.	55.20	49.51	18253.	0.878	49.43	0.09	0.256	0.369	0.0065	0.0128	1.205	45.84
87	75.46	60.20	27324.	1720.	1355.	54.23	48.57	17924.	0.878	48.59	0.09	0.249	0.357	0.0062	0.0121	1.201	44.65
87	75.46	66.20	27276.	1742.	1384.	53.98	48.36	17609.	0.878	47.88	0.08	0.244	0.346	0.0060	0.0114	1.194	44.21
87	75.46	71.20	27342.	1677.	1409.	71.10	65.66	17355.	0.878	48.25	0.08	0.259	0.337	0.0067	0.0108	1.143	61.66
89	75.16	1.00	7191.	744.	359.	41.94	34.83	5044.	1.073	32.66	1.83	0.792	1.636	0.0505	0.1939	1.470	32.85
89	75.16	3.50	7186.	908.	389.	29.78	21.87	4829.	1.044	21.10	1.85	0.619	1.531	0.0325	0.1699	1.611	18.47
89	75.16	7.50	7154.	1049.	438.	23.35	15.04	4515.	1.008	16.96	1.85	0.511	1.378	0.0230	0.1392	1.680	9.94
89	75.16	12.00	7225.	1167.	496.	19.74	11.30	4199.	0.983	14.87	1.87	0.441	1.228	0.0177	0.1119	1.703	4.48
89	75.16	18.00	7224.	1291.	574.	16.48	8.16	3836.	0.954	13.20	1.87	0.382	1.060	0.0136	0.0857	1.694	-0.64
89	75.16	26.00	7712.	1429.	680.	14.67	6.61	3427.	0.933	11.77	1.98	0.329	0.878	0.0104	0.0607	1.657	-4.67
89	75.16	36.10	7651.	1561.	817.	12.37	4.82	3017.	0.909	10.56	1.94	0.288	0.707	0.0082	0.0412	1.582	-8.95
89	75.16	46.10	7559.	1685.	950.	10.72	3.58	2704.	0.897	9.70	1.89	0.256	0.584	0.0066	0.0292	1.521	-12.67
89	75.16	54.20	7946.	1799.	1055.	10.02	3.13	2494.	0.889	9.08	1.97	0.231	0.507	0.0054	0.0226	1.491	-15.42
89	75.16	60.20	7808.	1850.	1135.	9.49	2.86	2358.	0.883	8.75	1.92	0.221	0.458	0.0050	0.0190	1.449	-16.85
89	75.16	66.20	7657.	1877.	1212.	9.35	2.98	2240.	0.880	8.51	1.86	0.216	0.418	0.0048	0.0161	1.398	-17.50
89	75.16	71.20	7906.	1640.	1275.	16.72	10.99	2150.	0.878	8.82	1.91	0.267	0.388	0.0071	0.0141	1.210	7.71
105	50.33	1.00	8855.	558.	394.	114.81	110.52	30191.	1.001	147.57	0.06	0.730	1.015	0.0604	0.1117	1.193	111.98
105	50.33	3.50	9342.	623.	400.	88.47	83.96	29921.	0.998	100.82	0.06	0.649	1.001	0.0487	0.1087	1.260	85.38
105	50.33	7.50	9616.	656.	411.	81.48	76.89	29482.	0.993	86.60	0.06	0.613	0.979	0.0439	0.1041	1.282	78.25
105	50.33	12.00	9823.	679.	424.	78.47	73.85	28988.	0.987	80.33	0.06	0.590	0.953	0.0409	0.0990	1.289	75.13
105	50.33	18.00	9997.	701.	440.	76.37	71.74	28342.	0.980	75.76	0.07	0.569	0.920	0.0382	0.0926	1.289	72.93
105	50.33	26.00	10523.	733.	464.	75.16	70.52	27492.	0.972	71.69	0.07	0.540	0.877	0.0349	0.0846	1.291	71.56
105	50.33	36.10	10704.	758.	494.	74.75	70.15	26460.	0.965	68.41	0.07	0.519	0.825	0.0325	0.0754	1.276	71.02
105	50.33	46.10	10970.	788.	526.	73.40	68.85	25486.	0.955	65.58	0.07	0.495	0.776	0.0299	0.0675	1.266	69.52
105	50.33	54.20	11082.	816.	551.	70.67	66.14	24737.	0.948	63.51	0.07	0.474	0.740	0.0277	0.0618	1.262	66.65
105	50.33	60.20	11220.	833.	570.	70.20	65.69	24205.	0.943	62.20	0.07	0.462	0.714	0.0264	0.0579	1.255	66.09
105	50.33	66.20	11359.	852.	590.	69.25	64.77	23689.	0.939	60.95	0.07	0.449	0.689	0.0251	0.0543	1.250	65.05
105	50.33	71.20	11268.	827.	606.	79.62	75.27	23275.	0.937	60.92	0.07	0.466	0.669	0.0268	0.0515	1.208	75.50
106	24.05	1.00	6655.	516.	343.	88.63	86.28	21533.	0.971	110.24	0.10	0.378	0.543	0.0334	0.0666	1.215	86.21
106	24.05	3.50	7067.	590.	351.	67.13	64.66	21291.	0.970	74.89	0.10	0.329	0.533	0.0260	0.0644	1.295	64.44
106	24.05	7.50	7287.	629.	363.	61.06	58.55	20898.	0.967	64.03	0.11	0.307	0.519	0.0228	0.0609	1.324	58.21
106	24.05	12.00	7481.	654.	378.	59.13	56.61	20459.	0.965	59.30	0.11	0.294	0.502	0.0211	0.0571	1.330	56.17
106	24.05	18.00	7619.	679.	398.	57.55	55.04	19889.	0.963	55.83	0.11	0.282	0.481	0.0195	0.0524	1.328	54.47
106	24.05	26.00	7923.	714.	425.	55.84	53.33	19154.	0.957	52.65	0.12	0.266	0.453	0.0176	0.0469	1.326	52.60
106	24.05	36.10	8088.	743.	461.	55.37	52.91	18281.	0.951	50.01	0.12	0.254	0.421	0.0162	0.0408	1.306	51.98
106	24.05	46.10	8342.	781.	499.	53.95	51.52	17470.	0.947	47.78	0.12	0.239	0.392	0.0146	0.0356	1.295	50.38
106	24.05	54.20	8608.	815.	527.	52.42	50.02	16847.	0.940	46.02	0.13	0.227	0.369	0.0132	0.0320	1.291	48.70
106	24.05	60.20	8743.	836.	552.	52.06	49.69	16405.	0.935	44.97	0.13	0.220	0.354	0.0126	0.0296	1.280	48.24
106	24.05	66.20	8817.	851.	574.	52.06	49.71	15982.	0.931	44.02	0.13	0.215	0.339	0.0120	0.0274	1.268	48.15
106	24.05	71.20	8746.	821.	594.	61.43	59.17	15646.	0.929	44.06	0.13	0.225	0.327	0.0131	0.0257	1.215	57.64

M	P	Z	QW	TW	TG	NUB	NUBC	REB	PRB	NUMCEL	A E6	TAW	TAG	PLNKW	PLNKB	TRAT	UBCHOT
107	71.05	1.00	10455.	554.	372.	126.47	120.93	33843.	1.050	163.04	0.06	1.039	1.502	0.0865	0.1729	1.219	123.68
107	71.05	3.50	11066.	621.	379.	99.60	93.72	33520.	1.045	111.19	0.06	0.920	1.480	0.0693	0.1679	1.289	96.55
107	71.05	7.50	11429.	661.	390.	90.44	84.39	32991.	1.036	95.01	0.06	0.858	1.444	0.0609	0.1600	1.319	87.22
107	71.05	12.00	11696.	685.	403.	87.53	81.41	32393.	1.027	87.94	0.06	0.825	1.404	0.0567	0.1514	1.326	84.19
107	71.05	18.00	11969.	712.	421.	84.20	78.02	31607.	1.014	82.50	0.07	0.788	1.351	0.0522	0.1409	1.330	80.73
107	71.05	26.00	12343.	744.	446.	81.79	75.59	30580.	0.999	77.81	0.07	0.749	1.282	0.0478	0.1277	1.328	78.17
107	71.05	36.10	12588.	770.	479.	81.08	74.91	29342.	0.985	73.91	0.07	0.718	1.201	0.0442	0.1128	1.311	77.31
107	71.05	46.10	12959.	806.	512.	78.79	72.62	28173.	0.973	70.57	0.07	0.679	1.125	0.0401	0.0999	1.303	74.83
107	71.05	54.20	13318.	839.	540.	76.55	70.40	27264.	0.962	68.06	0.07	0.647	1.067	0.0367	0.0908	1.299	72.43
107	71.05	60.20	13538.	859.	561.	75.71	69.59	26613.	0.956	66.50	0.07	0.628	1.025	0.0349	0.0845	1.292	71.49
107	71.05	66.20	13675.	876.	582.	75.21	69.13	25985.	0.950	65.11	0.08	0.612	0.986	0.0333	0.0787	1.282	70.90
107	71.05	71.20	13579.	853.	600.	84.61	78.71	25482.	0.946	64.93	0.07	0.633	0.955	0.0353	0.0742	1.239	80.39
108	48.98	1.00	4825.	539.	386.	68.09	63.93	13755.	1.002	79.11	0.15	0.737	1.005	0.0628	0.1124	1.181	65.33
108	48.98	3.50	5111.	613.	393.	49.62	45.22	13605.	0.999	53.73	0.16	0.643	0.988	0.0490	0.1087	1.258	46.58
108	48.98	7.50	5275.	657.	407.	44.13	39.62	13361.	0.993	45.85	0.17	0.596	0.961	0.0426	0.1030	1.289	40.90
108	48.98	12.00	5400.	679.	422.	42.91	38.38	13087.	0.986	42.45	0.17	0.574	0.930	0.0397	0.0969	1.292	39.58
108	48.98	18.00	5526.	708.	442.	41.19	36.64	12731.	0.978	39.81	0.18	0.547	0.891	0.0364	0.0893	1.295	37.71
108	48.98	26.00	5739.	742.	472.	40.34	35.80	12269.	0.969	37.56	0.18	0.518	0.840	0.0331	0.0800	1.290	36.70
108	48.98	36.10	5859.	772.	509.	40.14	35.66	11719.	0.960	35.65	0.19	0.494	0.781	0.0304	0.0697	1.271	36.34
108	48.98	46.10	6022.	809.	547.	38.98	34.55	11207.	0.949	33.97	0.19	0.466	0.726	0.0274	0.0611	1.261	35.00
108	48.98	54.20	6259.	846.	578.	37.99	33.59	10812.	0.941	32.71	0.20	0.441	0.685	0.0248	0.0549	1.258	33.82
108	48.98	60.20	6348.	868.	602.	37.52	33.15	10530.	0.937	31.93	0.20	0.427	0.655	0.0234	0.0507	1.251	33.23
108	48.98	66.20	6383.	884.	627.	37.75	33.43	10260.	0.933	31.29	0.20	0.417	0.628	0.0224	0.0469	1.237	33.37
108	48.98	71.20	6378.	855.	648.	45.62	41.43	10045.	0.930	31.29	0.20	0.435	0.606	0.0243	0.0439	1.187	41.34
109	24.78	1.00	4731.	526.	363.	64.81	62.42	13034.	0.969	74.24	0.18	0.382	0.535	0.0332	0.0629	1.198	62.30
109	24.78	3.50	5030.	607.	370.	46.95	44.42	12871.	0.967	50.20	0.19	0.329	0.525	0.0252	0.0605	1.285	44.14
109	24.78	7.50	5224.	658.	386.	41.45	38.87	12607.	0.965	42.73	0.20	0.301	0.508	0.0215	0.0568	1.322	38.43
109	24.78	12.00	5370.	698.	402.	39.59	37.00	12312.	0.963	39.44	0.20	0.286	0.490	0.0195	0.0529	1.332	36.44
109	24.78	18.00	5497.	716.	425.	38.41	35.83	11930.	0.957	36.99	0.21	0.273	0.467	0.0180	0.0482	1.329	35.12
109	24.78	26.00	5811.	756.	458.	37.72	35.17	11437.	0.952	34.79	0.22	0.256	0.437	0.0160	0.0425	1.325	34.25
109	24.78	36.10	5966.	792.	500.	37.20	34.68	10852.	0.947	32.91	0.23	0.242	0.401	0.0145	0.0363	1.305	33.53
109	24.78	46.10	6142.	835.	543.	36.00	33.54	10315.	0.937	31.26	0.23	0.227	0.370	0.0130	0.0313	1.291	32.15
109	24.78	54.20	6388.	875.	579.	35.08	32.65	9905.	0.931	30.05	0.24	0.214	0.346	0.0116	0.0277	1.285	31.03
109	24.78	60.20	6481.	898.	607.	34.83	32.43	9615.	0.927	29.31	0.25	0.207	0.329	0.0110	0.0254	1.273	30.67
109	24.78	66.20	6550.	918.	634.	34.76	32.40	9340.	0.924	28.65	0.25	0.201	0.314	0.0104	0.0232	1.260	30.49
109	24.78	71.20	6501.	878.	656.	42.99	40.71	9123.	0.922	28.72	0.25	0.213	0.302	0.0116	0.0216	1.199	38.86
110	74.33	1.00	5650.	539.	379.	76.93	71.34	16095.	1.051	91.05	0.13	1.118	1.549	0.0953	0.1760	1.191	74.19
110	74.33	3.50	6001.	614.	386.	56.73	50.73	15923.	1.045	61.75	0.14	0.974	1.524	0.0741	0.1703	1.270	53.69
110	74.33	7.50	6196.	658.	399.	50.76	44.57	15643.	1.036	52.66	0.15	0.903	1.483	0.0645	0.1613	1.301	42.78
110	74.33	12.00	6357.	683.	414.	48.88	42.62	15327.	1.024	48.60	0.15	0.865	1.436	0.0596	0.1520	1.308	40.60
110	74.33	18.00	6497.	711.	434.	47.06	40.75	14911.	1.010	45.50	0.16	0.826	1.376	0.0548	0.1401	1.310	38.44
110	74.33	26.00	6759.	748.	463.	45.56	39.21	14371.	0.995	42.77	0.16	0.778	1.298	0.0493	0.1255	1.309	36.49
110	74.33	36.10	6910.	779.	500.	45.14	38.82	13723.	0.981	40.49	0.17	0.741	1.206	0.0452	0.1092	1.291	35.66
110	74.33	46.10	7109.	817.	538.	43.84	37.56	13116.	0.965	38.50	0.17	0.699	1.121	0.0408	0.0956	1.280	34.83
110	74.33	54.20	7363.	855.	569.	42.51	36.23	12647.	0.955	37.02	0.18	0.661	1.056	0.0369	0.0858	1.277	38.31
110	74.33	60.20	7460.	874.	594.	42.33	36.10	12313.	0.948	36.14	0.18	0.642	1.010	0.0350	0.0792	1.266	38.03
110	74.33	66.20	7518.	892.	618.	42.30	36.11	11992.	0.943	35.36	0.18	0.626	0.967	0.0334	0.0731	1.254	37.89
110	74.33	71.20	7481.	861.	639.	50.56	44.59	11738.	0.939	35.35	0.18	0.655	0.933	0.0363	0.0685	1.202	46.27
111	24.70	1.00	2963.	514.	370.	45.61	43.26	7907.	0.967	50.26	0.30	0.390	0.524	0.0345	0.0605	1.173	43.12
111	24.70	3.50	3117.	592.	380.	32.07	29.60	7808.	0.966	34.08	0.31	0.337	0.514	0.0266	0.0583	1.252	29.32
111	24.70	7.50	3210.	641.	393.	27.72	25.19	7648.	0.964	28.99	0.32	0.309	0.498	0.0226	0.0547	1.290	24.75
111	24.70	12.00	3314.	672.	411.	26.45	23.92	7471.	0.961	26.76	0.33	0.293	0.480	0.0205	0.0510	1.299	23.36
111	24.70	18.00	3396.	703.	435.	25.36	22.83	7240.	0.956	25.07	0.34	0.278	0.457	0.0187	0.0465	1.300	22.13
111	24.70	26.00	3546.	740.	467.	24.82	22.32	6945.	0.951	23.60	0.36	0.262	0.428	0.0168	0.0411	1.295	21.41
111	24.70	36.10	3620.	775.	508.	24.49	22.03	6596.	0.945	22.33	0.37	0.248	0.394	0.0152	0.0352	1.275	20.90
111	24.70	46.10	3715.	818.	550.	23.44	21.02	6276.	0.936	21.20	0.38	0.232	0.364	0.0135	0.0304	1.266	19.65
111	24.70	54.20	3919.	860.	586.	23.02	20.64	6030.	0.930	20.38	0.40	0.218	0.340	0.0121	0.0270	1.262	19.04
111	24.70	60.20	3954.	882.	612.	22.74	20.39	5856.	0.927	19.88	0.40	0.211	0.324	0.0114	0.0247	1.252	18.64
111	24.70	66.20	3967.	899.	639.	22.92	20.60	5691.	0.924	19.46	0.40	0.206	0.309	0.0109	0.0226	1.236	18.73
111	24.70	71.20	3954.	853.	664.	30.28	28.06	5561.	0.922	19.58	0.40	0.220	0.298	0.0123	0.0211	1.169	26.25

M	P	Z	QW	TW	TG	NUB	NUBC	REB	PRB	NUMCEL	A B6	TAW	TAG	PLNKW	PLNKB	TRAT	UBCHOT
112	51.23	1.00	2901.	517.	387.	47.97	43.76	7583.	1.005	49.76	0.30	0.803	1.048	0.0707	0.1168	1.154	45.29
112	51.23	3.50	3050.	597.	396.	32.19	27.69	7493.	1.001	33.67	0.32	0.692	1.029	0.0539	0.1126	1.236	29.20
112	51.23	7.50	3145.	651.	410.	27.20	22.55	7349.	0.994	28.57	0.33	0.630	0.998	0.0454	0.1063	1.277	23.99
112	51.23	12.00	3256.	684.	427.	25.63	20.94	7187.	0.987	26.30	0.34	0.595	0.964	0.0409	0.0996	1.291	22.27
112	51.23	18.00	3341.	719.	449.	24.29	19.57	6976.	0.978	24.59	0.35	0.562	0.920	0.0370	0.0911	1.297	20.77
112	51.23	26.00	3563.	760.	482.	23.93	19.21	6699.	0.969	23.10	0.37	0.526	0.862	0.0329	0.0807	1.296	20.21
112	51.23	36.10	3652.	799.	522.	23.24	18.56	6367.	0.957	21.76	0.38	0.495	0.795	0.0295	0.0694	1.282	19.31
112	51.23	46.10	3749.	845.	566.	22.22	17.60	6060.	0.945	20.65	0.39	0.462	0.733	0.0261	0.0600	1.272	18.07
112	51.23	54.20	3943.	891.	601.	21.44	16.83	5825.	0.938	19.80	0.41	0.432	0.687	0.0231	0.0532	1.273	17.05
112	51.23	60.20	3993.	916.	629.	21.16	16.60	5657.	0.933	19.30	0.42	0.417	0.654	0.0217	0.0487	1.263	16.64
112	51.23	66.20	4007.	935.	656.	21.08	16.56	5498.	0.930	18.87	0.42	0.406	0.624	0.0206	0.0446	1.250	16.44
112	51.23	71.20	4003.	888.	680.	27.47	23.15	5372.	0.927	18.98	0.42	0.434	0.600	0.0233	0.0415	1.182	23.02
113	75.13	1.00	3015.	516.	383.	49.07	43.58	8010.	1.049	52.80	0.29	1.180	1.549	0.1041	0.1742	1.158	46.40
113	75.13	3.50	3159.	591.	392.	33.96	28.07	7920.	1.042	35.79	0.30	1.027	1.523	0.0809	0.1683	1.234	31.01
113	75.13	7.50	3253.	639.	404.	29.08	22.97	7775.	1.032	30.40	0.31	0.942	1.480	0.0690	0.1592	1.272	21.27
113	75.13	12.00	3358.	669.	420.	27.63	21.44	7611.	1.020	27.99	0.32	0.895	1.431	0.0629	0.1495	1.283	19.49
113	75.13	18.00	3438.	702.	442.	26.25	19.99	7395.	1.006	26.14	0.33	0.848	1.368	0.0570	0.1373	1.288	17.73
113	75.13	26.00	3590.	738.	472.	25.62	19.32	7115.	0.991	24.56	0.34	0.799	1.287	0.0513	0.1223	1.285	16.65
113	75.13	36.10	3674.	774.	512.	25.09	18.81	6779.	0.976	23.17	0.35	0.755	1.191	0.0464	0.1058	1.270	15.65
113	75.13	46.10	3767.	817.	552.	24.00	17.74	6466.	0.961	21.98	0.36	0.707	1.103	0.0412	0.0921	1.262	19.97
113	75.13	54.20	3951.	859.	586.	23.29	17.03	6224.	0.951	21.09	0.38	0.664	1.036	0.0368	0.0822	1.261	19.06
113	75.13	60.20	3993.	878.	613.	23.39	17.18	6051.	0.945	20.60	0.38	0.646	0.989	0.0351	0.0755	1.247	19.05
113	75.13	66.20	4013.	897.	638.	23.25	17.08	5887.	0.940	20.13	0.38	0.628	0.944	0.0333	0.0694	1.236	18.80
113	75.13	71.20	3995.	852.	660.	30.46	24.56	5756.	0.936	20.23	0.38	0.671	0.910	0.0376	0.0648	1.171	26.18
114	22.03	1.00	1281.	457.	305.	20.56	18.41	3180.	0.979	24.10	0.96	0.389	0.542	0.0379	0.0725	1.199	18.44
114	22.03	3.50	1310.	527.	316.	14.89	12.64	3129.	0.975	16.33	0.98	0.339	0.530	0.0295	0.0691	1.272	12.54
114	22.03	7.50	1323.	582.	332.	12.40	10.09	3050.	0.970	13.80	0.99	0.306	0.510	0.0245	0.0641	1.315	9.84
114	22.03	12.00	1371.	618.	352.	11.70	9.37	2963.	0.966	12.66	1.03	0.287	0.488	0.0218	0.0588	1.328	8.99
114	22.03	18.00	1400.	657.	377.	10.93	8.59	2851.	0.962	11.77	1.06	0.268	0.460	0.0191	0.0523	1.335	8.03
114	22.03	26.00	1567.	708.	416.	11.06	8.74	2704.	0.957	10.96	1.19	0.246	0.424	0.0164	0.0447	1.334	7.94
114	22.03	36.10	1593.	755.	466.	10.55	8.27	2531.	0.948	10.25	1.21	0.228	0.382	0.0143	0.0367	1.312	7.20
114	22.03	46.10	1620.	808.	517.	9.89	7.65	2377.	0.941	9.65	1.23	0.210	0.345	0.0124	0.0304	1.298	6.29
114	22.03	54.20	1756.	861.	560.	9.73	7.53	2260.	0.933	9.19	1.34	0.194	0.318	0.0107	0.0262	1.295	5.90
114	22.03	60.20	1767.	890.	595.	9.51	7.35	2178.	0.928	8.91	1.34	0.186	0.299	0.0100	0.0235	1.280	5.55
114	22.03	66.20	1755.	909.	629.	9.50	7.38	2102.	0.924	8.69	1.33	0.181	0.282	0.0095	0.0211	1.258	5.44
114	22.03	71.20	1780.	844.	656.	13.87	11.87	2042.	0.922	8.78	1.35	0.199	0.269	0.0112	0.0193	1.169	10.03
115	23.83	1.00	5229.	673.	378.	38.65	35.79	7709.	0.965	45.82	0.54	0.282	0.501	0.0196	0.0579	1.353	35.62
115	23.83	3.50	5693.	812.	390.	28.99	26.37	7573.	0.963	30.39	0.59	0.226	0.484	0.0132	0.0535	1.496	25.37
115	23.83	7.50	6039.	912.	418.	25.14	22.32	7289.	0.958	25.28	0.63	0.195	0.456	0.0101	0.0477	1.563	21.05
115	23.83	12.00	6397.	978.	453.	23.76	20.96	6975.	0.952	22.91	0.66	0.178	0.425	0.0086	0.0419	1.576	19.35
115	23.83	18.00	6691.	1045.	500.	22.41	19.65	6582.	0.946	21.06	0.69	0.163	0.387	0.0074	0.0352	1.568	17.67
115	23.83	26.00	7373.	1121.	567.	21.99	19.34	6089.	0.933	19.33	0.76	0.148	0.342	0.0062	0.0280	1.540	16.87
115	23.83	36.10	7628.	1190.	651.	20.88	18.36	5541.	0.922	17.82	0.79	0.136	0.292	0.0053	0.0210	1.486	15.38
115	23.83	46.10	8016.	1270.	745.	20.03	17.61	5071.	0.911	16.61	0.82	0.124	0.251	0.0045	0.0160	1.436	14.13
115	23.83	54.20	8546.	1346.	819.	19.47	17.07	4733.	0.902	15.68	0.88	0.114	0.223	0.0039	0.0130	1.412	13.17
115	23.83	60.20	8555.	1387.	875.	18.82	16.26	4504.	0.897	15.12	0.87	0.109	0.205	0.0035	0.0111	1.384	12.27
115	23.83	66.20	8722.	1432.	938.	18.64	16.77	4295.	0.893	14.65	0.88	0.104	0.189	0.0033	0.0096	1.353	11.87
115	23.83	71.20	8609.	1338.	977.	24.23	23.14	4154.	0.892	14.79	0.87	0.115	0.177	0.0039	0.0084	1.251	17.86
116	48.33	1.00	4839.	651.	367.	37.78	33.19	7016.	1.010	43.42	0.62	0.594	1.034	0.0428	0.1204	1.344	34.63
116	48.33	3.50	5271.	783.	383.	28.57	23.58	6857.	1.002	28.72	0.68	0.479	0.998	0.0291	0.1124	1.475	24.83
116	48.33	7.50	5595.	880.	411.	24.80	19.60	6599.	0.990	23.84	0.72	0.414	0.941	0.0225	0.1002	1.539	20.57
116	48.33	12.00	5886.	943.	443.	23.33	18.10	6314.	0.977	21.53	0.76	0.379	0.878	0.0191	0.0879	1.553	18.76
116	48.33	18.00	6145.	1008.	490.	21.96	16.76	5953.	0.964	19.73	0.80	0.347	0.799	0.0163	0.0737	1.545	17.04
116	48.33	26.00	6581.	1080.	556.	21.08	16.02	5508.	0.946	18.08	0.86	0.316	0.705	0.0138	0.0586	1.516	15.78
116	48.33	36.10	6834.	1146.	642.	20.25	15.42	5014.	0.931	16.67	0.89	0.291	0.603	0.0119	0.0441	1.458	14.58
116	48.33	46.10	7151.	1231.	730.	19.09	14.44	4590.	0.918	15.46	0.93	0.263	0.520	0.0099	0.0336	1.421	12.93
116	48.33	54.20	7807.	1319.	807.	18.55	14.03	4279.	0.907	14.54	1.00	0.238	0.461	0.0083	0.0272	1.404	11.91
116	48.33	60.20	7995.	1375.	866.	17.88	13.47	4066.	0.900	13.95	1.02	0.224	0.422	0.0074	0.0232	1.384	10.90
116	48.33	66.20	8103.	1418.	927.	17.61	13.32	3872.	0.896	13.49	1.03	0.214	0.388	0.0068	0.0199	1.354	10.37
116	48.33	71.20	7793.	1312.	975.	23.52	19.52	3726.	0.894	13.66	0.98	0.240	0.362	0.0084	0.0176	1.235	16.79

M	P	Z	QW	TW	TG	NUB	NUBC	REB	PRB	NUMCEL	A E6	TAW	TAG	PLNKW	PLNKB	TRAT	UBCHOT
117	72.35	1.00	5967.	649.	346.	45.12	38.87	8508.	1.082	51.46	0.55	0.893	1.621	0.0646	0.1976	1.376	37.38
117	72.35	3.50	6548.	784.	362.	34.70	27.77	8312.	1.063	33.87	0.61	0.716	1.565	0.0435	0.1843	1.513	25.42
117	72.35	7.50	6952.	878.	389.	30.57	23.27	7990.	1.039	27.99	0.65	0.622	1.473	0.0337	0.1634	1.576	20.06
117	72.35	12.00	7297.	935.	423.	29.06	21.67	7630.	1.014	25.20	0.69	0.573	1.371	0.0291	0.1425	1.581	17.77
117	72.35	18.00	7616.	997.	471.	27.52	20.16	7171.	0.990	22.99	0.72	0.527	1.243	0.0250	0.1185	1.565	15.41
117	72.35	26.00	8224.	1068.	539.	26.72	19.52	6602.	0.963	20.96	0.78	0.480	1.088	0.0212	0.0927	1.530	13.67
117	72.35	36.10	8530.	1128.	630.	25.96	19.09	5971.	0.940	19.25	0.80	0.445	0.922	0.0185	0.0685	1.457	12.11
117	72.35	46.10	8998.	1219.	724.	24.48	17.83	5433.	0.925	17.77	0.84	0.399	0.787	0.0152	0.0513	1.418	9.36
117	72.35	54.20	9827.	1317.	805.	23.39	16.89	5042.	0.910	16.59	0.91	0.357	0.692	0.0124	0.0409	1.405	6.93
117	72.35	60.20	10125.	1376.	869.	22.67	16.32	4774.	0.903	15.90	0.93	0.335	0.630	0.0111	0.0345	1.381	5.39
117	72.35	66.20	10184.	1404.	931.	22.87	16.72	4532.	0.898	15.40	0.94	0.325	0.575	0.0105	0.0293	1.340	5.09
117	72.35	71.20	9378.	1241.	984.	36.76	31.20	4355.	0.895	15.85	0.86	0.389	0.536	0.0146	0.0258	1.178	30.38
119	46.48	1.00	8398.	662.	354.	61.75	57.22	12792.	1.013	69.41	0.34	0.561	1.023	0.0399	0.1225	1.378	58.57
119	46.48	3.50	9231.	789.	370.	48.61	43.70	12505.	1.005	46.02	0.37	0.456	0.988	0.0275	0.1144	1.506	44.85
119	46.48	7.50	9773.	870.	396.	43.87	38.79	12038.	0.994	38.43	0.39	0.404	0.932	0.0221	0.1019	1.554	39.68
119	46.48	12.00	10175.	918.	428.	42.03	36.97	11523.	0.980	34.90	0.41	0.377	0.870	0.0195	0.0896	1.552	37.59
119	46.48	18.00	10576.	972.	473.	40.15	35.15	10873.	0.967	32.09	0.43	0.350	0.794	0.0170	0.0753	1.535	35.42
119	46.48	26.00	11203.	1037.	537.	38.63	33.76	10077.	0.950	29.51	0.46	0.321	0.703	0.0147	0.0601	1.502	33.56
119	46.48	36.10	11566.	1087.	618.	37.99	33.36	9196.	0.933	27.32	0.47	0.301	0.604	0.0130	0.0457	1.435	32.64
119	46.48	46.10	12240.	1179.	703.	35.65	31.15	8434.	0.923	25.32	0.49	0.269	0.523	0.0106	0.0350	1.409	29.77
119	46.48	54.20	13389.	1280.	778.	33.56	29.17	7871.	0.910	23.68	0.54	0.239	0.465	0.0086	0.0284	1.406	27.15
119	46.48	60.20	13696.	1327.	835.	32.81	28.53	7484.	0.903	22.80	0.55	0.227	0.426	0.0079	0.0243	1.380	26.13
119	46.48	66.20	14366.	1422.	892.	30.01	25.76	7124.	0.898	21.70	0.57	0.205	0.391	0.0065	0.0209	1.392	22.76
119	46.48	71.20	12975.	1231.	940.	46.95	43.13	6858.	0.895	22.50	0.51	0.253	0.366	0.0095	0.0185	1.208	40.67
120	75.33	1.00	9270.	656.	355.	69.58	63.16	14334.	1.077	78.17	0.29	0.918	1.651	0.0657	0.1970	1.369	61.74
120	75.33	3.50	10138.	774.	370.	55.43	48.38	14038.	1.061	51.91	0.32	0.757	1.600	0.0465	0.1850	1.487	46.24
120	75.33	7.50	10680.	844.	395.	50.66	43.35	13550.	1.040	43.43	0.34	0.680	1.515	0.0384	0.1661	1.525	40.56
120	75.33	12.00	11075.	886.	425.	48.89	41.56	13008.	1.017	39.42	0.36	0.640	1.422	0.0344	0.1473	1.521	38.26
120	75.33	18.00	11464.	933.	467.	47.06	39.75	12316.	0.994	36.24	0.37	0.599	1.304	0.0306	0.1252	1.502	35.80
120	75.33	26.00	12094.	991.	526.	45.59	38.39	11456.	0.970	33.30	0.39	0.553	1.161	0.0264	0.1009	1.472	33.55
120	75.33	36.10	12469.	1036.	604.	45.31	38.41	10491.	0.946	30.84	0.40	0.521	1.005	0.0237	0.0776	1.406	32.68
120	75.33	46.10	13227.	1124.	686.	42.73	35.95	9648.	0.933	28.59	0.42	0.466	0.874	0.0195	0.0600	1.382	28.90
120	75.33	54.20	14334.	1218.	755.	40.09	33.38	9022.	0.919	26.76	0.46	0.416	0.780	0.0159	0.0490	1.381	25.00
120	75.33	60.20	14700.	1268.	809.	38.92	32.35	8590.	0.910	25.71	0.47	0.393	0.717	0.0143	0.0422	1.361	23.15
120	75.33	66.20	15844.	1402.	866.	33.60	26.92	8181.	0.904	24.19	0.50	0.339	0.659	0.0110	0.0362	1.405	15.92
120	75.33	71.20	14064.	1190.	912.	54.74	48.85	7877.	0.900	25.25	0.44	0.430	0.617	0.0169	0.0322	1.203	48.70
121	25.63	1.00	16196.	659.	361.	121.94	119.23	31491.	0.970	141.06	0.10	0.311	0.555	0.0222	0.0654	1.362	118.92
121	25.63	3.50	17557.	758.	373.	100.29	97.43	30929.	0.968	94.94	0.11	0.264	0.540	0.0165	0.0619	1.462	96.84
121	25.63	7.50	18358.	814.	394.	93.22	90.31	30019.	0.965	80.52	0.12	0.242	0.516	0.0141	0.0565	1.492	89.49
121	25.63	12.00	18968.	851.	420.	90.15	87.26	29017.	0.960	73.92	0.12	0.229	0.489	0.0128	0.0511	1.491	86.25
121	25.63	18.00	19552.	892.	453.	87.00	84.14	27742.	0.953	68.73	0.13	0.216	0.456	0.0115	0.0448	1.480	82.90
121	25.63	26.00	20379.	943.	501.	84.08	81.27	26155.	0.947	64.13	0.13	0.201	0.415	0.0101	0.0375	1.459	79.71
121	25.63	36.10	21018.	984.	563.	83.01	80.32	24355.	0.934	60.09	0.14	0.190	0.369	0.0092	0.0304	1.411	78.45
121	25.63	46.10	22104.	1059.	624.	77.62	74.99	22739.	0.925	56.17	0.14	0.172	0.330	0.0076	0.0247	1.402	72.66
121	25.63	54.20	23813.	1148.	678.	72.41	69.81	21515.	0.921	53.07	0.16	0.154	0.301	0.0063	0.0208	1.413	66.99
121	25.63	60.20	24756.	1210.	720.	68.50	65.93	20651.	0.916	51.00	0.16	0.143	0.280	0.0055	0.0184	1.415	62.76
121	25.63	66.20	27605.	1389.	763.	56.56	53.92	19798.	0.909	47.39	0.18	0.117	0.261	0.0038	0.0162	1.512	49.84
121	25.63	71.20	24732.	1198.	802.	76.45	74.07	19143.	0.904	49.25	0.16	0.145	0.246	0.0056	0.0146	1.314	70.75
122	50.13	1.00	16504.	637.	366.	135.30	130.63	32281.	1.013	148.27	0.10	0.631	1.072	0.0464	0.1249	1.328	132.20
122	50.13	3.50	17850.	733.	378.	109.96	104.98	31740.	1.007	99.81	0.11	0.538	1.045	0.0347	0.1186	1.423	106.45
122	50.13	7.50	18645.	787.	398.	101.84	96.74	30860.	0.999	84.58	0.11	0.494	1.000	0.0298	0.1089	1.453	98.06
122	50.13	12.00	19214.	821.	422.	98.56	93.46	29883.	0.987	77.55	0.12	0.469	0.952	0.0272	0.0991	1.452	94.61
122	50.13	18.00	19822.	860.	455.	95.11	90.04	28630.	0.975	72.04	0.12	0.442	0.890	0.0245	0.0872	1.443	90.95
122	50.13	26.00	20627.	907.	500.	92.38	87.36	27055.	0.964	67.17	0.13	0.413	0.813	0.0217	0.0736	1.424	87.97
122	50.13	36.10	21166.	943.	559.	92.11	87.27	25253.	0.946	62.93	0.13	0.393	0.727	0.0198	0.0601	1.377	87.51
122	50.13	46.10	22438.	1022.	620.	85.69	80.90	23623.	0.934	58.74	0.14	0.353	0.651	0.0163	0.0491	1.373	80.67
122	50.13	54.20	24042.	1104.	672.	80.09	75.32	22380.	0.928	55.54	0.15	0.318	0.595	0.0135	0.0416	1.382	74.63
122	50.13	60.20	25125.	1170.	713.	75.09	70.33	21498.	0.922	53.27	0.15	0.293	0.556	0.0117	0.0368	1.390	69.27
122	50.13	66.20	28819.	1392.	756.	58.59	53.57	20611.	0.914	48.87	0.18	0.228	0.517	0.0074	0.0324	1.523	51.51
122	50.13	71.20	25564.	1188.	794.	80.22	75.75	19925.	0.909	50.96	0.15	0.287	0.488	0.0113	0.0292	1.314	74.28

M	P	Z	GW	TW	TG	NUB	NUBC	REB	PRB	NUMCEL	A E6	TAW	TAG	PLNKW	PLNKB	TRAT	UBCHOT
206	24.83	2.00	2651.	501.	340.	38.12	35.69	12794.	0.974	59.13	0.07	0.402	0.564	0.0364	0.0696	1.201	57.10
206	24.83	6.00	4413.	582.	350.	43.36	40.79	12594.	0.971	44.84	0.11	0.345	0.551	0.0275	0.0664	1.286	48.45
206	24.83	12.00	7695.	755.	377.	44.50	41.69	12106.	0.966	37.32	0.14	0.257	0.518	0.0161	0.0589	1.452	41.36
206	24.83	18.00	11292.	957.	420.	43.16	40.14	11410.	0.959	32.46	0.17	0.191	0.473	0.0095	0.0494	1.610	35.92
206	24.83	24.00	14761.	1183.	479.	39.40	36.24	10574.	0.949	28.55	0.19	0.143	0.419	0.0056	0.0394	1.750	31.32
206	24.83	29.90	17658.	1384.	553.	35.82	32.65	9695.	0.936	25.60	0.21	0.114	0.364	0.0038	0.0304	1.821	27.60
206	24.83	35.90	18745.	1531.	635.	31.54	28.46	8876.	0.924	23.51	0.22	0.098	0.315	0.0029	0.0233	1.818	24.66
206	24.83	41.90	17636.	1573.	710.	28.04	25.12	8189.	0.917	22.31	0.23	0.094	0.275	0.0026	0.0182	1.738	22.67
206	24.83	47.90	15833.	1552.	768.	25.80	23.10	7650.	0.906	21.69	0.24	0.096	0.245	0.0028	0.0148	1.612	21.25
206	24.83	53.90	12355.	1472.	850.	23.02	20.53	7254.	0.899	21.56	0.23	0.104	0.224	0.0032	0.0126	1.475	20.05
206	24.83	59.90	8609.	1352.	889.	20.66	18.35	6987.	0.896	21.81	0.19	0.118	0.209	0.0040	0.0112	1.343	18.74
206	24.83	65.90	5222.	1219.	922.	18.85	16.69	6822.	0.894	22.39	0.14	0.137	0.201	0.0053	0.0104	1.215	16.97
207	49.43	2.00	2741.	514.	355.	38.97	34.69	12076.	1.019	57.63	0.08	0.780	1.086	0.0691	0.1299	1.195	55.59
207	49.43	6.00	4512.	595.	366.	43.07	38.49	11888.	1.013	43.61	0.12	0.666	1.061	0.0519	0.1239	1.282	47.03
207	49.43	12.00	7817.	776.	393.	43.61	38.45	11431.	1.000	36.18	0.16	0.495	0.998	0.0303	0.1100	1.449	40.03
207	49.43	18.00	11444.	980.	437.	42.06	36.43	10774.	0.981	31.31	0.19	0.368	0.911	0.0178	0.0923	1.607	34.63
207	49.43	24.00	14935.	1206.	496.	38.59	32.60	9982.	0.964	27.50	0.21	0.277	0.806	0.0107	0.0734	1.742	30.16
207	49.43	29.90	17825.	1404.	572.	35.12	29.08	9145.	0.943	24.60	0.23	0.222	0.699	0.0072	0.0567	1.807	26.51
207	49.43	35.90	18801.	1542.	654.	31.16	25.28	8363.	0.929	22.60	0.25	0.193	0.603	0.0055	0.0432	1.797	23.71
207	49.43	41.90	17955.	1602.	739.	27.50	21.93	7708.	0.917	21.36	0.26	0.182	0.525	0.0050	0.0337	1.720	21.69
207	49.43	47.90	15822.	1574.	815.	25.13	19.98	7196.	0.906	20.77	0.27	0.187	0.467	0.0053	0.0273	1.595	20.31
207	49.43	53.90	12290.	1496.	876.	22.32	17.54	6823.	0.900	20.62	0.25	0.202	0.426	0.0060	0.0232	1.464	19.12
207	49.43	59.90	8578.	1379.	921.	20.09	15.65	6572.	0.896	20.85	0.21	0.228	0.399	0.0075	0.0206	1.332	17.86
207	49.43	65.90	5141.	1244.	953.	18.36	14.24	6417.	0.895	21.41	0.15	0.265	0.383	0.0099	0.0191	1.206	16.16
208	75.13	2.00	2864.	514.	356.	40.86	35.15	12565.	1.077	60.85	0.08	1.186	1.647	0.1051	0.1965	1.194	58.70
208	75.13	6.00	4690.	597.	366.	45.07	38.87	12379.	1.065	45.99	0.11	1.015	1.610	0.0791	0.1879	1.280	49.61
208	75.13	12.00	8136.	776.	392.	45.40	38.24	11924.	1.042	38.03	0.15	0.753	1.520	0.0461	0.1677	1.450	42.08
208	75.13	18.00	11936.	981.	435.	43.80	35.79	11261.	1.011	32.79	0.18	0.559	1.390	0.0270	0.1415	1.611	36.28
208	75.13	24.00	15612.	1206.	494.	40.33	31.67	10449.	0.984	28.72	0.20	0.421	1.234	0.0163	0.1131	1.747	31.48
208	75.13	29.90	18523.	1400.	567.	36.72	27.87	9583.	0.956	25.65	0.22	0.339	1.073	0.0110	0.0876	1.811	27.63
208	75.13	35.90	19615.	1532.	650.	32.86	24.19	8769.	0.938	23.58	0.24	0.296	0.926	0.0086	0.0669	1.795	24.71
208	75.13	41.90	18675.	1586.	733.	29.17	20.94	8084.	0.924	22.29	0.25	0.281	0.807	0.0078	0.0522	1.715	22.64
208	75.13	47.90	16465.	1550.	806.	26.96	19.35	7547.	0.911	21.67	0.26	0.291	0.718	0.0083	0.0423	1.588	21.21
208	75.13	53.90	12854.	1477.	869.	23.99	16.94	7153.	0.903	21.49	0.24	0.313	0.654	0.0095	0.0359	1.457	19.96
208	75.13	59.90	8980.	1367.	915.	21.44	14.91	6888.	0.899	21.70	0.20	0.351	0.612	0.0117	0.0318	1.329	18.60
208	75.13	65.90	5369.	1231.	945.	19.71	13.66	6725.	0.897	22.28	0.15	0.409	0.587	0.0155	0.0295	1.203	16.83
209	50.03	2.00	5695.	546.	350.	66.33	61.87	30293.	1.023	118.22	0.03	0.743	1.110	0.0626	0.1340	1.241	114.27
209	50.03	6.00	9611.	622.	360.	82.23	77.48	29891.	1.017	90.01	0.04	0.647	1.088	0.0487	0.1288	1.320	97.47
209	50.03	12.00	17078.	814.	383.	85.98	80.59	28882.	1.005	74.51	0.05	0.473	1.032	0.0277	0.1161	1.511	82.78
209	50.03	18.00	25363.	1038.	421.	84.13	78.15	27393.	0.987	64.38	0.06	0.345	0.951	0.0157	0.0991	1.700	71.56
209	50.03	24.00	33565.	1288.	476.	77.95	71.53	25547.	0.969	56.43	0.06	0.255	0.852	0.0092	0.0805	1.868	61.77
209	50.03	29.90	38193.	1474.	541.	70.17	63.68	23600.	0.951	50.96	0.07	0.209	0.749	0.0063	0.0636	1.933	54.69
209	50.03	35.90	40766.	1609.	614.	63.47	57.14	21775.	0.935	47.05	0.07	0.183	0.657	0.0050	0.0500	1.927	49.22
209	50.03	41.90	38759.	1644.	686.	57.21	51.21	20212.	0.926	44.88	0.08	0.177	0.580	0.0047	0.0398	1.836	45.72
209	50.03	47.90	35019.	1581.	751.	54.94	49.41	18956.	0.915	44.03	0.09	0.188	0.520	0.0052	0.0328	1.685	43.21
209	50.03	53.90	27076.	1429.	809.	53.01	48.04	18021.	0.907	44.60	0.08	0.219	0.477	0.0069	0.0281	1.489	41.52
209	50.03	59.90	18671.	1351.	849.	43.17	38.49	17354.	0.902	44.70	0.07	0.238	0.448	0.0081	0.0252	1.383	38.11
209	50.03	65.90	10854.	1201.	875.	37.55	33.23	17014.	0.900	46.10	0.05	0.282	0.431	0.0109	0.0235	1.244	34.50

EXECUTION TERMINATED

APPENDIX C

GENERAL TEST DATA

TABLE VI

UNIFORM FLUX SS-310 TEST SECTION FOR NITROGEN—TEST CONDITIONS

Run	Date	P (psia)	$Re_{b,in}$	T_{in} (°F)	T_{out} (°F)	Power (kw)	q" (Btu/hr-ft^2)	Qualifications*		
								Steady	Heat Balance	Consistency
50	6/13	76.39	3210	297.0	886.0	0.285	2482			
51	6/13	25.39	3389	304.0	858.5	0.290	2525			
52	6/13	25.39	3405	306.3	860.0	0.287	2499			
53	6/13	75.29	10484	306.0	846	0 79	6880	X		
54	6/20	25.14	9373	299.0	889.5	0.77	6706		X	
55	6/21	25.16	4283	308.5	828.5	0.340	2961	X		
56	6/21	25.56	9207	294.0	612.3	0.407	3544			
90	7/19	Unsuccessful						X	X	X
91	8/ 7							X	X	X
92	8/ 7	19.79	6947	76 0	786.0	0.574	4999			
93	8/ 7	20.00	3823	80.5	978.0	0.423	3679			

* X signifies unsatisfactory conditions.

TABLE VII

UNIFORM FLUX SS-310 TEST SECTION FOR STEAM—TEST CONDITIONS

Run	Date	P (psia)	$Re_{b,in}$	T_{in} (°F)	T_{out} (°F)	Power (kw)	q" (Btu/hr-ft^2)	Qualifications*		
								Steady	Heat Balance	Consistency
1	4/24	29.51	11800	675.5	862.5	0.70	6096	X		
2	4/24	29.81	18100	635.5	812.0	0.71	6183	X		
3-13	Heat Balance Check (no power)									
14	5/ 7	50.67	20800	698.0	865.5	1.00	8927	X		
15	5/ 7	50.17	19100	704.7	870.0	1.00	8927	X		
16	5/ 7	49.64	19100	718.0	883.0	0.99	8622			
17	5/ 7	50.47	20200	693.0	1030.5	1.98	17244	X		
18	5/ 7	49.77	19400	718.0	1062.1	1.98	17418	X		
19	5/ 9	50.64	34500	297.3	478.7	1.02	9057			
20	5/ 9	50.44	34000	302.7	481.0	1.01	8970			
21	5/ 9	50.14	34600	305.0	861.7	3.18	27868			
22	5/ 9	49.84	34000	306.7	863.5	3.11	27084			
23	5/ 9	25.24	25500	274.5	773.0	1.98	17418	X		
24	5/14	25.09	9900	278.8	906.5	1.03	8970			
25	5/14	50.64	9450	297.7	923.3	1.06	9231			
26	5/14	69.94	9200	341.0	934.5	1.15	10015			
27	5/14	69.94	8400	343.3	939.8	1.13	9928			
28	5/14	76.04	10000	712.0	1082.5	1.12	9754			
29	5/14	49.94	9400	705.2	1072.3	1.08	9362			
30	5/16	25.35	3100	259.6	1162.0	0.375	3266	X	X	X
31	5/16	24.95	3200	256.0	935.0	0.34	3309			
32	5/16	--	--	--	--	--	--	X	X	X
33	5/17	25.23	3200	263.7	891.0	0.34	2961			
34	5/17	25.63	3250	265.5	902.0	0.34	2961	X	X	
35	5/17	49.73	3205	317.0	965.0	0.42	3658			
36	5/17	75.53	3493	353.7	992.0	0.495	4311		X	
37	5/21	25.58	2829	698.7	1035.7	0.32	2787		X	X
38	5/21	50.73	2896	707.0	1035.0	0.37	3222			
39	5/21	50.53	2955	707.3	1037.7	0.37	3222			

* X signifies unsatisfactory conditions.

TABLE VII (Continued)

Run	Date	P (psia)	$Re_{b,in}$	T_{in} (°F)	T_{out} (°F)	Power (kw)	q" (Btu/hr-ft^2)	Qualifications*		
								Steady	Heat Balance	Consistency
40	5/21	75.23	2929	709.0	1028.5	0 368	3205			
41	5/23	25.56	3295	257.0	851.0	0.344	2994			
42	5/23	75.65	3652	337.5	885.5	0.435	3788	X	X	
43	5/28	24.85	13805	28.79	438.4	0.373	3248		X	
44	5/28	24 75	14520	287.3	394.4	0.373	2344		X	X
45	6/ 6	25.78	2173	272.0	972.0	0.290	2526	X	X	
46	6/ 6	51.78	2512	385.5	876.5	0.291	2534	X	X	
47	6/ 7	25.36	1873	408.0	1055 0	0.285	2482			
48	6/ 7	76.26	2748	481.7	1067.3	0.43	3745		X	
49	6/ 7	75.7	2175	716.3	1092 0	0.33	2874			
57	6/25	25.13	11367	711.0	1096.0	1.28	11147			
58	6/25	76.13	12383	698.0	1089.7	1.41	12279			
59	6/26	75.06	20103	705.0	1091 7	2.21	19247			
60	6/26	50.76	20751	691.5	1072.0	2.23	19421	X		X
61	6/26	25.46	22163	677.7	1044.5	2.22	19333			
62	6/27	75.03	17710	382.0	986.0	2.02	17679		X	
63	6/27	50.53	18089	382.5	982.0	2.07	18027			
64	6/27	50.53	17912	383.0	896.3	2.07	18027			
65	6/27	24.93	17774	378.6	991.0	2.035	17723			
66	6/28	75.10	21462	1099.7	1419.6	3.01	26214	X		
67	6/28	50.10	21486	1094.0	1403.8	2.90	25256	X		
68	6/28	65.01	25890	1087.5	1410.5	3.53	30742			
69	6/28	25.69	11223	1084.5	1430.5	1.75	15240			
70	7/ 1	76.23	9802	1145.0	1474.3	1.56	13586			
71	7/ 1	49.13	10845	1107.0	1446.0	1.71	14892			
72	7/ 1	75.73	3598	1097.3	1404.5	0.63	5487			
73	7/ 2	49.75	3568	1102.7	1408.7	0.635	5530			
74	7/ 2	25.25	3613	1109.0	1404.0	0.63	5487			
75	7/ 2	75.55	18312	364.5	1305.0	3.31	28826			
76	7/ 2	53.95	17730	343.4	1280.5	3.02	26300		X	
77	7/ 3	25.95	19831	346.0	1247.7	3.25	28304			

TABLE VII (Concluded)

Run	Date	P (psia)	$Re_{b,in}$	T_{in} (°F)	T_{out} (°F)	Power (kw)	q" (Btu/hr-ft^2)	Qualifications*		
								Steady	Heat Balance	Consistency
78	7/ 3	25.45	13511	298.0	1266.5	2.25	19595			
79	7/ 3	51.05	13692	327.0	1110.7	2.04	17766		X	X
80	7/ 8	76.60	12358	351.5	1215.0	2.03	17635			
81	7/ 8	51.20	12595	346.5	1112.5	1.77	15371			
82	7/10	25.88	3294	315.3	1303.7	0.59	5138			
83	7/10	50 88	4836	365.0	1244.7	0.85	7385			
84	7/10	75.28	3985	370.5	1311.0	0.785	6836			
85	7/16	24.96	17947	1064.3	1410.0	2.62	22774			
86	7/16	75.36	21773	1080.0	1413.5	3.11	27085			
87	7/16	75.46	21820	1074 0	1406.7	3.09	26910			
88	7/18	25.16	6013	355.5	1107.7	0 86	7516			
89	7/18	75.16	5044	380.0	1238.7	0.87	7577			

TABLE VIII

UNIFORM FLUX Zr-2 TEST SECTION FOR STEAM—TEST CONDITIONS

Run	Date	P (psia)	$Re_{b,in}$	T_{in} (°F)	T_{out} (°F)	Power (kw)	q" (Btu/hr-ft^2)	Qualifications*		
								Steady	Heat Balance	Consistency
101	9/18	51.0	17500	433.0	418.3	0	Heat Balance Check (no power)			
102	9/23	50.3	20000	584.0	547.0	0				
103	9/25	49.8	31000	707.0	690.0	0				
104	9/25	49.8	40000	882.0	856.0	0				
105	10/ 2	49.9	34000	396.5	605.2	1.2				
106	10/ 4	23.62	25000	348.5	593.5	0.925				
107	10/ 4	70.62	35500	373.0	602.0	1.44				
108	10/ 9	48.55	15000	396.0	645.5	0.67				
109	10/11	24.35	14000	371.3	653.5	0.675				
110	10/14	73.9	17000	379.5	640.5	0.788				
111	10/14	24 27	8400	389.0	659.0	0 416				
112	10/16	50.8	8000	386.0	681.5	0.413				
113	10/18	74.7	8500	338.0	660.5	0.42				
114	10/28	21.6	3000	394.0	628.5	0.181			X	
115	10/30	23.4	8400	388.0	974.0	0.865				X
116	11/ 1	47.9	7700	384.0	966.5	0.787				X
117	11/16	71.92	8800	376.0	962.0	0.98				X
118	11/16	23.5	15000	357.3	905.5	1.47				X
119	11/18	46.5	14000	383.0	924.0	1.35				X
120	11/20	74.9	15000	394.5	890.5	1.46				X
121	11/22	25.2	31000	376.0	798.0	2.48				X
122	11/23	49.7	33000	380.0	791.0	2.52				X
123	Test section failure									

* X signifies unsatisfactory conditions.

TABLE IX

NONUNIFORM FLUX SS-310 TEST SECTION FOR STEAM—TEST CONDITIONS

Run	Date	P (psia)	$Re_{b,in}$	T_{in} (°F)	T_{out} (°F)	Power (kw)	q''_{max} (Btu/hr-ft^2)	Qualifications*		
								Steady	Heat Balance	Consistency
201-205	Heat Balance Check (no power)									
206		24.83	12884	343.0	931.3	1.310	18645			
207		49.43	12169	357.7	962.0	1.320	18844			
208		75.13	12652	360.5	954.0	1.375	19570			
209		50.03	30350	357.0	895.0	2.920	40701			X

* X signifies unsatisfactory conditions.

APPENDIX D

SURFACE EMISSIVITY MEASUREMENTS

Surface samples were cut from the SS-310 dummy test section, the Zr-2 test section and the tubing as received for the measurement of normal spectral emissivity at several temperatures.

I. SAMPLE DESCRIPTION

Sample A: (SS-310) Exposed to steam at wall temperatures ranging from 300°F to 1500°F for a total of approximately 50 hrs. This sample was cut 2 to 3 in. from the exit of 36-in. long uniform dummy test section.

Sample B: (SS-310) Same exposure to steam as sample A with an additional exposure to nitrogen at wall temperatures from 300°F to 1100°F for a total of approximately 7 hrs. This sample was cut 2 to 3 in. from the exit of the 28-in. long uniform dummy test section (shortened by 8 in. due to cut of sample A).

Sample C: (SS-310) Tubing as received. Visual inspection of all of the SS-310 samples A, B, and C showed a characteristic rough appearance of the inside tube area along approximately half of the circumference while the remaining portion appeared to be more smooth. This surface texture is ascribed to the fabrication process. For this reason it was decided to select two samples, a rough and a smooth for each of the cases A, B and C, yielding a total of 6 samples.

Sample D: (Zr-2) Exposed to steam at wall temperatures of 500-1000°F for about 100 hrs. This sample was cut 4-3/4 in. downstream of the inlet to the heated length (see Figure 8). Surface appearance was dark.

Sample E: (Zr-2) Exposed to steam at wall temperatures of 800-1400°F for about 100 hrs. This sample was cut 31 in. downstream of the inlet. Surface appearance was light brown.

Sample G: (Zr-2) Tubing as received.

II. EXPERIMENTAL PROCEDURE

From each of the sample areas a 1/4 in. x 1/8 in. sample was cut. Care was exercised so as not to damage the inside surface. Each sample was soaked in acetone to remove any residual grease or oil from the machining process. Then samples were mounted in standard graphite holders, each having a machined cavity which served as black body reference points. Suspended from the thermocouple recording the surface and black body reference temperature the sample holder was positioned in the argon flushed furnace.

The normal spectral emissivity of the sample was obtained as the ratio of the sample to black body radiation intensities measured at 2-micron intervals over the range of 2 to 20 microns for each of three temperatures, approximately 1000°F, 1500°F and 2000°F, respectively, for the SS-310 samples and at 1000°F and 1500°F for the Zr-2 samples. In each case spectral measurements were made at the lowest temperature first, then at the higher temperatures in order of increasing temperature. No check was made at lower temperatures following the highest temperature level, since some materials show hysteresis effects. The experimental accuracy on emissivity was estimated to be less than 0.01. This does not include the variation in emissivity with location on the surface. Each sample was allowed to cool in the argon atmosphere of the furnace until nearly at room temperature to prevent further oxidation.

III. DISCUSSION OF SPECTRAL RESULTS

As seen from the data of Table X for normal spectral emissivity sample C exhibits the typical behavior of unoxidized electrical conductors, i.e., increasing emissivity with increasing temperature or decreasing wavelength of the radiation. For sample G this trend is reversed at low wavelengths, probably due to the presence of a thin oxide film. The smooth SS-310 sample shows a definitely smaller emissivity for higher wavelength than the sample appearing to have a rough surface.

The characteristic behavior of electrical conductors is exhibited by sample A above 6 microns for the rough and above 10-15 microns for the smooth sample, respectively. The rather complex behavior of the emissivity, particularly the pronounced changes with temperature at certain wavelengths, reflects the characteristics of the oxides formed on the surface resulting from exposure to the steam, although these results are not fully explained. As compared to sample C a definite increase in emissivity to a nearly constant value near 0.9 over the important range of wavelengths up to 6 microns is apparent.

The results for sample B agree most closely to those of sample A for the case of the rough surface having retained more of its metalic nature, however, similarities in general trends are apparent also for the case of the smooth surface. The significant dip near 4-6 microns for samples A and B at 2000°F

TABLE X

NORMAL SPECTRAL WALL EMISSIVITY DATA

(Samples A, B, C, D, E)

λ (micron)	(SS-310) A						(SS-310) B					
	Rough			Smooth			Rough			Smooth		
	1047°F	1422°F	2001°F	1076°F	1422°F	2006°F	1045°F	1430°F	2016°F	1066°F	1401°F	2021°F
2	.874	.886	.895	.894	.901	.912	.869	.878	.894	.848	.854	.894
4	.890	.892	.781	.864	.873	.877	.854	.851	.779	.894	.889	.772
6	.804	.908	.871	.863	.878	.846	.905	.902	.720	.886	.939	.873
8	.823	.840	.888	.921	.900	.826	.876	.863	.790	.756	.836	.877
10	.758	.787	.804	.936	.897	.849	.817	.816	.864	.683	.750	.781
12	.697	.737	.737	.943	.878	.860	.756	.762	.826	.633	.690	.702
14	.648	.695	.689	.879	.853	.838	.677	.708	.738	.601	.647	.648
16	.582	.640	.628	.620	.736	.702	.666	.630	.634	.558	.602	.603
18	.594	.619	.679	.538	.613	.686	.548	.579	.689	.573	.601	.668
20	.624	.648	.715	.635	.629	.620	.607	.614	.651	.600	.651	.685

λ (micron)	(SS-310) C						(Zr-2) D		(Zr-2) E		(Zr-2) G	
	Rough			Smooth								
	1049°F	1972°F	2004°F	1098°F	1468°F	2088°F	1004°F	1498°F	1004°F	1500°F	1000°F	1500°F
2	.745	.906	.862	.623	.916	.844	.905	.851	.907	.922	.848	.682
4	.602	.775	.774	.494	.789	.770	.919	.837	.908	.922	.830	.683
6	.544	.654	.644	.447	.618	.592	.785	.745	.916	.933	.832	.615
8	.519	.573	.590	.418	.533	.508	.705	.702	.935	.948	.606	.541
10	.519	.559	.572	.411	.489	.475	.641	.661	.961	.975	.555	.570
12							.795	.621	1.012	1.02	.445	.548
14	.516	.534	.581	.398	.431	.441	.758	.572	.840	.880	.434	.510
16	.508						.668	.550	.760	.790	.410	.489
18	.508						.639	.552	.690	.685	.410	.467
20	.511	.538	.574	.369	.421	.435						

(most pronounced for sample B, rough) is indicative of partial return to the unoxidized behavior for the low wavelength range, suggesting a possible change in surface film structure during the emissivity measurements.

It was furthermore noted that the color of each SS-310 sample before heating was a gray tone. After heating the samples all had a green tone resembling that of a nickel oxide. It is believed that the argon flush in the furnace is complete, and that oxygen trapped on the surface could have caused some oxidation.

In general it may be concluded that there appears to be little or no change in surface emissivity of SS-310 when exposure to steam is being followed by exposure to nitrogen.

The Zr-2 sample E, having a light brown appearence, shows a consistently high spectral emissivity depending little on temperature. The dark sample D, however, indicates a complex variation with wavelength and an inverse temperature effect reflecting the characteristics of thin oxide layers.

IV. WALL EMISSIVITY

The temperature dependent wall emissivity, $\epsilon_w(T)$, is taken to be the effective surface emissivity for black body radiation from a source at the temperature of the surface, and is obtained by numerical integration of the spectral data of Table X,

$$\epsilon_w(T) = \frac{\int_o^\infty \epsilon_{w\lambda}(T) E_{b\lambda}(T) d\lambda}{\int_o^\infty E_{b\lambda}(T) d\lambda} \cong \sum_{i=1}^{N} \epsilon_{w\lambda_i}(T) \int_{\lambda_i}^{\lambda_{i+1}} \frac{E_{b\lambda}(T)}{E_b(T)} d\lambda \qquad \text{(D-1)}$$

$$\epsilon_w(T) \cong \sum_{i=1}^{N} \epsilon_{w\lambda_i}(T) \frac{E_{b,o-\lambda_{i+1}}(T) - E_{b,o-\lambda_i}(T)}{E_b(T)}$$

where $E_{b\lambda}(T)$ is the Planck function and the integral $E_{b,o-\lambda_i}(T)/E_b(T)$ is taken from standard tables.[20] For SS-310 samples A and B mean values for rough and smooth surfaces were used in evaluating $\epsilon_{w\lambda_i}(T)$. Calculated values for $\epsilon_w(T)$ are tabulated below.

Sample A (SS-310)		Sample D (Zr-2)		Sample E (Zr-2)	
Temp. (°R)	$\epsilon_w(T)$	Temp. (°R)	$\epsilon_w(T)$	Temp. (°R)	$\epsilon_w(T)$
1000	0.830	--	--	--	--
1536	0.859	1464	0.819	1464	0.904
1882	0.877	1958	0.793	1960	0.920
2460	0.869	--	--	--	--

The temperature dependence of wall emissivity for metals is usually well approximated by an expression of the form

$$\epsilon_w(T) = \epsilon_A + \epsilon_B \ln T \qquad \text{(D-2)}$$

where T is measured in °R. For SS-310 the constants are $\epsilon_A = 0.371$ and $\epsilon_B =$ $= 0.0664$. The data for Zr-2 shows considerable scatter. The light brown oxide covered surface, sample E, shows a relatively high and increasing emissivity with temperature, typical of metal surfaces, $\epsilon_A \simeq 0.419$ and $\epsilon_B \simeq 0.0664$. The dark oxide covered surface, sample D, however, indicates an inverse temperature effect and lower values of emissivity. It is known[22] that thin oxide films may have a pronounced effect on surface emissivity, particularly at small wavelength (1-2μ) of magnitude comparable to that of the film thickness. Because of the limited data obtained for Zr-2 and the nonuniform conditions along the tube wall a single average value of 0.8 is used for the present study.

The values of emissivity measured for the Zr-2 sample as received and particularly for the samples exposed to steam are considerably higher than values quoted for the pure metal surface,[23] and somewhat higher than the value of 0.67 at 1470°F quoted for an oxide coated surface.[24]

REFERENCES

1. W. McAdams, Heat Transmission (Third Edition), McGraw-Hill, New York (1954) (Ch. 4 by H. C. Hottel).

2. W. M. Kays, Convective Heat and Mass Transfer, McGraw-Hill, New York (1966).

3. E. M. Sparrow, T. H. Hallman, and R. Siegel, "Turbulent Heat Transfer in the Thermal Entrance Region of a Pipe with Uniform Heat Flux," Appl. Sci. Res., A7, 37-52 (1958).

4. D. M. McEligot, P. M. Magee, and G. Leppert, "Effect of Large Temperature Gradients on Convective Heat Transfer: The Downstream Region," J. Heat Transfer, 87C, 67-76 (1965).

5. H. C. Perkins, and P. Worsoe-Schmidt, "Turbulent Heat and Momentum Transfer for Gases in a Circular Tube at Wall-to-Bulk Temperature Ratios to Seven," Int. J. Heat Mass Transfer, 8, 1011-1031 (1965).

6. B. S. Petuknov, V. V. Korillov, and V. N. Maidanik, "Heat Transfer Experimental Research for Turbulent Gas Flow in Pipes at High Temperature Difference Between Wall and Bulk Fluid Temperature," Proc., Third International Heat Transfer Conference, Vol. I, AIChE-ASME, 285-242 (1966).

7. L. V. Humble, et al., "Measurements of Average Heat Transfer and Friction Coefficients for Subsonic Flow of Air in Smooth Tubes at High Surface and Fluid Temperatures," NACA Report 1020 (1952).

8. M. F. Taylor, "Local Heat Transfer Measurements for Forced Convection of Hydrogen and Helium at Surface Temperatures Up to 5600°R," Proceedings of the 1963 Heat Transfer and Fluid Mechanics Institute, 251-272 (1963).

9. W. B. Hall and P. H. Price, "The Effect of Longitudinally Varying Wall Heat Flux on the Heat Transfer Coefficient for Turbulent Flow in a Pipe," International Developments in Heat Transfer, Part III, ASME (1961), pp. 607-613.

10. E. N. Seider and G. E. Tate, "Heat Transfer and Pressure Drop of Liquids in Tubes," Ind. Eng. Chem., 1429-1435 (1936).

11. C. A. Bankston, "Heat Transfer Turbulence and Interchannel Flow Stability in the Transition from Turbulent to Laminar Flow in Tubes," Ph.D. Thesis, Univ. of New Mexico, 1965.

12. H. C. Reynolds, Jr., "Internal Low Reynolds Number Turbulent Heat Transfer," Ph.D. Thesis, Univ. of Arizona, 1968. (EMMT Lab. TR-2, Engineering Experimental Station, College of Engineering, The University of Arizona, Tucson, Arizona.)

13. R. D. Cess, In E. M. Sparrow and R. D. Cess, Radiation Heat Transfer, Brooks-Cole, p. 219, 1966.

14. R. Viskanta, "Radiation Heat Transfer and Interaction of Convection with Radiation Heat Transfer," Advances in Heat Transfer, Vol. 3, Academic Press, pp. 175-251, 1966.

15. H. Lord, "Radiation-Convection Interaction in Grey Gas Duct Flow," Ph.D. Thesis, The University of Michigan, 1969 (to be published).

16. M. M. Abu-Romia and C. L. Tien, "Appropriate Mean Absorption Coefficients for Infrared Radiation of Gases," J. Heat Transfer (ASME), 321-237 (1967).

17. H. Schlichting, Boundary Layer Theory (Fourth Edition), McGraw-Hill, New York (1960).

18. H. W. Emmons, "The Laminar-Turbulent Transition in a Boundary Layer—Part I," J. Aeron. Sci., 490-498 (July 1951).

19. Freund, Mathematical Statistics, Prentice-Hall, 1962.

20. Krieth, Principles of Heat Transfer, International, 1962.

21. Eckert and Drake, Heat and Mass Transfer, McGraw-Hill, New York, 1959.

22. R. E. Rolling, et al., "Investigation of the Effect of Surface Conditions on the Radiant Properties of Metals," Report AFML-TR-64-363, Part II (April 1967).

23. A. Goldsmith, et al., Handbook of Thermophysical Properties of Solid Materials, Vol. II, McMillan, New York (1961).

24. W. D. Wood, et al., Zr-2 Properties, Report BMI-1154.